SIMULATION OF FLOW IN A HIGH-TEMPERATURE REACTOR CHAMBER

by

HUONG THI DO

Department of Chemical Engineering
McGill University
Montreal, Canada

March 1973

A thesis submitted to the Faculty of Graduate Studies and Research of McGill University in partial fulfillment of the requirements for the degree of Master of Engineering.

ABSTRACT

The flow pattern and temperature profile have been simulated for a very hot gas stream entering a cylindrical reactor chamber which may have cooled walls. The simulation is a preliminary to calculating the trajectories and reaction histories of particles injected at low solid loadings into the tail flame of an induction plasma torch. The numerical solution procedure suggested by Spalding and co-workers has been employed. The predictions for the isothermal form of the model have been shown to agree satisfactorily with the results of flow visualization in a cold model of the reactor, and with both numerical and experimental results obtained by other workers. The flow of an Argon "tail flame" in the reactor with cooled walls is predicted to be entirely different from the corresponding isothermal flow, due to variations of the fluid properties. The heat transfer to the wall shows a strong dependence on entry Reynolds number and entry temperature of the gas.

RÉSUMÉ

On a simulé l'écoulement et déduit le profil de température d'un courant gazeux chaud ou très chaud pénétrant dans un réacteur cylindrique dont les parois peuvent être refroidies. Lorsqu'on injecte une faible quantité de particules a l'extrémité de la "flamme" d'une torche à plasma, cette simulation est la première étape de l'établissement d'un modèle permettant de connaître les trajectoires des particules ainsi que l'évolution temporelle et spatiale d'éventuelles réactions chimiques. On a employé la méthode d'analyse numerique préconisée par Spalding et ses associés. Les résultats obtenus dans le cas particulier d'un reacteur isotherme furent comparés favorablement avec, d'une part une visualisation de l'écoulement dans un réacteur à temperature ambiante, d'autre part les résultats numeriques ou experimentaux d'autres auteurs.

Il a été constaté numériquement que l'écoulement d'Argon de la sortie de la "flamme" de la torche à travers ~~le~~ réacteur à parois refroidies est entièrement different de l'écoulement isotherme d'Argon à travers le même réacteur; la différence peut s'expliquer par les variations des propriétés du fluide. Le coefficient d'échange thermique le long des parois varie beaucoup avec, d'une part la valeur du nombre de Reynolds caracterisant l'entrée du réacteur, d'autre part la température d'entrée du gaz.

ACKNOWLEDGMENTS

The author wishes to express her gratitude to the many persons who have contributed either directly or indirectly to the work presented in this thesis.

In particular, she is indebted to:

Professor R. Clift for his generous guidance and constant support throughout the course of this investigation.

Mr. H.Q. Bui for his moral support and help in a variety of ways.

Mr. D. Bhaga, fellow graduate student, for his guidance in the Hydrogen Bubble Method, and for the use of his circuit.

Mr. B. Hoogendoorn for the construction of the electric circuit.

Mr. A. Krish and the Staff of the Chemical Engineering Workshop for the construction of the experimental equipment.

Mr. L. Allen, summer student, for his assistance in the set-up of the experimental apparatus.

The National Research Council of Canada for financial support for the present work.

The McConnell Foundation for financial support in the form of a Memorial Fellowship.

Drs. M. Boulos, S. Katta and A.S. Mujumdar for many useful discussions.

Finally, her thanks are due to Miss H. Levesque for typing this thesis.

TABLE OF CONTENTS

Page

Page

APPENDICES

LIST OF FIGURES

LIST OF TABLES

1. INTRODUCTION

A number of studies have been reported in the literature on the use of plasma reactors for chemical production and for processes requiring thermal treatment in the metallurgical, ceramic, and associated industries. At least some of the potential applications appear to have a promising future on a commercial scale (43,21). In the Canadian context, interest in chemical reactions using a plasma flame as the heat source is now centered in the field of metallurgical operations: the treatment of metal ores to produce pure high melting-point metals and refractories. Practical application is essentially limited to expensive products, due to the high installation and power costs associated with plasma systems. One possible technique for heterogeneous reactions, which is being studied by other workers in this laboratory, is the injection of particles at low solid-loadings into the laminar tail flame of an induction plasma generator. In order to calculate particle trajectories and reaction history, the flow pattern and temperature profile in the reactor chamber must be characterized completely. Experimental measurements are extremely difficult under these situations, and very little information is available in the literature, especially for laminar flows.

The present work presents a method for simulating the flow in the reactor by numerical solution of the equations of continuity, motion and energy. The approach suggested by Gosman and co-workers (17) was employed, using "upwind differences" to improve stability of the solution procedure. This is described in detail in Chapter II, together with the boundary conditions and specifications of the problem. The computer program developed is applicable to any axi-symmetric reactor geometry. The simulation was carried out for a laminar tail flame entering a cylindrical reactor with cooled walls as shown in Fig.2.1. The geometry assumed here represents a critical test, since the combination of a sudden expansion followed by a sudden contraction with cooled exterior walls gives particularly troublesome boundary conditions.

Numerical results are presented in Chapter III with the details of the computations. The existence and uniqueness of the solutions and factors influencing the accuracy, convergence and stability of the solution procedure are discussed. Results were obtained for both isothermal flow with constant properties and an Argon tail flame, with a range of reactor entry conditions. Argon was used since it is a common working-fluid for plasma processes; a different fluid would lead to slightly different results. Some predictions were also carried out for isothermal flow in a simple conduit expansion to enable a comparison with the results obtained by other workers, using a different finite-differencing scheme.

The validity of the predictions for the isothermal form of the model was compared with the results of flow visualization in a cold model of the reactor, with sucrose solution as the working fluid. The Hydrogen Bubble Method was used to visualize the flow. The experimental apparatus and techniques used are described in Chapter IV, with a comparison between the predicted and measured values of the dimensions of the laminar jet entering the reactor and the centerline velocity of the flow field.

Chapter V presents the conclusion of the work, with recommendations for further work.

II. THEORY

2.1 INTRODUCTION

The present work is concerned with flows of very hot gases, such as are generated by an induction or arc plasma in a chamber of the geometry shown in Fig. 2.1. The cross-section of the chamber is circular. The incoming gas is admitted into the chamber at Section AA', flows through a sudden expansion and contraction, and exits at Section BB'. The gas is chemically inert, and the chamber walls are all water-cooled, assumed to be impermeable and non-reacting.

The procedure for predicting the flow is based upon the conservation laws of mass, momentum and energy, expressed through partial differential equations in the general form applicable to a fluid whose properties vary with position. In the present chapter, these equations are developed in cylindrical polar coordinates for axi-symmetric flows. The equations are made dimensionless, and then cast into a finite-difference form which enables numerical solution by the technique developed by Gosman <u>et al</u> (17). In addition to the differential equations, algebraic equations describing the specification of the mathematical problem are derived from the boundary conditions and the thermodynamic and transport properties of the fluid. The present work is restricted to laminar axi-symmetric steady flows.

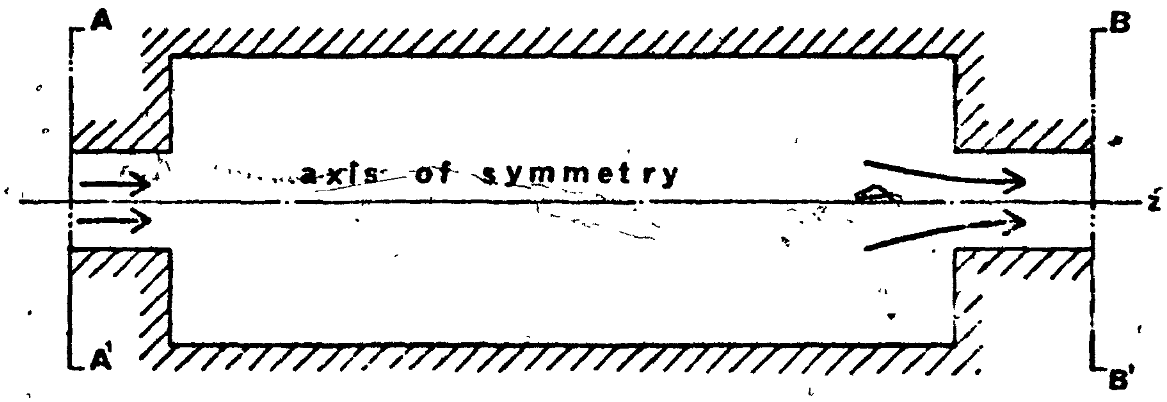

Fig.2.1 ILLUSTRATION OF THE GEOMETRY OF THE SYSTEM

2.2 BASIC EQUATIONS

2.2.1 The Differential Equations Based on the Conservation Laws

(a) Continuity equation - The conservation of mass law gives:

$$\bar{\nabla} \cdot (\hat{\rho}\hat{\underline{V}}) = 0 \qquad (2.2\text{-}1)$$

where $\hat{\rho}$ is the density of the fluid, and $\hat{\underline{V}}$ is the velocity vector.

The continuity equation for an axi-symmetric flow in cylindrical polar coordinates takes the form (for zero gradients in the θ-direction):

$$\frac{1}{\hat{r}} \frac{\partial}{\partial \hat{r}} (\hat{\rho} \hat{r} \hat{V}_r) + \frac{\partial}{\partial \hat{z}} (\hat{\rho} \hat{V}_z) = 0 \qquad (2.2\text{-}2)$$

where $\hat{V}_r$ and $\hat{V}_z$ are the velocity components in the $\hat{r}$ and $\hat{z}$ directions respectively.

(b) Equation of motion - The general equation of motion derived from the conservation law of momentum in the absence of the gravitational force takes the form:

$$\hat{\rho} \frac{D\hat{\underline{V}}}{Dt} = -\bar{\nabla}\hat{p} - \bar{\nabla} \cdot \underline{\underline{\tau}} \qquad (2.2\text{-}3)$$

where $\hat{p}$ is the fluid mechanic pressure, and $\underline{\underline{\tau}}$ the viscous stress tensor, determined by, for a Newtonian fluid:

$$\underline{\underline{\tau}} = -\hat{\mu}\,\underline{\underline{\Delta}}' + (\tfrac{2}{3}\hat{\mu} - \hat{\mu}')\,\underline{\underline{\delta}}(\bar{\nabla} \cdot \hat{\underline{V}})$$

in which $\hat{\mu}$ is the shear viscosity of the fluid and $\hat{\mu}'$ is the "bulk viscosity", which is identically zero for low density monatomic gases, and generally small in dense gases (5). In view of the above, the bulk viscosity is ignored so that the fluid mechanic and thermodynamic pressures are then equal. $\underline{\underline{\Delta}}$ denotes the rate of strain tensor, given by:

$$\Delta_{ij} = \frac{\partial \hat{V}_i}{\partial x_j} + \frac{\partial \hat{V}_j}{\partial x_i}$$

and $\underline{\underline{\delta}}$ is the unit tensor:

$$\underline{\underline{\delta}} = \begin{pmatrix} 1 & 0 & 0 \\ 0 & 1 & 0 \\ 0 & 0 & 1 \end{pmatrix}$$

The three components of the equation of motion in cylindrical polar coordinates for steady axi-symmetric flows take the forms:

(i) r-component:

$$\hat{\rho}[\hat{V}_r \frac{\partial \hat{V}_r}{\partial \hat{r}} - \frac{\hat{V}_\theta^2}{\hat{r}} + \hat{V}_z \frac{\partial \hat{V}_r}{\partial \hat{z}}] = -\frac{\partial \hat{p}}{\partial \hat{r}} + \frac{1}{\hat{r}} \frac{\partial}{\partial \hat{r}}[\hat{r}\ \hat{\mu}(2\frac{\partial \hat{V}_r}{\partial \hat{r}} - \frac{2}{3}\bar{\nabla}.\hat{\underline{V}})]$$

$$- \frac{\hat{\mu}}{\hat{r}}[2\frac{\hat{V}_r}{\hat{r}} - \frac{2}{3}\bar{\nabla}.\hat{\underline{V}}] + \frac{\partial}{\partial \hat{z}}[\hat{\mu}(\frac{\partial \hat{V}_z}{\partial \hat{r}} + \frac{\partial \hat{V}_r}{\partial \hat{z}})] \quad (2.2\text{-}4)$$

(ii) θ-component:

$$\hat{\rho}[\hat{V}_r \frac{\partial \hat{V}_\theta}{\partial \hat{r}} + \frac{\hat{V}_r \hat{V}_\theta}{\hat{r}} - \hat{V}_z \frac{\partial \hat{V}_\theta}{\partial \hat{z}}] = \frac{1}{\hat{r}^2}\frac{\partial}{\partial \hat{r}}[\hat{r}^3\ \hat{\mu}\ \frac{\partial}{\partial \hat{r}}(\frac{\hat{V}_\theta}{\hat{r}})]$$

$$+ \frac{\partial}{\partial \hat{z}}[\hat{\mu}\ \frac{\partial \hat{V}_\theta}{\partial \hat{z}}] \quad (2.2\text{-}5)$$

(iii) z-component:

$$\hat{\rho}\,[\hat{V}_r \frac{\partial \hat{V}_z}{\partial \hat{r}} + \hat{V}_z \frac{\partial \hat{V}_z}{\partial \hat{z}}] = -\frac{\partial \hat{p}}{\partial \hat{z}} + \frac{1}{\hat{r}} \frac{\partial}{\partial \hat{r}} [\hat{r}\, \hat{\mu}\, (\frac{\partial \hat{V}_z}{\partial \hat{r}} + \frac{\partial \hat{V}_r}{\partial \hat{z}})]$$

$$+ \frac{\partial}{\partial \hat{z}} [\hat{\mu}\, (2 \frac{\partial \hat{V}_z}{\partial \hat{z}} - \frac{2}{3} \bar{\nabla}.\hat{\underline{V}})] \qquad (2.2\text{-}6)$$

here, $\hat{V}_\theta$ is the velocity component in the θ-direction (i.e. the swirl velocity), and

$$\bar{\nabla}.\hat{\underline{V}} = \frac{1}{\hat{r}} \frac{\partial}{\partial \hat{r}} (\hat{r}\, \hat{V}_r) + \frac{\partial \hat{V}_z}{\partial \hat{z}}$$

(c) Energy equation - In the absence of gravitational forces, the general equation of thermal energy based on the law of conservation of energy takes the form (5):

$$\hat{\rho} \frac{D\hat{U}}{Dt} = -\bar{\nabla}.\underline{q} - \hat{p}\, \bar{\nabla}.\hat{\underline{V}} - \underline{\tau}:\bar{\nabla}\hat{\underline{V}} - \hat{Q}_R \qquad (2.2\text{-}7)$$

$\hat{\rho} \frac{D\hat{U}}{Dt}$	rate of gain of internal energy
$-\bar{\nabla}.\underline{q}$	rate of energy input by conduction
$-\hat{p}\, \bar{\nabla}.\hat{\underline{V}}$	reversible rate of energy increase by compression
$-\underline{\tau}:\bar{\nabla}\hat{\underline{V}}$	irreversible rate of energy increase by viscous dissipation
$-\hat{Q}_R$	rate of energy input by radiation

where $\hat{U}$ is the internal energy of the fluid per unit mass,

$\underline{q}$ is the conductive heat flux vector, and

$\hat{Q}_R$ is the rate of energy loss by radiation per unit volume.

The energy equation may be written in terms of the fluid temperature $\hat{T}$ and heat capacity at constant pressure $\hat{c}_p$ by using the fundamental thermodynamic relationships as follows:

$$\hat{U} = \hat{H} - \hat{p}\,\hat{v}$$

and

$$d\hat{H} = \hat{c}_p d\hat{T} + [\hat{v} - \hat{T}\,(\frac{\partial \hat{v}}{\partial \hat{T}})_{\hat{p}}]d\hat{p}$$

where $\hat{H}$ and $\hat{v}$ are the specific enthalpy and volume of the fluid respectively ($\hat{v} = 1/\hat{\rho}$). Combining the above two equations gives:

$$d\hat{U} = \hat{c}_p d\hat{T} - \hat{T}(\frac{\partial \hat{v}}{\partial \hat{T}})_{\hat{p}} d\hat{p} - \hat{p}\, d\hat{v}$$

The substantial derivative of $\hat{U}$ hence becomes:

$$\frac{D\hat{U}}{Dt} = \hat{c}_p \frac{D\hat{T}}{Dt} - \hat{T}\,(\frac{\partial \hat{v}}{\partial \hat{T}})_{\hat{p}} \frac{D\hat{p}}{Dt} - \hat{p}\,\frac{D\hat{v}}{Dt} \qquad (2.2\text{-}8)$$

With the aid of the continuity equation, $\frac{D\hat{\rho}}{Dt} = -\hat{\rho}(\overline{\nabla}.\underline{\hat{V}})$, the term $(D\hat{v}/Dt)$ may be transformed as follows:

$$\frac{D\hat{v}}{Dt} = \frac{D}{Dt}(\frac{1}{\hat{\rho}}) = -\frac{1}{\hat{\rho}^2}\frac{D\hat{\rho}}{Dt} = \frac{1}{\hat{\rho}}(\overline{\nabla}.\underline{\hat{V}})$$

Substituting this equation into Eq.(2.2-8) and the resulting equation into Eq.(2.2-7) yields:

$$\hat{\rho}\,\hat{c}_p \frac{D\hat{T}}{Dt} = -\overline{\nabla}\cdot\underline{q} + \hat{\rho}\hat{T}\left(\frac{\partial\hat{v}}{\partial\hat{T}}\right)_{\hat{p}} \frac{D\hat{p}}{Dt} - \underline{\underline{\tau}}:\overline{\nabla}\underline{\hat{V}} - \hat{Q}_R \qquad (2.2\text{-}9)$$

In order to proceed further, it is necessary to assume an appropriate value for the coefficient of thermal expansion of the fluid, $(\partial\hat{v}/\partial\hat{T})_{\hat{p}}$. The value used in the present work is that for an ideal gas*.

$$\left(\frac{\partial\hat{v}}{\partial\hat{T}}\right)_{\hat{p}} = M\frac{R}{\hat{p}}$$

with M the molecular weight of the gas and R the gas constant. The energy equation hence becomes:

$$\hat{\rho}\,\hat{c}_p \frac{D\hat{T}}{Dt} = -\overline{\nabla}\cdot\underline{q} + \frac{D\hat{p}}{Dt} - \underline{\underline{\tau}}:\overline{\nabla}\underline{\hat{V}} - \hat{Q}_R \qquad (2.2\text{-}10)$$

Fourier's law gives:

$$\underline{q} = -\hat{k}\,\overline{\nabla}\,\hat{T} \qquad (2.2\text{-}11)$$

where $\hat{k}$ is the thermal conductivity of the fluid.

The rate of energy loss by viscous dissipation is given by:

$$\underline{\underline{\tau}}:\overline{\nabla}\underline{\hat{V}} = -\hat{\mu}\,\Phi \qquad (2.2\text{-}12)$$

---

*As shown in appendix B the actual values for argon deviate from the ideal value by at most 28% over the temperature range of interest (up to 10,000°K), but for a polyatomic gas or mixture of gaseous components it might be necessary to use a different coefficient of thermal expansion.

where $\hat{\Phi}$ is known as the dissipation function and its form in cylindrical coordinates is (5):

$$\hat{\Phi} = 2[(\frac{\partial \hat{V}_r}{\partial \hat{r}})^2 + (\frac{\hat{V}_r}{\hat{r}})^2 + (\frac{\partial \hat{V}_z}{\partial \hat{z}})^2] - \frac{2}{3}(\bar{\nabla}.\underline{\hat{V}})[\frac{\partial \hat{V}_r}{\partial \hat{r}} + \frac{\hat{V}_r}{\hat{r}} + \frac{\partial \hat{V}_z}{\partial \hat{z}}]$$

$$+ [\hat{r} \frac{\partial}{\partial \hat{r}}(\frac{\hat{V}_\theta}{\hat{r}})]^2 + [\frac{\partial \hat{V}_z}{\partial \hat{r}} + \frac{\partial \hat{V}_r}{\partial \hat{z}}]^2 + [\frac{\partial \hat{V}_\theta}{\partial \hat{z}}]^2 \qquad (2.2\text{-}13)$$

Substituting Equations (2.2-11,12) into Equation (2.2-10) yields the final form of the steady-state energy equation:

$$\hat{\rho} c_p(\underline{\hat{V}}.\bar{\nabla})\hat{T} = \bar{\nabla}.(\hat{k}\,\bar{\nabla}\hat{T}) + (\underline{\hat{V}}.\bar{\nabla})\hat{p} + \hat{\mu}\,\hat{\Phi} - \hat{Q}_R \qquad (2.2\text{-}14)$$

For an axi-symmetric flow in cylindrical polar coordinates, the energy equation takes the form:

$$\hat{\rho} c_p(\hat{V}_r \frac{\partial \hat{T}}{\partial \hat{r}} + \hat{V}_z \frac{\partial \hat{T}}{\partial \hat{z}}) = \frac{1}{\hat{r}} \frac{\partial}{\partial \hat{r}}(\hat{r}\hat{k} \frac{\partial \hat{T}}{\partial \hat{r}}) + \frac{\partial}{\partial \hat{z}}(\hat{k} \frac{\partial \hat{T}}{\partial \hat{z}})$$

$$+ (\hat{V}_r \frac{\partial \hat{p}}{\partial \hat{r}} + \hat{V}_z \frac{\partial \hat{p}}{\partial \hat{z}}) + \hat{\mu}\,\hat{\Phi} - \hat{Q}_R \qquad (2.2\text{-}15)$$

Krey and Morris (26) have reported determinations of the radiation properties of the gases commonly used in plasma applications, including argon, nitrogen and oxygen. For temperatures in the range of interest of the present work, it was found that all the gases could be regarded as "optically thin": i.e. there is negligible absorption of thermal radiation from an element of the gas by surrounding elements. Assuming that the fluid is optically thin, all the energy radiated by the gas is absorbed by the walls; the heat lost by radiation may then be expressed as (51):

$$\hat{Q}_R = 4\varkappa\sigma(n^2\hat{T}^4 - n^2\hat{T}_w^4) \qquad (2.2\text{-}16)$$

where $\varkappa$ is the absorption coefficient, σ is the Boltzmann constant and n is the refractive index of the gas.

(d) Closure - We have now introduced all the differential equations derived from the conservation laws, which represent the foundation upon which the present prediction procedure is based. In the following section, these equations are presented in forms made dimensionless with reference to the inlet conditions.

2.2.2 Dimensionless Equations

The quantities in the above equations can be made dimensionless with reference to the upstream diameter D_o, the mean velocity V_o and the inlet fluid properties μ_o, ρ_o, c_{po}, k_o, to give:

$$r = \frac{\hat{r}}{D_o} \qquad z = \frac{\hat{z}}{D_o}$$

$$\rho = \frac{\hat{\rho}}{\rho_o} \qquad \mu = \frac{\hat{\mu}}{\mu_o} \qquad c_p = \frac{\hat{c}_p}{c_{p_o}} \qquad k = \frac{\hat{k}}{k_o}$$

$$V_r = \frac{\hat{V}_r}{V_o} \qquad V_\theta = \frac{\hat{V}_\theta}{V_o} \qquad V_z = \frac{\hat{V}_z}{V_o} \qquad p = \frac{\hat{p}}{\rho_o V_o^2}$$

$$T = \frac{\hat{T} - T_w}{T_o - T_w} \qquad Q_R = \frac{\hat{Q}_R}{\rho_o c_{p_o} V_o (T_o - T_w)/D_o}$$

.....(2.2-17)

here, T_o and T_w denote the fluid temperatures at the inlet and the wall respectively. The equations (2.2-2,4,5,6,15) become:

$$\frac{1}{r}\frac{\partial}{\partial r}(\rho r\ V_r) + \frac{\partial}{\partial z}(\rho V_z) = 0 \qquad (2.2\text{-}18)$$

$$\rho(V_r\frac{\partial V_r}{\partial r} - \frac{V_\theta^2}{r} + V_z\frac{\partial V_r}{\partial z}) = -\frac{\partial p}{\partial r} + \frac{1}{Re}\left\{\frac{1}{r}\frac{\partial}{\partial r}[r\,\mu(2\frac{\partial V_r}{\partial r} - \frac{2}{3}\,\overline{\nabla}.\underline{V})]\right.$$

$$\left. - \frac{\mu}{r}[2\frac{V_r}{r} - \frac{2}{3}\,\overline{\nabla}.\underline{V}] + \frac{\partial}{\partial z}[\mu(\frac{\partial V_z}{\partial r} + \frac{\partial V_r}{\partial z})]\right\} \qquad (2.2\text{-}19)$$

$$\rho(V_r\frac{\partial V_\theta}{\partial r} + \frac{V_r V_\theta}{r} + V_z\frac{\partial V_\theta}{\partial z}) = \frac{1}{Re}\left\{\frac{1}{r^2}\frac{\partial}{\partial r}[\mu\ r^3\frac{\partial}{\partial r}(\frac{V_\theta}{r})]\right.$$

$$\left. + \frac{\partial}{\partial z}(\mu\frac{\partial V_\theta}{\partial z})\right\} \qquad (2.2\text{-}20)$$

$$\rho(V_r\frac{\partial V_z}{\partial r} + V_z\frac{\partial V_z}{\partial z}) = -\frac{\partial p}{\partial z} + \frac{1}{Re}\left\{\frac{1}{r}\frac{\partial}{\partial r}[r\ \mu(\frac{\partial V_z}{\partial r} + \frac{\partial V_r}{\partial z})]\right.$$

$$\left. + \frac{\partial}{\partial z}[\mu\,(2\frac{\partial V_z}{\partial z} - \frac{2}{3}\,\overline{\nabla}.\underline{V})]\right\} \qquad (2.2\text{-}21)a$$

$$\rho c_p\left(V_r\frac{\partial T}{\partial r} + V_z\frac{\partial T}{\partial z}\right) = \frac{1}{RePr}\left[\frac{1}{r}\frac{\partial}{\partial r}\left(r\,k\frac{\partial T}{\partial r}\right) + \frac{\partial}{\partial z}\left(k\frac{\partial T}{\partial z}\right)\right]$$

$$+ \frac{Br}{Pr}\left[V_r\frac{\partial p}{\partial r} + V_z\frac{\partial p}{\partial z}\right] + \frac{Br}{RePr}\,\mu\phi + Q_R \qquad (2.2\text{-}22)$$

where Re is the Reynolds number, Pr is the Prandtl number and Br is the Brinkman number, defined by:

$$Re = \rho_o D_o V_o/\mu_o \qquad (2.2\text{-}23)$$

$$Pr = \mu_o c_{po}/k_o \qquad (2.2\text{-}24)$$

$$Br = \mu_o V_o^{\,2}/k_o(T_o - T_w) \qquad (2.2\text{-}25)$$

and

$$\bar{\nabla}.\underline{V} = \frac{1}{r}\frac{\partial}{\partial r}(rV_r) + \frac{\partial V_z}{\partial z} \qquad (2.2\text{-}26)$$

$$\phi = 2\left[\left(\frac{\partial V_r}{\partial r}\right)^2 + \left(\frac{V_r}{r}\right)^2 + \left(\frac{\partial V_z}{\partial z}\right)^2\right] - \frac{2}{3}(\bar{\nabla}.\underline{V})\left[\frac{\partial V_r}{\partial r} + \frac{V_r}{r} + \frac{\partial V_z}{\partial z}\right]$$

$$+ \left[r\frac{\partial}{\partial r}\left(\frac{V_\theta}{r}\right)\right]^2 + \left[\frac{\partial V_z}{\partial r} + \frac{\partial V_r}{\partial z}\right]^2 + \left[\frac{\partial V_\theta}{\partial z}\right]^2 \qquad (2.2\text{-}27)$$

2.2.3 The Introduction of Vorticity, ω, and Stream Function, ψ

Although the differential equations presented in the previous section contain all the background for the problem, they are not in every respect convenient to work with, for they contain differentials of the pressure as well as those of the velocity components, which are all unknown. This defect can be remedied if most of the terms involving velocity are expressed in terms of the stream function, and the vorticity is introduced as a main dependent variable to remove the pressure from the equations by combining the two equations (2.2-19) and (2.2-21) into one.

The scalar dimensionless stream function ψ and vorticity w are defined by:

$$\rho V_z = \frac{1}{r}\frac{\partial\psi}{\partial r} \qquad (2.2\text{-}28)$$

$$\rho V_r = -\frac{1}{r}\frac{\partial\psi}{\partial z} \qquad (2.2\text{-}29)$$

$$w = \frac{\partial V_r}{\partial z} - \frac{\partial V_z}{\partial r} \qquad (2.2\text{-}30)$$

These definitions lead to:

$$\frac{\partial}{\partial z}\left[\frac{1}{\rho r}\frac{\partial\psi}{\partial z}\right] + \frac{\partial}{\partial r}\left[\frac{1}{\rho r}\frac{\partial\psi}{\partial r}\right] + w = 0 \qquad (2.2\text{-}31)$$

Upon the introduction of the stream function, equation (2.2.20) becomes

$$\left\{\frac{\partial}{\partial z}\left[r\, V_\theta\frac{\partial\psi}{\partial r}\right] - \frac{\partial}{\partial r}\left[r\, V_\theta\frac{\partial\psi}{\partial z}\right]\right\} - \frac{1}{Re}\left\{\frac{\partial}{\partial z}\left[r^3\mu\frac{\partial}{\partial z}\left(\frac{V_\theta}{r}\right)\right]\right.$$

$$\left. + \frac{\partial}{\partial r}\left[r^3\mu\frac{\partial}{\partial r}\left(\frac{V_\theta}{r}\right)\right]\right\} = 0 \qquad (2.2\text{-}32)$$

The equation for vorticity is derived from the two equations (2.2-19) and (2.2-21) by differentiating the first with respect to z and the second with respect to r, and then subtracting one from the other. In this way, the pressure is removed entirely and, after the rearrangement, the equations take the form:

$$r^2\left\{\frac{\partial}{\partial z}\left[\frac{w}{r}\frac{\partial\psi}{\partial r}\right] - \frac{\partial}{\partial r}\left[\frac{w}{r}\frac{\partial\psi}{\partial z}\right]\right\} - \frac{1}{Re}\left\{\frac{\partial}{\partial z}\left[r^3\frac{\partial}{\partial z}\left(\mu\frac{w}{r}\right)\right] + \frac{\partial}{\partial r}\left[r^3\frac{\partial}{\partial r}\left(\mu\frac{w}{r}\right)\right]\right\}$$

$$- r\frac{\partial}{\partial z}(\rho V_\theta^2) + r^2 S_w = 0 \qquad (2.2\text{-}33)$$

where

$$S_w = \frac{\partial}{\partial z}\left[\frac{\rho}{r}V_r^2 - V_z\frac{\partial}{\partial r}(\rho V_z) + V_r\frac{\partial}{\partial z}(\rho V_z)\right]$$

$$+ \frac{\partial}{\partial r}\left[-\frac{\rho}{r}V_r V_z - V_z\frac{\partial}{\partial r}(\rho V_r) + V_r\frac{\partial}{\partial z}(\rho V_r)\right]$$

$$- \frac{2}{Re}\left\{\frac{\partial^2}{\partial z\partial r}\left[\mu\left(\frac{\partial V_r}{\partial r} - \frac{\partial V_z}{\partial z}\right)\right] + \frac{\partial^2}{\partial z^2}\left[\mu\frac{\partial V_z}{\partial r}\right]\right.$$

$$\left. - \frac{\partial}{\partial r}\left[r\frac{\partial}{\partial r}\left(\frac{\mu}{r}\frac{\partial V_r}{\partial z}\right) + 2\frac{\mu}{r}\frac{\partial V_r}{\partial z}\right] + \frac{1}{r}\frac{\partial}{\partial z}\left[\mu\left(\frac{\partial V_r}{\partial r} - \frac{V_r}{r}\right)\right]\right\}$$

$$\ldots\ldots(2.2\text{-}34)$$

The energy equation (2.2-22) becomes:

$$c_p\left\{\frac{\partial}{\partial z}\left[T\frac{\partial\psi}{\partial r}\right] - \frac{\partial}{\partial r}\left[T\frac{\partial\psi}{\partial z}\right]\right\} - \frac{1}{RePr}\left\{\frac{\partial}{\partial z}\left[rk\frac{\partial T}{\partial z}\right] + \frac{\partial}{\partial r}\left[rk\frac{\partial T}{\partial r}\right]\right\} =$$

$$\frac{Br}{RePr}\Phi + rQ_R \qquad (2.2\text{-}35)$$

where $\Phi = -\text{Re}\,\rho r[V_r(V_r\frac{\partial V_r}{\partial r} - \frac{V_\theta^2}{r} + V_z\frac{\partial V_r}{\partial z}) + V_z(V_r\frac{\partial V_z}{\partial r} + V_z\frac{\partial V_z}{\partial z})]$

$$+ \mu r\,[\{r\frac{\partial}{\partial r}(\frac{V_\theta}{r})\}^2 + \{\frac{\partial V_\theta}{\partial z}\}]$$

$$+ \frac{\partial}{\partial r}[r\,\mu\{V_r(2\frac{\partial V_r}{\partial r} - \frac{2}{3}\bar{\nabla}.\underline{V}) + V_z(\frac{\partial V_z}{\partial r} + \frac{\partial V_r}{\partial z})\}]$$

$$+ \frac{\partial}{\partial z}[r\,\mu\{V_r(\frac{\partial V_z}{\partial r} + \frac{\partial V_r}{\partial z}) + V_z(2\frac{\partial V_z}{\partial z} - \frac{2}{3}\bar{\nabla}.\underline{V})\}]$$

.....(2.2-36)

All these four equations (2.2-31,32,33,35) have a similar structure and are found to fit a general equation of the form:

$$a\{\frac{\partial}{\partial z}[\varphi\,\frac{\partial\psi}{\partial r}] - \frac{\partial}{\partial r}[\varphi\,\frac{\partial\psi}{\partial z}]\} - \frac{\partial}{\partial z}[b\,\frac{\partial}{\partial z}(c\varphi)] - \frac{\partial}{\partial r}[b\,\frac{\partial}{\partial r}(c\varphi)] + d = 0$$

.....(2.2-37)

if φ is taken as the dependent variable, and a,b,c,d represent various functions. The forms of these functions are shown in Table 1. This table shows clearly the similarities and differences between the differential equations. It is their similarity of form which renders all the equations soluble when a solution procedure has been found for one of them. The following section presents a numerical solution for the general equations (2.2-37).

φ	a	b	c	d
ψ	0	$1/\rho r$	1	$-w$
rV_θ	1	$\frac{r^3\mu}{Re}$	$\frac{1}{r^2}$	0
$\frac{w}{r}$	r^2	$\frac{r^3}{Re}$	μ	$-r\,\frac{\partial}{\partial z}(\rho V_\theta^2) + r^2 S_w$
T	c_p	$\frac{rk}{RePr}$	1	$-(\frac{Br}{RePr}\,\Phi + rQ_R)$

TABLE 1

The Functions a,b,c and d

2.3 NUMERICAL APPROACH

2.3.1 Introduction

The partial differential equations presented in the previous section are highly non-linear and coupled in various ways. Hence, they are too complicated for an analytical treatment, even under the most simplified cases, such as isothermal creeping flow. An alternative approach lies in numerical simulation using finite-difference methods. The solution procedure is as follows:

(i) Attention is confined to a finite number of points distributed throughout the flow field as the nodes of a two-dimensional grid at which values of the variables are calculated. The grid is so arranged that the boundaries of the flow field coincide with the outermost rows or columns. The nodes are chosen to be numerous in the regions where the gradients of the variables are steep, and more widely spread where gradients are small.

(ii) The partial differential equations are replaced by a set of simultaneous, algebraic finite-difference equations which relate the values of the variables at each node to the values which prevail at neighbouring nodes.

(iii) The algebraic equations are recast into a form suitable for solution by an iterative, successive-substitution technique. The Gauss-Seidel technique is selected for this purpose, for it is known to yield a rapid convergence (17,34,42). The solution will yield the distributions of the dependent variables w, V_θ, ψ, T throughout the flow, and consequently, the distributions of velocity and pressure may be obtained.

There are two common ways of deriving finite-difference equations from differential equations:

(1) using Taylor series expansions

(2) by integration over finite areas, together with assumptions about the distributions of the variables between the nodes of the grid.

The first is more popular, and has been used, for example, by Macagno and Hung (29) to predict the isothermal, laminar flow of a Newtonian fluid with uniform properties through an axi-symmetric conduit expansion. The second method is developed by Gosman and co-workers (17) and is chosen for the present work because it ensures that the conservation laws will be obeyed over arbitrarily large or small portions of the field. It also makes use of the upwind-difference techniques, developed by Courant et al (10), in place of the central-differences. A number of workers (4,6,10) have shown that the upwind difference form improves the stability of the solution procedure greatly.

The following sections present all the successive steps which lead to the replacement of the differential equations by a set of simultaneous algebraic equations and their successive solution procedure.

2.3.2 Derivation of the Finite-Difference Form of the General Differential Equation

Fig. 2-1 displays a part of the grid network, showing a typical node P with eight surrounding nodes N,S,W,E,NW,NE, SW and SE. The integration of the differential equations (2.2-37) is performed over the area enclosed by the dotted lines which lie midway between the neighbouring grid lines, as follows:

$$\int_{r_s}^{r_n}\int_{z_w}^{z_e} a\left\{\frac{\partial}{\partial z}\left(\varphi\frac{\partial\psi}{\partial r}\right) - \frac{\partial}{\partial r}\left(\varphi\frac{\partial\psi}{\partial z}\right)\right\} dz dr -$$

$$\int_{r_s}^{r_n}\int_{z_w}^{z_e} \left\{\frac{\partial}{\partial z}\left(b\frac{\partial}{\partial z}(c\varphi)\right) + \frac{\partial}{\partial r}\left(b\frac{\partial}{\partial r}(c\varphi)\right)\right\} dz dr + \int_{r_s}^{r_n}\int_{z_w}^{z_e} d\, dz dr = 0$$

.....(2.3-1)

With the assumption of a suitable average value for a, which may be the value at the centre of the rectangle P, the first integration can be performed to give:

$$a_P\left\{\int_{r_s}^{r_n}\left[\varphi_e\left(\frac{\partial\psi}{\partial r}\right)_e - \varphi_w\left(\frac{\partial\psi}{\partial r}\right)_w\right] dr - \int_{z_w}^{z_e}\left[\varphi_n\left(\frac{\partial\psi}{\partial z}\right)_n - \varphi_s\left(\frac{\partial\psi}{\partial z}\right)_s\right] dz\right\}$$

convection term

$$-\int_{r_s}^{r_n}\left[b_e\left(\frac{\partial}{\partial z}(c\varphi)\right)_e - b_w\left(\frac{\partial}{\partial z}(c\varphi)\right)_w\right]dr - \int_{z_w}^{z_e}\left[b_n\left(\frac{\partial}{\partial r}(c\varphi)\right)_n - b_s\left(\frac{\partial}{\partial r}(c\varphi)\right)_s\right]dz$$

diffusion term

$$+\int_{r_s}^{r_n}\int_{z_w}^{z_e} d\, dz dr = 0 \qquad (2.3\text{-}2)$$

source term

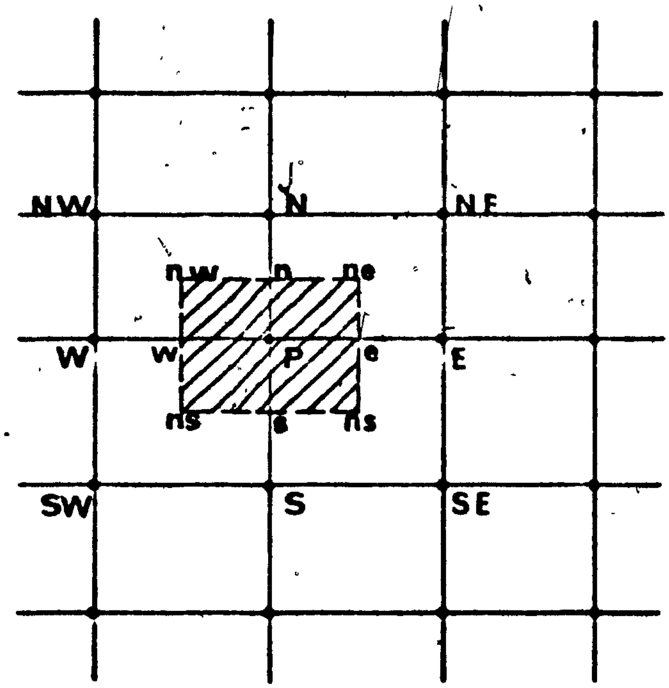

Fig.2.2 ILLUSTRATION OF A PORTION OF THE GRID

In order to proceed further, additional assumptions about the distributions of the variables between the nodes of the grid are required. The assumptions will differ according to the nature of the terms, so that each group must be considered separately.

(a) Convection term: consider the first integral of the four in the convection term, which we denote by the symbol I_c:

$$I_c \equiv a_p \int_{r_s}^{r_n} \varphi_e \left(\frac{\partial\psi}{\partial r}\right)_e dr \qquad (2.3\text{-}3)$$

If both φ and ψ are well-behaved functions, then there exists an average value of φ_e, say $\bar{\varphi}_e$, such that:

$$\bar{\varphi}_e \equiv \frac{\int_{r_s}^{r_n} \varphi_e \left(\frac{\partial\psi}{\partial r}\right)_e dr}{\int_{r_s}^{r_n} \left(\frac{\partial\psi}{\partial r}\right)_e dr} \approx \frac{I_c/a_p}{\psi_{ne} - \psi_{se}} \qquad (2.3\text{-}4)$$

therefore: $$I_c = a_p \bar{\varphi}_e (\psi_{ne} - \psi_{se}) \qquad (2.3\text{-}5)$$

To express $\bar{\varphi}_e$, ψ_{ne} and ψ_{se} in terms of values of the variables at the nodes of the grid, three assumptions are made:

(i) Assume that φ is uniform within each rectangle, and has the value which prevails at the centre of the rectangle.

(ii) $\bar{\varphi}_e$ takes on the φ-value possessed by the fluid upstream of the e-face of the rectangle. This is the implication of the "upwind differences". It is important to note that the direction of the flow across the e-face is connected to $(\partial\psi/\partial r)_e$ by eq.(2.2-28), and hence to $(\psi_{ne} - \psi_{se})$; in particular, if the latter quantity is positive, the direction of flow is from P to E, and it follows that $\bar{\varphi}_e$ must be equal to φ_P. If, however, $(\psi_{ne} - \psi_{se})$ is negative, the flow is from E to P, and $\bar{\varphi}_e$ must then be equal to φ_E. The quantity I_c in eq.(2.3-5) may now be expressed by

$$I_c \approx a_P[\varphi_E\left\{\frac{(\psi_{ne} - \psi_{se}) - |\psi_{ne} - \psi_{se}|}{2}\right\} + \varphi_P\left\{\frac{(\psi_{ne} - \psi_{se}) + |\psi_{ne} - \psi_{se}|}{2}\right\}] \qquad (2.3\text{-}6)$$

This form ensures that one of the two terms in ψ will be zero, and the term which remains will be that which represents the contribution from the node upstream of the e-face.

(iii) The value of the stream function at a particular corner of the rectangle is assumed to be equal to the average of the values on the four neighbouring nodes:

$$\psi_{se} = \frac{1}{4}(\psi_{SE} + \psi_E + \psi_P + \psi_S) \qquad (2.3\text{-}7)$$

The other three integrals in the convection term may be treated in a similar way. The convection term in eq.(2.3-2) can now be obtained by summing all four integrals. After rearrangement, it takes the form:

$$I_{cond} = (A_E^+\varphi_P - A_E^-\varphi_E) + (A_W^+\varphi_P - A_W^-\varphi_W) + (A_N^+\varphi_P - A_N^-\varphi_N) + (A_S^+\varphi_P - A_S^-\varphi_S) \qquad (2.3\text{-}8)$$

where

$$A_E^+ = \frac{a_P}{8}[(\psi_{NE} - \psi_{SE} + \psi_N - \psi_S) + |\psi_{NE} - \psi_{SE} + \psi_N - \psi_S|]$$

$$A_E^- = -\frac{a_P}{8}[(\psi_{NE} - \psi_{SE} + \psi_N - \psi_S) - |\psi_{NE} - \psi_{SE} + \psi_N - \psi_S|]$$

$$A_W^+ = -\frac{a_P}{8}[(\psi_{NW} - \psi_{SW} + \psi_N - \psi_S) - |\psi_{NW} - \psi_{SW} + \psi_N - \psi_S|]$$

$$A_W^- = \frac{a_P}{8}[(\psi_{NW} - \psi_{SW} + \psi_N - \psi_S) + |\psi_{NW} - \psi_{SW} + \psi_N - \psi_S|]$$

$$A_N^+ = -\frac{a_P}{8}[(\psi_{NE} - \psi_{NW} + \psi_E - \psi_W) - |\psi_{NE} - \psi_{NW} + \psi_E - \psi_W|]$$

$$A_N^- = \frac{a_P}{8}[(\psi_{NE} - \psi_{NW} + \psi_E - \psi_W) + |\psi_{NE} - \psi_{NW} + \psi_E - \psi_W|]$$

$$A_S^+ = \frac{a_P}{8}[(\psi_{SE} - \psi_{SW} + \psi_E - \psi_W) + |\psi_{SE} - \psi_{SW} + \psi_E - \psi_W|]$$

$$A_S^- = -\frac{a_P}{8}[(\psi_{SE} - \psi_{SW} + \psi_E - \psi_W) - |\psi_{SE} - \psi_{SW} + \psi_E - \psi_W|]$$

.....(2.3-9)

It may be observed that the A's can never become negative, although they may fall to zero. This is one of the features which enables a convergent solution procedure to be obtained. In each pair, such as A_E^+ and A_E^-, there is always one positive term while the other is identically zero.

(b) Diffusion term: consider the first integral in the diffusion term which we denote by I_d:

$$I_d \equiv \int_{r_s}^{r_n} b_e\left(\frac{\partial}{\partial z}(c\varphi)\right)dr \qquad (2.3\text{-}10)$$

Assuming that: $b_e \approx \frac{1}{2}(b_E + b_P)$ (2.3-11)

and $$\frac{\partial(c\varphi)}{\partial z} \approx \frac{c_E\varphi_E - c_P\varphi_P}{z_E - z_P} \qquad (2.3\text{-}12)$$

the above integral becomes:

$$I_d = \frac{b_E + b_P}{2} \cdot \frac{c_E\varphi_E - c_P\varphi_P}{z_E - z_P} \cdot \frac{r_N - r_S}{2} \qquad (2.3\text{-}13)$$

The other integrals may be evaluated in a similar way, and the sum of all four integrals will yield the diffusion term, which is:

$$I_{diff} = B_E(c_E\varphi_E - c_P\varphi_P) + B_W(c_W\varphi_W - c_P\varphi_P)$$
$$+ B_N(c_N\varphi_N - c_P\varphi_P) + B_S(c_S\varphi_S - c_P\varphi_P) \qquad (2.3\text{-}14)$$

where
$$B_E = \frac{b_E + b_P}{4} \cdot \frac{r_N - r_S}{z_E - z_P}$$
$$B_W = \frac{b_W + b_P}{4} \cdot \frac{r_N - r_S}{z_P - z_W}$$
$$B_N = \frac{b_N + b_P}{4} \cdot \frac{z_E - z_W}{r_N - r_P}$$
$$B_S = \frac{b_S + b_P}{4} \cdot \frac{z_E - z_W}{r_P - r_S}$$

(c) Source term: the final integral to be evaluated is:

$$I_{sor} \equiv \int_{r_s}^{r_n} \int_{z_w}^{z_e} d \, dzdr \qquad (2.3\text{-}16)$$

With the assumption that the quantity d is uniform over the area of integration and takes on the value at point P, the above equation may be integrated to yield:

$$I_{sor} \approx d_P \cdot \frac{z_E - z_W}{2} \cdot \frac{r_N - r_S}{2} \qquad (2.3\text{-}17)$$

The integration of the general differential equation is now complete. By summing the terms using eqs.(2.3-8, 14, 17) we have:

$$[A_E^+\varphi_P - A_E^-\varphi_E) + (A_W^+\varphi_P - A_W^-\varphi_W) + (A_N^+\varphi_P - A_W^-\varphi_N)$$
$$+ (A_S^+\varphi_P - A_S^-\varphi_S)] - [B_E(c_E\varphi_E - c_P\varphi_P) + B_W(c_W\varphi_W - c_P\varphi_P)$$
$$+ B_N(c_N\varphi_N - c_P\varphi_P) + B_S(c_S\varphi_S - c_P\varphi_P)] + d_P\frac{(z_E - z_W)(r_N - r_S)}{4}$$
$$= 0$$

Rearrangement yields:

$$\varphi_P = C_E\varphi_E + C_W\varphi_W + C_N\varphi_N + C_S\varphi_S + D \qquad (2.3\text{-}18)$$

where

$$\begin{aligned} C_E &= (B_E c_E + A_E^-)/\Sigma_{AB} \\ C_W &= (B_W c_W + A_W^-)/\Sigma_{AB} \\ C_N &= (B_N c_N + A_N^-)/\Sigma_{AB} \\ C_S &= (B_S c_S + A_S^-)/\Sigma_{AB} \\ D &= -d_P \frac{(z_E - z_W)(r_N - r_S)}{4}/\Sigma_{AB} \end{aligned} \qquad (2.3\text{-}19)$$

and

$$\Sigma_{AB} = (B_E + B_W + B_N + B_S)\,c_P + A_E^+ + A_W^+ + A_N^+ + A_S^+$$

The general differential equation (2.2-37) has now been replaced by the algebraic equation (2.3-18), a successive substitution formula which forms the core of the solution procedure. However, this formula can now only be applied at the interior nodes of the grid, for it was derived from the general differential equation which describes the flow only within the boundaries. In order to complete the problem, additional substitution formulae are required for the nodes which lie on the boundaries, and this will be presented in section (2.4).

2.3.3 Solution of the Set of Algebraic Equations

Successive-substitution techniques are employed to solve the set of algebraic equations for ψ, w/r, rV_θ and T, having the general form represented by eq.(2.3-18). Initial guesses for the values of the variables are substituted into the successive-substitution formulae (2.3-18), and new values are computed. These values are used to generate guesses for the next iteration, and the process is completed until no further changes result in the dependent variables. Relaxation factors, a_R, are introduced to stabilize and improve the speed of convergence of the computations as follows:

$$\varphi_P^m = \varphi_P^{m-1} + a_R\,[\varphi_P{}^m - \varphi_P{}^{m-1}] \qquad (2.3\text{-}20)$$

where the subscript m denotes the mth value calculated and φ denotes the value φ calculated by using eq.(2.3-18).

The iteration will be continued until the following condition is satisfied for all the dependent variables:

$$|\varphi_P^m - \varphi_P^{m-1}|/\varphi_O \le \lambda \qquad (2.3\text{-}21)$$

In which λ is the convergence criterion, and φ_O represents the reference values for the dependent variables.

2.4 ADDITIONAL ALGEBRAIC EQUATIONS

This section completes the mathematical specification of the problem by presenting the additional algebraic equations which embody the boundary conditions of the problem, and which link the various dependent variables together by means of the thermodynamic and transport properties of the fluid.

2.4.1 Boundary Conditions

Presented below is a set of boundary conditions that are encountered in practical circumstances, used for the present investigation. Other conditions are possible.

(a) At the inlet: In most cases, the condition of the entering fluid is known, so that the distributions of temperature, velocity, etc. may be specified. From these, the distributions of stream function and vorticity may be desired. The present predictions are obtained for a laminar flow entering the field of calculation, so that the velocity distribution at the inlet takes a parabolic form as follows:

$$\hat{V}_r = 0 \qquad (2.4\text{-}1)$$

and

$$\hat{V}_z = 2V_o[1 - (\frac{\hat{r}}{R_o})^2] \qquad (2.4\text{-}2)$$

where R_o is the radius of the inlet, $D_o/2$. Hence, the dimensionless velocity components are:

$$V_r = 0 \qquad (2.4\text{-}3)$$

$$V_z = 2(1 - 4r^2) \qquad (2.4\text{-}4)$$

Consequently, the dimensionless vorticity is given by:

$$\left(\frac{w}{r}\right) = 16 \qquad (2.4\text{-}5)$$

The temperature of the entering fluid is assumed to be uniform, except for a thin layer adjacent to the wall. From the definition (2.2-17), the dimensionless temperature takes the form:

$$T = 1 \qquad (2.4\text{-}6)$$

With this assumption, the fluid density is constant at the inlet, and the stream function can then be derived from the velocity distribution (2.4-3,4) to yield:

$$\psi = r^2(1 - 2r^2) + \psi_o \qquad (2.4\text{-}7)$$

where ψ_o denotes the value of ψ at the axis-of-symmetry (r=0).

(b) <u>At the walls</u>: The walls are characterized by a no-slip condition:

$$V_z = 0 \qquad (2.4\text{-}8)$$

and by the condition appropriate to an impermeable boundary:

$$V_r = 0 \tag{2.4-9}$$

Hence the value of the stream function is constant over the walls.

The walls of the reactor are kept at constant temperature by being water-cooled. The dimensionless temperature then takes the value zero as defined in eq.(2.2-17).

The vorticity at a wall is not often known at the start, so that the boundary condition for vorticity must be deduced from the other information, which is the no-slip condition at the wall. Gosman et al (17) derived a boundary condition for vorticity at the wall by assuming that gradients of vorticity in the direction parallel to the wall are much smaller than those in the normal direction, and that vorticity and density vary linearly near the wall. With these assumptions, they showed that:

$$\left(\frac{w}{r}\right)_P = g_1 + g_2 \left(\frac{w}{r}\right)_{NP} \tag{2.4-10}$$

where P indicates the value at a node on the wall and NP indicates the adjacent interior node, as shown in Fig.2-3. The functions g_1 and g_2 are:

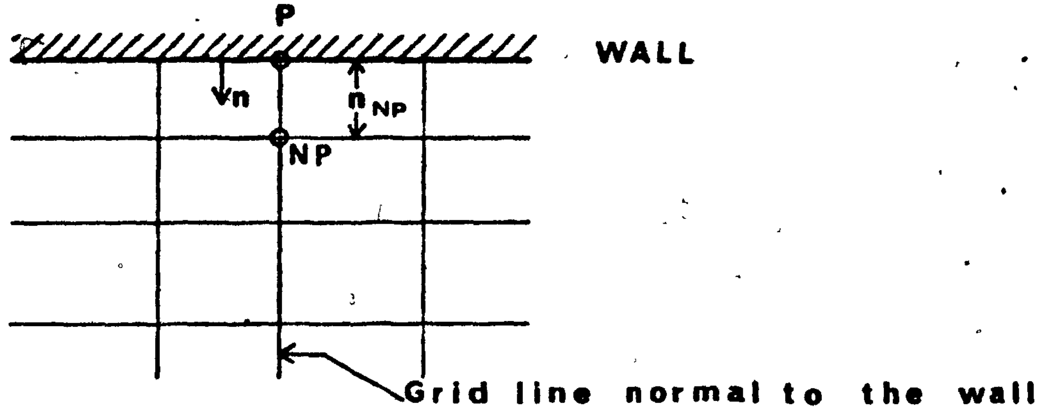

Fig. 2.3 NOMENCLATURE FOR THE SUBSTITUTION FORMULAE FOR THE WALLS

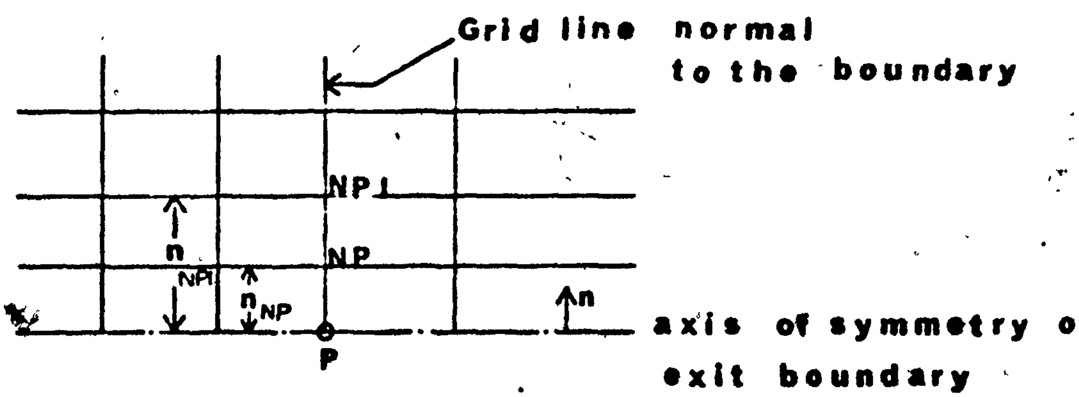

Fig. 2.4 NOMENCLATURE FOR THE SUBSTITUTION FORMULAE FOR THE AXIS-OF-SYMMETRY AND FOR THE EXIT BOUNDARY

$$g_1 = \frac{(\psi_P - \psi_{NP})}{n_{NP}^2 R_w [\rho_P(\frac{R_w}{3} - \frac{5}{24} n_{NP}) + \Delta\rho(\frac{5}{24} R_w - \frac{3}{20} n_{NP})]}$$

$$g_2 = -\frac{(R_w - n_{NP})[\rho_P(\frac{R_w}{6} - \frac{n_{NP}}{8}) + \Delta\rho(\frac{R_w}{8} - \frac{n_{NP}}{10})]}{R_w[\rho_P(\frac{R_w}{3} - \frac{5}{24} n_{NP}) + \Delta\rho(\frac{5}{24} R_w - \frac{3}{10} n_{NP})]} \qquad (2.4\text{-}11)$$

for a wall parallel to the axis-of-symmetry, and reduce to:

$$g_1 = \frac{\psi_P - \psi_{NP}}{r^2 n_{NP}^2(\frac{\rho_P}{3} + \frac{5}{24}\Delta\rho)}$$

$$g_2 = -\frac{\frac{\rho_P}{6} + \frac{\Delta\rho}{8}}{\frac{\rho_P}{3} + \frac{5\Delta\rho}{24}} \qquad (2.4\text{-}12)$$

for a wall normal to the axis-of-symmetry. In equation (2.4-11), R_w denotes the distance of the wall from the axis-of-symmetry, n_{NP} is the distance along the normal between two points P and NP, and $\Delta\rho = \rho_{NP} - \rho_P$.

(c) <u>On the axis-of-symmetry</u>: Along the axis-of-symmetry of the flow, the stream function must have a constant value and, for convenience, this was taken as zero. This condition expresses the fact that the radial component of velocity must be zero at the axis, following the law of mass continuity.

Moreover, since the axial velocity is finite, the definition of stream function (2.2-28) implies that the gradient of ψ with respect to r must tend to zero at the same rate as r near the axis. It follows that the $\psi \sim r$ distribution is parabolic in the immediate vicinity of the axis. From the symmetry requirements, it must take the form:

$$\psi - \psi_o \approx Ar^2 + Br^4 \qquad (2.4\text{-}13)$$

where A and B are constants, for fixed z. This equation, together with the definition of vorticity (2.2-30) imply that the vorticity at the axis must be zero. On the other hand, w/r is finite, and takes the form:

$$\left(\frac{w}{r}\right)_P = -\frac{8B}{\rho_P} \qquad (2.4\text{-}14)$$

Assuming that equation (2.4-13) holds at the interior nodes which are once or twice removed from a node P on the axis of symmetry, denoted by NP and NPI respectively, as shown in Fig. 2-4, the value of the constant B can be determined and eq.(2.4-14) becomes:

$$\left(\frac{w}{r}\right)_P = \frac{8}{\rho_P}\left[\frac{(\psi_{NPI} - \psi_P)/r_{NPI}^2 - (\psi_{NP} - \psi_P)/r_{NP}^2}{r_{NP}^2 - r_{NPI}^2}\right] \qquad .....(2.4\text{-}15)$$

For reasons of continuity, the gradients with respect to r of temperature and of the axial component of velocity, i.e. $\partial T/\partial r$ and $\partial V_z/\partial r$, must be zero at the axis. A three-point quadratic approximation for the first derivative yields:

$$V_{zP} = \frac{r_{NPI}^2}{r_{NPI}^2 - r_{NP}^2} V_{z,NP} - \frac{r_{NP}^2}{r_{NPI}^2 - r_{NP}^2} V_{z,NPI} \quad (2.4\text{-}16)$$

$$T_P = \frac{r_{NPI}^2}{r_{NPI}^2 - r_{NP}^2} T_{NP} - \frac{r_{NP}^2}{r_{NPI}^2 - r_{NP}^2} T_{NPI} \quad (2.4\text{-}17)$$

(d) <u>At the exit</u>: The distributions of the variables at the exit are not normally known. Fortunately, it is recognized that the exact nature of the downstream conditions has little effect on the solutions of the equations (17,31). In this work, a special sort of gradient condition is applied at the exit: the streamlines are taken as parallel to the duct walls, and all fluid properties are taken as uniform along streamlines. This implies that the radial velocity and the gradient of the dependent variables normal to the exit boundary are zero. A three-point quadratic approximation enables the evaluation of the exit value, φ_P, from information at two nearby nodes along the normal as follows

$$\varphi_P = \left[\frac{n_{NPI}^2}{n_{NPI}^2 - n_{NP}^2}\right] \varphi_{NP} - \left[\frac{n_{NP}^2}{n_{NPI}^2 - n_{NP}^2}\right] \varphi_{NPI} \quad (2.4\text{-}18)$$

where subscripts NP and NPI refer to the two adjacent points, as shown in Fig.2-4, n is the normal distance from the boundary and φ_P stands for V_z, ψ, $(\frac{W}{r})$ or T.

2.4.2 Thermodynamic and Transport Properties of the Fluid

At this stage, the energy equation (2.2-35) cannot be solved for T, since it contains more than one unknown: the temperature T and the fluid properties ρ, μ, c_p and k, which in turn, vary with temperature. Hence, additional thermodynamic relationships which connect the fluid properties with its temperature are required. In the present problem, large variations of the fluid properties are expected throughout the flow field, as a result of the steep temperature gradients. These thermodynamic and transport relationships become much more complex at high temperatures, especially when thermal dissociation and ionization occur. Properties of hot gases, specifically plasmas, are fundamentally different from those of the same material at low temperatures. This problem has been studied intensely by various workers (2,7,12,13,30,40,47), and most of the thermodynamic and transport properties of gases at very high temperatures have been computed theoretically since direct experimental measurements at such temperatures are not feasible.

Appendix A presents the data used in the present work for density, viscosity, thermal enthalpy and conductivity, and heat capacity at constant pressure for Argon at temperatures up to 15,000 $^{\circ}$K and atmospheric pressure. Values of density and heat capacity at constant pressure, and those of viscosity, thermal enthalpy and conductivity at temperatures below 5000°K, were calculated theoretically by Amdur and Mason (2) using statistical mechanics and kinetic theory combined with the molecular beam scattering techniques. Values of density and viscosity for Argon from 5000°K to 15,000°K were computed by Dre-Ilishak et al (13) using tabulated data for observed atomic energy levels to calculate the internal partition functions for the Argon atom and the first four Argon ions.

Lagrangian four-point-interpolation was used in the numerical predictions to obtain the local properties of the fluid in the flow field from the tabulated data.

2.4.3 Heat Loss by Radiation

When the gas temperature is very high, the radiation heat loss from the hot gas core to the confining walls becomes significant. The mechanism of heat transfer by radiation in an absorbing, emitting and scattering fluid is extremely complicated. In section (2.2-1) it was shown that the radiation heat loss may be predicted approximately by eq.(2.2-16), based on the assumptions that the fluid is a non-participating medium so that the walls of the reactor absorb all the energy radiated from the enclosed gas. This requires a knowledge of the absorption coefficient and refractive index of the fluid throughout the temperature field. Another alternative approach lies in the experimental results. Considerable experimental work has been reported on the total line radiation loss for

Nitrogen, Oxygen, Hydrogen and Argon plasmas. Appendix B presents the results obtained by Krey and Morris (26) for Argon at temperatures from 9000 to 15,000°K and at atmospheric pressure. It shows that the radiation heat loss is negligible at temperatures below 10,000°K, but increases exponentially with temperature so that it rapidly becomes significant at higher temperatures.

2.5 CLOSURE

In the present chapter, the problem has been described completely through the basic differential equations and the boundary conditions. The differential equations have been reduced into analogous algebraic equations, with a procedure of solving them. The next chapter presents the numerical solutions obtained for the systems considered, with the aid of the digital computer.

III. COMPUTATIONAL PROCEDURE AND RESULTS

3.1. INTRODUCTION

Solutions were obtained for laminar flows within the axi-symmetric conduits illustrated in Fig.3.1, in the absence of swirl (i.e. $V_\theta = 0$). The geometry shown in Figure 3.1a was chosen as a possible design for a high-temperature heterogeneous reactor, while the simple expansion of Figure 3.1b was included to enable comparison with the results of other workers (22,29). Numerical solutions were obtained for two distinct cases. In the first, which will be called the isothermal approach, the working fluid is at uniform temperature and has uniform thermodynamic and transport properties throughout the flow field. In the second, or non-isothermal approach, the flow of a hot gas was considered, whose properties vary with temperature and hence with position. The calculated streamlines and contours of vorticity and temperature are presented in this chapter as functions of the Reynolds number of the entering flow. Results obtained for the conduit expansion presented in Figure 3.1b are compared with the numerical solution of Macagno & Hung (29). Details of the computational procedure are presented, together with the discussions on the existence and uniqueness of the solution, and the factors which may influence the convergence and accuracy of the procedure.

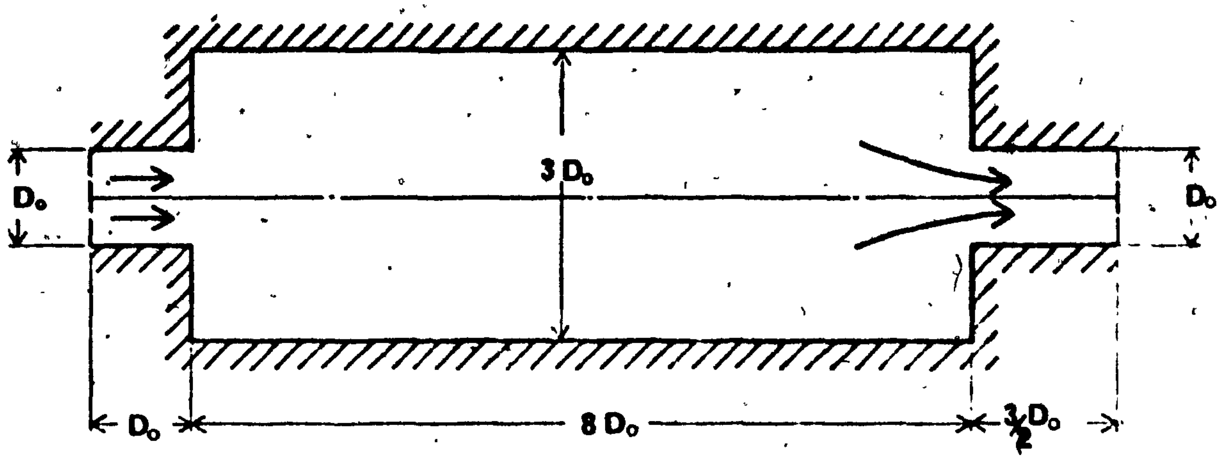

(a) A CYLINDRICAL REACTOR CHAMBER

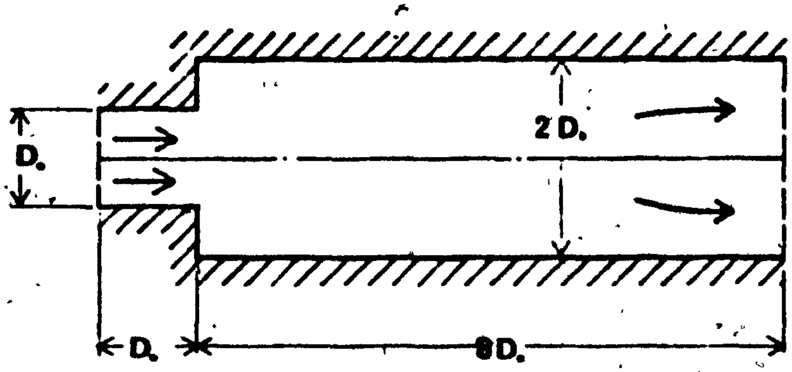

(b) AN AXI-SYMMETRIC CONDUIT EXPANSION

Fig.3.1 ILLUSTRATIONS OF THE GEOMETRIES CONSIDERED

3.2 EXISTENCE AND UNIQUENESS OF THE SOLUTION

The problems of existence and uniqueness of solutions to the Partial Differential Equations of fluid flow and their analogous Finite-Difference Equations are far from settled (2,3,4,38). Since the boundary conditions and equations considered here clearly correspond to real physical situations, heuristic reasoning suggests that existence is not a problem: it is reasonable to assume that any numerical solution which proceeds from a physically reasonable initial condition must exist.

The question of uniqueness of an attained numerical solution is more worrisome, simply because there exist some cases, physical and purely mathematical, in which the steady-solutions do not possess uniqueness (1,38). In the present investigation, as a means of testing the uniqueness of the computational solutions, different sets of initial conditions were applied to the same flow. Were the system computationally unstable, or non-unique, they would fail to converge to the same final solution. The results of these tests showed that the same final solution is attained, within reasonable accuracy, for flows under precisely the same circumstances but having different initial conditions. This is regarded as confirmation of the uniqueness of the solution.

3.3 FACTORS WHICH MAY INFLUENCE THE STABILITY, CONVERGENCE AND ACCURACY OF THE COMPUTATIONAL PROCEDURE

3.3.1 The Influence of the Initial Conditions

It is obvious that the closer the initial guesses of the distributions of the variables are to the final solutions, the fewer will be the iterations required to reach the solution. The procedure followed was to start with an approximate flow pattern as the initial conditions for the lowest Reynolds number in the working range. The final solutions were then used as the initial conditions for calculation with a higher Reynolds number, and so on.

3.3.2 The Influence of the Boundary Conditions

It has been observed that the specification of computational boundary conditions, besides affecting numerical stability, greatly affects the rate of convergence and accuracy of the finite difference equation solution (17,33,34). In particular, it appears that when the boundary condition for a dependent variable is in the form of prescribed gradients (such as for vorticity), convergence is significantly slower (17). This effect results fromthe upwind-differencing scheme, which causes errors in a given initial approximation to the final solution to be diffused and advected in the direction of the velocity during the iterative process. When they reach the boundaries of the flow, the error vanishes if the value of the variable is specified. On the other hand, if the boundary condition is of prescribed normal gradient, a portion of the error will remain and diffuse back into the interior field during the next cycle. This may be the reason why the vorticity equation was found to converge slowly and, under some circumstances, divergence occured. There are two remedies suggested by Gosman et al (17). The first is under-relaxation, which will be discussed in the next section. The second is the removal of the wall vorticities from the substitution formula (2.3-18) for the near-wall nodes by once-for-all algebraic elimination. Thus, for example, for an interior node P which lies adjacent to a wall node N as shown in Fig.3.2, the following modified substitution formulae must be applied for the evaluation of vorticity, using the boundary condition (2.4-10):

$$\left(\frac{w}{r}\right)_P = \frac{C_E(w/r)_E + C_W(w/r)_W + C_N(g_1)_N + C_S(w/r)_S + D}{1 - C_N(g_2)_N} \qquad \ldots\ldots(3.3\text{-}1)$$

The wall value, $(w/r)_N$, does not appear explicitly, for it has been eliminated through the use of eq.(2.4-10).

3.3.3 The Influence of Vorticity at the Sharp Corners

The wall vorticity is an important parameter, since at no-slip boundaries vorticity is produced and advected into the flow field. In particular, the computational conditions for vorticity at the sharp corners B and C shown in Fig.3.2 require special considerations. The vorticity at the exit corner C presents no important problem, since it is found to have little effect on the solutions of the flow field within the conduit. However, this effect is critical at the protruding corner B. There are several alternatives for the evaluation of $(w/r)_B$, for there is a discontinuity in vorticity at this geometric singularity, and the no-slip wall conditions for vorticity can be applied in a number of ways. Seven different methods have been applied by various workers (17,18,20,23,29, 31,32,33,34,42), five of which were more or less successful (34). Some involved rounding off the corner, whereas others involved using upstream wall values or otherwise biasing the results toward the usual anticipation of separation occuring at the corner. However, the correct formulation is still in question and no generally applicable results has been decided. In the present investigation, three different methods used by Macagno and Hung (20,29), by Gosman et al.(17,31) and by Roach and Muller (33,34) were tried. The most appropriate form was selected from the results of the flow visualization studies, presented in the next chapter. It was found that the most reliable predictions resulted from the use of discontinuous values for vorticity at the corner B as suggested by Gosman et al.(17) and Roach and Muller (33,34). Referring to Fig.3.2, when $(w/r)_B$ is needed in a substitution formula about node (IB,JB-1) upstream of the corner, the value is obtained from the boundary eq.(2.4-10), considering the corner as part of the upstream wall. When $(w/r)_P$ is required for the node downstream from the corner, (IB+1,JB), the value of $(w/r)_P$ which is evaluated by considering the corner as part of the expanded wall is used. This boundary condition was found to yield a slight contraction in the entering jet beyond the protruding corner for isothermal flows at Reynolds numbers from 40 to 100. The flow visualization study described in Chapter IV indicated that the edge of the recirculation region starting from the sharp corner is in fact very straight in the vicinity of the corner. Hence this form of the boundary condition was only used for the low Reynolds number isothermal flows and for the non-isothermal runs. For isothermal flows with Re $\geq$ 40, the method of Gosman et al. was used, in which $(w/r)_B$ is not used at all for the evaluation of vorticity at the downstream node (IB+1,JB); instead, $(w/r)_{IB+1,JB}$ was determined from eq.(2.3-18) with the stipulation that the value of stream function at this point is the same as that at the corner B. This particular boundary condition assumes implicitly that recirculation occurs, but this is known to be true in isothermal flows in this range of Reynolds numbers. At the exit corner C, the average of the vorticities obtained from upstream and downstream nodes was used, since the flow round this corner is smooth and no separation occurs.

3.3.4 The Influence of the Grid

It is obvious that the finer the grid, the more accurate is the solution. However, when the number of grid nodes is increased, the computing time required for each cycle of iteration increases roughly in proportion, and, in addition, the number of iterations required for convergence usually increases. Hence, the mesh size was kept as large as possible, compatible with the desired accuracy. Also, the use of a variable grid spacing as described below improves the accuracy of the solution without increasing the number of nodes. However, it is found that non-uniformity in the grid spacing between the grid lines which are adjacent and parallel to the walls may sometimes lead to divergence. This may be averted, as suggested by Gosman et al.(17) by keeping the ratio of the intervals between the nodes near the wall close to unity.

3.4 DETAILS OF THE COMPUTATIONS

3.4.1 Grid

To minimize computing time and still cover the area of steep gradients effectively, a nonuniform grid was employed. Fig.3.2 shows the grid used for the reaction chamber. The grid nodes are closely-spaced in the corners of the chamber where steep gradients of the dependent variables are expected, and more widely spaced elsewhere. The spacing of the grid lines in the r-direction is uniform, except near the wall and the axis-of-symmetry where it is made smaller. The spacing within the chamber in the z-direction is caused to increase progressively according to the formula

$$z_1 = \ell \tan(hf)/\tan(h) \qquad (3.4\text{-}1)$$

where z_1 denotes the distance from the expansion or contraction

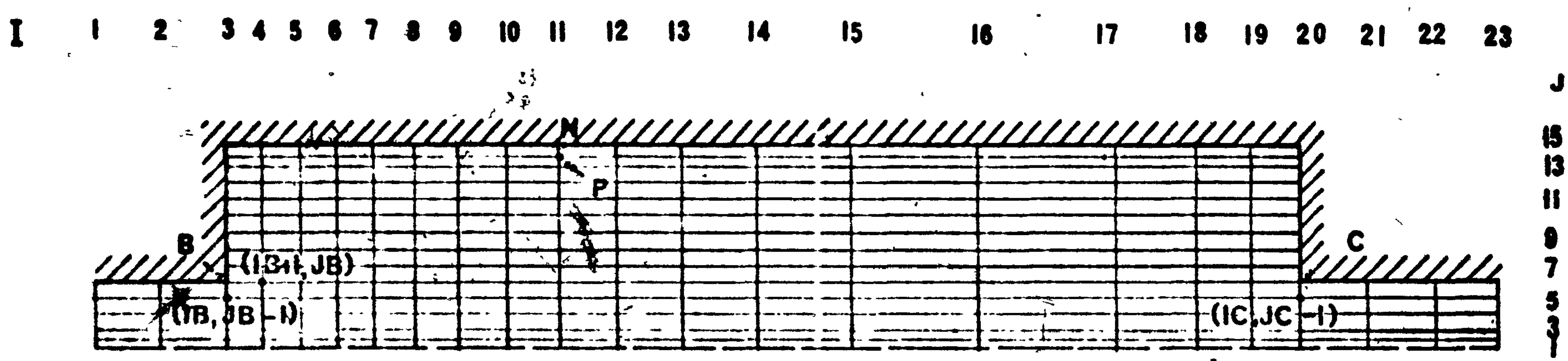

Fig.3.2 ILLUSTRATION OF A PORTION OF THE GRID

of the chamber in the z-direction, ℓ is the length of the section to be subdivided and f is a fraction which increases from 0 to 1 in equal increments. Various values of the constant h were used, ranging from 0.9 to 1.3 with increasing Reynolds numbers. A 22 x 11 grid was employed for flows within the abrupt conduit expansion, with a total of 232 internal grid nodes. For flows entering the reaction chamber of Fig. 3.1a, 22 x 16 and 23 x 15 grids providing 334 internal nodes were used. An equally-spaced rectangular grid was also employed in a few cases, to give a consistency check.

3.4.2 Convergence Criterion

The computations were terminated when λ in equation (2.3-17) was less than 0.001 for all dependent variables.

3.4.3 Under-/Over-relaxation Factors

Relaxation factors were introduced to improve the stability and speed of convergence. For isothermal flow, over-relaxation was used in the prediction of stream function, in which the relaxation parameter in eq. (2.3-20) took values between 1.2 and 1.3, while the vorticity equation was under-relaxed with a factor of 0.7 or 0.6, for it usually oscillates slightly. For the non-isothermal case the solutions converged with more difficulty so under-relaxation was used for all the dependent variables. A relaxation parameter between 0.65 and 0.75 was used for vorticity and temperature, whereas stream function required an even smaller value, which was chosen between 0.4 and 0.55.

3.4.4 Computing Time

All the computational predictions presented in this chapter were obtained with a digital computer IBM 360, Model 75. Each calculation for the isothermal flow in the conduit expansion required about two minutes of computing time, while the same flow in the reactor chamber required about three minutes. For the non-isothermal flow, the computing time was about six minutes.

A listing of the program used is presented in Appendix C, along with typical results obtained for both isothermal and non-isothermal flows in the reactor chamber.

3.5 COMPUTATIONAL RESULTS

This section is divided into two main parts. In the first, results of isothermal flows in a conduit expansion and in a reaction chamber are obtained, assuming uniformity in the temperature and properties of the fluid. In the second part, flows at high temperature entering a reaction chamber having cooled walls are studied with a range of reactor entry conditions.

3.5.1 Isothermal Flows

Flow patterns of an isothermal flow in an abrupt circular conduit expansion having a diameter ratio of 2:1 are predicted for Reynolds numbers ranging from 10 to 100. The results are presented in Figures 3.3,4 and 5, in which the upper half consists of vorticity contours and the lower half

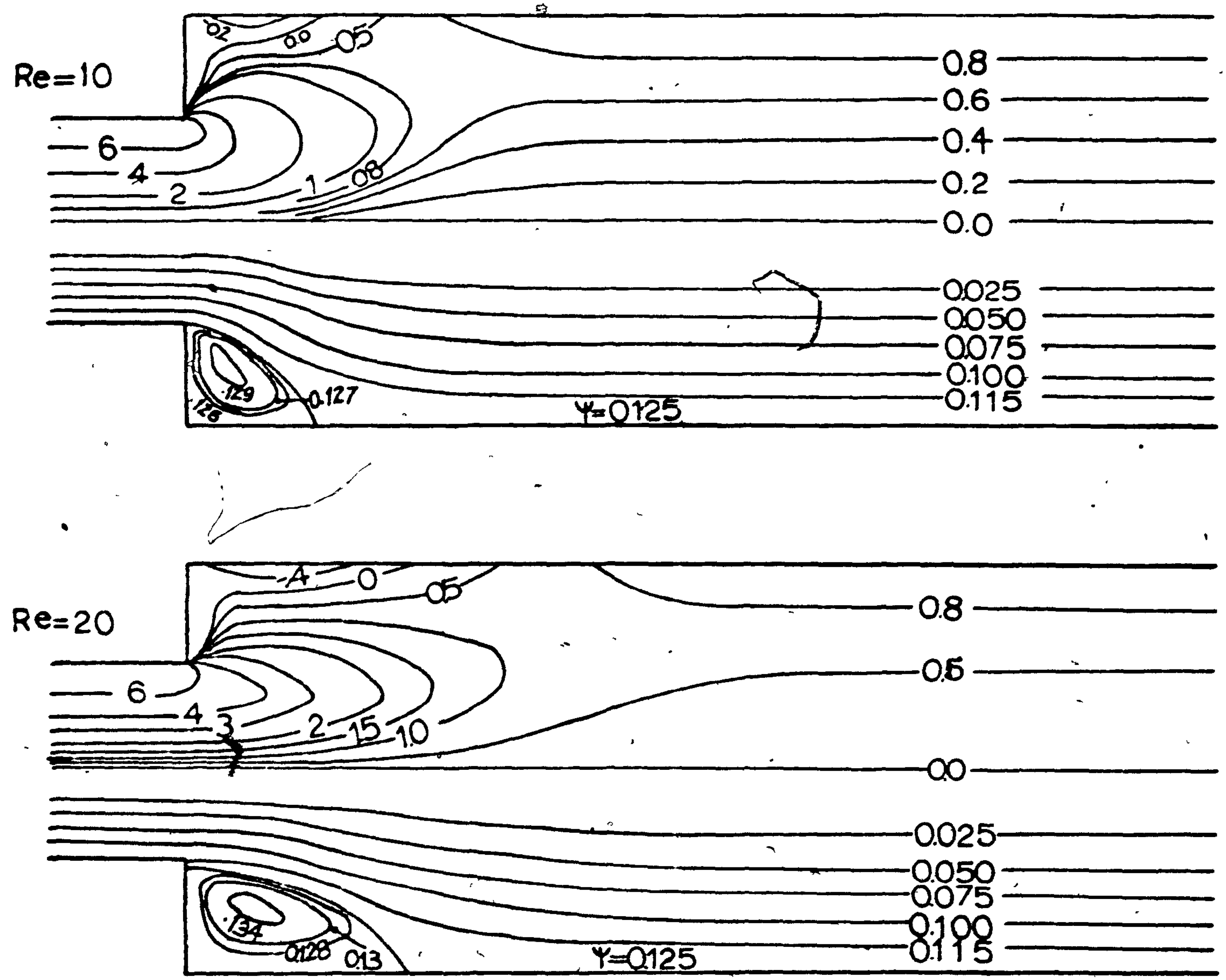

Fig.3.3 VORTICITY CONTOURS AND STREAMLINES FOR ISOTHERMAL FLOW IN A CIRCULAR CONDUIT EXPANSION

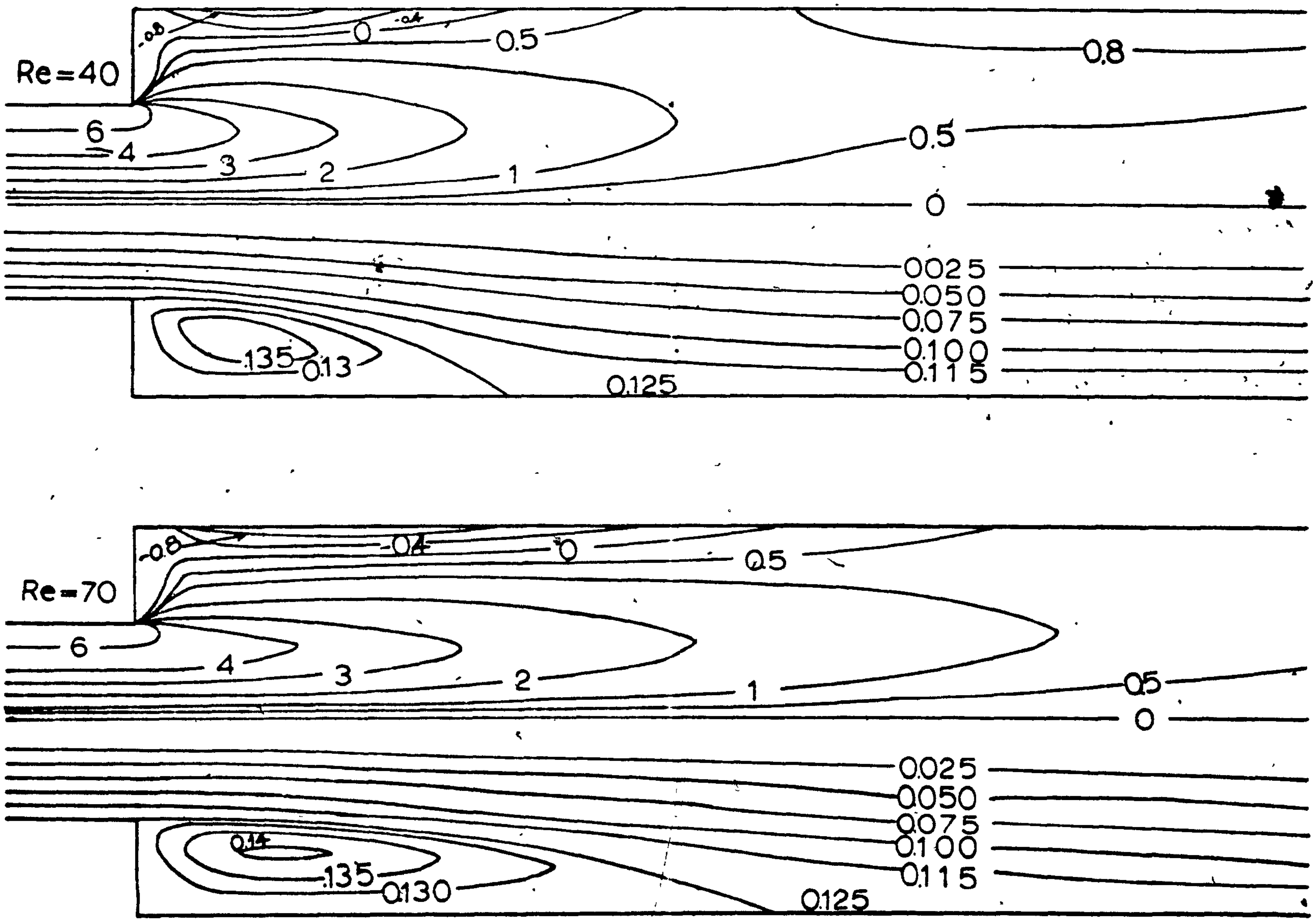

Fig.3.4 VORTICITY CONTOURS AND STREAMLINES FOR ISOTHERMAL FLOW IN A CIRCULAR CONDUIT EXPANSION

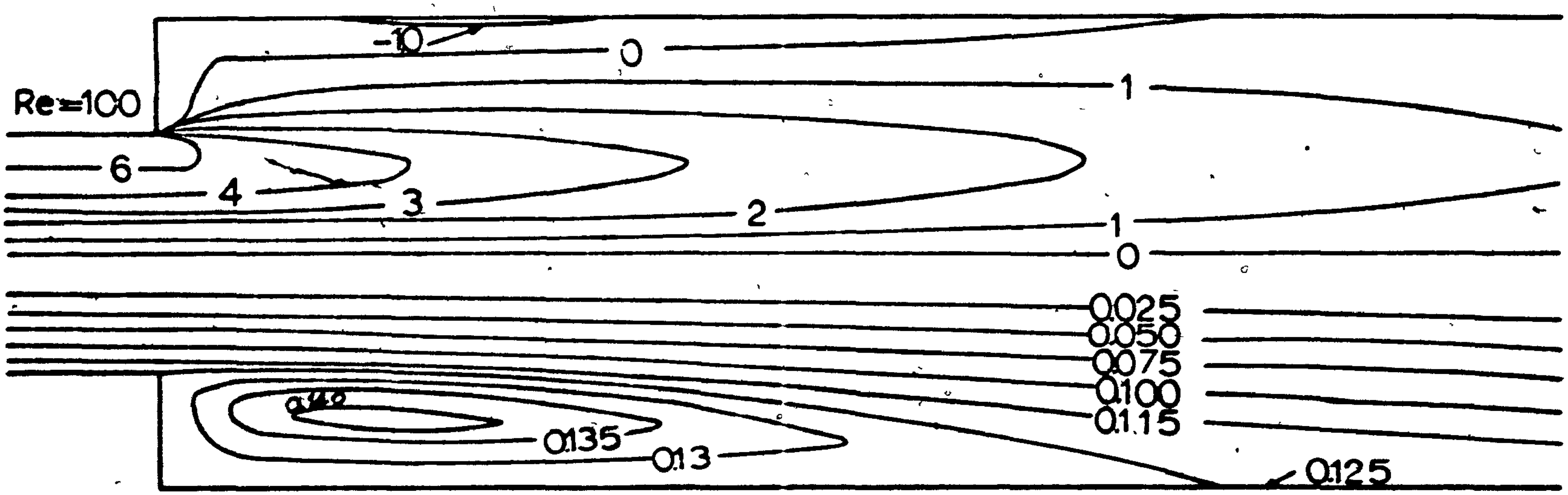

Fig.3.5 VORTICITY CONTOURS AND STREAMLINES FOR ISOTHERMAL FLOW IN A CIRCULAR CONDUIT EXPANSION

the streamlines. Dimensionless values are given. These figures show a captive eddy in the corner immediately following the sudden expansion of the chamber. It can be seen that, as the Reynolds number increases, the eddy becomes longer: the reattachment point and the "eye" of the eddy move downstream. The vorticity contour lines are stretched downstream by convection, while the effects of diffusion become smaller. The heavy concentration of contour lines around the sharp corner indicates a high vorticity gradient in this region, as expected. As Re increases, these gradients become more severe.

Fig.3.6 shows the comparison between the predictions of the present procedure and those obtained by Macagno and Hung (39), who used Taylor-series expansions for finite differencing. The relative eddy length L_e/D_o and the position of the eddy center L_c/D_o are shown as functions of the Reynolds number. Also presented in this figure are the experimental values obtained by Macagno and Hung (29), determined from photographic records using suspended aluminum powder to visualize the flow, and from direct observations of the direction in which dyed fluid would move. The agreement of the present predictions with their experimental results is quite satisfactory. Although the present results and their predictions fit the experimental results equally well, there is some difference between the two curves. This is due mainly to the difference in the boundary conditions used. The curves obtained are nearly straight, showing that the relative length

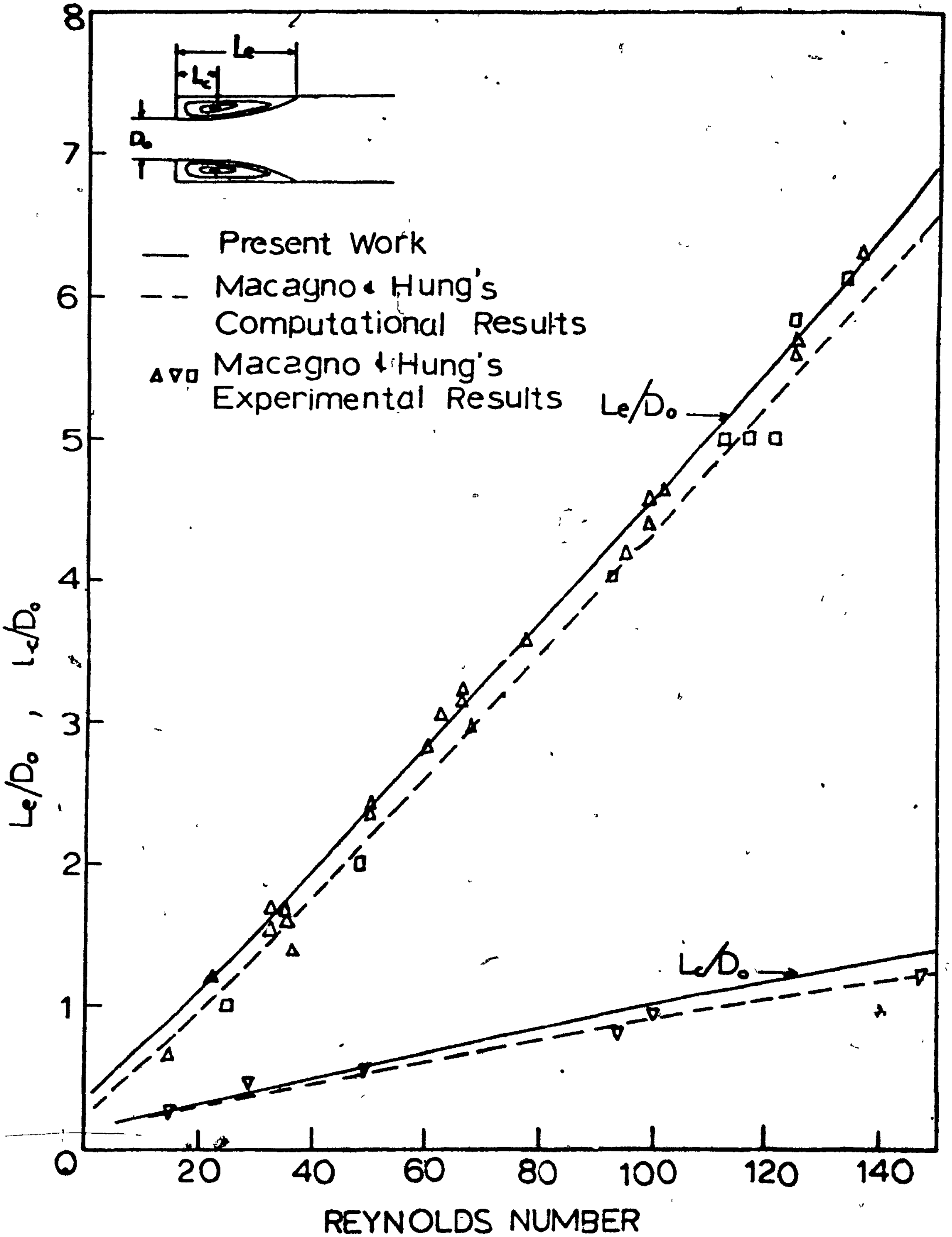

Fig.3.6 RELATIVE EDDY LENGTH AND POSITION OF EYE OF EDDY AS FUNCTIONS OF Re FOR ISOTHERMAL FLOW IN A CIRCULAR CONDUIT EXPANSION

of the eddy and the relative location of the "eye" of the eddy are nearly linear functions of Re in the range of Re = 20 to Re = 110. It is worth noticing the trend of the curves, both computational and experimental, as the Reynolds number becomes smaller and smaller. The results imply that a zone of separation would exist for creeping flow and this has also been recognized by Kawaguti (24). Macagno and Hung (29) reported that L_e/D_o takes a value of 0.27 at Re = 0, and carried out a calculation for a very low Reynolds number of 0.2 for a confirmation. However, this existence of an eddy at Re = 0 is ignored by Roach and Muller (33) who used a different boundary condition for vorticity at the corner.

A series of vorticity contours and streamlines of an isothermal flow entering the reaction chamber is presented in Figs. 3.7,8,9, for various Reynolds numbers from 10 to 100. The reaction chamber has a diameter ratio of 3:1, where the exit pipe diameter is the same as the inlet, and a length of 8 inlet diameters. The flow patterns predicted are qualitatively similar to those obtained in the simple conduit expansion; however, the degree of recirculation of the flow is accentuated strongly by the presence of the sudden contraction following the sudden expansion. This is shown clearly in Fig.3.10, presenting the growth of the recirculation region with the Reynolds number. The curve representing the relative length of the eddy is nearly straight in the range Re = 10 to Re = 50, above which it curves upwards. The position of the "eye" of

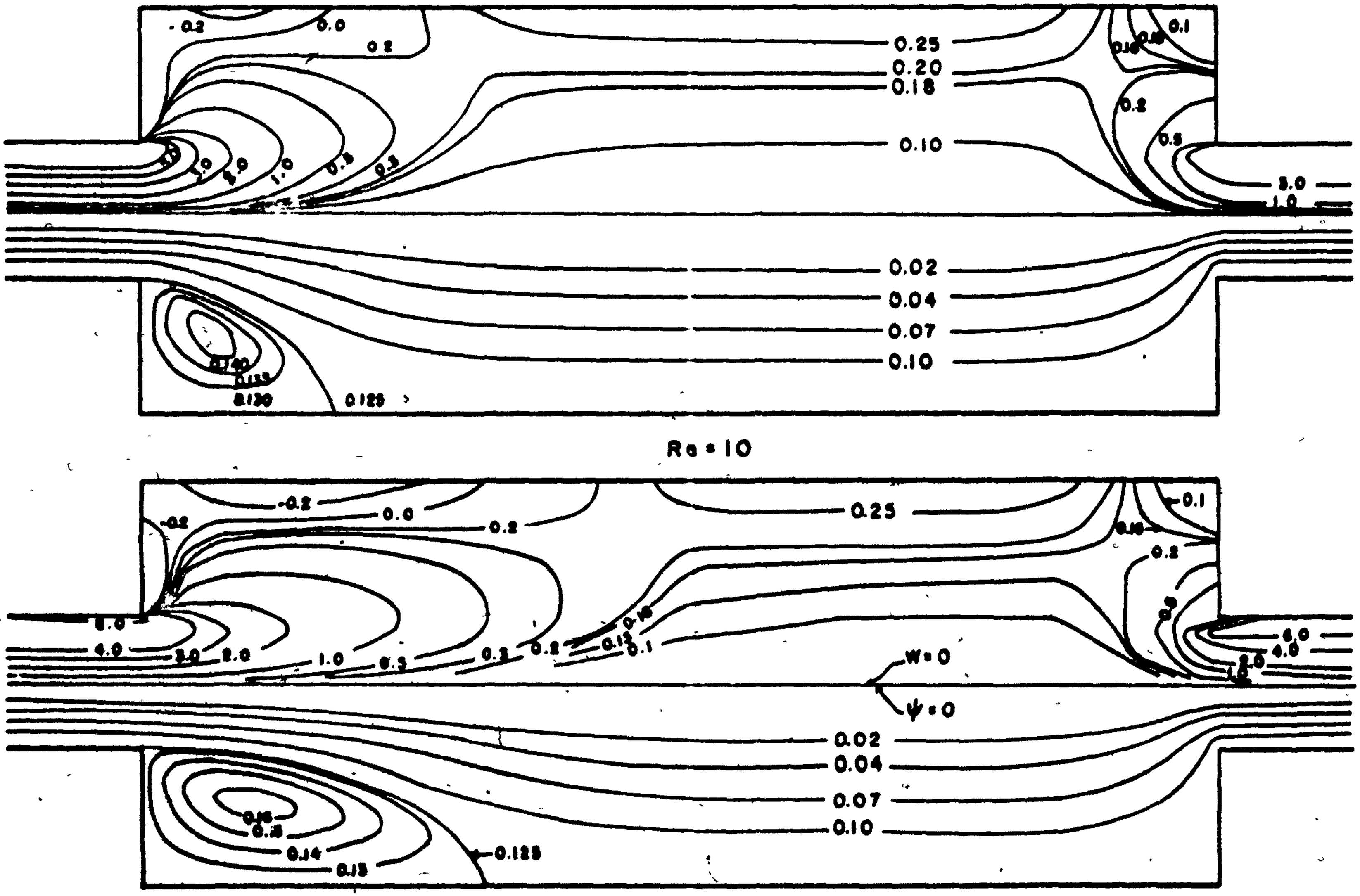

Re = 10

Re = 20

Fig.3.7 VORTICITY CONTOURS AND STREAMLINES FOR ISOTHERMAL FLOW IN REACTOR CHAMBER

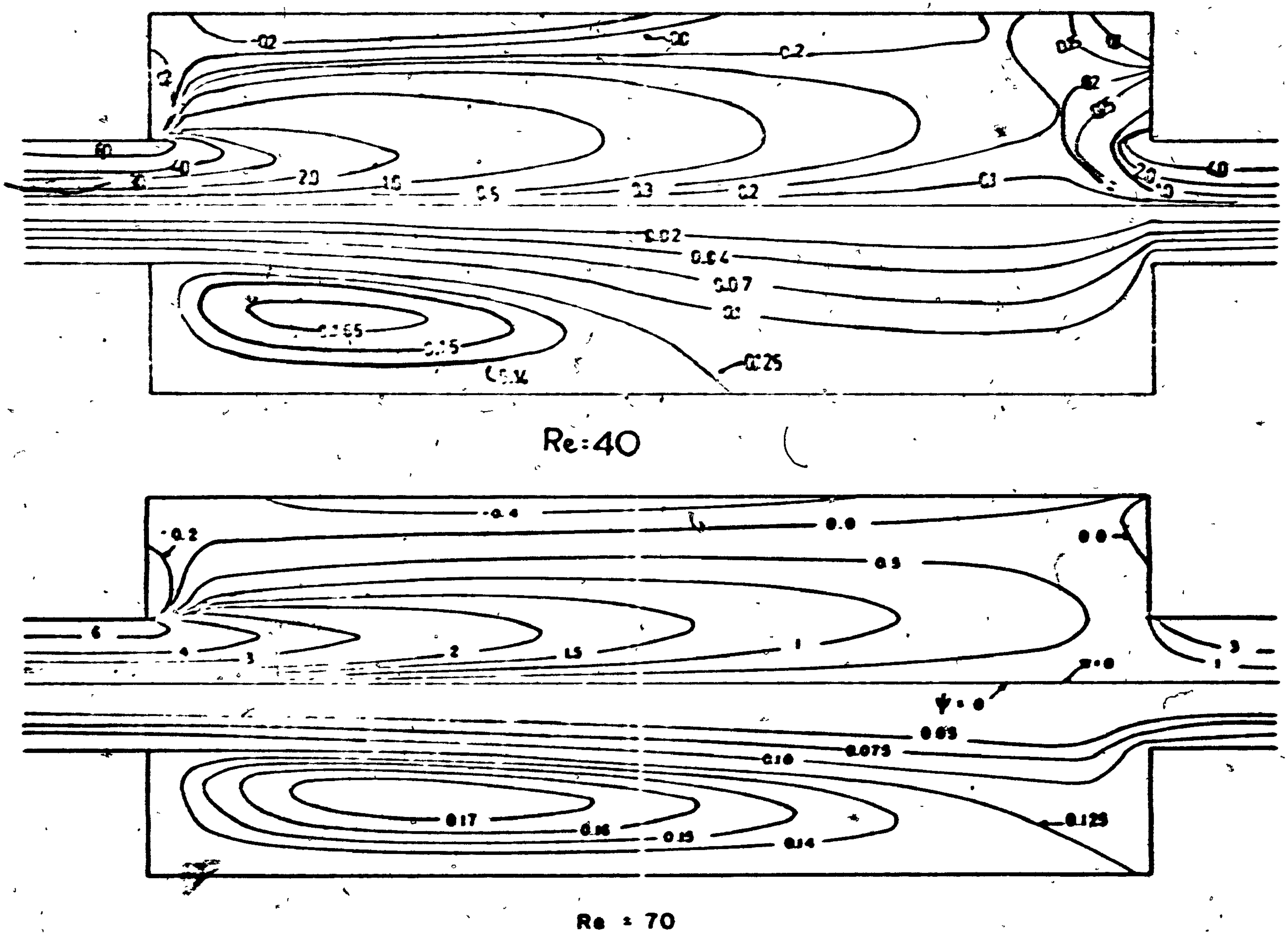

Fig.3.8 VORTICITY CONTOURS AND STREAMLINES FOR ISOTHERMAL FLOW IN REACTOR CHAMBER

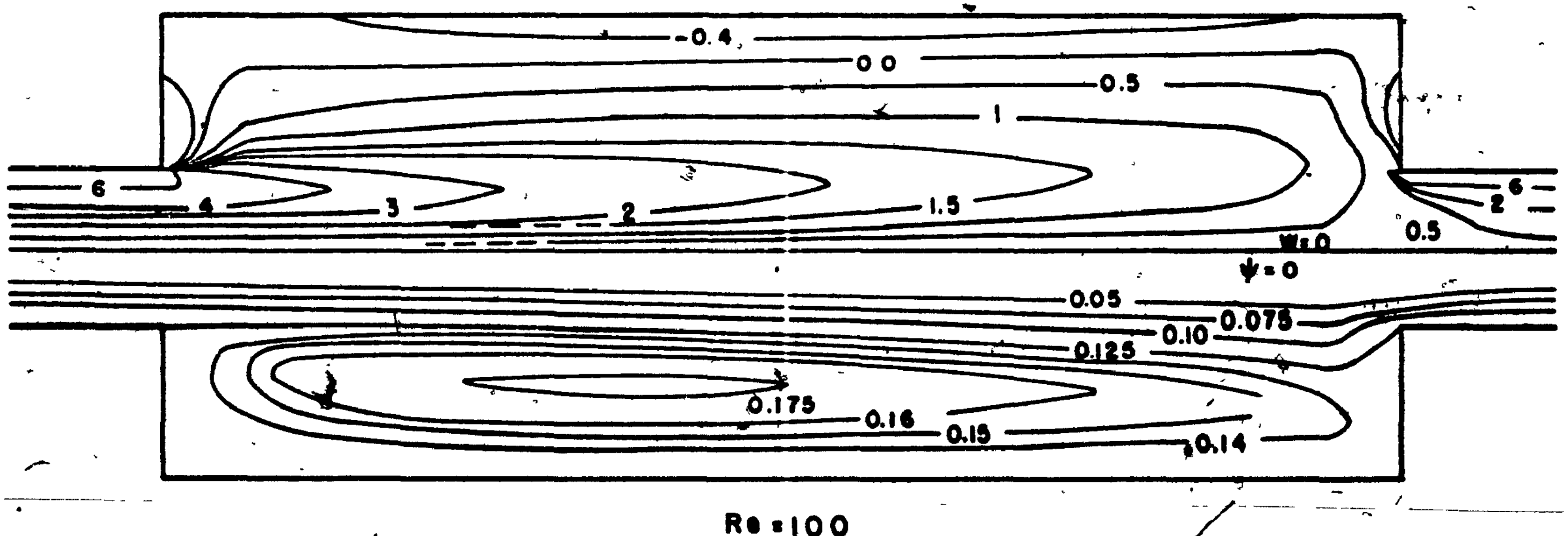

Fig.3.9 VORTICITY CONTOURS AND STREAMLINES FOR ISOTHERMAL FLOW IN REACTOR CHAMBER

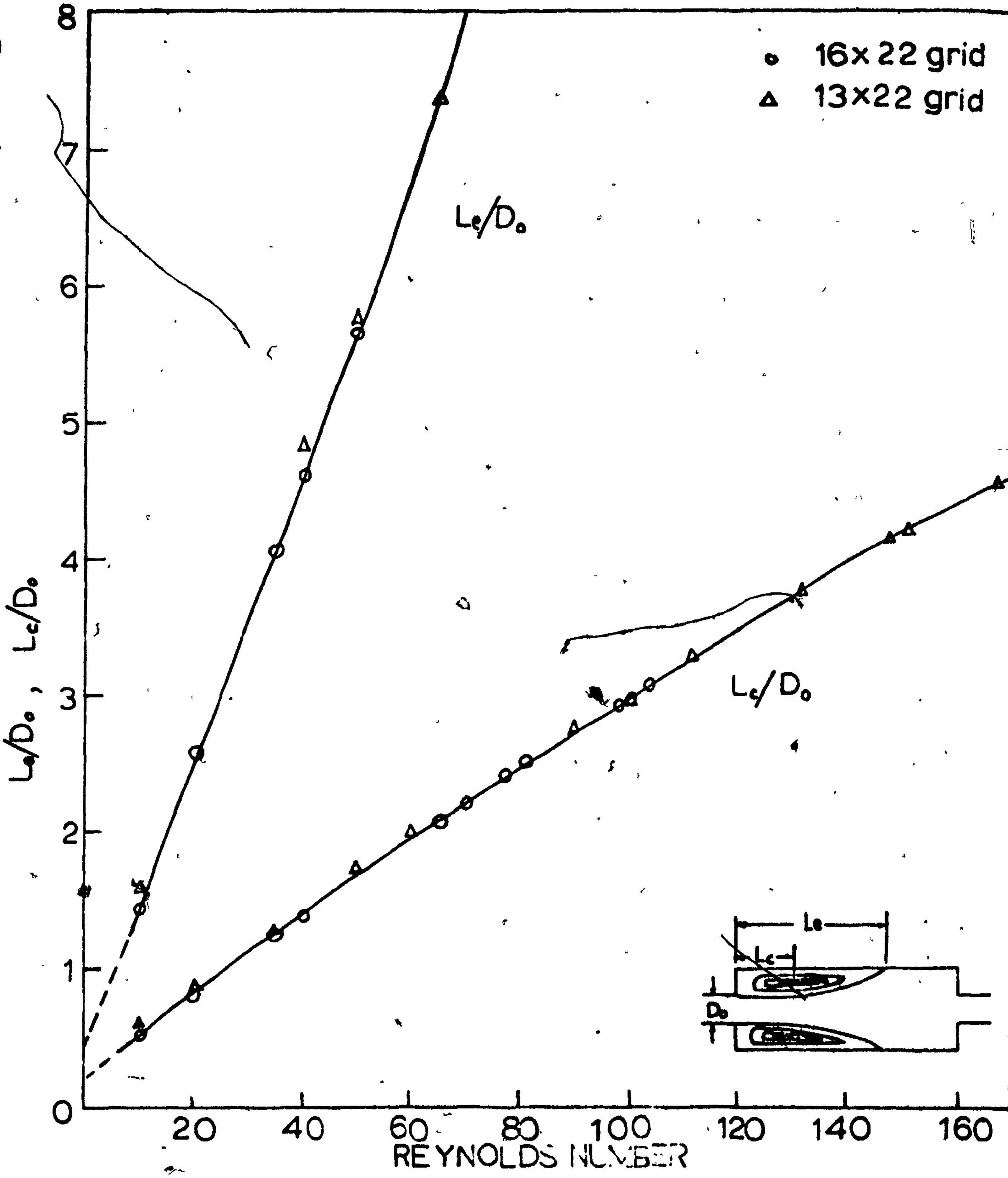

Fig.3.10 RELATIVE EDDY LENGTH AND POSITION OF EYE OF EDDY AS FUNCTIONS OF Re FOR ISOTHERMAL FLOW IN REACTOR CHAMBER.

the eddy is no longer linear as in the case of a sudden expansion which is not followed by a sudden contraction; instead the curve is concave. From Re = 70.5, the recirculation region occupies the whole length of the tube, and the reattachment point moves along the contracting wall towards the exit corner. Neither curve shown in Fig.3.10 passes through the origin, again implying that recirculation occurs even in creeping flow.

It is interesting to note that although there is no recirculation in the downstream corner above the sudden contraction of the chamber, the negative values of vorticity on the wall of the corner implies that recirculation would occur at much higher Reynolds numbers. The existence of such recirculation has been reported by Greenspan (18).

The validity of these numerical predictions for the reaction chamber will be discussed in the next chapter, where a comparison is made with the results of flow visualization studies.

3.5.2 Non-Isothermal Flow

Predictions of flow patterns and temperature distributions have been obtained for an Argon tail-flame entering a reactor having cooled walls. The three independent parameters of this investigation are the entry Reynolds number, the temperature of the entry flame, and the temperature of the walls of the reactor. For the range of the entry temperature of the flame investigated in this work ($2000^{o}K$ to $4000^{o}K$), radiation losses are assumed to be negligible compared to the heat transfer by other mechanisms. This is justified by experimental results reported by Krey and Morris (26). Properties of Argon at high temperature and atmospheric pressure presented in Appendix B were used for the present predictions, since Argon is a common working fluid in plasma processes. The use of a different gas having different properties would lead to slightly different results.

Figures 3.11 and 13 present the flow pattern and temperature distributions predicted for an Argon tail flame at $3000^{o}K$ entering the reactor having the walls at $300^{o}K$, with entry Reynolds numbers ranging from 1 to 100. As for the isothermal model, a captive eddy is predicted at the expansion. Although the flow pattern is qualitatively similar to that in the isothermal case, Fig.3.11 shows that the rapid density changes in the entry region enhance the recirculation strongly and increase the jet mass velocity. Even at a Reynolds number as low as 1, a large captive eddy is predicted in the entrant corner, much larger than in the corresponding isothermal flow. It increases rapidly with the entry Reynolds number, and already occupies the whole length of the chamber at Re = 5 . It is interesting to note that the separation in both cases is indicated below the sharp corner, even though the same boundary condition as in isothermal flow was assumed at the corner. A similar separation has been predicted in

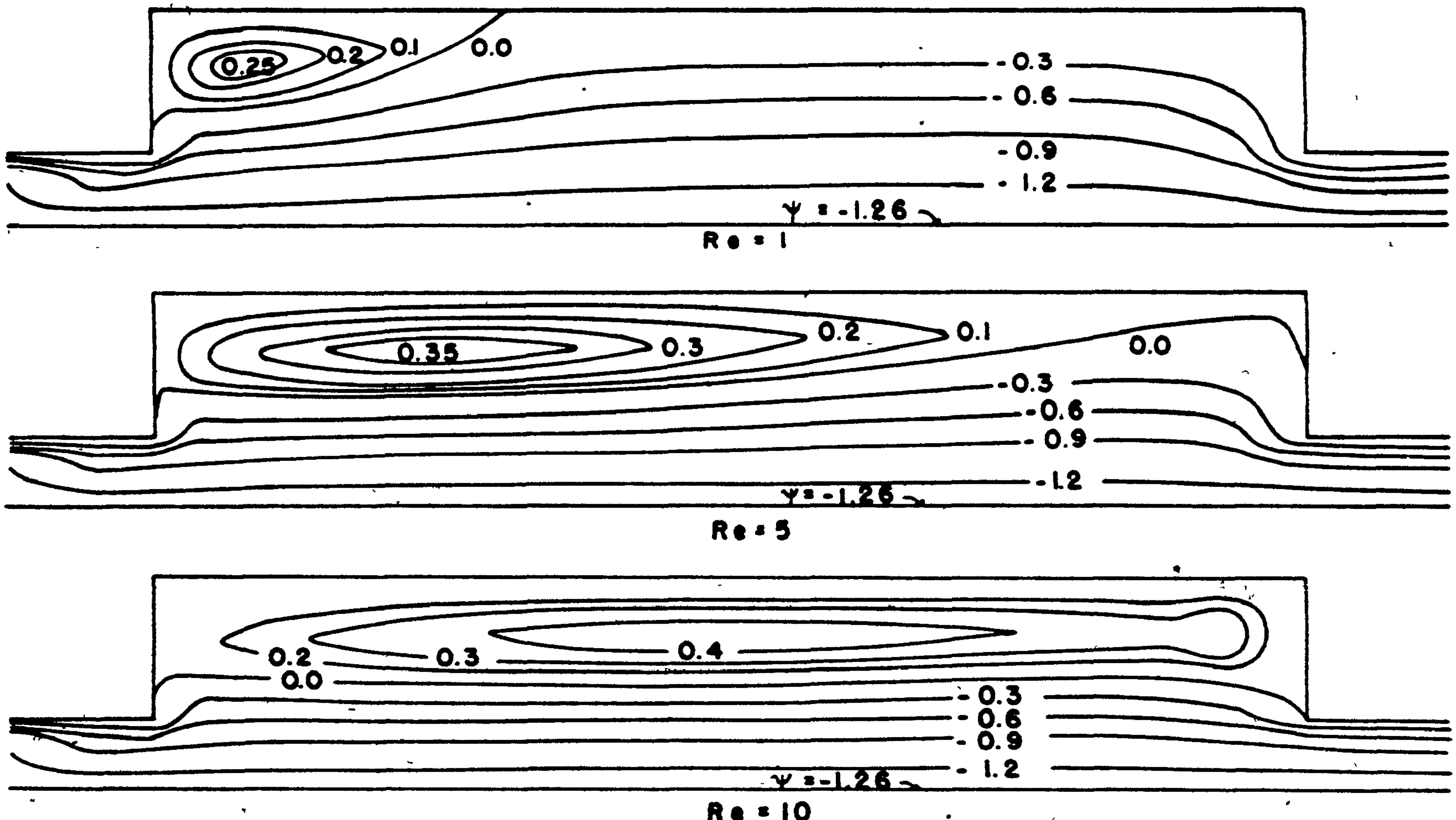

FIG. 3.11 - STREAMLINES FOR NON-ISOTHERMAL FLOW IN REACTOR CHAMBER, $T_o = 3000^oK$, $T_w = 300^oK$

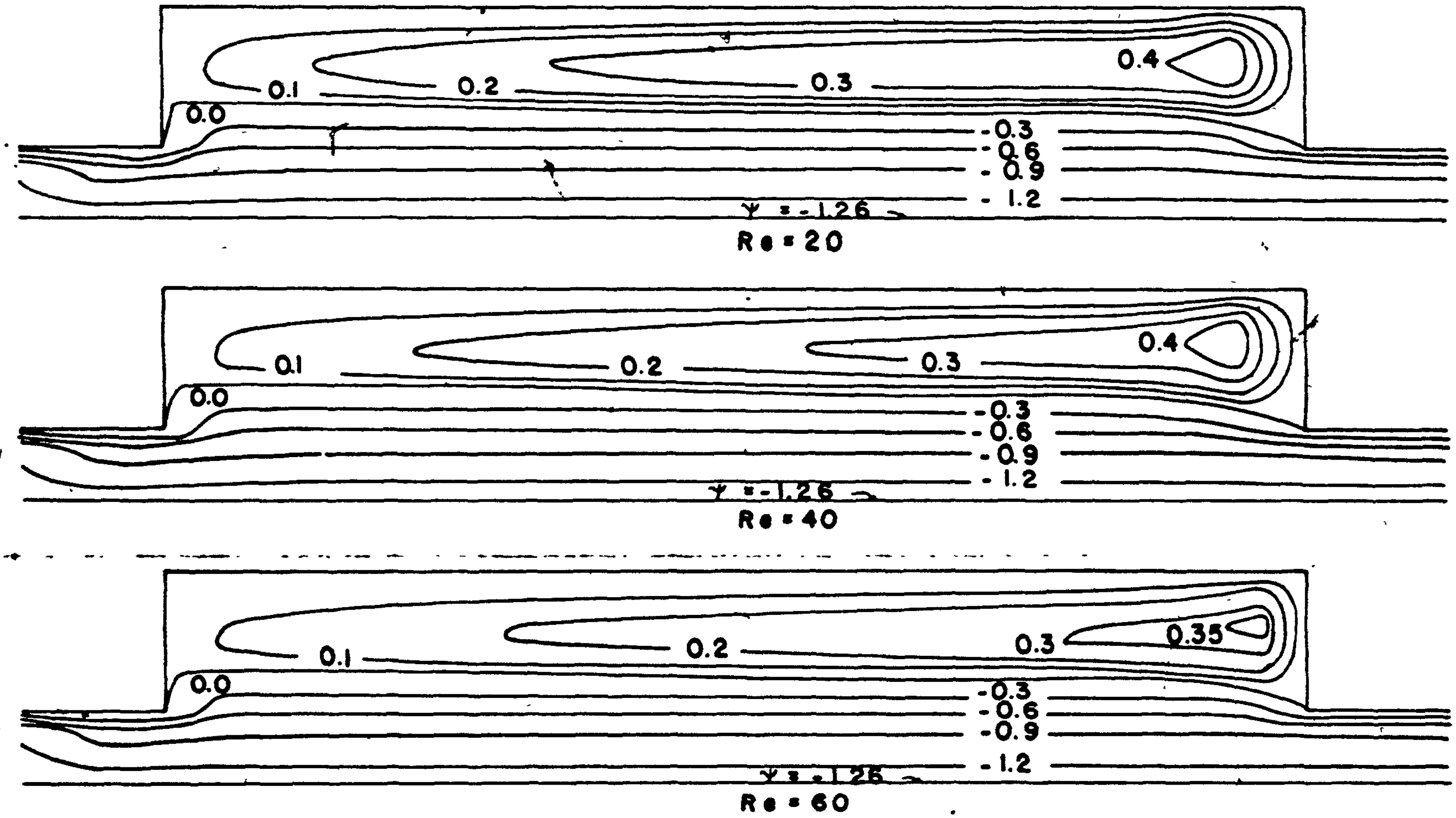

FIG. 3.11 (cont'd) - STREAMLINES FOR NON-ISOTHERMAL FLOW IN REACTOR CHAMBER, T_o = 3000°K, T_w = 300°K

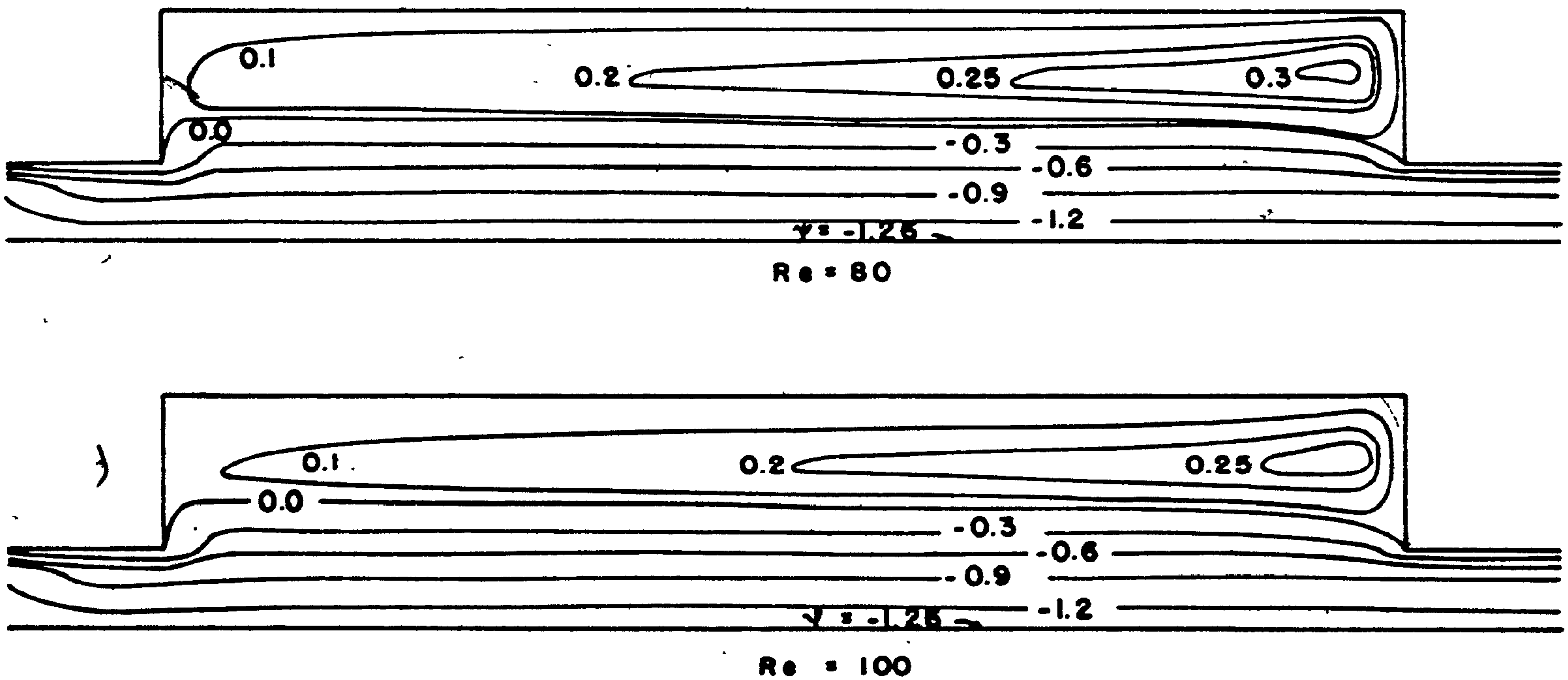

FIG. 3.11 (cont'd) - STREAMLINES FOR NON-ISOTHERMAL FLOW IN REACTOR CHAMBER, T_o = 3000°K, T_w = 300°K

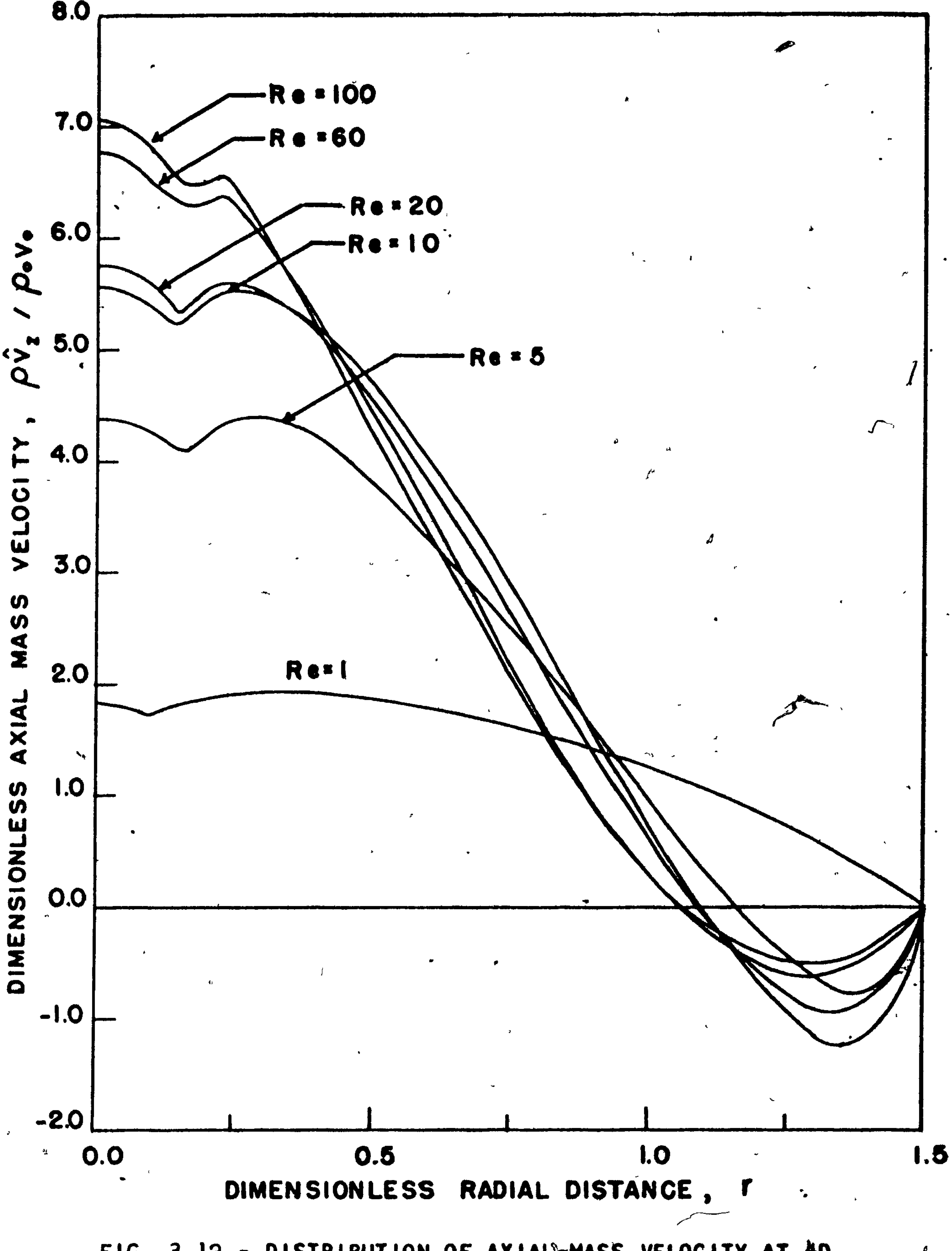

FIG. 3.12 - DISTRIBUTION OF AXIAL-MASS VELOCITY AT $4D_o$ FROM EXPANSION

plane flow over a step by Roache and Mueller (33). However, the fact that separation was predicted at the sharp corner for isothermal flow in this work suggests that the displaced separation point may result from the property gradients. Certainly separation below the corner of a step or expansion has been observed or predicted quite frequently for compressible flows (e.g. 52,53). Above Re = 5, as Re increases, the "eye" of the captive eddy moves rapidly downstream and is locked in that corner at a point which is essentially independent of Re for Re = 40 ; the separation and reattachment points of the recirculation move towards the shoulders of the reactor; while the flow in the central core becomes more parallel to the axis. Above Re = 40, the dimensionless stream function at the eye of the eddy decreases with increasing Re, showing that the recirculating velocities increase less rapidly than the inlet flow, this seems realistic, since the walls represent "no slip" boundaries and the eye of the eddy is stationary.

The radial profile of axial mass velocity at the middle of the reactor is presented in Fig.3.12. It shows that in all cases, the axial mass velocity exhibits a maximum at the axis and another maximum at some distance from the axis. This second maximum is the consequence of the rapid decay of temperature and hence the rapid increase in density with distance from the axis, as shown in Figs.3.13 and 14. This agrees qualitatively with the numerical results obtained by Swearingen and McEligot for a laminar gas flow between heated parallel plates (41).

Figure 3.13 presents the contour plots of temperature for the same flow conditions as in Fig.3.11. As the entry Reynolds number increases, the increasing effect of convection relative to conduction causes the hot gas core to extend further downstream, and at the same time contract slightly. On the other hand, the gas layer adjacent to the wall gets colder, especially in the upstream region, as shown in Figs. 3.13 and 14, the latter showing the radial temperature profile at the middle of the reactor. In Fig.3.13 it can be seen that at higher Reynolds numbers, the small region around the eye of the eddy gets warmer, due to convection by the recirculating fluid.

As a result of the decrease in temperature of the gas layer adjacent to the wall when Re increases, a decrease in local and overall rates of heat transfer to the wall is predicted. This is shown clearly in Figs.3.15 and 16, presenting the variations of thelocal heat transfer coefficient and Nusselt number respectively along the reactor. This local heat transfer coefficient, h_{coef}, is calculated from the rate of heat transfer to the wall and the bulk-to-wall temperature difference. The local bulk temperature of the fluid is defined by:

$$T_b = \frac{\int_0^{2\pi}\int_0^{R_w} \hat{c}_p\hat{\rho}\hat{V}_z\hat{T}\,\hat{r}d\hat{r}d\theta}{\int_0^{2\pi}\int_0^{R_w} \hat{c}_p\hat{\rho}\hat{V}_z\hat{r}d\hat{r}d\theta} \qquad (3.5\text{-}2)$$

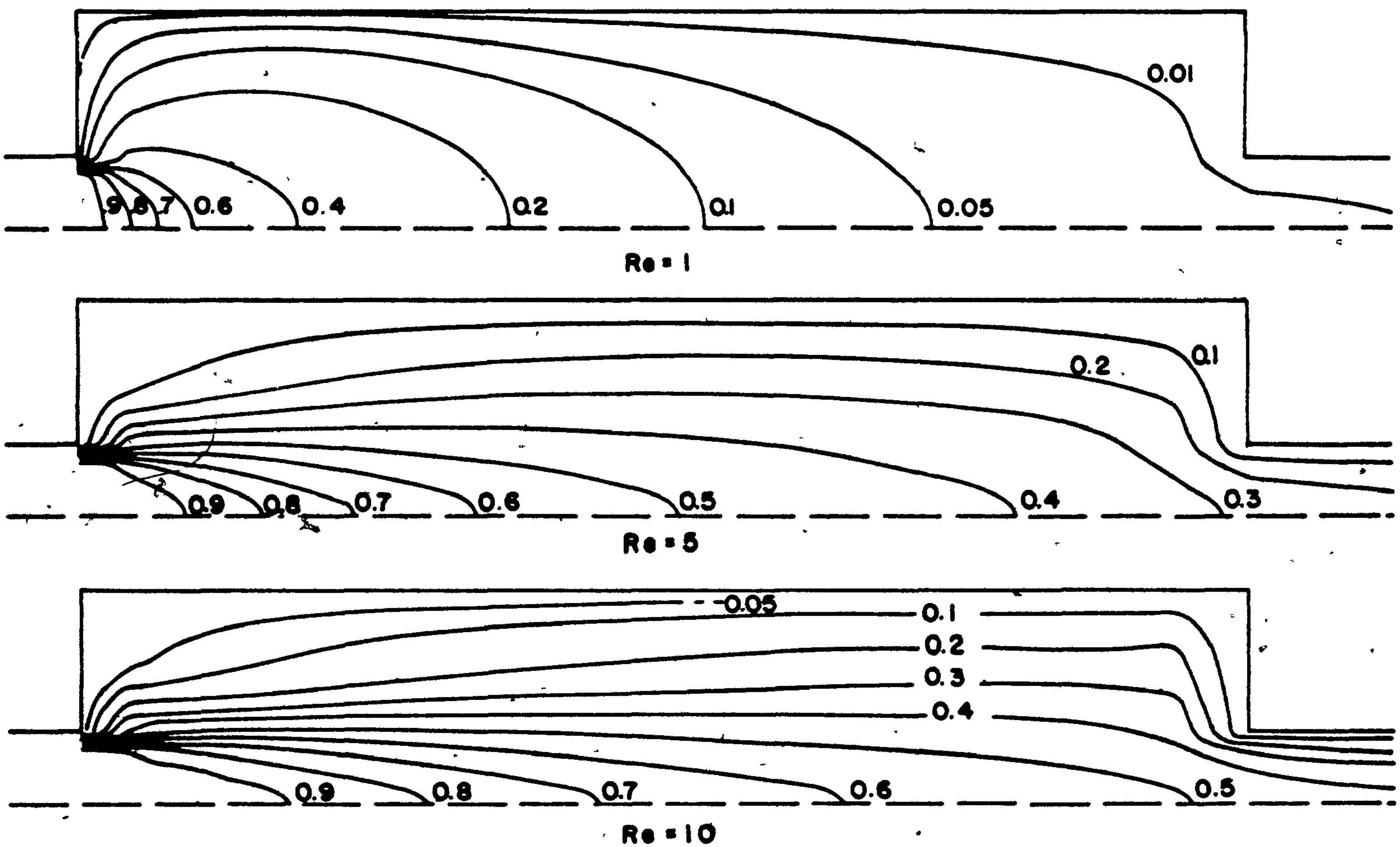

FIG. 3.13 - TEMPERATURE CONTOURS FOR NON-ISOTHERMAL FLOW IN REACTOR CHAMBER, T_o = 3000°K, T_w = 300°K

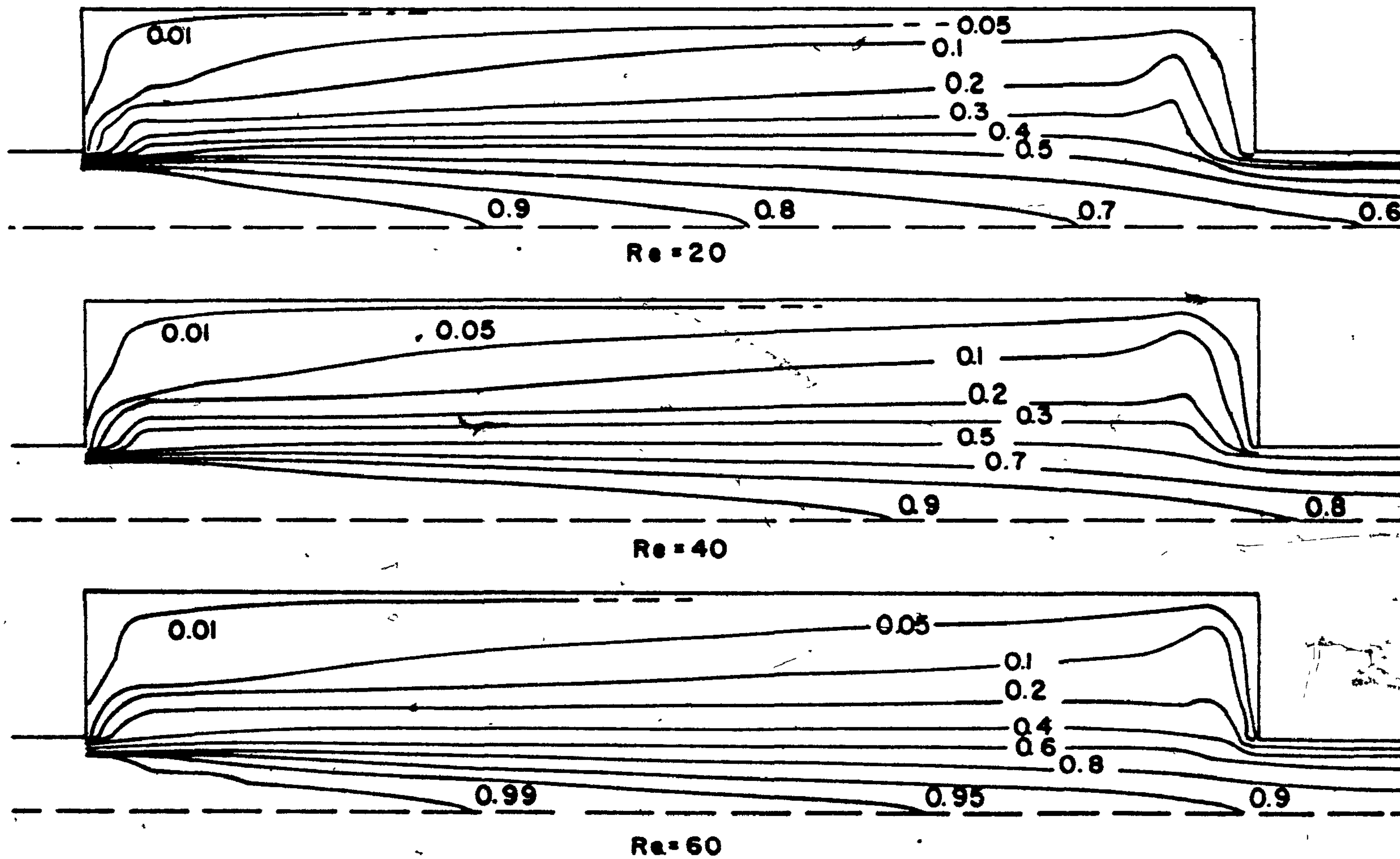

FIG. 3.13 (cont'd) - TEMPERATURE CONTOURS FOR NON-ISOTHERMAL FLOW IN REACTOR CHAMBER, T_o = 3000°K, T_w = 300°K

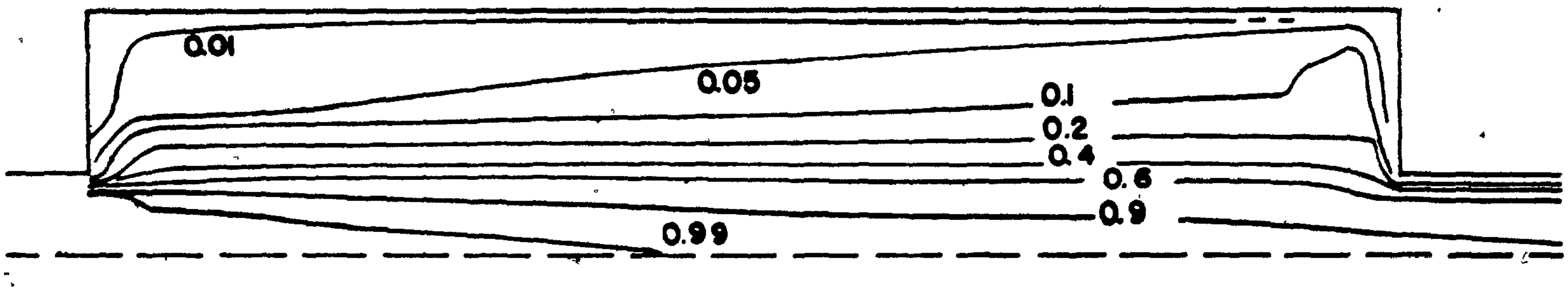

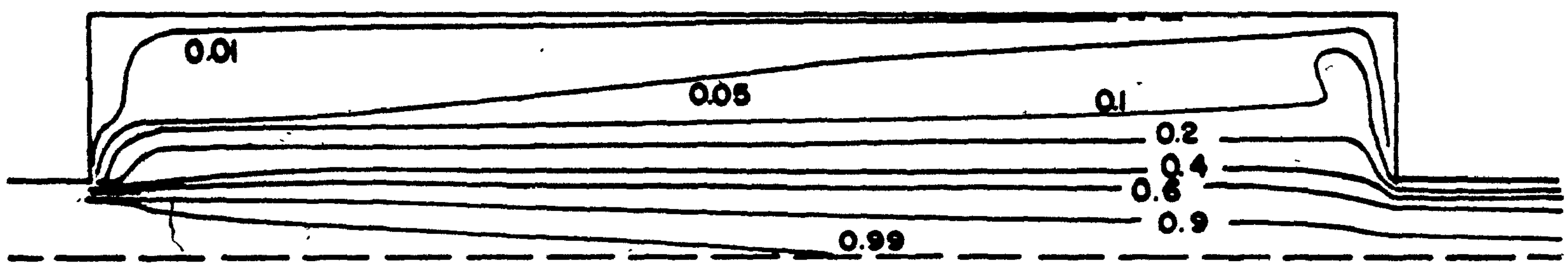

FIG. 3.13 (cont'd) - TEMPERATURE CONTOURS FOR NON-ISOTHERMAL FLOW IN REACTOR CHAMBER, $T_o = 3000^oK$, $T_w = 300^oK$

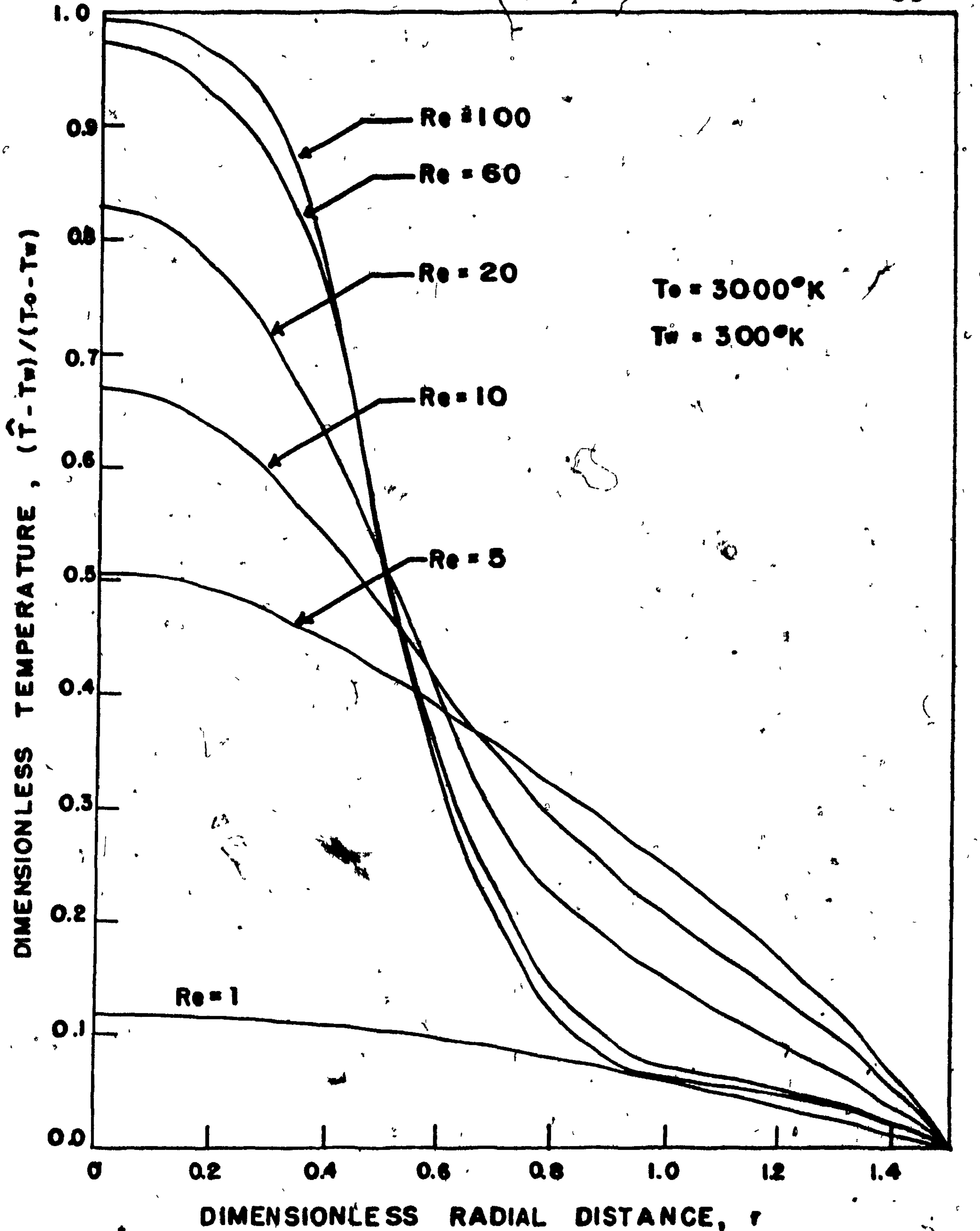

FIG. 3.14 – TEMPERATURE PROFILE AT $4D_o$ EXPANSION, T_o = 3000°K, T_w = 300°K

and the local Nusselt number is:

$$Nu = h_{coef} D_i / k_b \qquad (3.5\text{-}2)$$

where D_i is the diameter of the reactor and k_b is the thermal conductivity of the fluid evaluated at bulk temperature.

Figure 3.15 shows the dependence of the local heat transfer coefficient on the entry Reynolds number. As Re increases from 1 to 5, h_{coef} increases, and this corresponds to the increase in the length of the recirculation region (see Fig.3.11). The maximum in h_{coef} for Re = 1 occurs slightly downstream of the reattachment point. These findings are in agreement with the experimental results reported by Emerson (15), Krall and Sparrow (25) and Zemanick and Dougall (48) for separated turbulent flows. From Re = 5, an increase in Re results in a decrease in h_{coef}, whereas the recirculation length remains unchanged, and the maximum in h_{coef} moves to the downstream corner. In all cases, h_{coef} exhibits a minimum in the region of the upstream corner, which Fig.3.13 shows to be a zone of almost stagnant, cold gas. This is again in agreement with Emerson's results (15). Fig.3.16 shows the distribution of the local Nusselt number along the reactor. Since the bulk temperature of the gas increases with increasing Re, the resulting increase in the thermal conductivity leads to a remarkable decrease in the Nusselt number with Re. Both Figures 3.15 and 16 show that the effect of the entry Reynolds

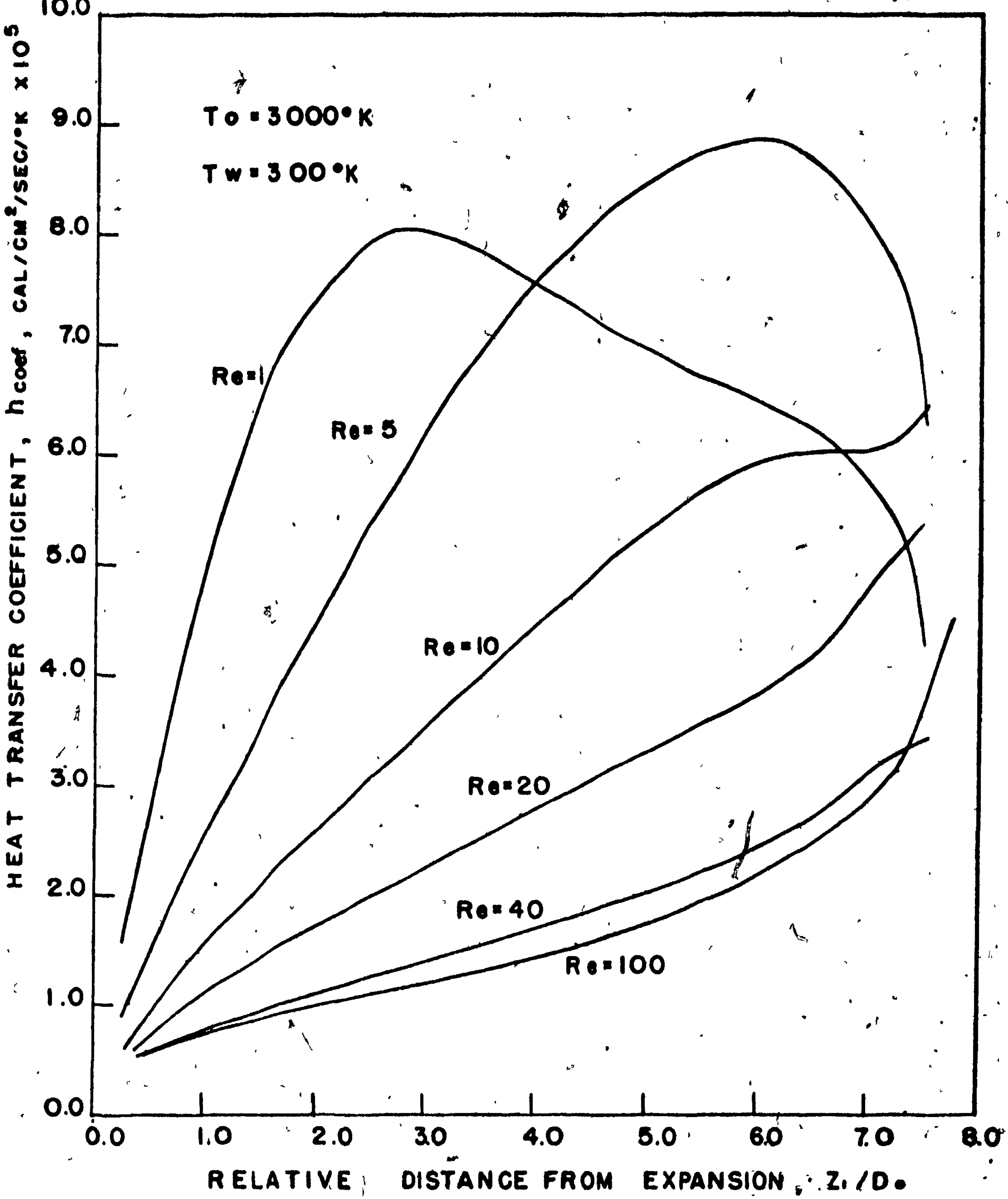

FIG. 3.15: VARIATIONS OF LOCAL HEAT TRANSFER COEFFICIENT, T_o = 3000°K, T_w = 300°K

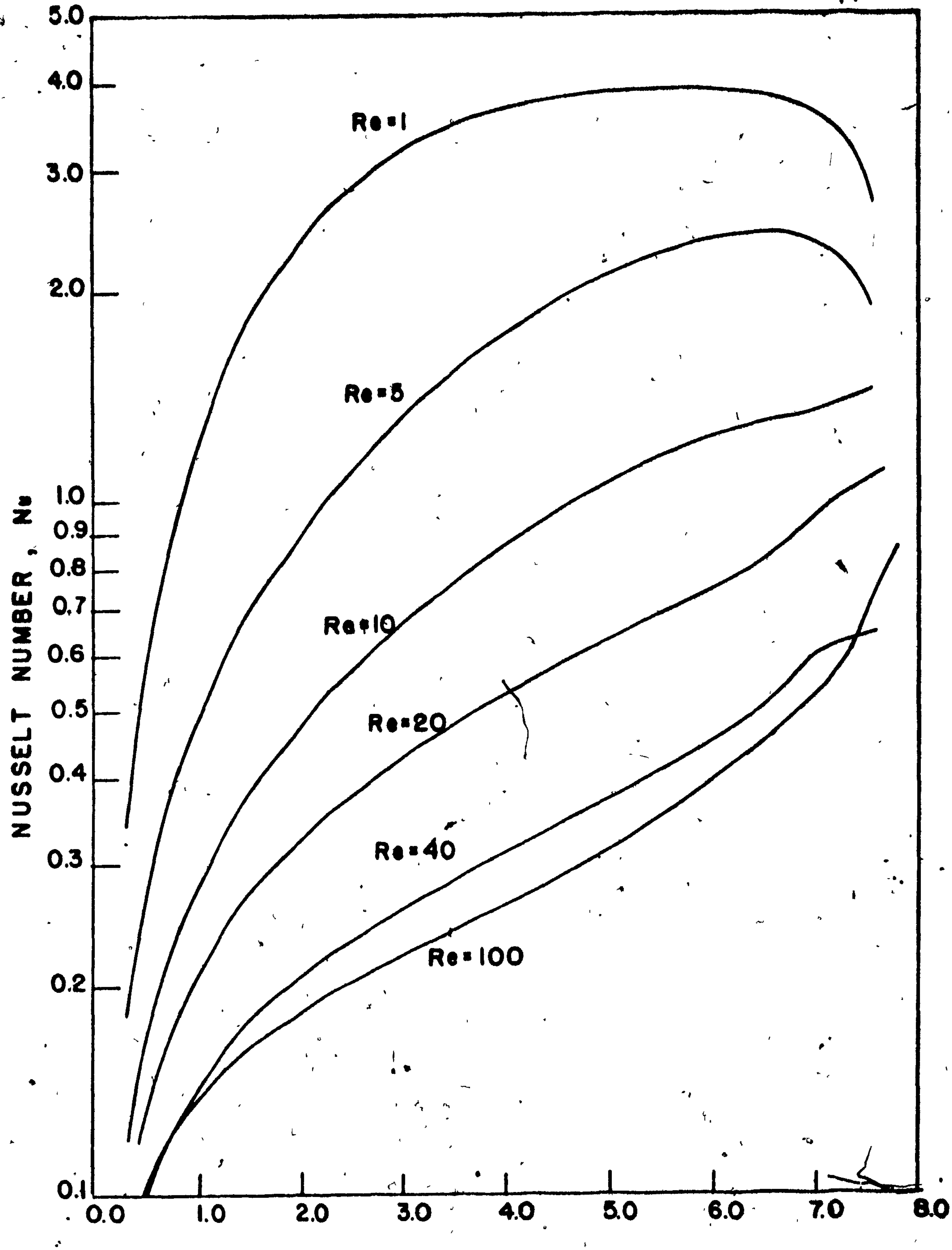

FIG. 3.16: VARIATIONS OF LOCAL NUSSELT NUMBER, T_o = 3000°K, T_w = 300°K

number becomes less important at higher Re.

The effect of the temperature of the entry tail flame is shown in Figs. 3.17 to 19, presenting respectively the flow pattern and temperature distribution of the flow field and the variations of the local Nusselt number for a flow atentry Re = 40 with the reactor walls at 300°K. Figure 3.17 shows that an increase in the inlet temperature leads to a stronger recirculation. It must be noted that an increase in the inlet temperature for the same entry Reynolds number corresponds to an increase in the mass flux since the viscosity of the fluid increases with temperature. Hence, an increase in the temperature of the entry flow would yield qualitatively similar effects to an increase in the Reynolds number. This can be seen clearly in Figs. 3.18 and 19: the hot gas core contracts and persists longer, and the local Nusselt number decreases as the entry temperature increases. However the heat transfer to the wall is increased with increasing entry temperature, the reverse trend in the Nusselt number resulting from the increase in the wall-to-bulk temperature difference is observed.

Similar effects are also obtained for a decrease in the wall temperature, since both an increase in the inlet temperature or a decrease in the wall temperature results in an increase in the inlet-to-wall temperature difference. Higher velocity (due to lower density) and thermal conductivity near the wall as T_w is increased cause the heat transfer rate and Nusselt number to increase with T_w. This is shown clearly

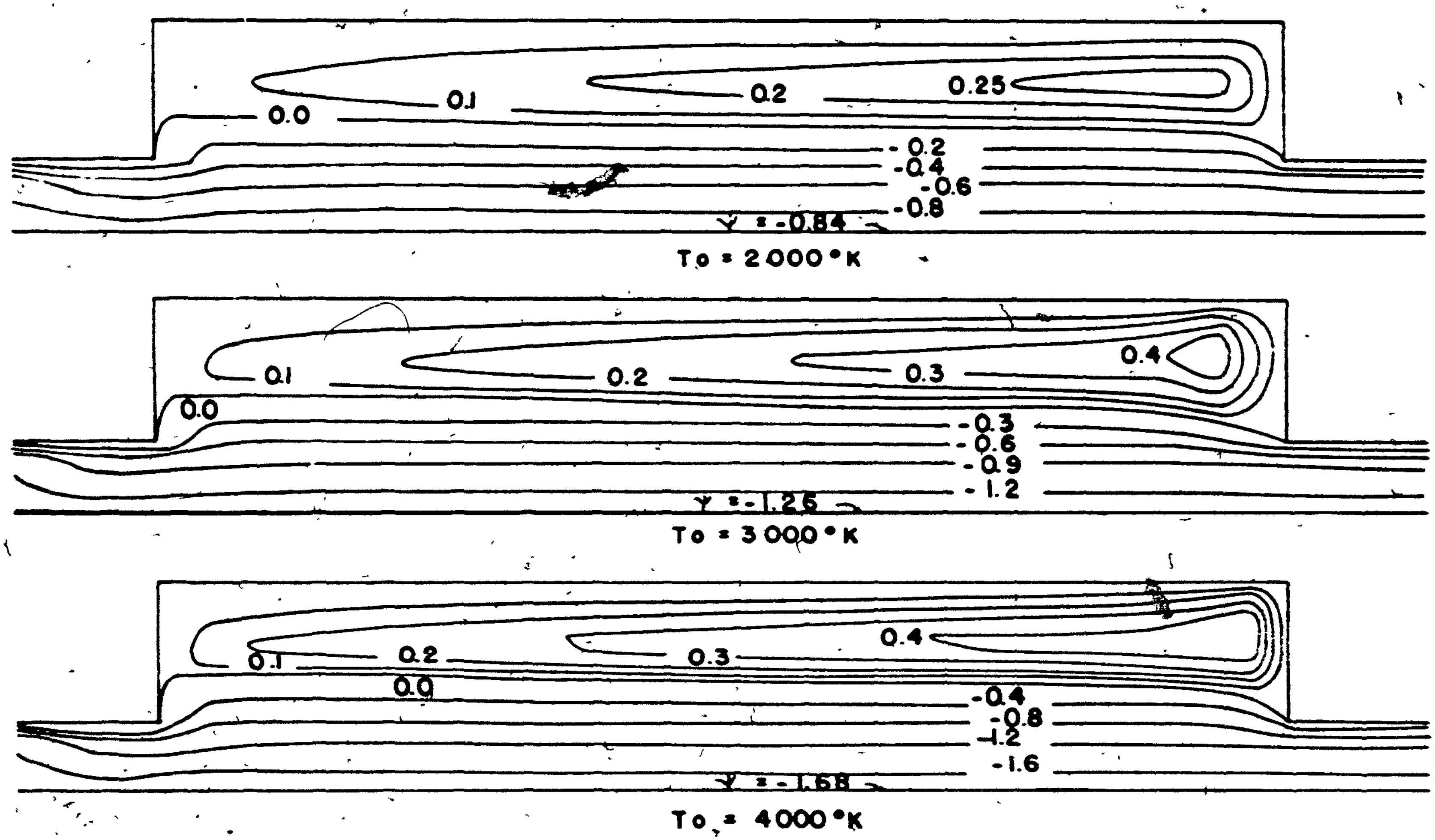

FIG. 3.17: EFFECT OF ENTRY TEMPERATURE ON FLOW IN REACTOR CHAMBER, T_w = 300°K, Re = 40

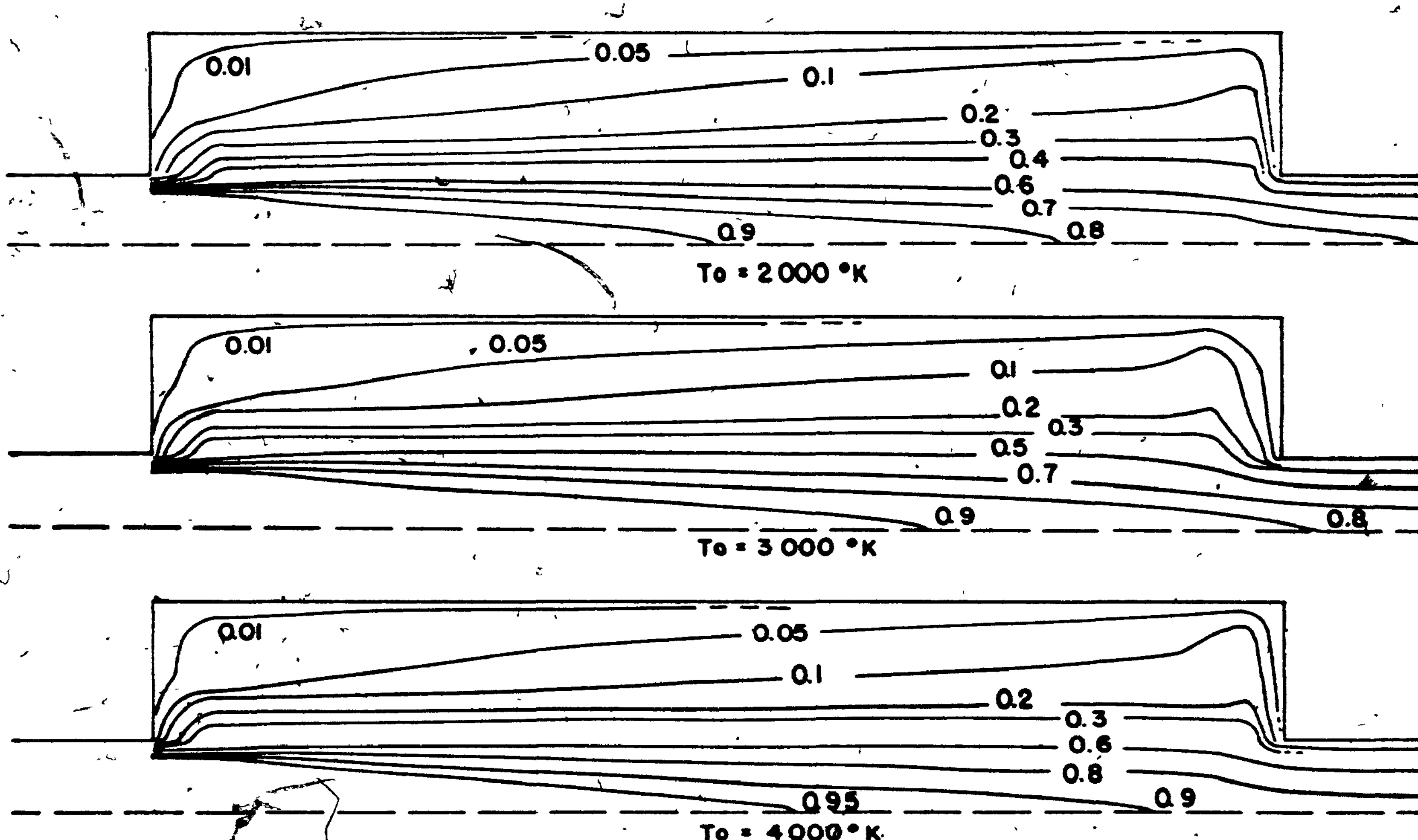

FIG. 3.18: EFFECT OF ENTRY TEMPERATURE ON TEMPERATURE DISTRIBUTION IN REACTOR CHAMBER, T_w = 3000°K, Re = 40

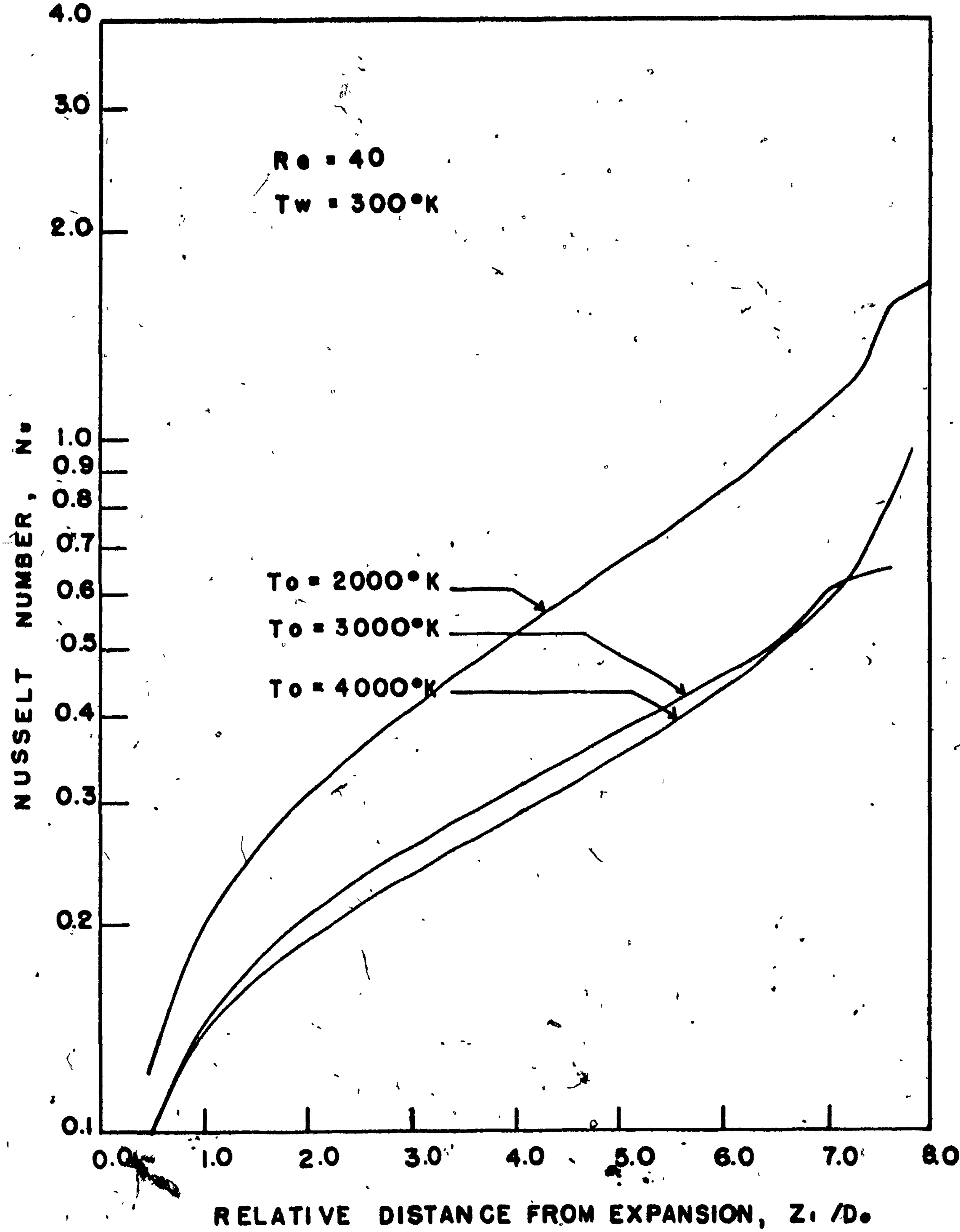

FIG. 3.19: EFFECT OF ENTRY TEMPERATURE ON LOCAL NUSSELT NUMBER, T_w = 300°K, Re = 40

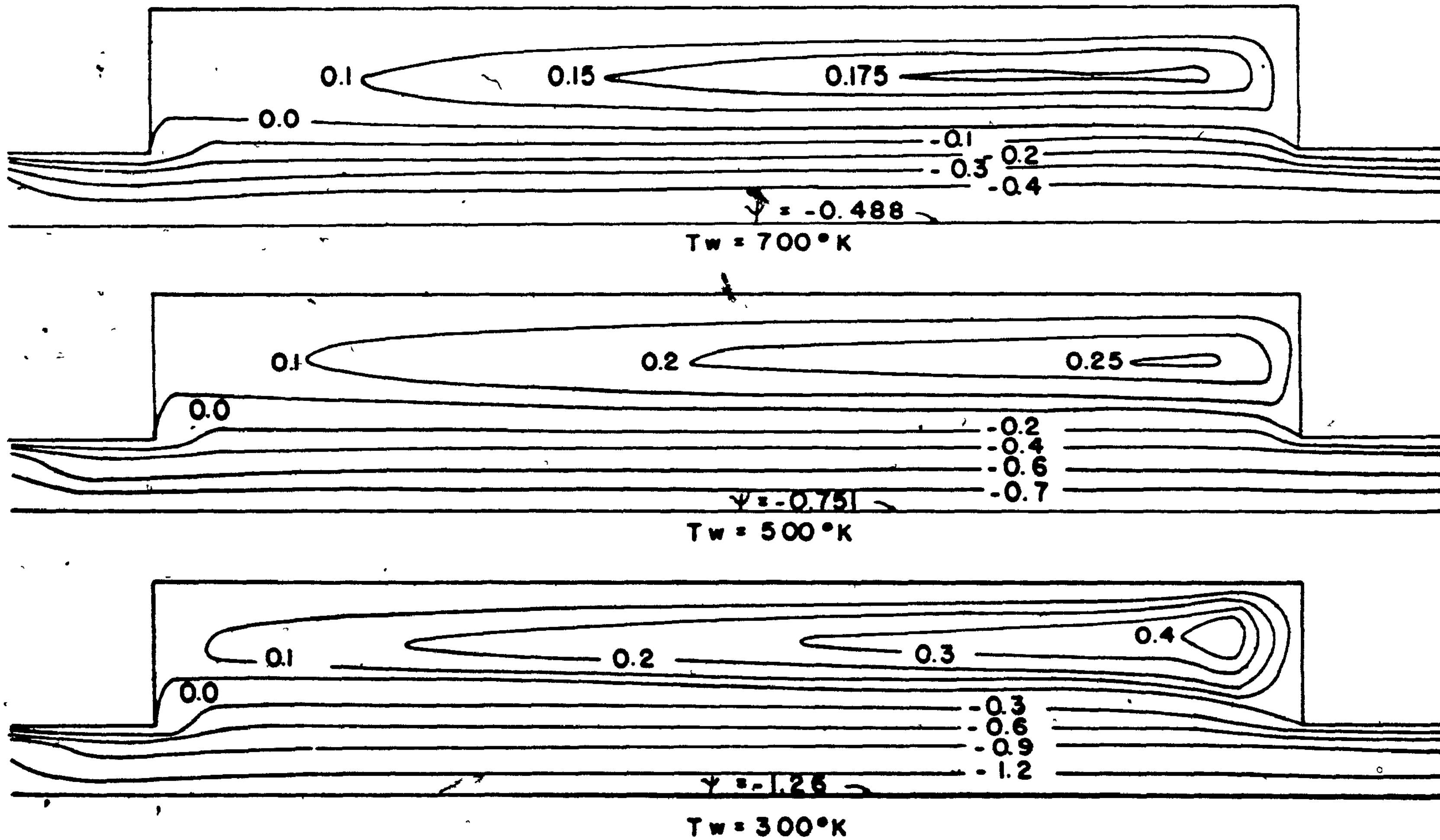

FIG. 3.20: EFFECT OF WALL TEMPERATURE ON FLOW IN REACTOR CHAMBER.
T_o = 3000°K, Re = 40

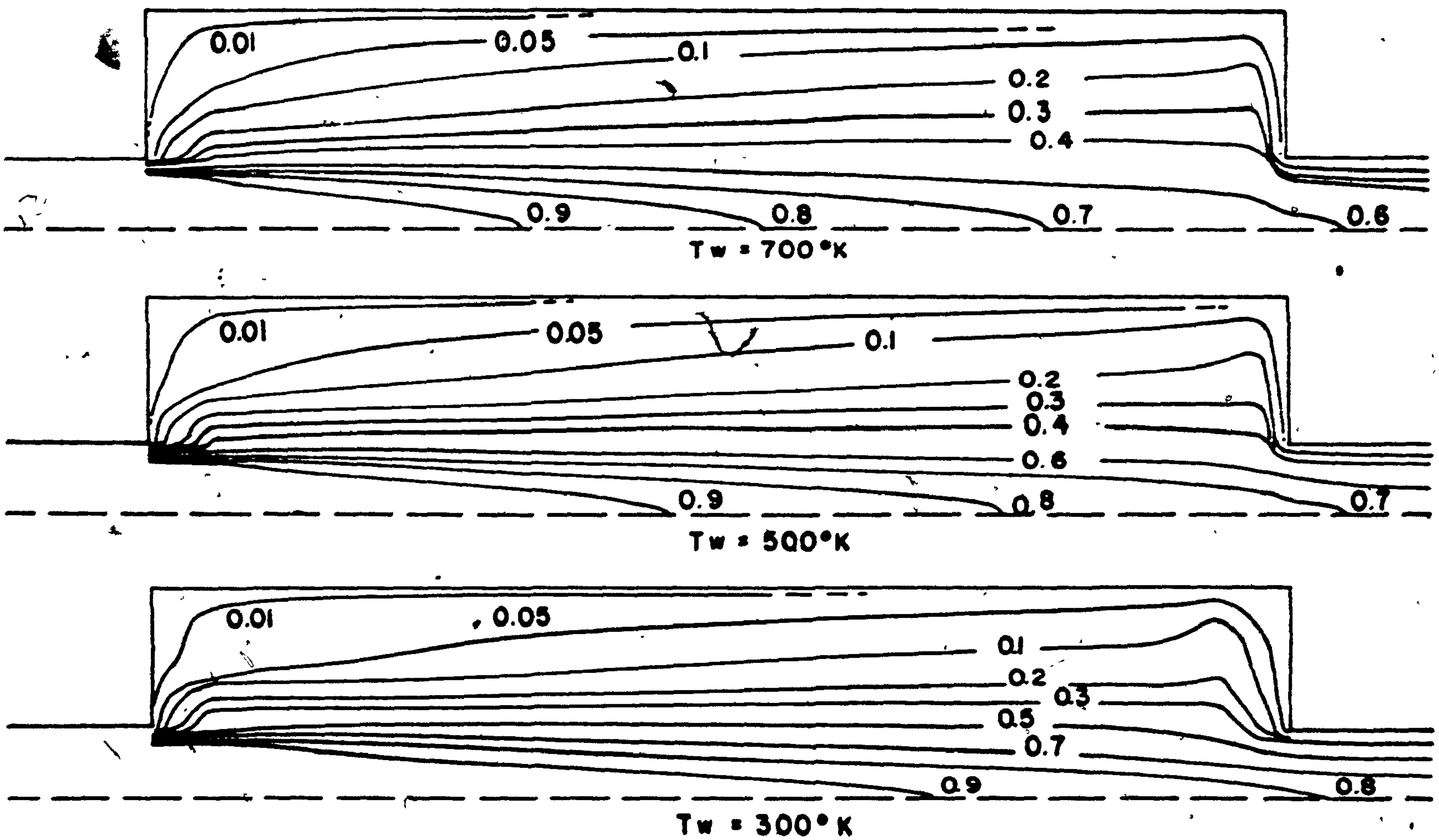

FIG. 3.21: EFFECT OF WALL TEMPERATURE ON TEMPERATURE DISTRIBUTIONS IN REACTOR CHAMBER, T_o = 3000°K, Re = 40

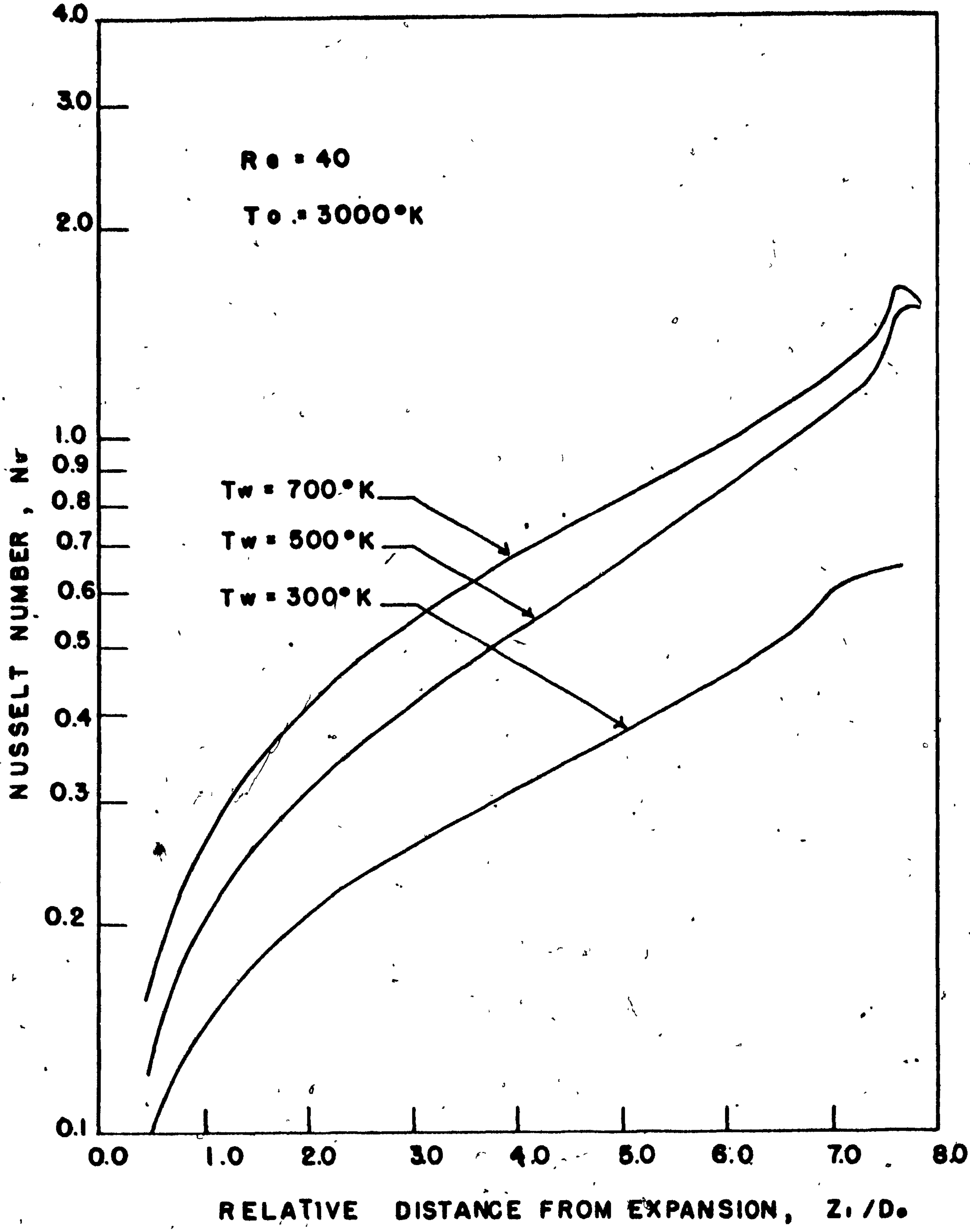

FIG. 3.22: EFFECT OF WALL TEMPERATURE ON LOCAL NUSSELT NUMBER, T_o = 3000°K, Re = 40

in Figs. 3.20 to 22, showing the effect of the wall temperature on the flow pattern and temperature distribution of the flow and on the variation of the local Nusselt number along the reactor. It may also be noted that the changes in the flow on raising T_w are generally tending towards the isothermal predictions, as should be expected.

3.6. CLOSURE

The numerical procedure used in this work predicts flow patterns following a sudden expansion in a circular conduit which agree quantitatively with previous simulations and with available experimental data. For isothermal flow in a sudden expansion and in the reactor geometry, it is predicted that recirculation occurs even at very low Reynolds number. The recirculation is very much stronger fow an Argon tail flame with temperature in the range of 2000°K to 4000°K entering a reactor whose walls are maintained at 300°K to 700°K. It is also predicted that the heat transfer coefficient depends largely on the length of the separation region. The local Nusselt number for heat transfer to the outside wall decreases as the Reynolds number or the entry temperature is increased, and as the wall temperature is decreased.

IV. EXPERIMENTS

An R.F. induction plasma generator has been installed in this laboratory, but experiments in a reactor attached to the generator were not feasible within the time-scale of the present project. Instead, a cold model of this reactor was used, designed to give approximate dynamic similarity. Sugar solutions were used for a low range of Reynolds numbers up to 130. The recirculation region and the velocity distributions at the center-line in the chamber were measured for comparison with the numerical solutions obtained for isothermal flows. The apparatus and methods used for the determinations of the flow field are now described in detail.

4.1 EXPERIMENTAL APPARATUS AND TECHNIQUES

4.1.1 Apparatus

A sketch of the apparatus used is shown in fig.4.1. The unit consists of a 65-gal. sugar-solution reservoir connected to a constant head tank. From here, the sugar solution flows through a gate valve, into a vertical pipe of 1-in.dia., and through the model, which is aligned with the axis of the pipe. The model itself consists of a conduit of 3-in. dia. and 8-in. long. The entry pipe is 10-feet long, enabling the flow, at Reynolds numbers below 2000, to attain a fully-developed parabolic profile before entering the model. This ensures agreement with a boundary condition used in the

Fig.4.1 EXPERIMENTAL APPARATUS

1,2. Reservoirs
3. Constant-Head Tank
4. Entry Pipe
5. Model
6. Exit Pipe
7. Rotameter
8. Bubble-generating wires
9. Anode
10. Plexiglass tank
11. Spot-lights
12. Circuit
13. Pulse generator
14. Pulse-counter
15. Pump

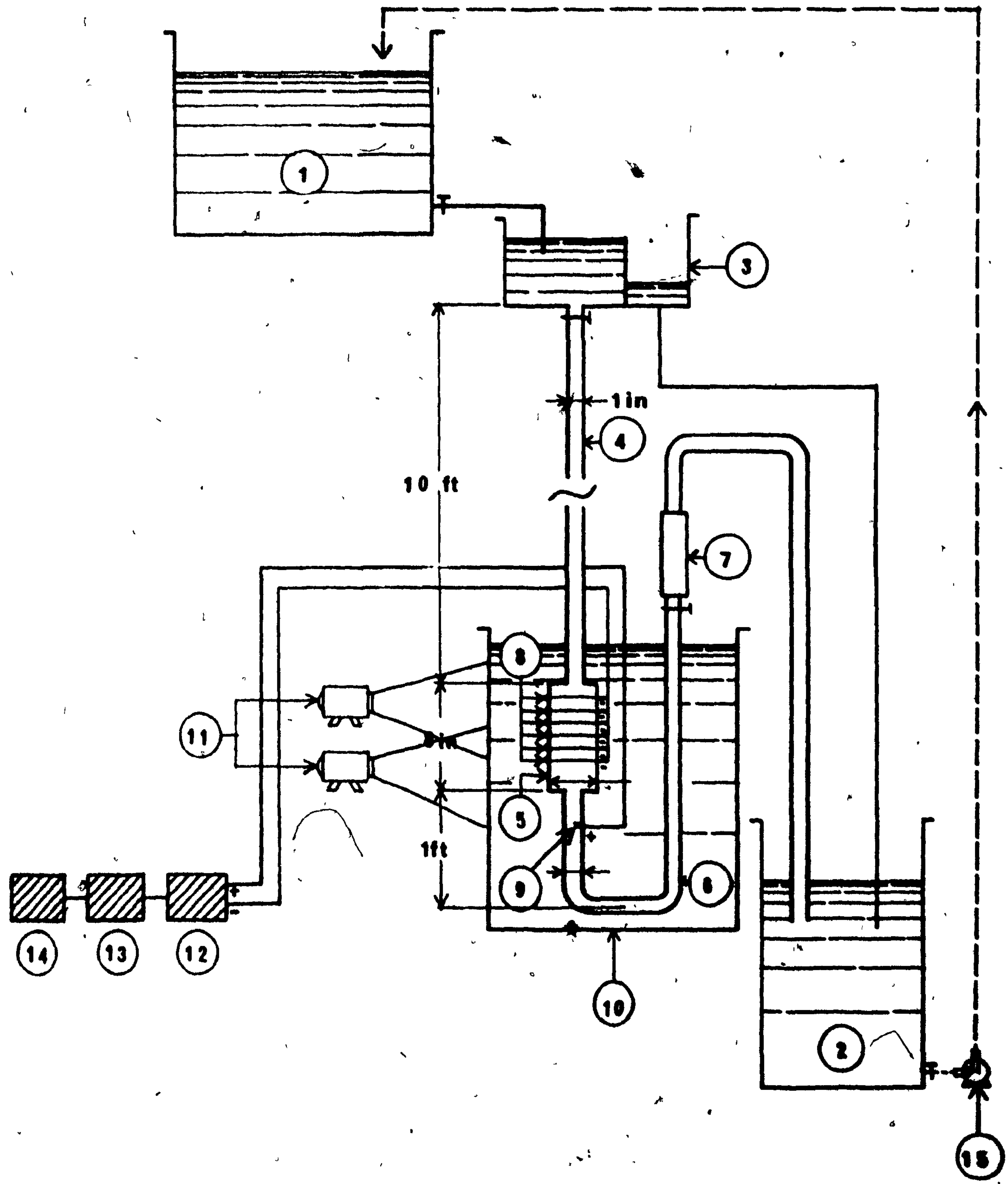

Fig. 4.1 EXPERIMENTAL APPARATUS

numerical analysis, as presented in section (2.4-10). The outlet of the model is another pipe of 1-in.dia., connected to a rotameter and a globe valve which enables control of the flow rate. From the control valve, the solution passes into a second reservoir. Both the model and the entrance and exit pipes were constructed of clear acrylic polymer ("plexiglass"). Between experimental runs, the solution was pumped back from the lower to the upper reservoir.

The flow within the model was observed by means of the Hydrogen bubble method developed by Geller (16). Electrolysis is used to generate Hydrogen bubbles to act as flow tracers. By proper control of working conditions, very fine Hydrogen bubbles could be made, to provide a visualization of the flow patterns that could be recorded photographically. In order to eliminate optical distortion due to the curvature of the surface of the chamber and the difference in refractive indexes of the media, the chamber was immersed in a rectangular tank filled with the working solution and photographed in a direction normal to the face of the outer tank.

4.1.2 Hydrogen Bubble-Method

Electrolysis was achieved by employing a fine wire of 0.001-in. dia. as the cathode of a D.C. circuit. The wire was strung across the chamber, normal to the direction of the flow, by means of two needles inserted in the center of rubber stoppers attached to the walls, as shown in Fig.4.6. The metal anode was inserted in the exit pipe downstream from the model, so that it did not interfere with the flow. The Hydrogen bubbles, formed at the wire, are swept off by hydrodynamic forces and, providing they are sufficiently small, follow the flow. The electric circuit employed is shown in Fig.4-2. Since the wire generating Hydrogen bubbles is so fine, it scarcely disturbs the flow pattern. The size of the Hydrogen bubbles formed at the wire is of the order of one-half of the wire diameter (36), so that their rise velocity is negligibly small.

The voltage required is a function of electrolyte concentration, the distance between electrodes, and the geometry. A variable working-voltage supply from about 10 to 400 volts was used, and Sodium Sulfate was added to the solution as electrolyte. About 0.15g/liter of Na_2SO_4 was sufficient in most cases. With solutions more viscous than about 0.10 poise, it was found that the Hydrogen bubbles tended to adhere to the wire until they coalesced to form large bubbles, which then detached. To eliminate this problem, surface active agents were used: about 0.02 g/liter of Sodium Lauryl Sulfate and 1.5% of iso-propyl alcohol were added to the sugar solution.

The voltage applied to the wire was pulsed at regular intervals of time to generate a series of rows of Hydrogen bubbles, so called "timelines", that assumed the shape of the

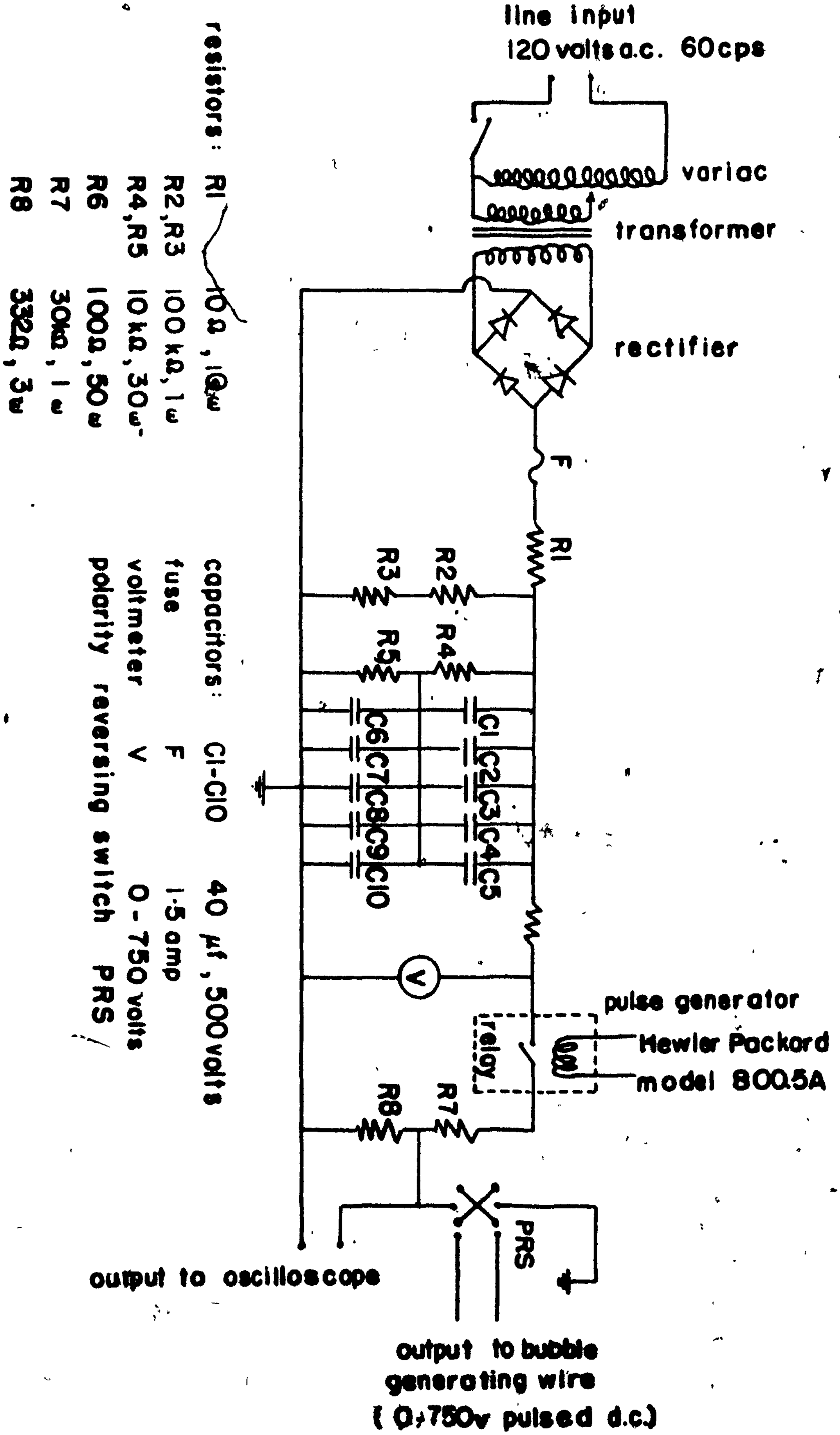

Fig.4.2 CIRCUIT DIAGRAM

velocity profile.in the chamber. This pulsing was accomplished by an electric pulse generator, manufactured by Hewlet-Packard Company, model 8005A, that gave pulse frequencies from 0.3 Hz to 10 MHz and pulse widths from 01. μsec to 3 sec duration.

The wire was made of Platinum with 13% Rhodium. Platinum was chosen because it does not corrode and appears to accumulate dirt less rapidly (36), while platinum with added rhodium is stronger and has a better electrochemical property than the pure metal (28).

Since Hydrogen is soluble in water, the bubbles generated at the wire rapidly dissolve. The half-life of the bubbles is very short, typically 3 sec. for the bubble size used in this work (36). To remedy this problem and provide a complete visualization within the model, 6 wires were inserted at different locations in the flow field. By using one wire at a time as the cathode, a complete picture of the whole flow field was obtained.

4.1.3 Lighting

The bubbles generated from the wire are hardly visible and require careful illumination. The optical arrangement is shown in Fig.4.3. The light source consisted of two spotlights with 1000 W, 120 volts tungsten iodine bulbs. The source was adjusted to give a plane 1/2 to 3/4 in. thick of intense light in order to prevent stray light from scattering in the water. According to Tory and Haywood (44) and Schraub

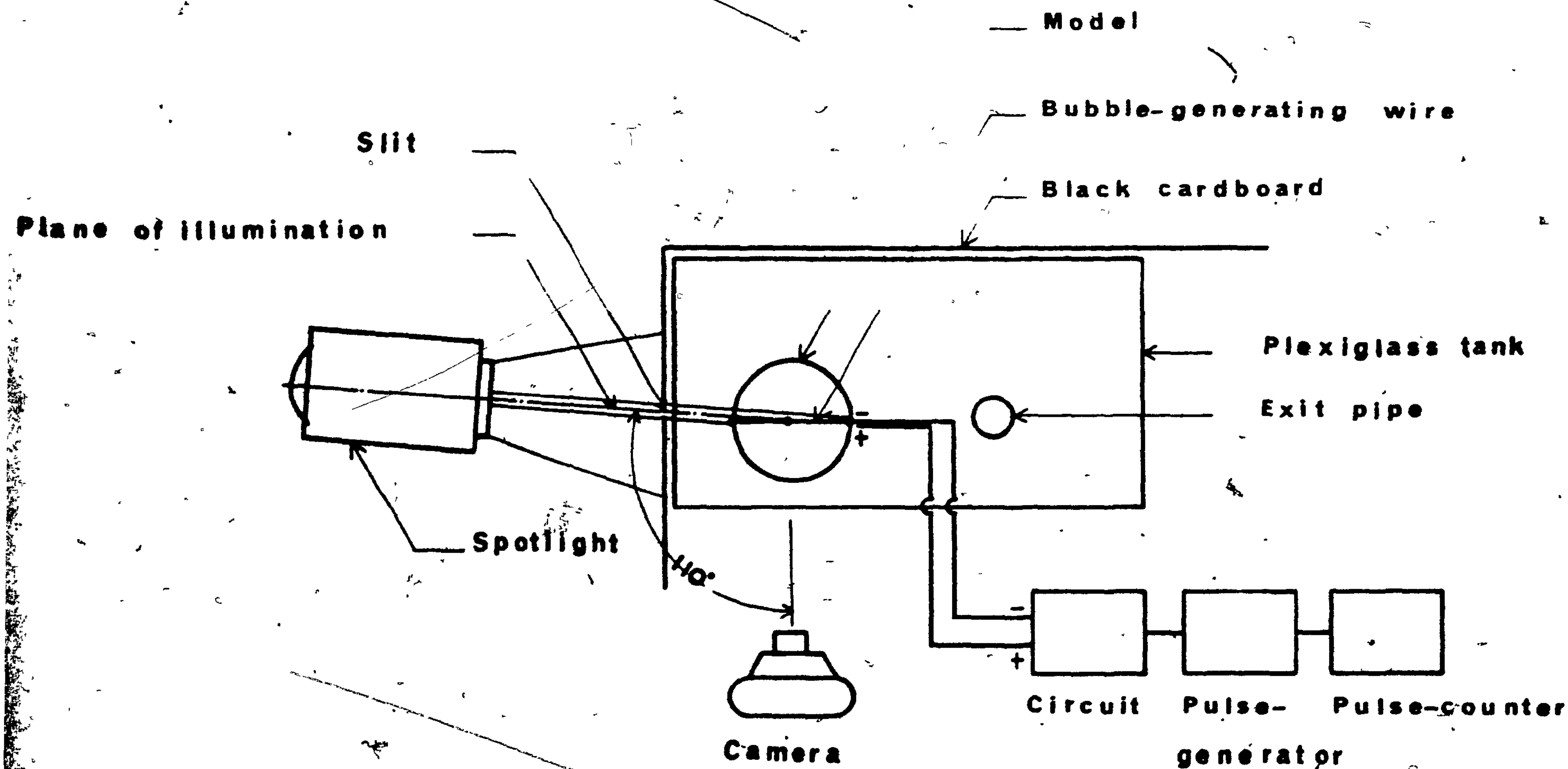

Fig.4.3 OPTICAL ARRANGEMENT

and Kline (36), the best illuminated view is obtained when, due to refraction, the plane of illumination is approximately 110° from the viewing angle. Dark background was used and all incident light other than the collimated sheet was minimized.

Photographic records were obtained with a fast film (400 ASA).

4.2 EXPERIMENTAL RESULTS AND DISCUSSIONS

4.2.1 Qualitative Observations

The Hydrogen bubble rows generated from the wires, one at a time, at regular intervals of time enabled a visualization of the flow field in the reactor model. For all Reynolds numbers up to 150, an annular captive eddy in the corner below the expansion was observed. The free boundary layer which lies between the recirculation region and the entering jet was rendered clearly visible, as shown in Figs. 4-6-12.

An interesting aspect of the flow was observed in this region during the early stages of the development of the flow: this is a varicose instability, similar to that reported by otherworkers for pipe jets at higher Reynolds numbers (22,49,50). Axisymmetric waves starting from the shoulder of the expansion were observed to grow in amplitude as they were propagated along the free boundary layer. Eventually, they became so strong that the boundary layer was broken and rolled back into a succession of ring vortices, which disintegrated as they approached the reattachment point. The resulting flow pattern is sketched in Fig. 4-4. However, these fluctuations died out quickly with time, and the flow appeared smoother and more stable. After this initial disturbance in the upstream region had died away, another transient feature became apparent in the downstream flow beyond the reattachment point. A region of flow reversal was observed between the positive velocity core and the wall. The disturbance was asymmetric,

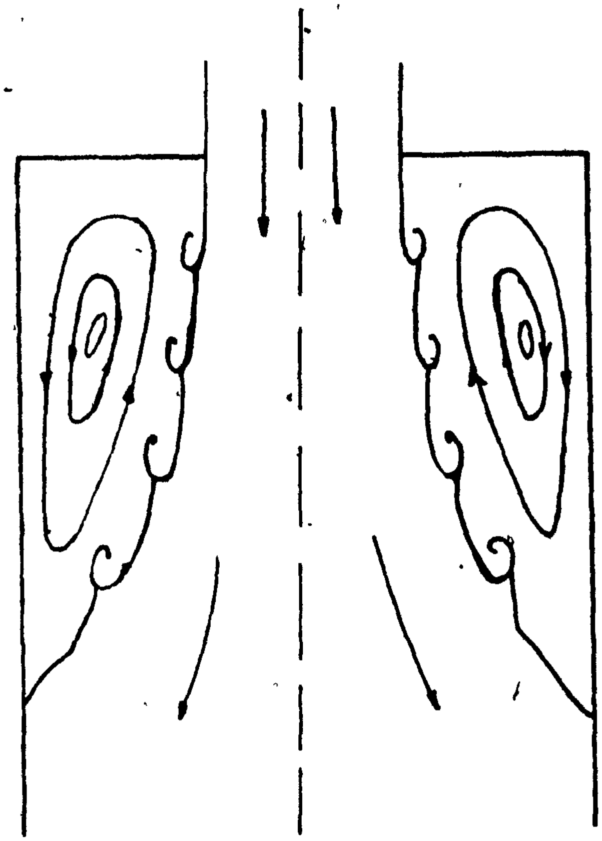

Fig.4.4 VARICOSE FLUCTUATIONS IN THE DEVELOPMENT OF THE FLOW

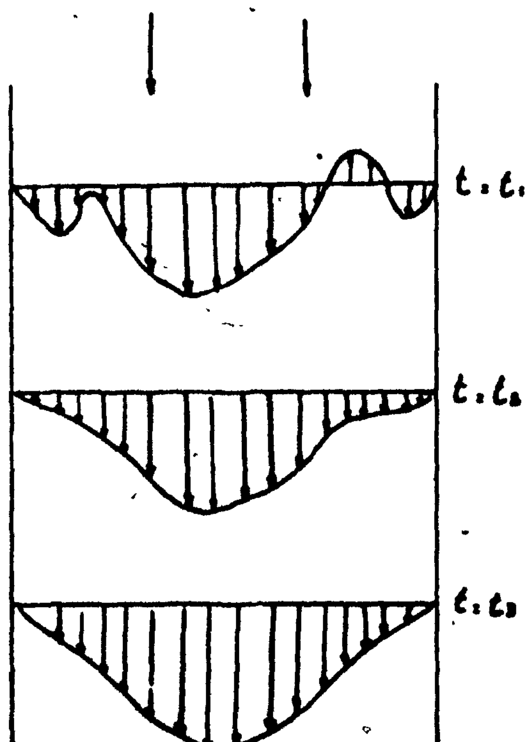

Fig.4.5 DEPARTURE FROM AXI-SYMMETRY IN THE DEVELOPMENT OF THE FLOW: VELOCITY PROFILE OF DOWNSTREAM FLOW AT DIFFERENT TIMES, $t_3 > t_2 > t_1$

with stronger backflow on one side of the reactor than on the other. A sketch of a typical velocity profile in this region at different times is shown in Fig.4-5. A similar phenomenon has been reported by Iribarne et al (22). The departure from axi-symmetry damped out gradually and finally, the flow became completely stable and axi-symmetric. At this point, steady-state was assumed to have been attained. Iribarne et al (22) reported that regular oscillations in the detached shear layer and fluctuations of the reattachment point were present even at the steady state for a pipe jet in an abrupt expansion, but these were not apparent in steady flows in the present experiments.

4.2.2 Quantitative Results and Discussions

Typical photographs of the hydrogen bubble rows generated from the wires are presentedin Figures 4.6-12, for a range of entry Reynolds numbers up to 103. The hydrogen bubble rows, as well as the dimensions of the laminar jet in the conduit are rendered clearly visible, thus enabling quantitative measurements.

Figures 4.13 and 14 show a comparison of the width of the jet within the conduit, bounded by the edge of the recirculation region, between the experimental measurements and the computational predictions for flow with the same entry Reynolds number. The agreement is satisfactory for the upstream half of the conduit, where the experimental measurements are obtainable.

'Figure 4.6

PHOTOGRAPH OF HYDROGEN BUBBLE ROWS FOR FLOW IN THE REACTOR MODEL AT Re = 34.8

Figure 4.7

PHOTOGRAPH OF HYDROGEN BUBBLE ROWS FOR FLOW IN THE REACTOR MODEL AT Re = 34.8

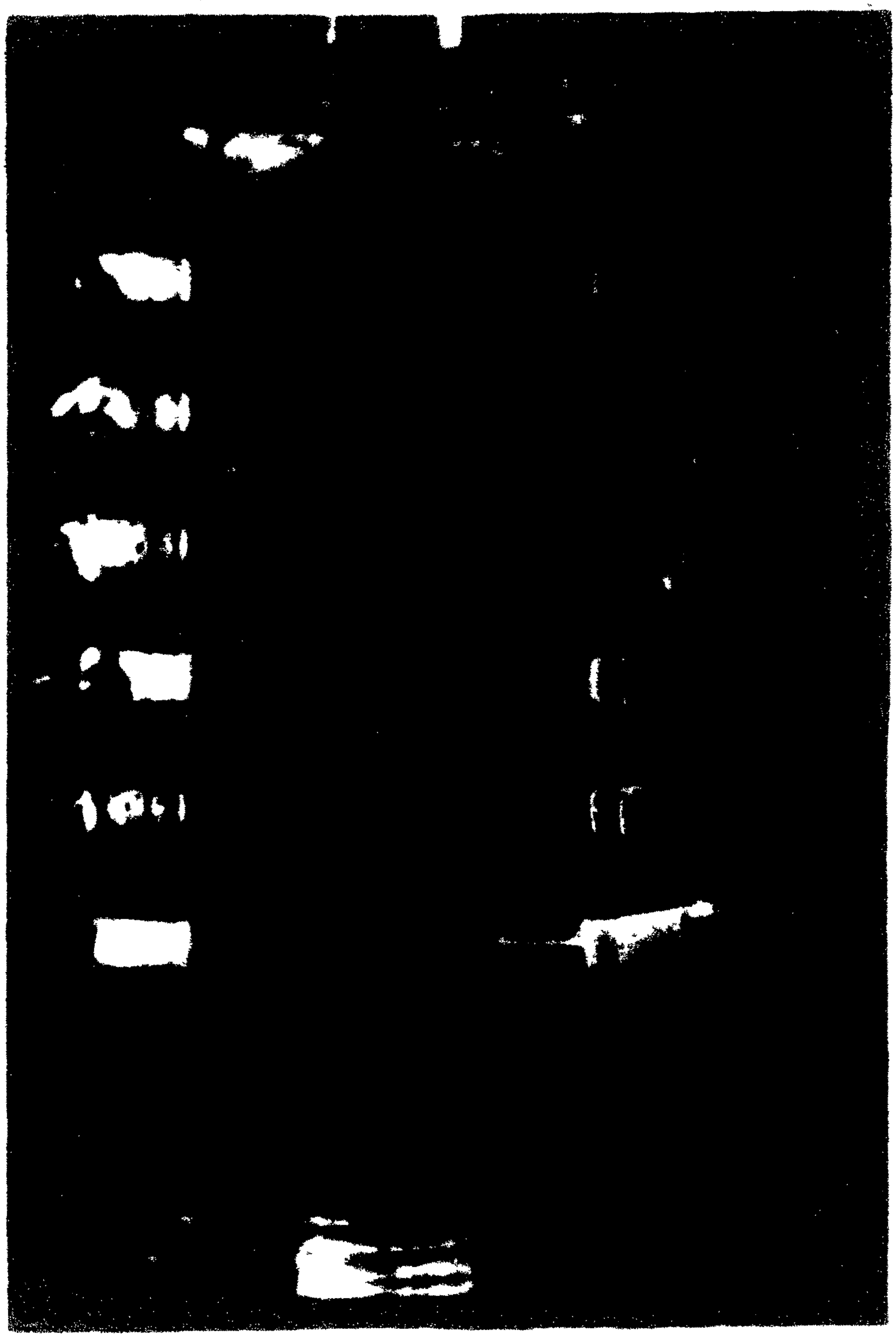

Figure 4.8

PHOTOGRAPH OF HYDROGEN BUBBLE ROWS FOR FLOW IN THE REACTOR MODEL AT Re = 49.6

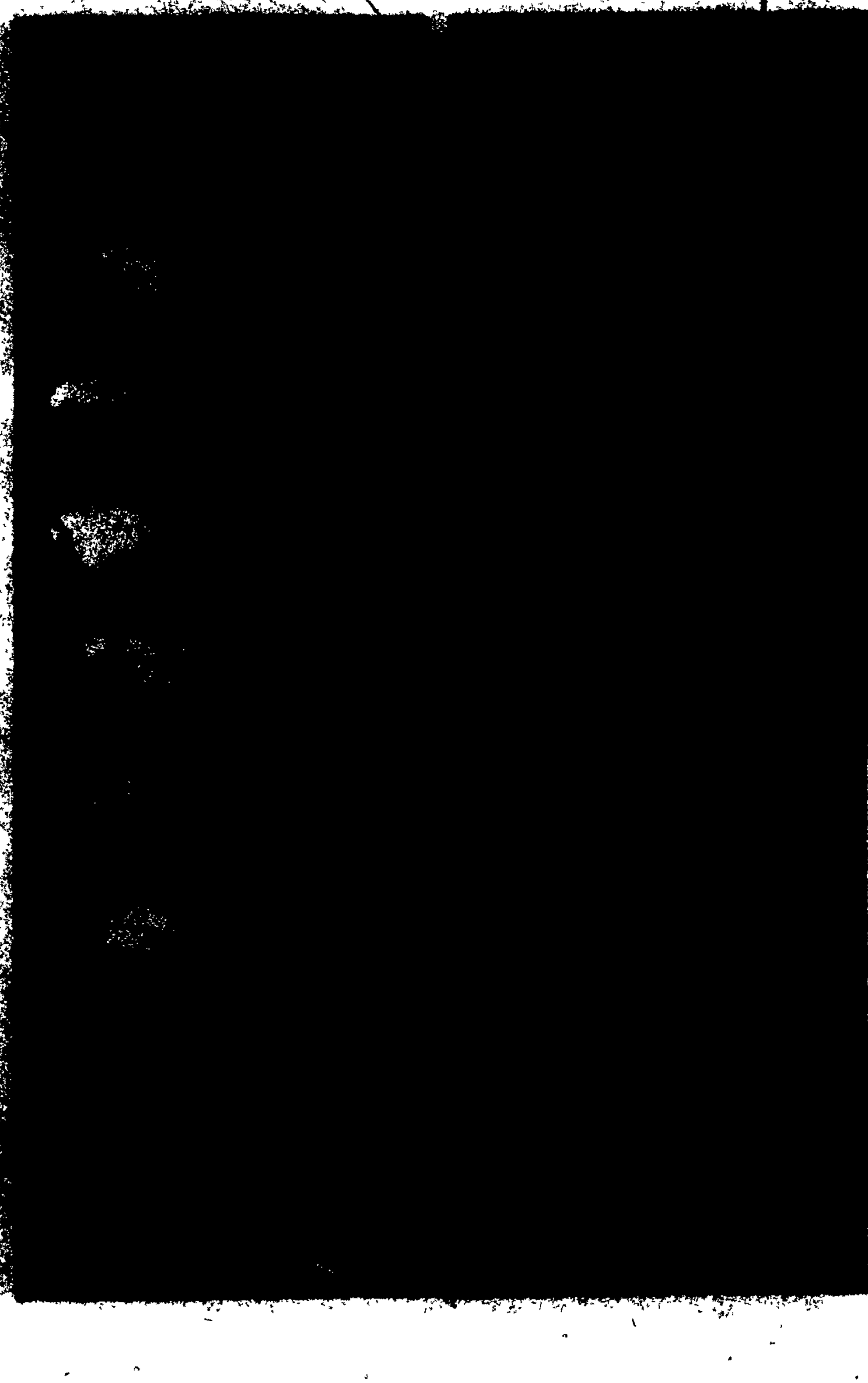

Figure 4.9

PHOTOGRAPH OF HYDROGEN BUBBLE ROWS FOR FLOW IN THE REACTOR MODEL AT Re = 64.55

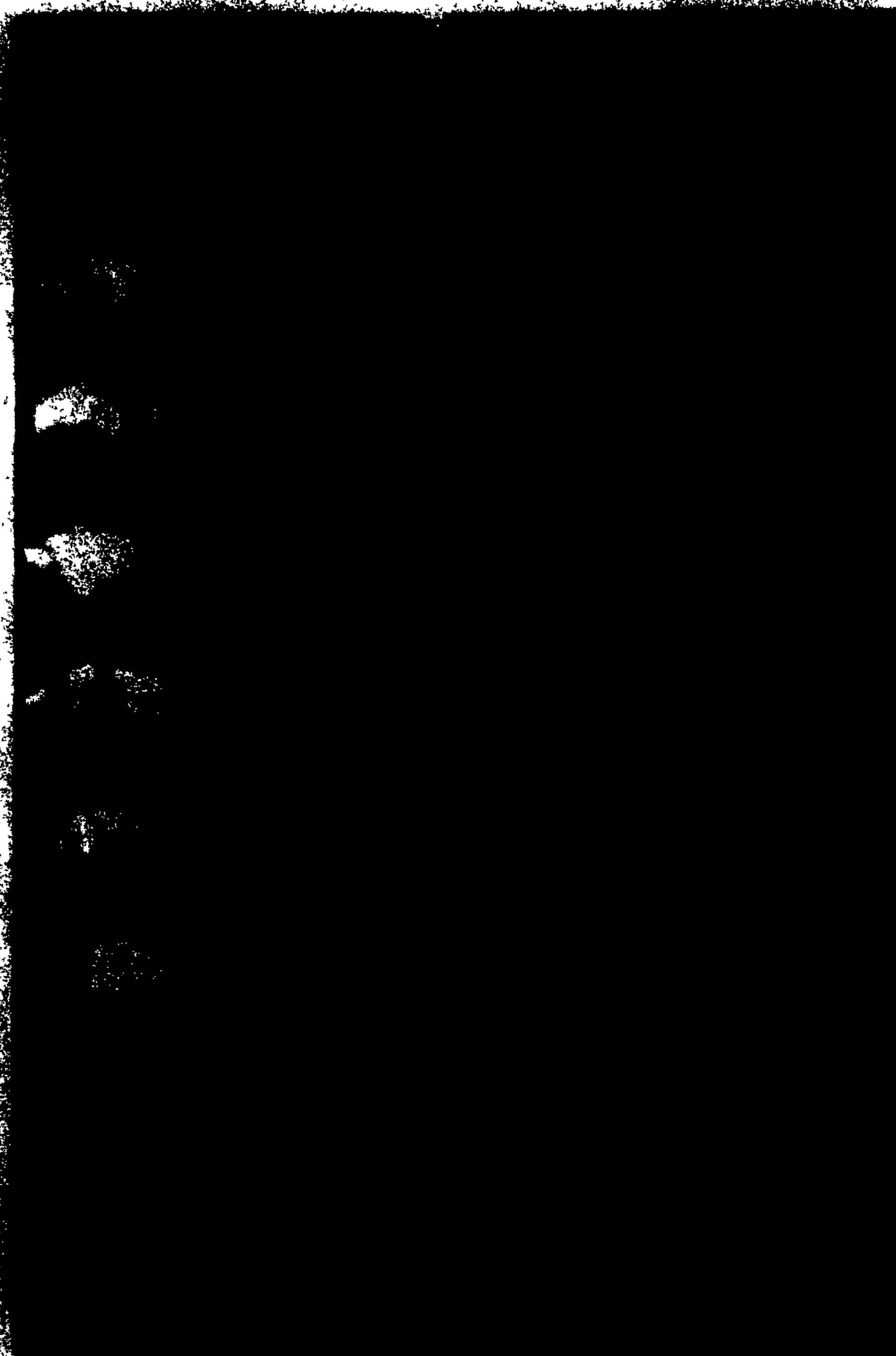

Figure 4.10

PHOTOGRAPH OF HYDROGEN BUBBLE ROWS FOR FLOW IN THE REACTOR MODEL AT Re = 77.5

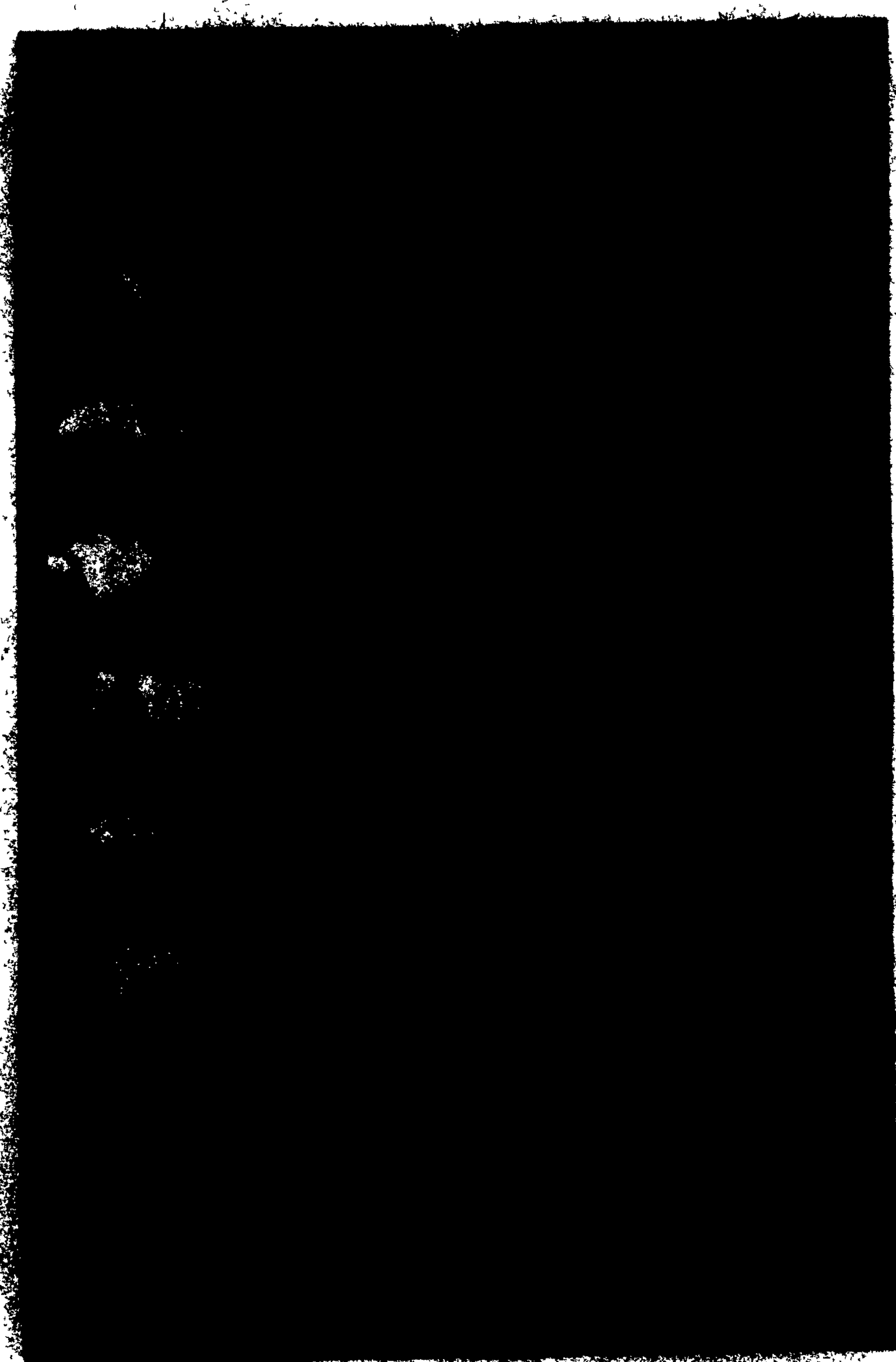

Figure 4.11

PHOTOGRAPH OF HYDROGEN BUBBLE ROWS FOR FLOW IN THE REACTOR MODEL AT Re = 77.5

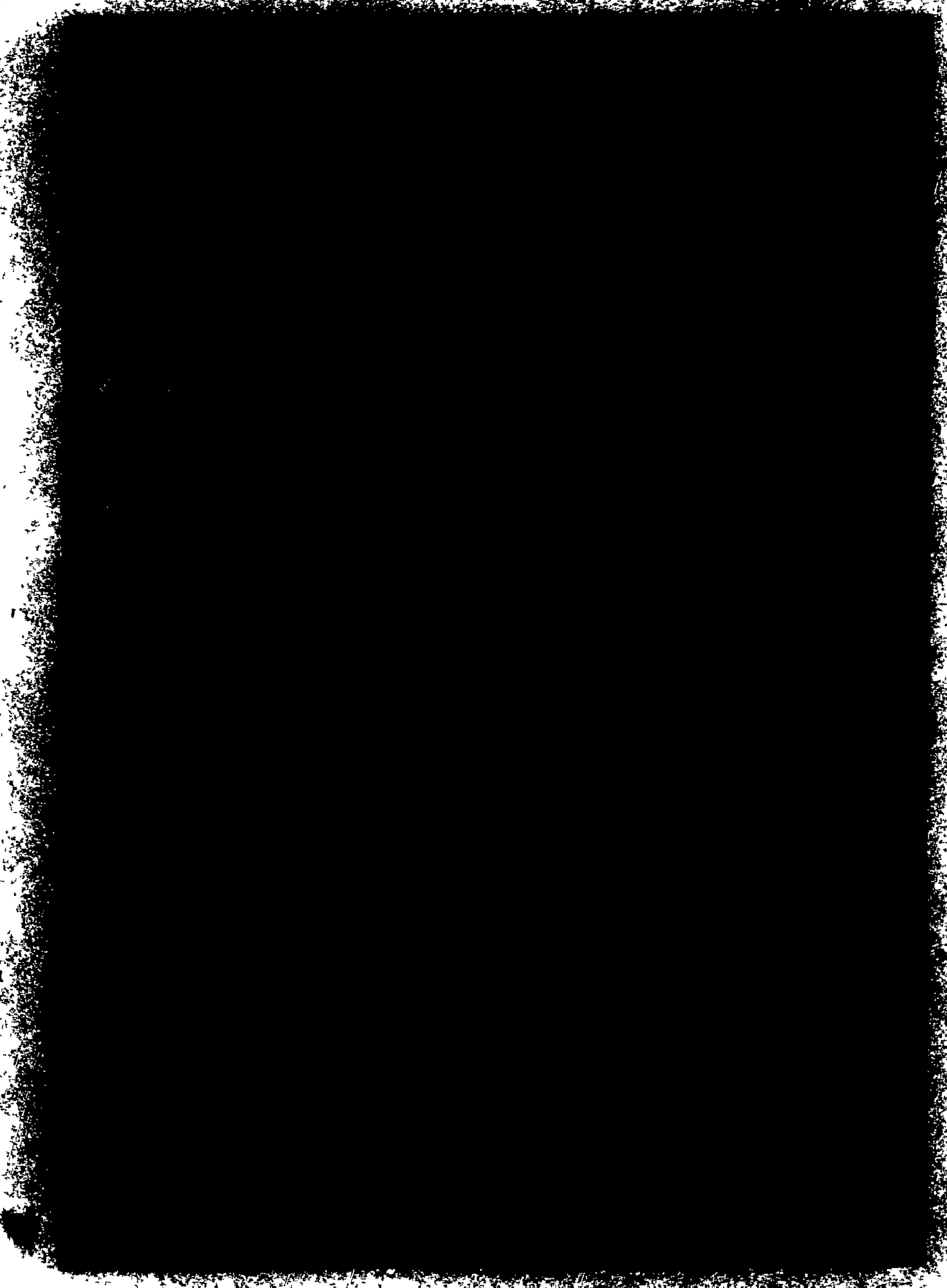

Figure 4.12

PHOTOGRAPH OF HYDROGEN BUBBLE ROWS FOR FLOW IN THE REACTOR MODEL AT Re = 103.76

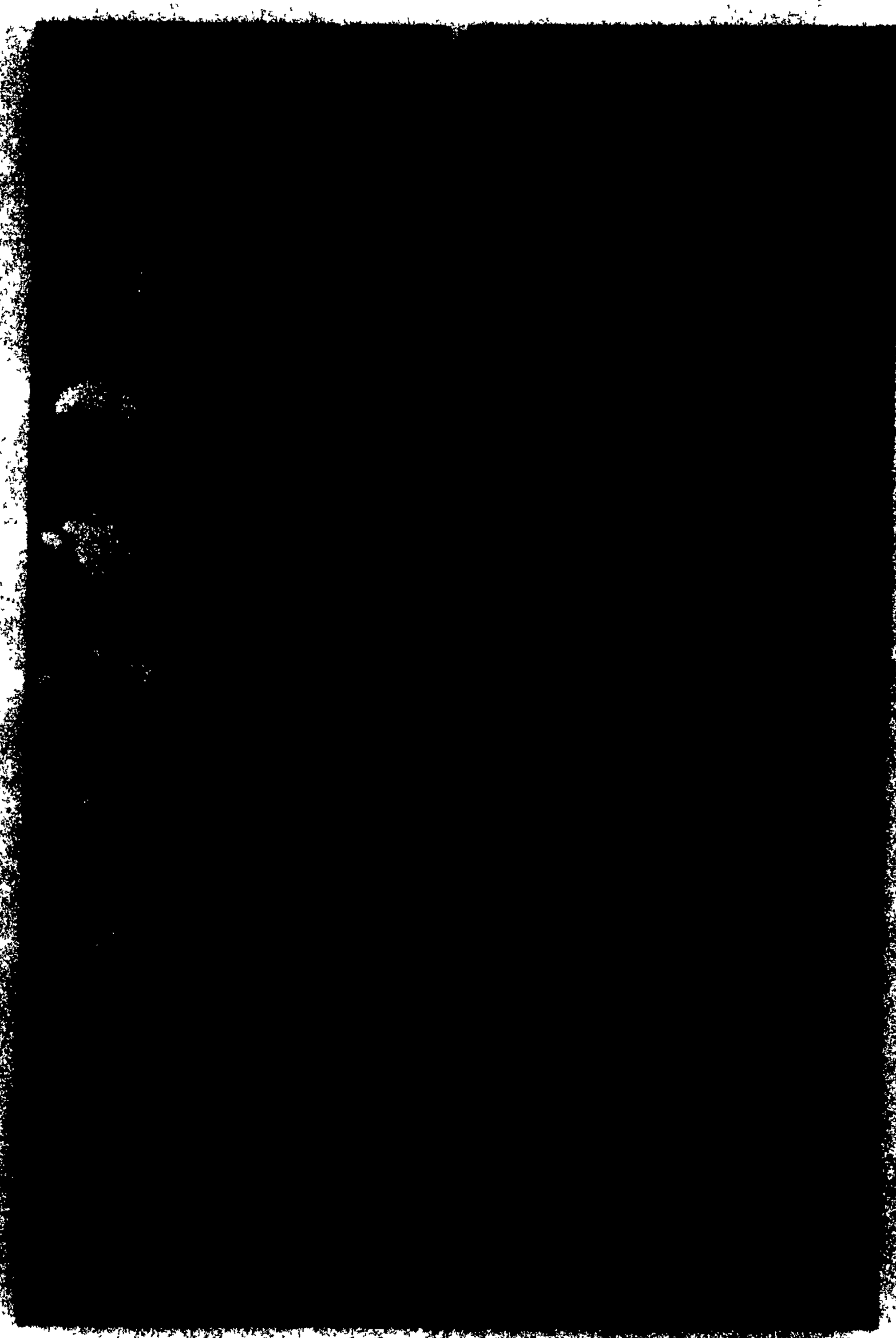

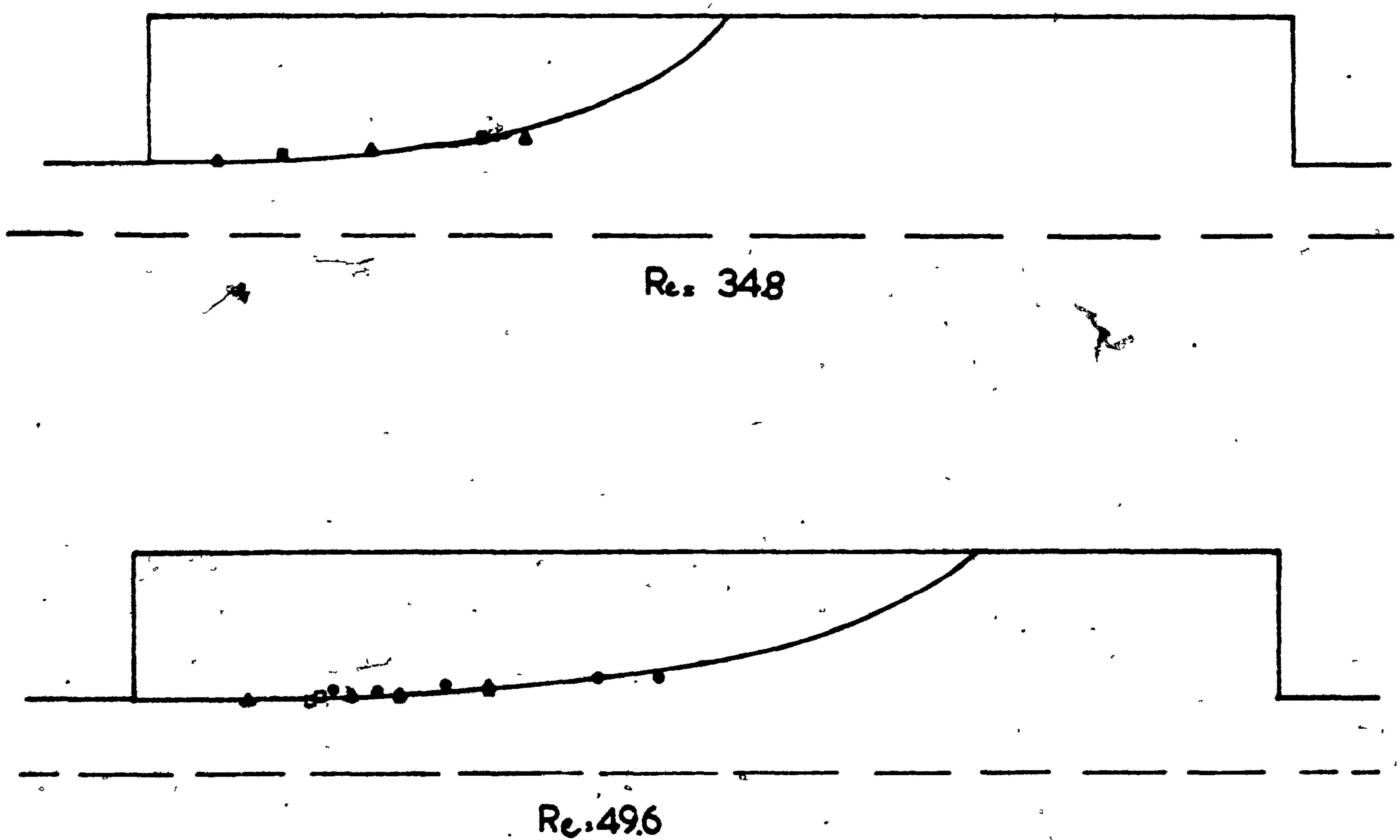

Fig.4.13 COMPARISON OF RESULTS FOR THE EDGE OF RECIRCULATING EDDY

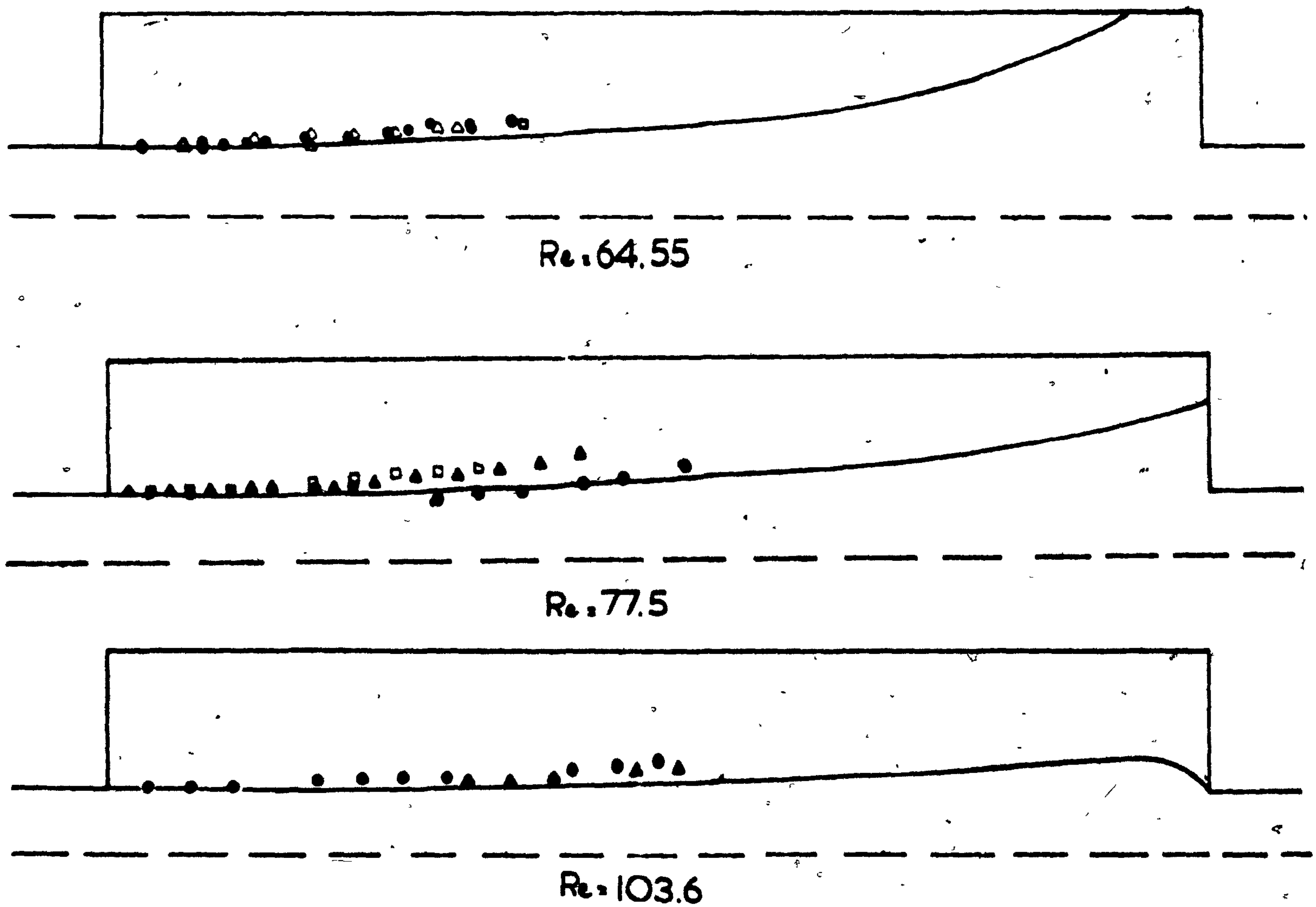

Fig.4.14 COMPARISON OF RESULTS FOR THE EDGE OF RECIRCULATING EDDY

The local space average of the center-line velocity was determined by measuring the distance between the peaks of the bubble rows which lie along the center line, applying a space scale factor and dividing by the time between the electric impulses. It must be noted that, at the centerline, the radial velocity of the fluid is zero, while the rise velocity of the bubbles owing to buoyant effect and the velocity defect caused by the wake behind the wire, discussed below, are in the axial direction. Hence, the pathline of the bubbles which are originally on the centerline would be the centerline itself. Figs. 4.16-20 present the dimensionless centerline velocity measured at different entry Reynolds numbers, along with the computed curve. It is obvious that the measured values differ appreciably from those predicted. This difference is believed to be the results of one or both of the following causes. There may be a significant slip velocity between the bubbles and the surrounding fluid, or the wires may disturb the flow and cause a velocity defect on the centerline. These are discussed separately in the following sections.

(a) Motion of Hydrogen bubbles relative to the surrounding fluid

As soon as the hydrogen bubbles are free from the wire, they start to rise in the vertical direction under the action of the buoyant force. The highest entry Reynolds number that was investigated in the present experiments was 105. The bubble generating wire used was 0.001 in. in dia., and therefore, the Reynolds number based on bubble diameter, assumed to be of the order of the wire diameter at the largest, and center-line-velocity must be 0.17 or less. For such small bubbles in the presence of surface active agents, the terminal rise velocity of the bubbles may be approximated by using Stokes solution for solid spheres (8). The result is:

$$v_B = \frac{2(\rho - \rho_B)}{g\mu} a_B^2 \qquad (4.2\text{-}1)$$

For bubbles of 0.001 in. dia. (a_B = 0.0005 in.) in sugar solution with a kinematic viscosity of 18.68 centistokes, the terminal rise velocity attained will be 1.9 x 10^{-6} cm/sec, which is completely negligible compared to the surrounding fluid velocity, as confirmed by other workers (9,11,16,36,44).

(b) Velocity defect behind the bubble generating wire - The disturbance to the overall flow pattern because of the existence of the bubble generating wire is the factor that limits the applicability of the method to the low Reynolds number regime. This disturbance is shown in Fig.4.15, where Fig.4.15a represents the velocity distribution which would exist in the tube if there were no wire present, and Fig.4.15b represents the velocity distribution in a plane perpendicular to the wire, downstream of the wire. Clearly the Hydrogen bubbles shed by the wire must be in the wake of the wire, and therefore will indicate a flow velocity which differs from the undisturbed

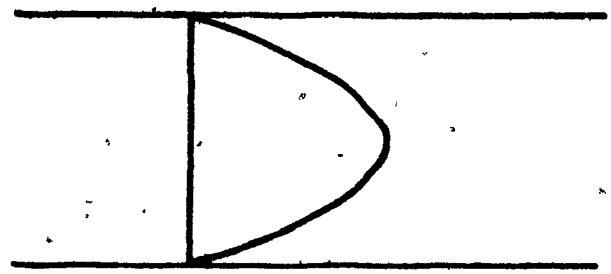

4-15 (a) velocity distribution when no wire is present

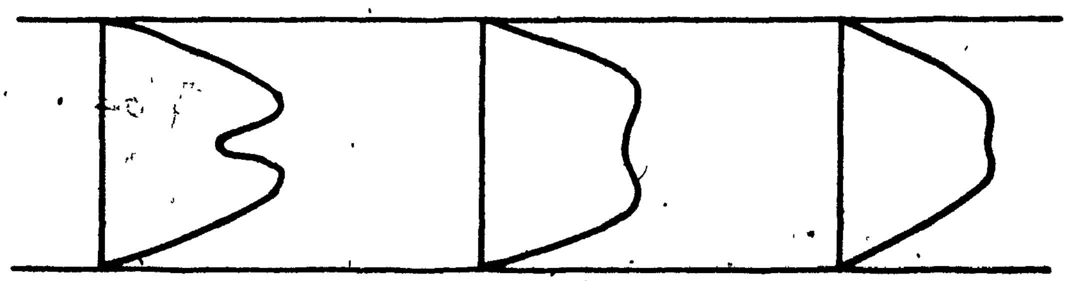

4-15 (b) velocity distribution downstream of the wire

Fig.4.15 VELOCITY DEFECT CAUSED BY THE WAKE OF THE BUBBLE GENERATING WIRE

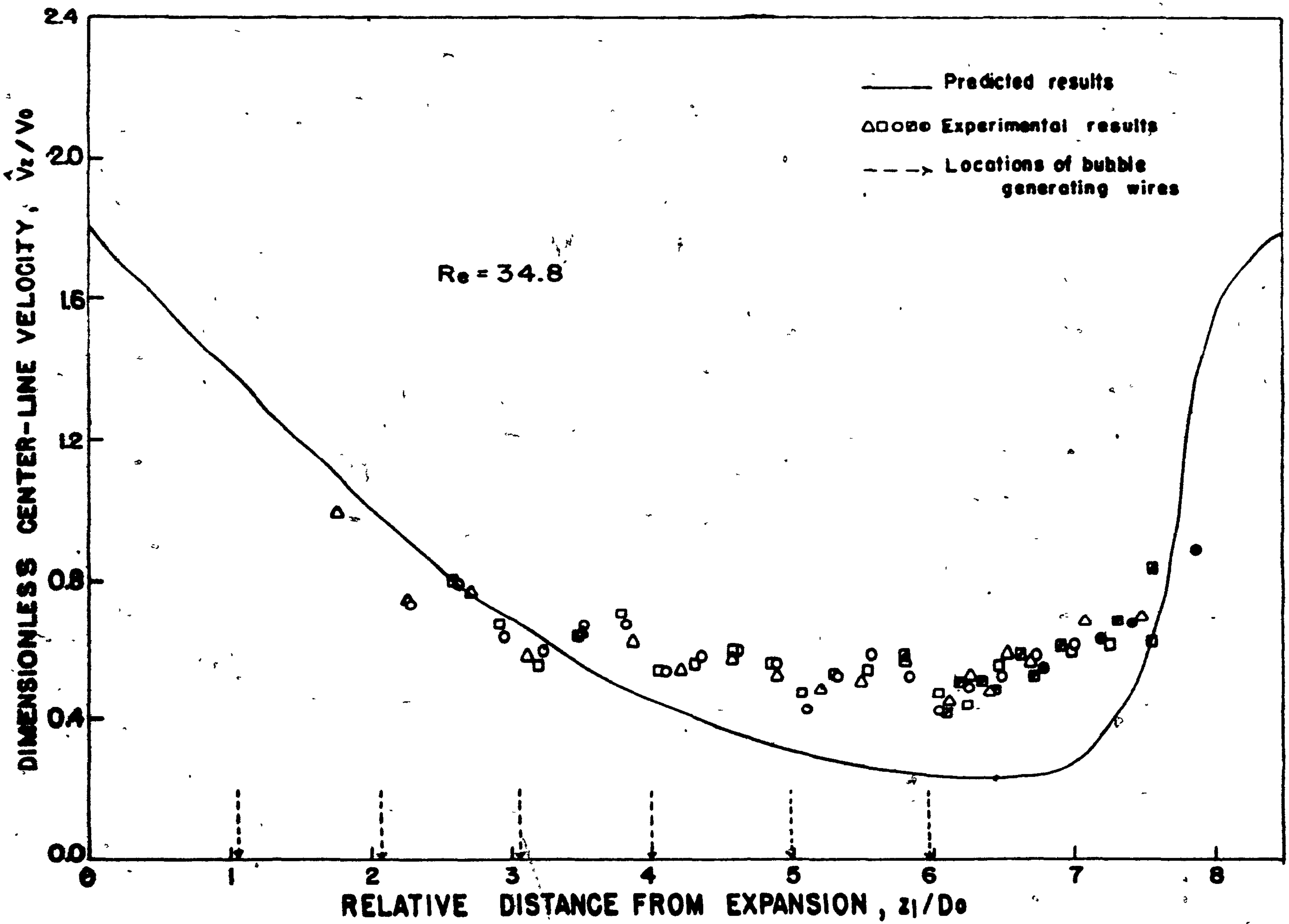

Fig.4.16 COMPARISON OF RESULTS FOR THE CENTERLINE VELOCITY

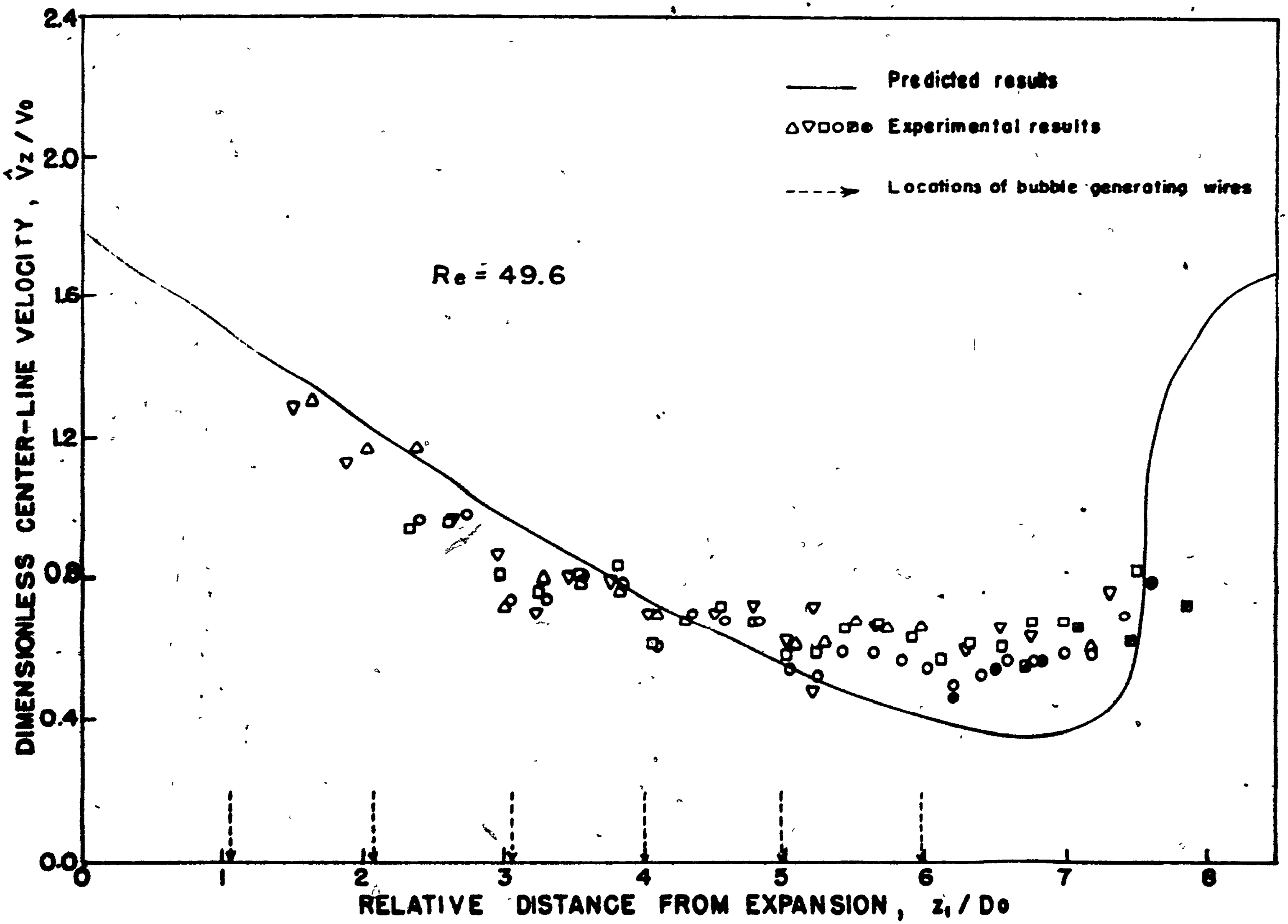

Fig.4.17 COMPARISON OF RESULTS FOR THE CENTERLINE VELOCITY

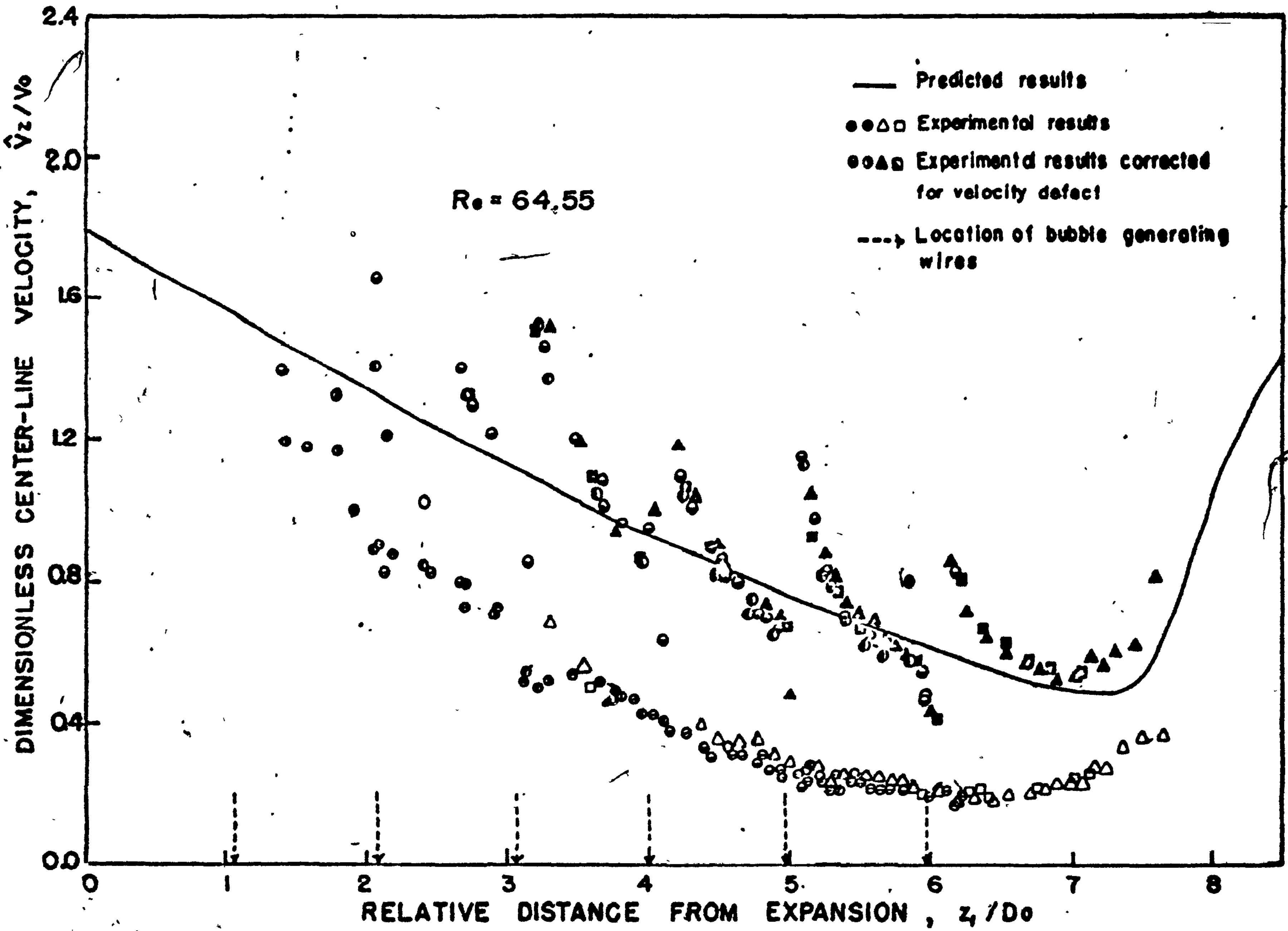

Predicted results
Experimental results
Experimentd results corrected for velocity defect
Location of bubble generating wires
Re = 64.55
DIMENSIONLESS CENTER-LINE VELOCITY, $\hat{V}_z/V_0$
RELATIVE DISTANCE FROM EXPANSION, z/D_0
2.4
2.0
1.6
1.2
0.8
0.4
0.0
0
1
2
3
4
5
6
7
8

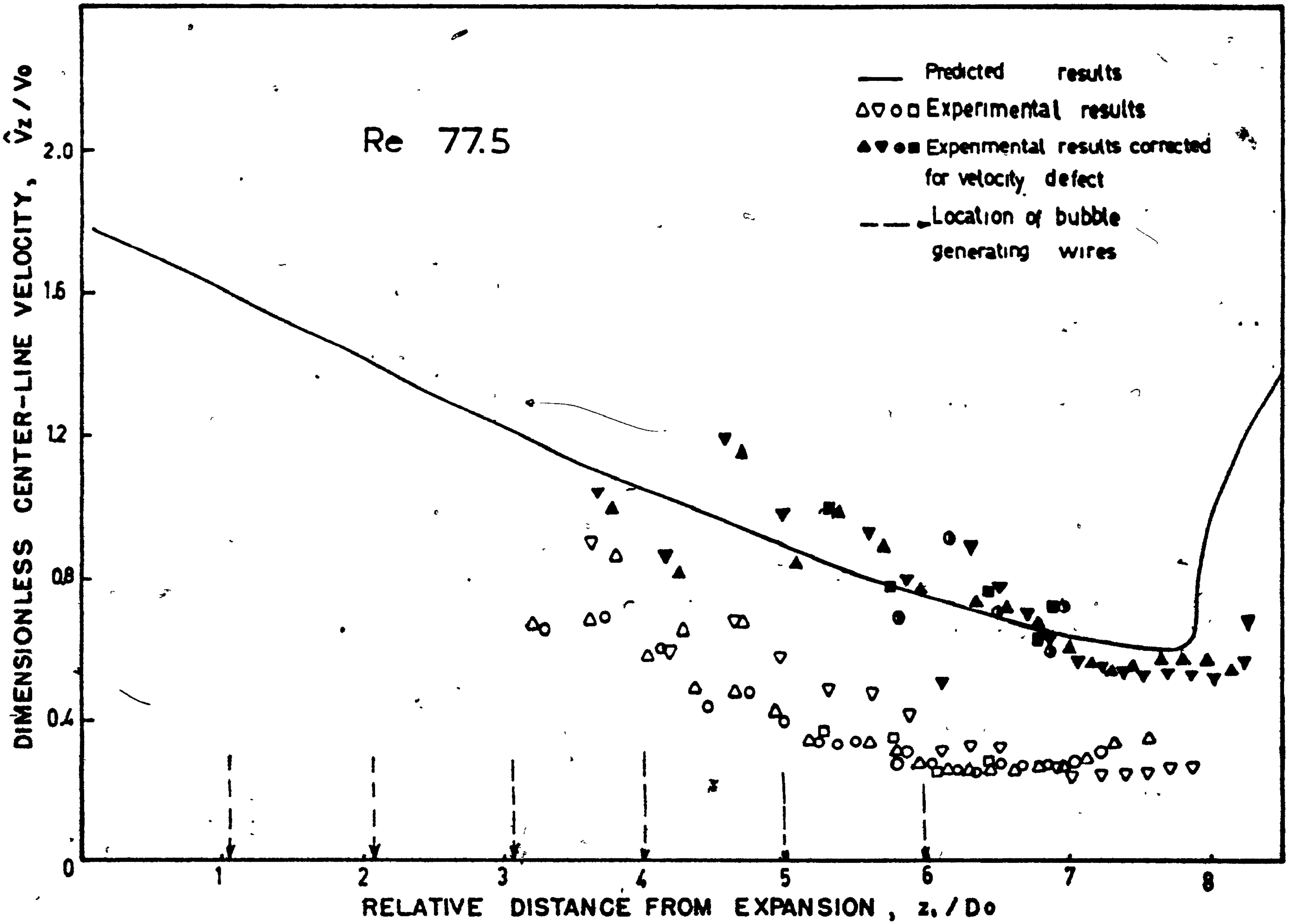

Fig. 4.19 COMPARISON OF RESULTS FOR THE CENTERLINE VELOCITY

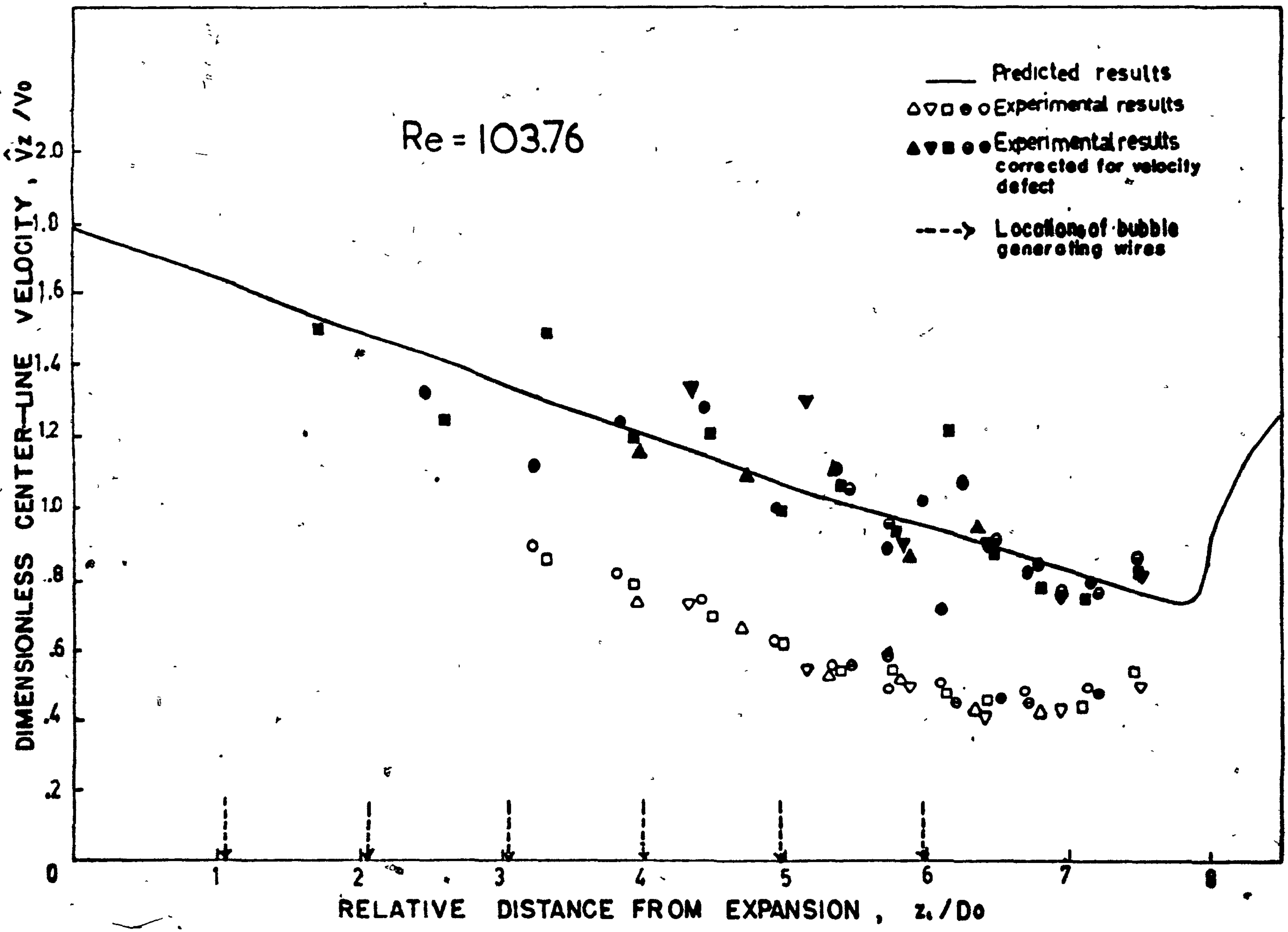

Fig.4.20 COMPARISON OF RESULTS FOR THE CENTERLINE VELOCITY

flow by the amount of the velocity defect, which decreases with distance downstream from the wire.

According to Clutter and Smith (9), the hydrogen bubble method is not applicable to flow with velocity higher than about 0.6 m/sec, but below this limit is a well-defined range in which the velocity defect is very small (16,36) and dies out quickly in less than 70 wire diameters (36). The present work leads to a different conclusion, although the maximum centerline velocity encountered was only about 0.14 m/sec, which falls in the supposed safe range of operation. Probably, the reason is the use of sugar solution as working fluid in the present work, while results reported by other workers are based on experiments with water. In the present experiments, the disturbance of the wire, accentuated by the presence of six wires, is so serious that its evidence is shown clearly through the photographs shown in Figs. 4.6..12: different separation zones are formed between the wires, quite unexpectedly. Figs. 4.6 and 10 show some bubble rows which distort as they pass the wire. The measured values of the centerline velocity, presented in Figs. 4.16 and 17, show sharp breaks at positions where the wires were located; the velocity shows a distinct minimum just behind each wire, where the defect is largest. Also, for flows at low Reynolds numbers, such as shown in Figs. 4.16 and 17, obtained from the photographs presented in Figs. 4.6-8, the observed values of the downstream centerline velocity are, surprisingly, higher than predicted.

This is explained by the observation that the disturbing effect of the wire increases with decreasing Reynolds number. As shown in Figs. 4-6..8, this effect makes the separation region persist longer, hence narrows the width of the core jet and consequently increases the velocity there. Obviously, this disturbing effect would become more and more serious in the downstream flow, due to the cumulative effect of all the wires.

The problem of flow over the wires is complicated by the fact that the flow is not uniform. However, since the maximum Reynolds number based on the wire diameter is 0.17, the velocity defect may be approximated by the asymptotic laminar wake solution for an infinite circular cylinder. Oseen's fundamental solution for the outer field of a uniform flow past a cylinder, given by Rosenhead (54) and Van Dyke (55), was chosen for this purpose, using the predicted velocity as the velocity of the approaching flow. The velocity defect on the centerline is given by:

$$V_d = -\frac{2\vartheta}{\ln(\frac{3.703}{R_a})}\left\{\frac{\partial}{\partial(R_x)}[\ln R_x + e^{R_x/2}K_o(\frac{R_x}{2})] - e^{R_x/2}K_o(\frac{R_x}{2})]\right\} \qquad \text{.........(4.2.2)}$$

where ϑ is the velocity of the approaching flow, K_o is the Bissel function of the second kind, and R_a and R_x are the Reynolds numbers based on the wire diameter a and the distance x from the wire respectively. For positions close to the wires, the Stokes expansion was used to give (8,27):

$$V_d = \vartheta\left\{1 - \frac{1}{\ln(\frac{3.703}{R_a})}[\ln(\frac{x}{a}) - \frac{1}{2}(1 - \frac{a^2}{x^2})]\right\} \qquad \text{.........(4.2.3)}$$

Special attention must be paid to the wire which generates bubbles. Since there exists a gas sheath around this wire, as reported by Schraub and Kline (36), a different defect may be expected. Hence, the effective diameter of this wire was assumed to be of the order of 1.5 the bare wire diameter. The corrected centerline velocities are presented in the same graphs in Figs. 4-15.21, showing that, although scattered, they fall close to the predicted curves. This scatter in the corrected values shows that eq. (4.2-2) over-estimates the velocity defect at positions close to the wires, for a non-uniform flow, whereas eq. (4.2-3) under-estimates it.

4.3 CONCLUSION

The numerical solutions for isothermal flow and the experimental results have been found to agree satisfactorily in the dimensions of the jet entering the reactor, and the centerline velocity of the fluid. This confirms the validity of the computed solutions, with the appropriate formulation of the boundary conditions. It also gives a strong support to the validity of the numerical solutions for non-isothermal flow, since the former is only a simple case of the latter. However, the Hydrogen Bubble Method used is not recommended for further work for flows of the type in the present work, since the disturbing effects of the wires introduce significant inaccuracies in the velocity measurements. In addition to the upper bound on the validity of this technique recognized by other authors, a lower limit appears to exist corresponding to the wire Reynolds number at which disturbance to the flow becomes significant.

V. CONCLUSIONS

A method of simulating the flow pattern and temperature distributions for laminar flow at high temperature entering a reactorhas been obtained. It provides a powerful means for investigating flows which cannot yet be determined by measurements, and hence for developing the design of high-temperature chemical reactors.

The predictions for the isothermal flow in a circular conduit expansion have been found to agree satisfactorily with both numerical and experimental results obtained by other workers. For isothermal flows in the reactor chamber, an annular captive eddy was predicted for all Reynolds numbers investigated, even at very low Re. The predictions are shown to agree with experimental results of flow visualization in a cold model of the reactor. The predicted flow pattern for an Argon tail flame in the reactor with cooled walls was found to be very different from the corresponding isothermal flow. The recirculation was very much stronger th an in the corresponding isothermal flow. Local heat transfer to the wall, resulting from conduction, was found to decrease with increasing entry Reynolds number, or increasing inlet temperature, or decreasing wall temperature.

The computer programme seems already to be working very satisfactorily with a modest computing time requirement. The range of the entry Reynolds number and the entry temperature investigated can be extended further, to conditions under which the radiation heat loss is significant, and a swirl velocity may be present. This is the next step for further work. Different gases besides Argon and different reactor dimensions and geometrics should also be used.

The validity of the isothermal form of solutions have been confirmed. However, the validity of the predictions for non-isothermal flow can not be properly assessed without additional experimental information. The main task for the future is the comparison of the resulting predictions with experimental data. Although measurements in a high-temperature reactor are very difficult, some can still be obtained, such as the heat transfer to the outside wall, the temperature of the effluent, etc. The assumption of constant wall temperature, used as boundary condition for the presented predictions, is somewhat artificial. A more realistic boundary condition for temperature at the walls of the reactor will surely lead to more successful predictions.

NOTATION

Symbol		Equation of First Mention
a	a coefficient in the general elliptic equation	(2.2-37)
a_B	radius of the hydrogen bubble generated from the wire	(4.2-1)
a_d	radius of the hydrogen bubble generating wire	(4.2-2)
a_R	relaxation factor	(2.3-20)
A_E, A_W, A_N, A_S	coefficients in the convection terms of the difference equation	(2.3-8)
b	a coefficient in the general elliptic equation	(2.2-37)
B_E, B_W, B_N, B_S	coefficients in the diffusion terms of the difference equation	(2.3-14)
Br	Brinkman number, based on inlet conditions, $\mu_o V_o^2/k_o(T_o-T_w)$	(2.2-35)
c	a coefficient in the general elliptic equation	(2.2-37)
c_E, c_W, c_N, c_S	values of the coefficient c evaluated at the points E, W, N, S	(2.3-14)
$\hat{c}_p$	specific heat at constant pressure of the fluid	(2.2-8)
c_p	dimensionless specific heat at constant pressure of the fluid	(2.2-17)
c_{p_o}	specific heat at constant pressure of the inlet fluid	(2.2-17)
C_E, C_W, C_N, C_S	coefficients in the general substitution formula	(2.3-18)
d	source term in the general elliptic equation	(2.2-37)

Symbol		Equation of First Mention
D	source term in the general substitution formula	(2.3-18)
D_i	diameter of the reactor chamber	(3.5-1)
f	fraction used in eq.(3.4-1)	(3.4-1)
g_1, g_2	functions in the boundary equation for vorticity	(2.4-11)
h	a constant used in eq.(3.4-1)	(3.4-1)
h_{coef}	heat transfer coefficient	
$\hat{H}$	specific enthalpy of the fluid	(2.2-8)
$\hat{k}$	thermal conductivity of the fluid	(2.2-11)
k	dimensionless thermal conductivity of the fluid	(2.2-17)
k_b	thermal conductivity of the fluid evaluated at local bulk temperature	(3.5-1)
k_o	thermal conductivity of the inlet fluid	(2.2-17)
ℓ	length of the section of the grid to be subdivided	(3.4-1)
L_e	length of the annular captive eddy	
L_c	position of the "eye" of the eddy downstream from the sudden expansion	
M	molecular weight of the gas	
n	refractive index of the gas	(2.2-16)
n_{NP}	distance along a normal to a boundary surface	(2.4-11)
Nu	Nusselt number, based on local conditions, $h_{coef} D_i / k_b$	(3.5-1)
$\hat{p}$	the fluid pressure	(2.2-7)

Symbol		Equation of First Mention
p	dimensionless dynamic pressure of the fluid, $\hat{p}/\rho_o V_o^2$	(2.2-17)
Pr	Prandtl number, based on inlet conditions, $\mu_o c_{p_o}/k_o$	(2.2-7)
$\hat{Q}_R$	rate of energy loss by radiation per unit volume	(2.2-7)
Q_R	dimensionless rate of energy loss by radiation per unit volume	(2.2-17)
$\hat{r}$	radial distance in cylindrical coordinates	(2.2-2)
r	dimensionless radial distance, $\hat{r}/D_o$	(2.2-17)
R	gas constant	
R_W	dimensionless distance of a wall from the axis-of-symmetry	(2.4-11)
R_1, R_2	ratios defined by eq.(4.2-3)	(4.2-2)
Re	Reynolds number of the inlet fluid, $\rho_o D_o V_o/\mu_o$	(2.2-22)
S_W	source term in the vorticity equation	(2.2-33)
t	time	
$\hat{T}$	absolute temperature of the fluid	(2.2-8)
T	reduced temperature of the fluid, $(\hat{T} - T_W)/(T_o - T_W)$	(2.2-17)
T_o	absolute temperature of the inlet fluid	(2.2-17)
T_W	absolute temperature of the fluid at the walls	(2.2-17)
$\hat{U}$	internal energy of the fluid per unit mass	(2.2-7)

Symbol		Equation of First Mention
$\hat{v}$	specific volume of the fluid	(2.2-8)
v_B	terminal rise velocity of the Hydrogen bubble owing to buoyancy	(4.2-1)
$\hat{\underline{V}}$	velocity vector	(2.2-1)
$\underline{V}$	dimensionless velocity vector, $\underline{V}/V_o$	(2.2-26)
V_o	mean inlet velocity	(2.2-17)
$\hat{V}_z, \hat{V}_r, \hat{V}_\theta$	components of the velocity vector in z-, r- and θ-directions	(2.2-2) (2.2-5)
V_z, V_r, V_θ	components of the dimensionless velocity vector in z-, r- and θ-directions	(2.2-17)
V_d	velocity defect caused by the wake of the bubble generating wire	
ϑ	velocity of the flow approaching the bubble generating wire	(4.2-2)
w	dimensionless vorticity	(2.2-30)
x	distance from the axis of the bubble generating wire	(4.2-2)
$\hat{z}$	axial distance in cylindrical coordinates	
z	dimensionless axial distance	(2.2-17)
z_1	axial distance from the expansion or contraction of the reactor	(3.4-1)

Symbol		Equation of First Mention
γ	Euler's constant	(4.2-2)
$\underline{\underline{\Delta}}$	rate of strain tensor	
Δ_{ij}	component of the rate of strain tensor	
$\underline{\underline{\delta}}$	unit tensor	
θ	angle in cylindrical coordinates	
κ	absorption coefficient	(2.2-16)
λ	convergence criterion	(2.3-21)
$\hat{\mu}$	viscosity of the fluid	(2.2-4)
μ	dimensionless viscosity of the fluid, $\hat{\mu}/\mu_o$	(2.2-17)
μ_o	viscosity of the inlet fluid	(2.2-17)
ν	kinematic viscosity of the fluid	
$\hat{\rho}$	density of the fluid	(2.2-1)
ρ	dimensionless density of the fluid, $\hat{\rho}/\rho_o$	(2.2-17)
ρ_o	density of the inlet fluid	(2.2-17)
ρ_B	density of the hydrogen bubble	(4.2-1)
σ	Boltzmann constant	(2.2-16)
ϕ	dependent variable of the general elliptic equation	(2.2-37)
$\underline{\underline{\tau}}$	stress tensor	(2.2-3)
$\hat{\Phi}$	dissipation function in the energy equation	(2.2-12)
ϕ	dimensionless dissipation function	(2.2-22)
Φ	dimensionless function in the energy equation	(2.2-35)
ψ	dimensionless stream function	(2.2-28)

REFERENCES

1. AMES, W.F., Nonlinear Partial Differential Equations in Engineering, Academic Press, New York, 1965.

2. AMDUR, I. and MASON, A.E., "Properties of Gases at Very High Temperature", Phys. Fluids, Vol.1, 370 (1958).

3. ASASUMA, T. and TAKEDA, S., "A Study on the Flow Visualization by the Hydrogen Bubble Method", Bull. of JSME, Vol.8, No.32, 599 (1965).

4. BARAKAT, H.Z. and CLARK, J.A., "Analytical and Experimental Study of Transient Laminar Natural Convection Flows in Partially Filled Containers", Proc. 3rd Int. Heat Transfer Conf. Chicago, Vol. II, paper No. 57, 152 (1966).

5. BIRD, R.B., STEWART, W.E., and LIGHTFOOT, E.M., Transport Phenomena, John Wiley & Sons, Inc., 1960.

6. BLAIR, A., METROPOLIS, N., TAUB, A.H. and TSINGOU, M., "A Study of a Numerical Solution to a Two-dimensional Hydrodynamic Problem", Physics and Mathematics, LA-2165 (TID-4500, 13th ed., rev.), 1957.

7. BROKAW, R., "Alignment Charts for Transport Properties Viscosity, Thermal Conductivity and Diffusion Coefficients for Non-polar Gases and Gas Mixtures at Low Density", NASA Tr R-81, 1961.

8. CLIFT, R., GRACE, J.R., and WEBER, M.E., "Bubbles, Drops and Particles", to be published (Academic Press, 1974).

9. CLUTTER, D.W. and SMITH, A.M.O., "Flow Visualization by Electrolysis of Water", Aerospace Engineering, January 1961.

10. COURANT, R., ISAACSON, E. and REES, M., "On the Solution of Non-linear Hyperbolic Differential Equations by Finite Differences", Communications on Pure and Applied Mathematics, Vol. 5, 243 (1952).

11. DAVIES, W. and FOX, R.W., "An Evaluation of the Hydrogen Bubble Technique for the Quantitative Determination of Fluid Velocity within Clear Tubes", Journal of Basic Engineering, Trans. ASME, Series D, Vol. 89, 771 (1967).

12. DAWE, R.A. and SMITH, E.B., "Viscosity of Argon at High Temperatures", Science J., 675 (1969).

13. DRELLISHAK, K.S., KNOPP, C.F. and CAMBEL, A.B., "Partition Functions and Thermodynamic Properties of Argon Plasma", Arnold Engineering Development Center, Report No. AEDC. TDR.63.146 (1963).

14. EDE, A.J., HISLOP, E.I. and MORRIS, R., "Effect on the Local Heat Transfer Coefficient in a Pipe of an Abrupt Disturbance of the Fluid Flow: Abrupt Convergence and Divergence of Diameter Ratio 2/1", Proceedings of the Institution of Mechanical Engineers, London, Vol. 170, No. 38, 1113 (1956).

15. EMERSON, W.H., "Heat Transfer in a Duct in Regions of Separated Flow", Proceeding of the Third International Heat Transfer Conference, Paper No. 26, Aug., 267 (1966).

16. GELLER, E.W., "An Electrochemical Method of Visualizing the Boundary Layer", Master's Thesis, Dept. of Aeronautical Engineering, Mississippi State College, Aug. 1954.

17. GOSMAN, A.D., PUN, W.M., RUNCHAL, A.K., SPALDING, D.B. and GOLFSHTEIN, M., Heat and Mass Transfer in Recirculating Flows, Academic Press, 1969.

18. GREENSPAN, D., "Numerical Studies of Steady, Viscous, Incompressible Flow in a Channel with a Step", J. of Engineering Mathematics, Vol. 3, No.1, 21 (1969).

19. HANSON, F.B. and RICHARDSON, P.D., "Mechanics of Turbulent Separated Flows as Indicated by Heat Transfer: A Review", Symposium on Fully Separated Flows as Indicated by Heat Transfer: A Review", Symposium on Fully Separated Flows", Hansen, A.G., Editor, The American Society of Mechanical Engineers, 27 (1964).

20. HUNG, T.K. and MACAGNO, E.O., "Laminar Eddies in a Two-dimensional Conduit Expansion", La Houille Blanche, Vol. 21, No.4, 391 (1966).

21. IBBERSON, V.J. and THRING, M.W., "Plasma Chemical and Process Engineering", Ind. Eng. Chem., Vol. 61, No. 11, 48 (1969).

22. IRIBARNE, A., FRANTISAK, F., HUMMEL, R.L. and SMITH, J.W., "An Experimental Study of Instabilities and other Flow Properties of a Laminar Pipe Jet", AIChE Journal, Vol. 18, No.4, 689 (1972).

23. KACKER, S.C. and WHITELAW, J.H., "Prediction of Wall-Jet and Wall-Wake Flows", J. Mechanical Engineering Science", Vol.12, No.6, 404 (1970).

24. KAWAGUTI, M., "Numerical Solution of Navier-Stokes Equations for the Flow in Two-dimensional Cavity", J. Physical Society of Japan, Vol. 16, 2307 (1961).

25. KRALL, K.M. and SPARROW, E.M., "Turbulent Heat Transfer in the Separated, Reattached and Redevelopment Regions of Circular Tube", J. Heat Transfer, Trans. ASME, Series C, 131 (1966).

26. KREY, R.U. and MORRIS, J.C., "Experimental Total and Total Line Radiation of Nitrogen, Oxygen, and Argon Plasmas", Physics of Fluids, Vol.13, 1483 (1970).

27. LAMB, H., Hydrodynamics, Cambridge, The University Press, 6th edition, 1932.

28. LENNEMANN, E. and HOWARD, J.H.G., "Unsteady Flow Phenomena in Rotating Centrifugal Impeller Passages". An ASME publication, presented at the Gas Turbine Conference and Products Show, Cleveland, Ohio, March 1969 of the American Society of Mechanical Engineers.

29. MACAGNO, E.O. and HUNG, T.K., "Computational and Experimental Study of a Captive Annular Eddy", J. Fluid Mech., Vol.28, part 1, 43 (1967).

30. MATHUR, G.P. and THODOS, G., "The Thermal Conductivity and Diffusivity of Gases for Temperatures up to 10,000°K.

31. PUN, W.M. and SPALDING, D.B., "A Procedure for Predicting the Velocity and Temperature Distribution in a Confined, Steady, Turbulent, Gaseous, Diffusion Flame", XVIII Intern. Astronautical Congress, Belgrade 1967, Pergamon Press, Polish Scientific Publishers 1968.

32. RICHARDSON, L.F., "The Approximate Arithmetical Solution by Finite Differences of Physical Problems Involving Differential Equations, with an Application to the Stresses in a Masonry Dam", Trans. of the Royal Society of London, Series A, Vol. 210, 307 (1910).

33. ROACHE, P.J. and MUELLER, T.J., "Numerical Solutions of Laminar Separated Flows", AIAA J., Vol.8, No.3, 530 (1970).

34. ROACHE, P.J., Computational Fluid Dynamics, Hermosa Publishers, 1972.

35. SAMUELSEN, G.S. and STARKMAN, E.S., "Analytical and Experimental Investigation of an Ammonia/Air Opposed Reacting Jet", Combustion Science and Technology, Vol.5, 31 (1972).

36. SCHRAUB, F.A., KLINE, S.J., HENRY, J., RUNSTADLER, P.W., Jr., and LITTELL, A., "Use of Hydrogen Bubbles for Quantitative Determination of Time-Dependent Velocity Fields in Low-Speed Water Flows", J. of Basic Engineering, Trans. ASME, Series D, Vol. 87, 429 (1965).

37. SKRIVAN, J.F. and JASKOWSKY, W.V., "Heat Transfer from Plasmas to Water-Cooled Tubes", I&EC Process Designs Development, Vol.4, No.4, 371 (1965).

38. SNEDEKER, R.S. and du P. DONALDSON, C., "Observation of a Bistable Flow in a Hemispherical Cavity", AIAA J., Vol.4, No.4, 735 (1966).

39. SPARROW, E.M. and CESS, R.D., Radiation Heat Transfer, Brooks/Cole Publishing Company, 1966.

40. SVEHLA, R.A., "Estimated Viscosities and Thermal Conductivities of Gases at High Temperatures", NASA, Technical Report R-132.

41. SWEARINGEN, T.B. and McEligot, D.M., "Internal Laminar Heat Transfer with Gas Property Variation", J. Heat Transfer, Trans. ASME, Series C, Nov., 432 (1971).

42. THOM, A. and APELT, C.J., Field Computations in Engineering and Physics, C. Van Nostrand Company Ltd, 1961.

43. THORPE, M.L. and WILKS, P.H., "Electric-Arc Furnace Turns Zircon Sands to Zirconia", Chem. Eng., Nov. 15, 1971.

44. TORY, A.C. and HAYWOOD, K.H., "Flow Visualization in the Lecture Theatre", Poull. Mech. Engineering Education, Vol. 7, 19 (1968).

45. TORY, A.C. and HAYWOOD, K.H., "The Hydrogen Bubble Technique of Flow Visualization - Factors Affecting Bubble Size and Buoyancy", An ASME publication No.71-FE-36, presented at the Fluids Engineering Conference, Pittsburgh, PA, May 1971 of the American Society of Mechanical Engineers.

46. WILLIAMS, P.S. and KNUDSEN, J.G., "Local Rates of Heat Transfer and Pressure Losses in the Vicinity of Annular Orifices", Canadian Journal of Chemical Engineering, Vol.41, 56 (1963).

47. YUN, K.S., WEISSMAN, S. and MASON, A.E., "High Temperature Transport Properties of Dissociating Nitrogen and Dissociating Oxygen", Physics of Fluids, Vol.5, 672 (1962).

48. ZEMANICK, P.P. and DOUGALL, R.S., "Local Heat Transfer Downstream of Abrupt Circular Channel Expansion", J. Heat Transfer, Trans. ASME, Series C, February, 53 (1970).

49. BEVERS, G.S. and WILSON, T.A., "Vortex Growth in Jets", J. Fluid Mech., Vol. 44, 97 (1970).

50. BECKER, H.A. and MASSARD, T.A., "Vortex Evolution in a Round Jet", J. Fluid Mech., Vol. 31, No. 3, 435 (1968).

51. VISKANTA, R., "Interation of Heat Transfer by Conduction, Convection, and Radiation in a Radiating Fluid", J. Heat Transfer, Trans. ASME, Nov. 318 (1963).

52. HAMA, F.R., "Experimental Studies on the Lip Shock", AIAA Journal, Vol. 6, No. 2, 212 (1968).

53. DONALDSON, I.S., "On the Separation of a Supersonic Flow at a Sharp Corner", AIAA Journal, Vol. 5, No. 6, 1086 (1967).

54. ROSENHEAD, L., Laminar Boundary Layers, Oxford at the Clarendon Press, 1963.

55. VAN DYKE, M., Perturbation Methods in Fluid Mechanics, Academic Press, 1964.

APPENDIX A

PROPERTIES OF ARGON AT HIGH TEMPERATURES

Temp °K	Density GM/CC x10^5	Thermal Enthalpy CAL/GM x10^3	Specific Heat at Constant Pressure CAL/GM/°K	Viscosity GM/CM/SEC x10^3	Thermal Conductivity CAL/CM/SEC/°K x10^4
1000	48.67	0.124	0.124	0.541	1.01
1500	32.40	0.186	0.124	0.708	1.32
2000	24.30	0.248	0.124	0.886	1.65
2500	19.45	0.310	0.124	1.05	1.96
3000	16.20	0.372	0.124	1.21	2.26
3500	13.88	0.434	0.124	1.37	2.56
4000	12.15	0.496	0.124	1.53	2.85
4500	10.80	0.558	0.124	1.68	3.13
5000	9.732	0.6213	0.124	1.83	3.41
5100	9.541	0.6341	0.124		
5200	9.358	0.6468	0.124		
5300	9.181	0.6594	0.124		
5400	9.011	0.6720	0.124		
5500	8.847	0.6846	0.124	1.97	3.67
5600	8.689	0.6971	0.124		
5700	8.537	0.7096	0.124		
5800	8.390	0.7220	0.124		
5900	8.247	0.7345	0.124		
6000	8.110	0.7469	0.124	2.11	3.94
6100	7.977	0.7593	0.124		
6200	7.848	0.7716	0.124		
6300	7.724	0.7841	0.124		
6400	7.603	0.7965	0.124		
6500	7.486	0.8089	0.124	2.25	4.20
6600	7.373	0.8215	0.125		
6700	7.262	0.8340	0.126		
6800	7.155	0.8467	0.127		
6900	7.051	0.8594	0.128		

APPENDIX A (cont'd)

Temp °K	Density GM/CC x10^5	Thermal Enthalpy CAL/GM x10^3	Specific Heat at Constant Pressure CAL/GM/°K	Viscosity GM/CM/SEC x10^3	Thermal Conductivity CAL/CM/SEC/°K x10^3
7000	6.950	0.8723	0.129	2.38	4.44
7100	6.851	0.8853	0.131		
7200	6.756	0.8984	0.132		
7300	6.663	0.9117	0.134		
7400	6.572	0.9252	0.136		
7500	8.484	0.9389	0.134	2.51	4.68
7600	6.398	0.9524	0.137		
7700	6.314	0.9662	0.139		
7800	6.231	0.9803	0.143		
7900	6.151	0.9947	0.146		
8000	6.073	1.010	0.150	2.63	4.90
8100	5.996	1.025	0.155		
8200	5.922	1.040	0.160		
8300	5.848	1.057	0.165		
8400	5.776	1.073	0.171		
8500	5.706	1.091	0.171	2.75	5.13
8600	5.637	1.108	0.178		
8700	5.569	1.126	0.185		
8800	5.502	1.145	0.194		
8900	5.436	1.165	0.203		

APPENDIX A (cont'd)

Temp °K	Density GM/CC x10^5	Thermal Enthalpy CAL/GM x10^3	Specific Heat at Constant Pressure CAL/GM/°K	Viscosity GM/CM/SEC x10^3	Thermal Conductivity CAL/CM/SEC/°K x10^4
9000	5.372	1.186	0.213	2.87	5.35
9100	5.308	1.207	0.224		
9200	5.245	1.230	0.236		
9300	5.183	1.255	0.248		
9400	5.122	1.280	0.262		
9500	5.062	1.307	0.270	2.98	5.56
9600	5.002	1.335	0.286		
9700	4.943	1.364	0.303		
9800	4.884	1.395	0.321		
9900	4.825	1.428	0.340		
10000	4.768	1.463	0.361	3.10	5.78
10100	4.710	1.500	0.383		
10200	4.653	1.540	0.406		
10300	4.596	1.582	0.431		
10400	4.539	1.626	0.457		
10500	4.482	1.672	0.487		
10600	4.425	1.722	0.517		
10700	4.369	1.775	0.548		
10800	4.312	1.832	0.580		
10900	4.255	1.891	0.615		

APPENDIX A (cont'd)

Temp °K	Denisty GM/CC x10^5	Thermal Enthalpy CAL/GM x10^3	Specific Heat at Constant Pressure CAL/GM/°K	Viscosity GM/CM/SEC x10^3	Thermal Conductivity CAL/CM/SEC/°K x10^4
11000	4.198	1.955	0.650	3.33	6.82
11100	4.142	2.022	0.688		
11200	4.085	2.092	0.726		
11300	4.028	2.167	0.767		
11400	3.970	2.246	0.809		
11500	3.913	2.322	0.875		
11600	3.855	2.417	0.921		
11700	3.798	2.512	0.968		
11800	3.740	2.611	1.017		
11900	3.682	2.715	1.066		
12000	3.623	2.825	1.117	3.55	6.64
12100	3.565	2.939	1.168		
12200	3.506	3.059	1.221		
12300	3.448	3.182	1.28		
12400	3.389	3.314	1.33		
12500	3.330	3.451	1.45		
12600	3.272	3.599	1.51		
12700	3.213	3.753	1.56		
12800	3.155	3.912	1.62		
12900	3.097	4.077	1.67		

APPENDIX A (cont'd)

Temp °K	Density GM/CC $\times 10^5$	Thermal Enthalpy CAL/GM $\times 10^3$	Specific Heat at Constant Pressure CAL/GM/°K	Viscosity GM/CM/SEC $\times 10^3$	Thermal Conductivity CAL/CM/SEC/°K $\times 10^4$
13000	3.039	4.247	1.73	3.76	7.04
13100	2.981	4.422	1.78		
13200	2.924	4.603	1.83		
13300	2.868	4.788	1.88		
13400	2.812	4.978	1.92		
13500	2.757	5.173	2.04		
13600	2.703	5.379	2.08		
13700	2.649	5.589	2.12		
13800	2.594	5.803	2.16		
13900	2.543	6.020	2.19		
14000	2.492	6.240	2.24	3.98	7.44
14100	2.442	6.463	2.24		
14200	2.394	6.688	2.25		
14300	2.347	6.914	2.27		
14400	2.301	7.141	2.28		
14500	2.256	7.367	2.26		
14600	2.213	7.592	2.25		
14700	2.171	7.817	2.25		
14800	2.131	8.042	2.24		
14900	2.092	8.265	2.23		
15000	2.054	8.487	2.21	4.18	7.85

APPENDIX B

TOTAL LINE RADIATION HEAT LOSS OF ARGON PLASMA

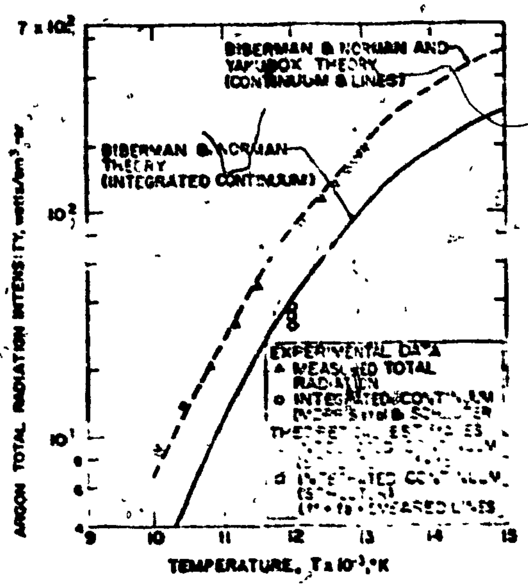

. Temperature dependence of the total radiation [illegible] continuum and line contributions (0.2μ < λ < [illegible]).

(Krey, R.U. and Morris, J.C., "Experimental Total and Total Line Radiation of Nitrogen, Oxygen and Argon Plasmas", Physics of Fluids, Vol. 13, 1483 (1970))

APPENDIX C

COMPUTER PROGRAM

- i Program Listing
- ii Typical Output for an Isothermal Flow in the Reactor Chamber
- iii Typical Output for a Non-isothermal Flow at High Temperature in the Reactor Chamber

```
LEVEL 21.6 ( MAY 72 )                                    OS/360   FORTRAN H

      COMPILER OPTIONS - NAME=  MAIN,OPT=02,LINECNT=56,SIZE=0000K,
                              SOURCE,EBCDIC,NOLIST,DECK,LOAD,NOMAP,NOEDIT,ID,NOXREF
 ISN 0002            COMMON/CVP/A(23,15,3),G1(23,15),G2(23,15),V1(23,15),V2(23,15)
 ISN 0003            COMMON/CNUMBR/NW,NF,NT,IE,IN,JN,INM,JNM,JA,JB,IB,IC,
                    1          JAM,JBM,IBP,ICM
 ISN 0004            COMMON/CGRID/Z(23),R(15),DELZ(23),DELR(15),IMIN(15),IMAX(15)
 ISN 0005            COMMON/CPROP/RO(23,15),ZMU(23,15),ZK(23,15),CP(23,15)
 ISN 0006            COMMON/CPARAM/VINL,RE,PR,BR
 ISN 0007            COMMON/CCHECK/RSDU(3),CC,NMAX,IRS(3),JRS(3),REFVAL(3),RELAX(3)
                    4,RSH,RSL
 ISN 0008            COMMON/CNAME/ANAME(9,7)
 ISN 0009            COMMON/CREF/ROREF,ZMUREF,CPREF,ZKREF,TINL,TWALL
 ISN 0010            COMMON/CDATA/TEMP(100),PROP(100,4),DEL
 ISN 0011            DIMENSION AO(23,15,7)
 ISN 0012            EQUIVALENCE(A(1,1,1),AO(1,1,1))
               C
 ISN 0013            READ(5,111) ANAME
 ISN 0014            PR=ZMUREF*CPREF/ZKREF
               C
               C***  COMPUTE GRID CO-ORDINATES AND SPECIFY CHAMBER DIMENSIONS
 ISN 0015            CALL GRID
               C
               C***  READ IN TABULATED GAS PROPERTIES AT DIFFERENT TEMPERATURES
               C
 ISN 0016            DEL=100.
 ISN 0017            DO 100  I=1,61
 ISN 0018      100   READ(5,112) TEMP(I),(PROP(I,K),K=1,4)
               C
               C
               C***  READ IN INITIAL VALUES FOR VORTICITY, STREAM FUNCTION,
               C     TEMPERATURE AND MASS VELOCITY COMPONENTS
               C
 ISN 0019            DO 2   K=1,5
 ISN 0020            DO 2   J=1,JN
 ISN 0021            I1=IMIN(J)
 ISN 0022            I2=IMAX(J)
 ISN 0023      2     READ(5,401) (AO(I,J,K),I=I1,I2)
               C
               C
               C***  SETTING BOUNDARY CONDITIONS
               C
               C***  FOR TEMPERATURE AND FLUID PROPERTIES
               C
               C     INLET
 ISN 0024            DO 300  J=1,JAM
 ISN 0025            A(1,J,NT)=1.
 ISN 0026            RO(1,J)=1.
 ISN 0027            ZMU(1,J)=1.
 ISN 0028            ZK(1,J)=1.
 ISN 0029      300   CP(1,J)=1.
               C
               C     AT THE WALLS
 ISN 0030            T=0.
 ISN 0031            CALL PROPTY(T,ROW,ZMUW,ZKW,CPW)
```

```
ISN 0032          DO 301   I=1,IB
ISN 0033          A(I,JA,NT)=0.
ISN 0034          RO(I,JA)=ROW
ISN 0035          ZMU(I,JA)=ZMUW
ISN 0036          ZK(I,JA)=ZKW
ISN 0037   301    CP(I,JA)=CPW
ISN 0038          DO 302   I=IC,IN
ISN 0039          A(I,JB,NT)=0.
ISN 0040          RO(I,JB)=ROW
ISN 0041          ZMU(I,JB)=ZMUW
ISN 0042          ZK(I,JB)=ZKW
ISN 0043   302    CP(I,JB)=CPW
ISN 0044          DO 303   I=IB,IC
ISN 0045          A(I,JN,NT)=0.
ISN 0046          RO(I,JN)=ROW
ISN 0047          ZMU(I,JN)=ZMUW
ISN 0048          ZK(I,JN)=ZKW
ISN 0049   303    CP(I,JN)=CPW
ISN 0050          DO 304   J=JA,JNM
ISN 0051          A(IB,J,NT)=0.
ISN 0052          RO(IB,J)=ROW
ISN 0053          ZMU(IB,J)=ZMUW
ISN 0054          ZK(IB,J)=ZKW
ISN 0055   304    CP(IB,J)=CPW
ISN 0056          DO 305   J=JB,JNM
ISN 0057          A(IC,J,NT)=0.
ISN 0058          RO(IC,J)=ROW
ISN 0059          ZMU(IC,J)=ZMUW
ISN 0060          ZK(IC,J)=ZKW
ISN 0061   305    CP(IC,J)=CPW
           C
           C
           C***   FOR MASS VELOCITIES
           C
           C      LAMINAR PARABOLIC INLET-VELOCITY DISTRIBUTIONS
ISN 0062   411    DO 400  J=1,JAM
ISN 0063          G1(1,J)=RO(1,J)*2.*(1.0-4.0*R(J)**2)
ISN 0064   400    G2(1,J)=0.
           C
           C      NO-SLIP AT THE WALLS
ISN 0065          DO 101   I=IB,IC
ISN 0066          G1(I,JN)=0.
ISN 0067   101    G2(I,JN)=0.
ISN 0068          DO 102  I=1,IB
ISN 0069          G1(I,JA)=0.
ISN 0070   102    G2(I,JA)=0.
ISN 0071          DO 103   I=IC,IN
ISN 0072           G1(I,JB)=0.
ISN 0073   103    G2(I,JB)=0.
ISN 0074          DO 104   J=JA,JNM
ISN 0075          G1(IB,J)=0.
ISN 0076   104    G2(IB,J)=0.
ISN 0077          DO 105   J=JB,JNM
ISN 0078          G1(IC,J)=0.
```

```
ISN 0079      105    G2(IC,J)=0.
              C
              C      ZERO RADIAL VELOCITY AT THE AXIS-OF-SYMMETRY AND AT THE EXIT
              C
ISN 0080             DO 106  I=1,IN
ISN 0081      106    G2(I,1)=0.
ISN 0082             DO 107  J=2,JB
ISN 0083      107    G2(IN,J)=0.
              C
              C***   FOR STREAM FUNCTION
              C
              C      INLET
ISN 0084             A(1,JA,NF)=0.
ISN 0085             A(1,1,NF)=-RO(1,JA)*R(JA)**2*(1.0-2.0*R(JA)**2)
ISN 0086             DO 205  J=2,JAM
ISN 0087      205    A(1,J,NF)=RO(1,J)*R(J)**2*(1.0-2.0*R(J)**2)+A(1,1,NF)
              C
              C      ON THE AXIS-OF-SYMMETRY
ISN 0088             DO 204  I=2,IN
ISN 0089      204    A(I,1,NF)=A(1,1,NF)
              C
              C      ON THE WALLS
ISN 0090             DO 201  I=IB,IC
ISN 0091      201    A(I,JN,NF)=0.0
ISN 0092             DO 202  I=1,IB
ISN 0093      202    A(I,JA,NF)=0.0
ISN 0094             DO 203  I=IC,IN
ISN 0095      203    A(I,JB,NF)=0.0
ISN 0096             DO 206  J=JA,JN
ISN 0097      206    A(IB,J,NF)=0.0
ISN 0098             DO 207  J=JB,JN
ISN 0099      207    A(IC,J,NF)=0.0
              C
              C**    FOR VORTICITY
              C
              C      INLET
ISN 0100             DO 16   J=1,JA
ISN 0101      16     A(1,J,NW)=16.0
              C
              C
              C***   SPECIFY REFERENCE VALUES OF VARIABLES FOR RESIDUAL-NORMALIZATION
              C
ISN 0102             REFVAL(NW)=A(1,JA,NW)
ISN 0103             REFVAL(NF)=A(1,1,NF)
ISN 0104             REFVAL(NT)=A(1,1,NT)
              C
              C
              C***   CALCULATE INITIAL VALUES FOR VELOCITY COMPONENTS AND
              C      FLUID PROPERTIES
              C
              C
ISN 0105             DO 6   J=1,JN
ISN 0106             I1=IMIN(J)
ISN 0107             I2=IMAX(J)
```

```
ISN 0108          DO 6  I=I1,I2
ISN 0109          IF(J.EQ.JN.OR.I.EQ.IMIN(J)) GO TO 7
ISN 0111          IF(I.EQ.IC.AND.J.GE.JB) GO TO 7
ISN 0113          CALL PROPTY(A(I,J,NT),RO(I,J),ZMU(I,J),ZK(I,J),CP(I,J))
ISN 0114     7    V1(I,J)=G1(I,J)/RO(I,J)
ISN 0115     6    V2(I,J)=G2(I,J)/RO(I,J)
             C
             C
ISN 0116          VINL=RE*ZMUREF/ROREF/(2.*R(JA))
ISN 0117          BR=ZMUREF*VINL**2/(ZKREF*(4.184E+07)*(TINL-TWALL))
             C
             C***  WRITE PROBLEM-SPECIFICATION INFORMATION
             C
ISN 0118          WRITE(6,601)
ISN 0119          WRITE(6,602) RE,PR,BR,ROREF,ZMUREF,CPREF,ZKREF,TINL,TWALL,
                 1VINL,(K,RELAX(K),K=1,IE),CC,IN,JN
             C
             C***  PRINT OUT COORDINATES AND INITIAL VALUES OF VARIABLES
ISN 0120          WRITE(6,501)  (Z(I),I=1,IN)
ISN 0121          WRITE(6,502)  (R(J),J=1,JN)
ISN 0122          CALL PRINCT
             C
             C
ISN 0123          CALL SOLVE
ISN 0124          CALL PRINCT
ISN 0125          CALL HEAT
ISN 0126          DO 699  K=1,5
ISN 0127          DO 699  J=1,JN
ISN 0128          I1=IMIN(J)
ISN 0129          I2=IMAX(J)
ISN 0130   699    WRITE(7,698)  (A0(I,J,K),I=I1,I2)
             C
             C
ISN 0131   111    FORMAT(18A4)
ISN 0132   112    FORMAT(F10.1,4E15.4)
ISN 0133   401    FORMAT(7E11.3)
ISN 0134   501    FORMAT(' DISTANCES IN DIRECTION-1'/(1H ,8(F13.3)))
ISN 0135   502    FORMAT(' DISTANCES IN DIRECTION-2'/(1H ,8(F13.3)))
ISN 0136   601    FORMAT(1H1/25X,'FINITE-DIFFERENCE ITERATIVE SOLUTION IS UNDERCONSI
                 1DERATION FOR THE CASE OF'/25X,'-----------------------------------
                 2-----------------------------------------'//' LAMINAR COMPRESSIBLE
                 3HOT GAS FLOW IN A PIPE WITH A SUDDEN ENLARGEMENT AND A SUDDEN CONT
                 4RACTION'///' THE INITIAL INFORMATION SUPPLIED IS'/)
ISN 0137   602    FORMAT(10X,'RE,      REYNOLDS NUMBER BASED ON INLET DIAMETER    =',
                 1 F8.2/10X, 'PR,      PRANDTL NUMBER BASED ON INLET PROPERTIES =',
                 1 F8.2/10X, 'BR,      BRINKMANN NUMBER     . . . . . . . . . . . . =',
                 11PE11.2/10X,'ROREF,  REFERENCE DENSITY FOR THE FLUID  . . . . =',
                 21PE11.2,'  GM/CC'/10X,'ZMUREF, REFERENCE VISCOSITY FOR THE FLUID
                 2. . . =',1PE11.2,'  GM/CM/SEC'/10X,'CPREF,  REFERENCE HEAT CAPACIT
                 3Y FOR THE FLUID  . =',1PE11.2,'  CAL/GM/DEG K'/10X,'ZKREF,  REFERE
                 4NCE HEAT CONDUCTIVITY FOR THE FLUID=',1PE11.2,'  CAL/CM/SEC/DEG K'
                 5/10X,'TINL,   INLET TEMPERATURE OF THE FLUID . . . . . =',0PF8.2,
                 6'  DEG K'/10X,'TWALL,  TEMPERATURE AT THE WALLS . . . . . . . . =',
                 7,0PF8.2,'  DEG K'/10X, 'VINL,   MEAN INLET FLOW RATE . . . . . . . . . .
```

```
                                  4 . . . =',0PF8.2,'  CM/SEC'/10X,'RELAX''S, RELAXATION PARAMETERS F
                                  5OR DEPENDENT VARIABLES ARE'/ 10X,3('RELAX(',I1,')=',0PF5.2,', ')/
                                  5         10X,'CC.       THE CONVERGENCY CRITERION . . . . . . . . =',
                                  61PE11.2/10X,'IN.         THE NUMBER OF COLUMNS (Z-DIRECTION)   . . =',
                                  7 I5/    10X,'JN.       THE NUMBER OF ROWS . .(R-DIRECTION)   . . =',
                                  8 I6//)
    ISN 0138          698     FORMAT(7(1PE11.3))
    ISN 0139                  STOP
    ISN 0140                  END

*OPTIONS IN EFFECT*        NAME=  MAIN,OPT=02,LINECNT=56,SIZE=0000K,

*OPTIONS IN EFFECT*        SOURCE,EBCDIC,NOLIST,DECK,LOAD,NOMAP,NOEDIT,ID,NOXREF

*STATISTICS*     SOURCE STATEMENTS =      139 ,PROGRAM SIZE =      5338

*STATISTICS*  NO  DIAGNOSTICS GENERATED

****** END OF COMPILATION ******                                          31K BYTES OF CORE N
```

```
FORTRAN IV G1  RELEASE 1.1              BLK DATA          DATE = 73219          02/52/20

 0001                 BLOCK DATA
 0002                 COMMON/CNUMBR/NW,NF,NT,IE,IN,JN,INM,JNM,JA,JB,IB,IC,
                     1          JAM,JBM,IBP,ICM
 0003                 COMMON/CCHECK/RSDU(3),CC,NMAX,IRS(3),JRS(3),REFVAL(3),RELAX(3)
             O       4,RSH,RSL
 0004                 COMMON/CPARAM/VINL,RE,PR,BR
 0005                 COMMON/CREF/ROREF,ZMUREF,CPREF,ZKREF,TINL,TWALL
 0006                 COMMON/CSCALE/C1,C2,ZL1,ZL2
             C
 0007                 DATA JN,IN,JA,JB,IB,IC/15,23,6,6,3,20/
 0008                 DATA ROREF,ZMUREF,CPREF,ZKREF,TINL,TWALL/1.62E-04,1.21E-03,
                     1 0.124,2.26E-04,3000.,300./
 0009                 DATA RELAX/0.75,0.55,0.75/,CC/0.001/,RSH,RSL/0.05,0.001/
 0010                 DATA NMAX/200/
 0011                 DATA NW,NF,NT,IE/1,2,3,3/,RE/60./
 0012                 DATA C1,C2,ZL1,ZL2/0.8,1.0,3.6,4.4/
             C
 0013                 END

  *OPTIONS IN EFFECT*  NOTERM,ID,EBCDIC,SOURCE,NOLIST,NODECK,LOAD,NOMAP,NOTEST
  *OPTIONS IN EFFECT*  NAME = BLK DATA, LINECNT =       56
  *STATISTICS*  NO DIAGNOSTICS GENERATED
```

```
0001          SUBROUTINE GRID
0002          COMMON/CGRID/Z(23),R(15),DELZ(23),DELR(15),IMIN(15),IMAX(15)
0003          COMMON/CNUMBR/NW,NF,NT,IE,IN,JN,INM,JNM,JA,JB,IB,IC,
             1              JAM,JBM,IBP,ICM
0004          COMMON/CSCALE/C1,C2,ZL1,ZL2
0005          DIMENSION X1(15)
        C**************************************************************
        C     SUBROUTINE FOR CALCULATION OF GRID COORDINATES
        C**************************************************************
        C
        C
        C***  CALCULATE ORDINATES IN R-DIRECTION
        C
0006          JNM=JN-1
0007          JAM=JA-1
0008          JBM=JB-1
0009          R(1)=0.
0010          R(2)=0.050
0011          R(3)=0.125
0012          JNMM=JNM-1
0013          DO 2  J=4,JNMM
0014    2     R(J)=R(J-1)+0.125
0015          R(JNM)=R(JNMM)+0.065
0016          R(JN)=R(JNM)+0.06
        C
        C***  CALCULATE ORDINATES IN Z-DIRECTION
        C
0017          INM=IN-1
0018          IBP=IB+1
0019          ICM=IC-1
0020          DO 10  I=1,IB
0021    10    Z(I)=0.5*(I-1)
        C
0022          II=7
0023          DO 20  I=1,II
0024          ZZ=C1*FLOAT(I)/FLOAT(II)
0025          X1(I)=TAN(ZZ)/TAN(C1)*ZL1
0026    20    Z(IB +I)=Z(IB )+X1(I)
        C
0027          Z(IC)=Z(IB)+ZL1+ZL2
0028          II=10
0029          IIM=II-1
0030          DO 21  I=1,IIM
0031          ZZ=C2*FLOAT(I)/FLOAT(II)
0032          X1(I)=TAN(ZZ)/TAN(C2)*ZL2
0033    21    Z(IC -I)=Z(IC )-X1(I)
        C
0034          II=IC+1
0035          DO 22  I=II,IN
0036    22    Z(I)=Z(IC)+0.5*(I-IC)
        C
        C***  CALULATE DELR'S AND DELZ'S
        C
0037          DELR(1)=R(2)-R(1)
```

```
0038                 DELR(JN)=R(JN)-R(JNM)
0039                 DO 40  J=2,JNM
0040          40     DELR(J)=0.5*(R(J+1)-R(J-1))
0041                 DELZ(1)=Z(2)-Z(1)
0042                 DELZ(IN)=Z(IN)-Z(INM)
0043                 DO 41  I=2,INM
0044          41     DELZ(I)=0.5*(Z(I+1)-Z(I-1))
              C
              C***   SPECIFY IMIN'S AND IMAX'S
              C
0045                 DO 30  L=1,JA
0046                 IMIN(L)=1
0047          30     IMAX(L)=IN
0048                 JA1=JA+1
0049                 DO 31  L=JA1,JN
0050                 IMIN(L)=IB
0051          31     IMAX(L)=IC
              C
0052                 RETURN
0053                 END
```

```
*OPTIONS IN EFFECT*  NOTERM,ID,EBCDIC,SOURCE,NOLIST,NODECK,LOAD,NOMAP,NOTEST
*OPTIONS IN EFFECT*  NAME = GRID     , LINECNT =       56
*STATISTICS*    SOURCE STATEMENTS =         53,PROGRAM SIZE =      1758
*STATISTICS*  NO DIAGNOSTICS GENERATED

*STATISTICS*  NO DIAGNOSTICS THIS STEP
```

```
LEVEL 21.6 ( MAY 72 )                                   OS/360  FORTRAN H

          COMPILER OPTIONS - NAME=  MAIN,OPT=02,LINECNT=56,SIZE=0000K,
                              SOURCE,EBCDIC,NOLIST,DECK,LOAD,NOMAP,NOEDIT,ID,NOXREF
  ISN 0002              SUBROUTINE SOLVE
  ISN 0003              COMMON/CVP/A(23,15,3),G1(23,15),G2(23,15),V1(23,15),V2(23,15)
  ISN 0004              COMMON/CNUMBR/NW,NF,NT,IE,IN,JN,INM,JNM,JA,JB,IB,IC,
                      1                  JAM,JBM,IBP,ICM
  ISN 0005              COMMON/CGRID/Z(23),R(15),DELZ(23),DELR(15),IMIN(15),IMAX(15)
  ISN 0006              COMMON/CCHECK/RSDU(3),CC,NMAX,IRS(3),JRS(3),REFVAL(3),RELAX(3)
                      4,RSH,RSL
  ISN 0007              COMMON/CPOST/IM,IP,JM,JP,IL,IH
  ISN 0008              COMMON/CPROP/RO(23,15),ZMU(23,15),ZK(23,15),CP(23,15)
  ISN 0009              DIMENSION AQ(23,15,7)
  ISN 0010              EQUIVALENCE(A(1,1,1),AQ(1,1,1))
                  C*************************************************************
                  C     THIS SUBROUTINE INITIATES AND CONTROLS THE ITERATION PROCESS
                  C*************************************************************
                  C
  ISN 0011              WVW(DELF,RAD,DNNP,ROP,DELRO,WNP)=-(DELF/(RAD*DNNP)**2/(ROP/3.
                      1                           +5.*DELRO/24.)+WNP*(ROP/6.+DELRO/8.)/
                      2                           (ROP/3.+3.*DELRO/24.))
  ISN 0012              WHW(DELF,RAD,DNNP,ROP,DELRO,WNP)=-(DELF/DNNP**2/RAD/(ROP*(RAD/3.
                      3                           -5.*DNNP/24.)+DELRO*(5.*RAD/24.-3.*DNNP/
                      4                           20.)) + WNP*(RAD-DNNP)*(ROP*(RAD/6.-DNNP/
                      5                           8.)+DELRO*(RAD/8.-DNNP/10.))/RAD/(ROP*
                      6                           (RAD/3.-5.*DNNP/24.)+DELRO*(5.*RAD/24.
                      7                           -3.*DNNP/10.)))
                  C
                  C
  ISN 0013              NITER=0
  ISN 0014              WRITE(6,21)
  ISN 0015              DO 9  K=1,IE
  ISN 0016          9   RSDU(K)=0.
                  C
                  C
                  C***  CAUSE ONE CYCLE OF ITERATION TO BE PERFORMED
  ISN 0017          1   NITER=NITER+1
  ISN 0018              DO 10  J=2,JNM
  ISN 0019              IL=IMIN(J)+1
  ISN 0020              IH=IMAX(J)-1
  ISN 0021              IF(J.EQ.JA)  IL=IB+1
  ISN 0023              IF(J.EQ.JB)  IH=IC-1
  ISN 0025         20   DO 10  I=IL,IH
  ISN 0026              IM=I-1
  ISN 0027              IP=I+1
  ISN 0028              JM=J-1
  ISN 0029              JP=J+1
  ISN 0030         10   CALL FULON(I,J)
  ISN 0031              CALL BOUND
  ISN 0032              WRITE(6,22) NITER,(RSDU(K),IRS(K),JRS(K),K=1,IE)
  ISN 0033         99   RES=0.
  ISN 0034              DO 3  K=1,IE
  ISN 0035              IF(ABS(RSDU(K)).GT.ABS(RES)) RES=RSDU(K)
  ISN 0037          3   RSDU(K)=0.
                  C
```

```
                C***   TEST IF MAXIMUM NUMBER OF ITERATION REACHED
   ISN 0039     89     IF(NITER.GT.NMAX) GO TO 5
                C
                C
                C
                C***   TEST IF CONVERGENCE CRITERION SATISFIED
   ISN 0040     50     IF(ABS(RES).GT.CC) GO TO 1
                C
                C
                C***   WALL VORTICITIES ARE CALCULATED HERE
                C
   ISN 0042     5      DO 12  I=2,IB
   ISN 0043     12     A(I,JA,NW)=WHW(A(I,JAM,NF)-A(I,JA,NF),R(JA),R(JA)-R(JAM),
                      2                 RO(I,JA),RO(I,JAM)-RO(I,JA),A(I,JAM,NW))
   ISN 0044            JA1=JA+1
   ISN 0045            JB1=JB+1
   ISN 0046            DO 14  J=JA1,JNM
   ISN 0047     14     A(IB,J,NW)=WVW(A(IBP,J,NF)-A(IB,J,NF),R(J),Z(IBP)-Z(IB),
                      3                 RO(IB,J),RO(IBP,J)-RO(IB,J),A(IBP,J,NW))
   ISN 0048            DO 15  J=JB1,JNM
   ISN 0049     15     A(IC,J,NW)=WVW(A(ICM,J,NF)-A(IC,J,NF),R(J),Z(IC)-Z(ICM),
                      4                 RO(IC,J),RO(ICM,J)-RO(IC,J),A(ICM,J,NW))
   ISN 0050            DO 11  I=IB,IC
   ISN 0051     11     A(I,JN,NW)=WHW(A(I,JNM ,NF)-A(I,JN,NF),R(JN),R(JN)-R(JNM),
                      1                 RO(I,JN),RO(I,JNM)-RO(I,JN),A(I,JNM,NW))
   ISN 0052            DO 13  I=IC,IN
   ISN 0053     13     A(I,JB,NW)=WHW(A(I,JBM,NF)-A(I,JB,NF),R(JB),R(JB)-R(JBM),
                      5                 RO(I,JB),RO(I,JBM)-RO(I,JB),A(I,JBM,NW))
                C
   ISN 0054     21     FORMAT(1H1/2X,'MAXIMUM RESIDUAL FOR EACH VARIABLE'//2X,'NITER',12X
                      1 ,'STREAM FCN',13X,'VORTICITY',13X,'TEMPERATURE'//)
   ISN 0055     22     FORMAT(2X,I4,5X,6(1PE14.3,' (',I2,',',I2,') '))
   ISN 0056            RETURN
   ISN 0057            END

*OPTIONS IN EFFECT*      NAME=  MAIN,OPT=02,LINECNT=56,SIZE=0000K,

*OPTIONS IN EFFECT*      SOURCE,EBCDIC,NOLIST,DECK,LOAD,NOMAP,NOEDIT,ID,NOXREF

*STATISTICS*     SOURCE STATEMENTS =       56 ,PROGRAM SIZE =      3138

*STATISTICS*  NO  DIAGNOSTICS GENERATED

****** END OF COMPILATION ******                                        59K BYTES OF CORE
```

```
LEVEL 21.6 ( MAY 72 )                                    OS/360  FORTRAN H

          COMPILER OPTIONS - NAME=  MAIN,OPT=02,LINECNT=56,SIZE=0000K,
                            SOURCE,EBCDIC,NOLIST,DECK,LOAD,NOMAP,NOEDIT,ID,NOXREF
  ISN 0002              SUBROUTINE FDEQN(I,J)
  ISN 0003              COMMON/CVP/A(23,15,3),G1(23,15),G2(23,15),V1(23,15),V2(23,15)
  ISN 0004              COMMON/CNUMBR/NW,NF,NT,IE,IN,JN,INM,JNM,JA,JB,IB,IC,
                   1                 JAM,JBM,IBP,ICM
  ISN 0005              COMMON/CGRID/Z(23),R(15),DELZ(23),DELR(15),IMIN(15),IMAX(15)
  ISN 0006              COMMON/CCHECK/RSDU(3),CC,NMAX,IRS(3),JRS(3),REFVAL(3),RELAX(3)
                   4,RSM,RSL
  ISN 0007              COMMON/CCOEF/BE,BW,BN,BS,CE,CW,CN,CS,CPP
  ISN 0008              COMMON/CPROP/RO(23,15),ZMU(23,15),ZK(23,15),CP(23,15)
  ISN 0009              COMMON/CPUST/IM,IP,JM,JP,IL,IH
                C**********************************************************
                C     FINITE-DIFFERENCE-EQUATION SUBROUTINE
                C**********************************************************
                C
  ISN 0010              FG1H(DELF,RAD,DNNP,ROP,DELRO)=-DELF/DNNP**2/RAD/(ROP*(RAD/3.-
                   1                   5.*DNNP/24.) +DELRO*(5.*RAD/24.-3.*DNNP/20.))
  ISN 0011              FG2H(RAD,DNNP,ROP,DELRO)=-(RAD-DNNP)*(ROP*(RAD/6.-DNNP/8.)+
                   2                   DELRO*(RAD/8.-DNNP/10.))/RAD/(ROP*(RAD/3.-
                   3                   5.*DNNP/24.) +DELRO*(5.*RAD/24.-3.*DNNP/10.))
  ISN 0012              FG1V(DELF,RAD,DNNP,ROP,DELRO)=-DELF/(RAD*DNNP)**2/(ROP/3.
                   4                   +5.*DELRO/24.)
  ISN 0013              FG2V(ROP,DELRO)=-(ROP/6.+DELRO/8.)/(ROP/3.+5.*DELRO/24.)
                C
                C
  ISN 0014              DO 100  K=1,IE
  ISN 0015              IF(K.EQ.NT.AND.I.LE.IB) GO TO 100
                C
                C***    CALCULATE SOURCE TERM
  ISN 0017      24      CALL SORCE(I,J,K,SOURCE)
                C
                C***    CALCULATE DIFFUSION TERM
  ISN 0018              CALL DCOEF(I,J,K)
                C
  ISN 0019              IF(K.NE.NW) GO TO 110
                C
                C***    IMPLICIT TREATMENT OF WALL VORTICITY BOUNDARY
                C
  ISN 0021              ZM=3.
  ISN 0022              ZMM=0.
  ISN 0023              ZWVU=0.
  ISN 0024              IF(I.EQ.IL.AND.J.GE.JA) GO TO 500
  ISN 0026              IF(I.EQ.IM) GO TO 600
  ISN 0028              GO TO 700
                C
                C       THE CURRENT NODE IS ADJACENT TO A WEST WALL
  ISN 0029      500     LIE=IM
  ISN 0030              COE=9.
  ISN 0031              DELT=Z(IBP)-Z(IB)
  ISN 0032              GO TO 555
                C
                C       THE CURRENT NODE IS ADJACENT TO AN EAST WALL
  ISN 0033      600     IF(J-JB) 799,800,601
```

```
ISN C034      601    LIEW=IP
ISN 0035             COEW=BE
ISN 0036             DELT=Z(IC)-Z(ICM)
ISN CC37      555    A(LIEW,J,NW)=FG1V(A(I,J,NF)-A(LIEW,J,NF),R(J),DELT,RO(LIEW,J),
                    1                    RO(I,J)-RO(LIEW,J))
ISN 0038             ZW=FG2V(RO(LIEW,J),RO(I,J)-RO(LIEW,J))
ISN 0039             ZWMU=ZWMU+COEW*ZW*ZMU(LIEW,J)
ISN 0040             IF(J.EQ.JNM) GO TO 501
ISN 0042             GO TO 999
ISN C043      700    IF(J.EQ.JNM) GO TO 501
ISN CC45             IF(J.EQ.(JAM).AND.I.LE.IB) GO TO 502
ISN 0047             IF(J.NE.JBM) GO TO 999
ISN 0049             IF(I-IC) 999,800,503
              C
              C      THE CURRENT NODE IS ADJACENT TO A NORTH WALL
ISN 0050      501    RAD=R(JN)
ISN 0051             DELT=R(JN)-R(JNM)
ISN 0052             GO TO 666
ISN 0053      502    RAD=R(JA)
ISN 0054             DELT=R(JA)-R(JAM)
ISN 0055             GO TO 666
ISN 0056      503    RAD=R(JB)
ISN 0057             DELT=R(JB)-R(JBM)
ISN 0058      666    LJNS=JP
ISN 0059             CONS=BN
ISN C060             A(I,LJNS,NW)=FG1H(A(I,J,NF)-A(I,LJNS,NF),RAD,DELT,RO(I,LJNS),
                    3                    RO(I,J)-RO(I,LJNS))
ISN 0061             ZWH=FG2H(RAD,DELT,RO(I,LJNS),RO(I,J)-RO(I,LJNS))
ISN 0062             ZWMU=ZWMU+CONS*ZWH*ZMU(I,LJNS)
ISN CC63             GO TO 999
              C
              C***   VORTICITY AT THE DOWNSTREAM CORNER
ISN 0064      800    A(IC,JB,NW)=0.5*(FG1V(A(ICM,JB,NF)-A(IC,JB,NF),R(JB),Z(IC)-Z(ICM),
                    1                      RO(IC,JB),RO(ICM,JB)-RO(IC,JB)) +
                    2                  FG1H(A(IC,JBM,NF)-A(IC,JB,NF),R(JB),R(JB)-R(JBM),
                    3                      RO(IC,JB),RO(IC,JBM)-RO(IC,JB)))
ISN CC65             IF(I.EQ.IC) GO TO 801
ISN 0C67             ZW =0.5*(FG2V(RO(IC,JB),RO(ICM,JB)-RO(IC,JB)) +
                    6          FG2H(R(JB),R(JB)-R(JBM),RO(IC,JB),RO(IC,JBM)-RO(IC,JB)))
ISN 0068             ZWMU=ZWMU+BE*ZWH*ZMU(IC,JB)
ISN 0069             GO TO 999
ISN 0C70      801    ZWH=0.5*(FG2V(RO(IC,JB),RO(ICM,JB)-RO(IC,JB)) +
                    6          FG2H(R(JB),R(JB)-R(JBM),RO(IC,JB),RO(IC,JBM)-RO(IC,JB)))
ISN 0071             ZWMU=ZWMU+BN*ZWH*ZMU(IC,JB)
ISN C072      999    CONTINUE
              C
              C
              C***   COMPUTE CONVECTION TERMS AUI AND ZUI
              C
ISN C073      110    AUI=0.
ISN 0074             ZUI=0.
ISN 0075             IF(K.EQ.NF) GO TO 140
              C
              C***   CALCULATE MEAN MASS FLOW RATE AT 4 TUBES OF THE TANK
```

```
                 C
ISN 0077                DZR=1./(4.*DELZ(I)*DELR(J))
ISN 0078                GM1E=+DZR*(A(I,JP,NF)-A(I,JM,NF)+A(IP,JP,NF)-A(IP,JM,NF))
ISN 0079                GM1W=-DZR*(A(I,JP,NF)-A(I,JM,NF)+A(IM,JP,NF)-A(IM,JM,NF))
ISN 0080                GM2S=+DZR*(A(IP,J,NF)-A(IM,J,NF)+A(IP,JM,NF)-A(IM,JM,NF))
ISN 0081                GM2N=-DZH*(A(IP,J,NF)-A(IM,J,NF)+A(IP,JP,NF)-A(IM,JP,NF))
                 C
ISN 0082                IF(GM1W)2,3,1
ISN 0083         1      ZUI=GM1W
ISN 0084                GO TO 3
ISN 0085         2      AUI=-GM1W*A(IM,J,K)
ISN 0086                IF(K.EQ.NW.AND.(I.EQ.IL.AND.J.GE.JA)) GO TO 200
ISN 0088         3      IF(GM2S)5,6,4
ISN 0089         4      ZUI=ZUI+GM2S
ISN 0090                GO TO 6
ISN 0091         5      AUI=AUI-GM2S*A(I,JM,K)
ISN 0092         6      IF(GM1E)7,9,8
ISN 0093         7      AUI=AUI-GM1E*A(IP,J,K)
ISN 0094                IF(K.EQ.NW.AND.(I.EQ.IH.AND.J.GE.JB)) GO TO 202
ISN 0096                GO TO 9
ISN 0097         8      ZUI=ZUI+GM1E
ISN 0098         9      IF(GM2N)10,12,11
ISN 0099         10     AUI=AUI-GM2N*A(I,JP,K)
ISN 0100                IF(K.NE.NW) GO TO 23
ISN 0102                IF(J.EQ.JNM) GO TO 203
ISN 0104                IF(J.EQ.(JAM).AND.I.LE.IB) GO TO 203
ISN 0106                IF(J.EQ.(JBM).AND.I.GE.IC) GO TO 203
ISN 0108                GO TO 21
ISN 0109         11     ZUI=ZUI+GM2N
ISN 0110         12     GO TO (140,21,23),K
                 C
ISN 0111         200    ZUI=ZUI+GM1W*ZW
ISN 0112                GO TO 3
ISN 0113         202    ZUI=ZUI+GM1E*ZW
ISN 0114                GO TO 9
ISN 0115         203    ZUI=ZUI+GM2N*ZWH
                 C
                 C
ISN 0116         21     AUI=AUI*R(J)**2
ISN 0117                ZUI=ZUI*R(J)**2
ISN 0118                GO TO 140
ISN 0119         23     AUI=AUI*CP(I,J)
ISN 0120                ZUI=ZUI*CP(I,J)
                 C
                 C***   CALCULATE VALUE OF THE DEPENDENT VARIABLE AT THE CURRENT NODE
                 C
ISN 0121         140    ANJM=BE*CE*A(IP,J,K)+BW*CW*A(IM,J,K)+BN*CN*A(I,JP,K)+
                     B        BS*CS*A(I,JM,K)+AUI+SOURCE
ISN 0122                ADNM=(BE+BW+BN+BS)*CPP+ZUI
ISN 0123                IF(K.EQ.NW) ADNM=ADNM-ZWMU
ISN 0125                AOLD=A(I,J,K)
ISN 0126                A(I,J,K)=ANJM/ADNM
ISN 0127         222    CONTINUE
                 C
```

```
                C***  UNDER/OVER-RELAXATION
                C
 ISN 0128             DIF=A(I,J,K)-AOLD
 ISN 0129             RS=DIF/REFVAL(K)
 ISN 0130             IF(ABS(RS).GE.RSH) GO TO 70
 ISN 0132             IF(ABS(RS).LE.RSL) GO TO 80
 ISN 0134             RLX=RELAX(K)-0.3*(RS-RSL)/(RSH-RSL)
 ISN 0135             GO TO 40
 ISN 0136       70    RLX=RELAX(K)-0.3
 ISN 0137             GO TO 40
 ISN 0138       80    RLX=RELAX(K)
 ISN 0139       40    A(I,J,K)=AOLD+RLX*DIF
 ISN 0140             IF(ABS(RS).LE.ABS(RSDU(K))) GO TO 101
 ISN 0142             RSDU(K)=RS
 ISN 0143             IRS(K)=I
 ISN 0144             JRS(K)=J
                C
 ISN 0145       101   GO TO(102,100,103),K
                C***  CALCULATE VELOCITY COMPONENTS
                C
 ISN 0146       102   DO 50  L=IM,IP
 ISN 0147             IF(L.EQ.1) GO TO 50
 ISN 0149             IF(L.EQ.IB.AND.J.GE.JA) GO TO 50
 ISN 0151             IF(L.EQ.IC.AND.J.GE.JB) GO TO 50
 ISN 0153             G2(L,J)=-ADF(L,J,1,NF)/R(J)
 ISN 0154             V2(L,J)=G2(L,J)/RO(L,J)
 ISN 0155       50    CONTINUE
                C
 ISN 0156             DO 31  L=JM,JP
 ISN 0157             IF(L.EQ.1.OR.L.EQ.JN) GO TO 31
 ISN 0159             IF(L.EQ.JA.AND.I.LE.IB) GO TO 31
 ISN 0161             IF(L.EQ.JB.AND.I.GE.IC) GO TO 31
 ISN 0163             G1(I,L)= ADF(I,L,2,NF)/R(L)
 ISN 0164             V1(I,L)=G1(I,L)/RO(I,L)
 ISN 0165       31    CONTINUE
 ISN 0166             IF(J.NE.2) GO TO 100
 ISN 0168             BBR=1./(1.-(R(2)/R(3))**2)
 ISN 0169             G1(I,1)=BBR*G1(I,2)-(BBR-1.)*G1(I,3)
 ISN 0170             V1(I,1)=G1(I,1)/RO(I,1)
 ISN 0171             GO TO 100
                C
                C***  CALCULATE DENSITY,VISCOSITY, THERMAL CONDUCTIVITY AND
                C     SPECIFIC HEAT
 ISN 0172       103   CALL  PROPTY(A(I,J,NT),RO(I,J),ZMU(I,J),ZK(I,J),CP(I,J))
                C
 ISN 0173       100   CONTINUE
 ISN 0174             RETURN
 ISN 0175             END

*OPTIONS IN EFFECT*       NAME=  MAIN,OPT=02,LINECNT=56,SIZE=0000K,

*OPTIONS IN EFFECT*       SOURCE,EBCDIC,NOLIST,DECK,LOAD,NOMAP,NOEDIT,ID,NOXREF

*STATISTICS*      SOURCE STATEMENTS =      174 ,PROGRAM SIZE =      4802
```

```
LEVEL 21.6 ( MAY 72 )                                  OS/360  FORTRAN H

          COMPILER OPTIONS - NAME=  MAIN,OPT=02,LINECNT=56,SIZE=0000K,
                             SOURCE,EBCDIC,NOLIST,DECK,LOAD,NOMAP,NOEDIT,ID,NOXREF
  ISN 0002            SUBROUTINE DCOEF(I,J,K)
  ISN 0003            COMMON/CGRID/Z(23),R(15),DELZ(23),DELR(15),IMIN(15),IMAX(15)
  ISN 0004            COMMON/CPARAM/VINL,RE,PR,BR
  ISN 0005            COMMON/CPOST/IM,IP,JM,JP,IL,IH
  ISN 0006            COMMON/CPROP/RO(23,15),ZMU(23,15),ZK(23,15),CP(23,15)
  ISN 0007            COMMON/CCOEF/BE,BW,BN,BS,CE,CW,CN,CS,CPP
                C*****************************************************************
                C     SUBROUTINE FOR CALCULATION OF DIFFUSION COEFFICIENTS
                C*****************************************************************
                C
  ISN 0008            GO TO(2,1,5),K
                C
                C***  FOR VORTICITY
                C
  ISN 0009      1     BBP=R(J)**3/RE
  ISN 0010            BBE=BBP
  ISN 0011            BBW=BBP
  ISN 0012            BBN=R(JP)**3/RE
  ISN 0013            BBS=R(JM)**3/RE
  ISN 0014            CPP=ZMU(I,J)
  ISN 0015            CE=ZMU(IP,J)
  ISN 0016            CW=ZMU(IM,J)
  ISN 0017            CN=ZMU(I,JP)
  ISN 0018            CS=ZMU(I,JM)
  ISN 0019            GO TO 20
                C
                C***  FOR STREAM FUNCTION
                C
  ISN 0020      2     BBP=1./(R(J)*RO(I,J))
  ISN 0021            BBE=1./(R(J)*RO(IP,J))
  ISN 0022            BBW=1./(R(J)*RO(IM,J))
  ISN 0023            BBN=1./(R(JP)*RO(I,JP))
  ISN 0024            IF(J.EQ.2) GO TO 3
  ISN 0026            BBS=1./(R(JM)*RO(I,JM))
  ISN 0027            GO TO 4
  ISN 0028      3     BBS=8./(R(J)+R(JM))/(RO(I,J)+RO(I,JM))-BBP
  ISN 0029      4     CPP=1.
  ISN 0030            CE=1.
  ISN 0031            CW=1.
  ISN 0032            CN=1.
  ISN 0033            CS=1.
  ISN 0034            GO TO 20
                C
                C***  FOR TEMPERATURE
                C
  ISN 0035      5     REPR=RE*PR
                C
                C
  ISN 0036            BBP=ZK(I,J)*R(J)/REPR
  ISN 0037            BBE=ZK(IP,J)*R(J)/REPR
  ISN 0038            BBW=ZK(IM,J)*R(J)/REPR
  ISN 0039            BBN=ZK(I,JP)*R(JP)/REPR
```

```
ISN 0040          BBS=ZK(I,JM)*R(JM)/REPR
ISN 0041          CPP=1.
ISN 0042          CE=1.
ISN 0043          CW=1.
ISN 0044          CN=1.
ISN 0045          CS=1.
            C
            C***  FOR ALL DEPENDENT VARIABLES
            C
ISN 0046    20    BE=(BBP+BBE)/(2.*DELZ(I)*(Z(IP)-Z(I)))
ISN 0047          BW=(BBP+BBW)/(2.*DELZ(I)*(Z(I)-Z(IM)))
ISN 0048          BN=(BBN+BBP)/(2.*DELR(J)*(R(JP)-R(J)))
ISN 0049          BS=(BBS+BBP)/(2.*DELR(J)*(R(J)-R(JM)))
ISN 0050          RETURN
ISN 0051          END
*OPTIONS IN EFFECT*      NAME=  MAIN,OPT=02,LINECNT=56,SIZE=0000K,

*OPTIONS IN EFFECT*      SOURCE,EBCDIC,NOLIST,DECK,LOAD,NOMAP,NOEDIT,ID,NOXREF

*STATISTICS*     SOURCE STATEMENTS =       50 ,PROGRAM SIZE =     1178

*STATISTICS*  NO  DIAGNOSTICS GENERATED

****** END OF COMPILATION ******                                   67K BYTES OF CORE
```

LEVEL 21.6 (MAY 72)　　　　　　　　　　　OS/360　FORTRAN H

```
              COMPILER OPTIONS - NAME=  MAIN,OPT=02,LINECNT=56,SIZE=0000K,
                                  SOURCE,EBCDIC,NOLIST,DECK,LOAD,NOMAP,NOEDIT,ID,NOXREF
ISN 0002                 SUBROUTINE PROPTY(TT,RO,ZMU,ZK,CP)
ISN 0003                 COMMON/CREF/ROREF,ZMUREF,CPREF,ZKREF,TINL,TWALL
ISN 0004                 COMMON/CDATA/TEMP(100),PROP(100,4),DEL
ISN 0005                 DIMENSION Y(4),VAL(4)
                   C
                   C*************************************************************************
                   C     SUBROUTINE FOR CALCULATION OF DENSITY,VISCOSITY,
                   C     THERMAL CONDUCTIVITY AND SPECIFIC HEAT AT CONSTANT PRESSURE
                   C*************************************************************************
                   C
                   C     PROP(I,1) : DENSITY GM/CC
                   C     PROP(I,2) : VISCOSITY GM/CM/SEC
                   C     PROP(I,3) : THERMAL CONDUCTIVITY CAL/CM/SEC/DEG K
                   C     PROP(I,4) : SPECIFIC HEAT AT CONSTANT PRES
                   C
                   C***  CONVERT DIMENSIONLESS TEMPERATURE TO DIMENSIONAL ONE
                   C
ISN 0006                 T=TT*(TINL-TWALL)+TWALL
                   C
                   C***  LAGRANGE INTERPOLATION FOR EQUAL INTERVALS
ISN 0007                 IT=IFIX(T)/100 +1
ISN 0008                 IF(T.EQ.TEMP(IT)) GO TO 60
ISN 0010                 H=T-TEMP(IT)
ISN 0011                 IF(IT.LT.2) GO TO 20
ISN 0013                 DO 200  KK=1,4
ISN 0014                 DO 201  N=1,4
ISN 0015           201   VAL(N)=PROP(IT+N-2,KK)
ISN 0016           200   Y(KK)=(-VAL(1)/(H+DEL) +3.*VAL(2)/H -3.*VAL(3)/(H-DEL)
                       1       +VAL(4)/(H-2.*DEL))*(H+DEL)*H*(H-DEL)*(H-2.*DEL)/
                       2       (6.*DEL**3)
ISN 0017                 GO TO 400
                   C
ISN 0018           20    DO 800  KK=1,4
ISN 0019                 DO 801  I=1,4
ISN 0020           801   VAL(I)=PROP(I,KK)
ISN 0021           800   Y(KK)=(-VAL(1)/H +3.*VAL(2)/(H-DEL) -3.*VAL(3)/(H-2.*DEL)
                       4       +VAL(4)/(H-3.*DEL))*H*(H-DEL)*(H-2.*DEL)*(H-3.*DEL)/
                       5       (6.*DEL**3)
ISN 0022                 GO TO 400
                   C
ISN 0023           60    DO 300  KK=1,4
ISN 0024           300   Y(KK)=PROP(IT,KK)
                   C
                   C***  MAKE FLUID PROPERTIES DIMENSIONLESS
                   C
ISN 0025           400   RO=Y(1)/ROREF
ISN 0026                 ZMU=Y(2)/ZMUREF
ISN 0027                 ZK=Y(3)/ZKREF
ISN 0028                 CP=Y(4)/CPREF
ISN 0029                 RETURN
ISN 0030                 END
*OPTIONS IN EFFECT*      NAME=  MAIN,OPT=02,LINECNT=56,SIZE=0000K,
```

```
LEVEL 21.6 ( MAY 72 )                                        OS/360  FORTRAN H

              COMPILER OPTIONS - NAME=  MAIN,OPT=02,LINECNT=56,SIZE=0000K,
                         SOURCE,EBCDIC,NOLIST,DECK,LOAD,NOMAP,NOEDIT,ID,NOXREF
 ISN 0002               SUBROUTINE SORCE(I,J,K,SOURCE)
 ISN 0003               COMMON/CVPV/A(23,15,9),G1(23,15),G2(23,15),V1(23,15),V2(23,15)
 ISN 0004               COMMON/CGRID/Z(23),R(15),DELZ(23),DELR(15),IMIN(15),IMAX(15)
 ISN 0005               COMMON/CNUMBR/NN,NF,NT,IE,IN,JN,INM,JNM,JA,JB,IB,IC,
                       1          JAM,JBM,IBP,ICM
 ISN 0006               COMMON/CPROP/RO(23,15),ZMU(23,15),ZK(23,15),CP(23,15)
 ISN 0007               COMMON/CREF/ROREF,ZMUREF,CPREF,ZKREF,TINL,TWALL
 ISN 0008               COMMON/CPARAM/VINL,RE,PR,BR
 ISN 0009               COMMON/CPOST/IM,IP,JM,JP,IL,IH
 ISN 0010               DIMENSION DV1DZ(23,15),DV1DR(23,15),DV2DZ(23,15),DV2DR(23,15)
 ISN 0011               DIMENSION AO(23,15,9)
 ISN 0012               EQUIVALENCE (A(1,1,1),AO(1,1,1))
                  C*************************************************************
                  C     SUBROUTINE FOR CALCULATION OF SOURCE TERMS
                  C*************************************************************
                  C
 ISN 0013               GO TO(2,1,3),K
                  C
                  C***  FOR VORTICITY
                  C
 ISN 0014         1     DO 22  LI=IM,IP
 ISN 0015               DO 21  LJ=JM,JP
 ISN 0016               DV2DR(LI,LJ)=ADF(LI,LJ,2,7)
 ISN 0017               DV1DZ(LI,LJ)=ADF(LI,LJ,1,6)
 ISN 0018         21    AO(LI,LJ,8)=ZMU(LI,LJ)*(DV2DR(LI,LJ)-DV1DZ(LI,LJ))
 ISN 0019         22    AO(LI,J,9)=ADF(LI,J,2,8)
                  C
 ISN 0020               IMM=IM-1
 ISN 0021               IPP=IP+1
 ISN 0022               IF(IMM.LT.1) IMM=1
 ISN 0024               IF(IMM.LT.IB.AND.J.GT.JA) IMM=IB
 ISN 0026               IF(IPP.GT.IN) IPP=IN
 ISN 0028               IF(IPP.GT.IC.AND.J.GT.JB) IPP=IC
 ISN 0030               DO 25 LI=IMM,IPP
 ISN 0031               DV1DR(LI,J)=ADF(LI,J,2,6)
 ISN 0032         25    AO(LI,J,8)=ZMU(LI,J)*DV1DR(LI,J)
                  C
 ISN 0033               DO 24  LI=IM,IP
 ISN 0034         24    AO(LI,J,9)=-2.*(AO(LI,J,9)+ADF(LI,J,1,8)+ZMU(LI,J)/R(J)*
                       1          (DV2DR(LI,J)-V2(LI,J)/R(J)))/RE -V1(LI,J)*
                       2          ADF(LI,J,2,4) +V2(LI,J)*ADF(LI,J,1,4)
                       3          +G2(LI,J)*V2(LI,J)/R(J)
 ISN 0035               SOURCE=ADF(I,J,1,9)
                  C
 ISN 0036               JMM=JM-1
 ISN 0037               JPP=JP+1
 ISN 0038               IF(JMM.LT.1) JMM=1
 ISN 0040               IF(JPP.GT.JN) JPP=JN
 ISN 0042               IF(JPP.GT.JA.AND.I.LT.IB) JPP=JA
 ISN 0044               IF(JPP.GT.JB.AND.I.GT.IC) JPP=JB
 ISN 0046               DO 33  LJ=JMM,JPP
 ISN 0047               IF(LJ.EQ.1.OR.LJ.EQ.JN) GO TO 61
```

```
ISN 0049          DV2DZ(I,LJ)=ADF(I,LJ,1,7)
ISN 0050          AQ(I,LJ,8)=ZMU(I,LJ)*DV2DZ(I,LJ)
ISN 0051          GO TO 33
ISN 0052     61   DV2DZ(I,LJ)=0.0
ISN 0053          AQ(I,LJ,8)=0.
ISN 0054     33   CONTINUE
             C
ISN 0055     36   DO 32  LJ=JM,JP
ISN 0056          AQ(I,LJ,9)=2.*ADF(I,LJ,2,8)/RE -V1(I,LJ)*ADF(I,LJ,2,5)
                 1             +V2(I,LJ)*ADF(I,LJ,1,5)
ISN 0057          IF(LJ.EQ.1) GO TO 360
ISN 0059          AQ(I,LJ,9)=AQ(I,LJ,9)-(G2(I,LJ)*V1(I,LJ)-2.*ZMU(I,LJ)*
                 5                            DV2DZ(I,LJ)/RE)/R(LJ)
ISN 0060          GO TO 32
ISN 0061     360  F1=R(LJ+2)/(R(LJ+2)-R(LJ+1))
ISN 0062          AQ(I,LJ,9)=AQ(I,LJ,9)-F1*(G2(I,LJ+1)*V1(I,LJ+1)-2.*ZMU(I,LJ+1)
                 1                                  *DV2DZ(I,LJ+1)/RE)/R(LJ+1)
                 2                    -(1.-F1)*(G2(I,LJ+2)*V1(I,LJ+2)-2.*ZMU(I,LJ+2)
                 3                                  *DV2DZ(I,LJ+2)/RE)/R(LJ+2)
ISN 0063     32   CONTINUE
ISN 0064          SOURCE=-(SOURCE+ADF(I,J,2,9))*R(J)**2
ISN 0065          RETURN
             C
             C
             C***  FOR STREAM FUNCTION
             C
ISN 0066     2    SOURCE=A(I,J,NW)*R(J)
ISN 0067          RETURN
             C
             C
             C***  FOR TEMPERATURE
             C
ISN 0068     3    SOURCE=0.
             C
ISN 0069          RETURN
ISN 0070          END

*OPTIONS IN EFFECT*      NAME=  MAIN,OPT=02,LINECNT=56,SIZE=0000K,

*OPTIONS IN EFFECT*      SOURCE,EBCDIC,NOLIST,DECK,LOAD,NOMAP,NOEDIT,ID,NOXREF

*STATISTICS*     SOURCE STATEMENTS =       69 ,PROGRAM SIZE =     7916

*STATISTICS*  NO  DIAGNOSTICS GENERATED

****** END OF COMPILATION ******                                    59K BYTES OF CORE N
```


7905810

```
LEVEL 21.6 ( MAY 72 )                                   OS/360  FORTRAN H

        COMPILER OPTIONS - NAME= MAIN,OPT=02,LINECNT=56,SIZE=0000K,
                           SOURCE,EBCDIC,NOLIST,DECK,LOAD,NOMAP,NOEDIT,ID,NOXREF
  ISN 0002              SUBROUTINE BOUND
  ISN 0003              COMMON/CVP/A(23,15,3),G1(23,15),G2(23,15),V1(23,15),V2(23,15)
  ISN 0004              COMMON/CGRID/Z(23),R(15),DELZ(23),DELR(15),IMIN(15),IMAX(15)
  ISN 0005              COMMON/CPROP/RO(23,15),ZMU(23,15),ZK(23,15),CP(23,15)
  ISN 0006              COMMON/CNUMBR/NW,NF,NT,IE,IN,JN,INM,JNM,JA,JB,IB,IC,
                1                  JAM,JBM,IBP,ICM
                C*****************************************************
                C      SUBROUTINE FOR CALCULATION OF BOUNDARY VALUES FOR
                C      ALL THE DEPENDENT VARIABLES
                C*****************************************************
                C
                C
                C*****FOR STREAM FUNCTION ...A(I,J,NF)
                C
                C***   EXIT (ASSUMING ZERO AXIAL GRADIENT)
  ISN 0007              BB=1./(1.-((Z(IN)-Z(INM))/(Z(IN)-Z(IN-2)))**2)
  ISN 0008              BB1=BB-1.
  ISN 0009      2       DO 210  J=2,JB
  ISN 0010      210     A(IN,J,NF)=BB*A(INM,J,NF)-BB1*A(IN-2,J,NF)
                C
                C
                C*****FOR VORTICITY...A(I,J,NW)
                C
                C***   EXIT
  ISN 0011              DO 18  J=2,JB
  ISN 0012      18      A(IN,J,NW)=BB*A(IN-1,J,NW)-BB1*A(IN-2,J,NW)
                C
                C***   ON THE AXIS-OF-SYMMETRY
  ISN 0013      111     DO 10  I=2,IN
  ISN 0014      10      A(I,1,NW)=A(I,2,NW)+(R(2)/(R(3)-R(2)))*(A(I,2,NW)-A(I,3,NW))
                C
                C
                C*****FOR TEMPERATURE ...A(I,J,NT)
                C
                C***   EXIT
  ISN 0015              DO 300  J=2,JBM
  ISN 0016      300     A(IN,J,NT)=BB*A(INM,J,NT)-BB1*A(IN-2,J,NT)
                C
                C***   ON THE AXIS-OF-SYMMETRY
  ISN 0017              BBR=1./(1.-(R(2)/R(3))**2)
  ISN 0018              BBR1=BBR-1.
  ISN 0019              DO 301  I=2,IN
  ISN 0020      301     A(I,1,NT)=BBR*A(I,2,NT)-BBR1*A(I,3,NT)
                C
                C*****FOR VELOCITIES
                C
                C***   ZERO AXIAL GRADIENTS AT EXIT
                C
  ISN 0021      41      DO 401  J=2,JBM
  ISN 0022              G1(IN,J)=BB*G1(INM,J)-BB1*G1(IN-2,J)
  ISN 0023      401     V1(IN,J)=G1(IN,J)/RO(IN,J)
                C
```

7905211

```
                C***  ON THE AXIS OF SYMMETRY
                C
  ISN 0024            DO 402  I=2,IN
  ISN 0025            G1(I,1)=BBP*G1(I,2)-BBP1*G1(I,3)
  ISN 0026      402   V1(I,1)=G1(I,1)/RO(I,1)
                C
                C
  ISN 0027            RETURN
  ISN 0028            END

*OPTIONS IN EFFECT*       NAME=  MAIN,OPT=02,LINECNT=56,SIZE=0000K,

*OPTIONS IN EFFECT*       SOURCE,EBCDIC,NOLIST,DECK,LOAD,NOMAP,NOEDIT,ID,NOXREF

*STATISTICS*      SOURCE STATEMENTS =       27 ,PROGRAM SIZE =      1048

*STATISTICS*  NO  DIAGNOSTICS GENERATED

****** END OF COMPILATION ******                                    67K BYTES OF CORE N
```

```
LEVEL 21.6 ( MAY 72 )                                   OS/360  FORTRAN H

          COMPILER OPTIONS - NAME=  MAIN,OPT=02,LINECNT=56,SIZE=0000K,
                             SOURCE,EBCDIC,NOLIST,DECK,LOAD,NOMAP,NOEDIT,ID,NOXREF
  ISN 0002              FUNCTION ADF(I,J,LX,KQ)
  ISN 0003              COMMON/CVP/A(23,15,9),G1(23,15),G2(23,15),V1(23,15),V2(23,15)
  ISN 0004              COMMON/CNUMBR/NW,NF,NT,IE,IN,JN,INM,JNM,JA,JB,IB,IC,
                       1                JAM,JPM,IBP,ICM
  ISN 0005              COMMON/CGRID/Z(23),R(15),DELZ(23),DELR(15),IMIN(15),IMAX(15)
  ISN 0006              COMMON/CPOST/IM,IP,JM,JP,IL,IH
  ISN 0007              DIMENSION BENQ(9),BWSR(9),BP(9),AQ(23,15,9)
  ISN 0008              EQUIVALENCE (A(1,1,1),AQ(1,1,1))
                  C*****************************************************************
                  C     THIS FUNCTION EVALUATES FIRST DERIVATIVES IN TERMS OF
                  C     CENTRAL DIFFERENCES
                  C*****************************************************************
  ISN 0009              DF(PN,BENQ,BWSR,BP,XENQ,XWSR)=((BENQ-BP)*XWSR**2
                       1                    +(BP-BWSR)*XENQ**2)/
                       2                    (XENQ*XWSR*(PN*XENQ+XWSR))
                  C
                  C***  DEPENDING ON THE POSITION OF THE POINT (I,J) ,THERE ARE 5 DIFFERENT
                  C     EXPRESSIONS FOR THE DERIVATIVE
                  C***  LX INDICATES THE TYPE OF DERIVATIVE
                  C       LX=1: PARTIAL DERIVATIVE W.R.T. Z
                  C       LX=2: PARTIAL DERIVATIVE W.R.T. R
                  C     AQ(I,J,8) & AQ(I,J,9) : TEMPORARY DEPENDENT VARIABLES
                  C
  ISN 0010              PN=1.
  ISN 0011              IF(J.EQ.1) GO TO 2
  ISN 0013              IF(I.EQ.1) GO TO 3
  ISN 0015              IF(I.EQ.IN)GO TO 5
  ISN 0017              IF(J.EQ.JN) GO TO 4
  ISN 0019              IF(J.EQ.JA.AND.(I.LT.IB))  GO TO 4
  ISN 0021              IF(J.EQ.JB.AND.(I.GT.IC))  GO TO 4
  ISN 0023              IF(I.EQ.IB.AND.(J.GT.JA))  GO TO 3
  ISN 0025              IF(I.EQ.IC.AND.(J.GT.JB))  GO TO 5
                  C
                  C***  M=1 :FOR POINTS NOT ON ANY OF THE BOUNDARIES
                  C
  ISN 0027        1     IF(LX.EQ.1) GO TO 12
  ISN 0029        13    BENQ(KQ)=AQ(I,J+1,KQ)
  ISN 0030              BWSR(KQ)=AQ(I,J-1,KQ)
  ISN 0031              BP(KQ)=AQ(I,J,KQ)
  ISN 0032              XENQ=R(J+1)-R(J)
  ISN 0033              XWSR=R(J)-R(J-1)
  ISN 0034              GO TO 100
  ISN 0035        12    BENQ(KQ)=AQ(I+1,J,KQ)
  ISN 0036              BWSR(KQ)=AQ(I-1,J,KQ)
  ISN 0037              BP(KQ)=AQ(I,J,KQ)
  ISN 0038              XENQ=Z(I+1)-Z(I)
  ISN 0039              XWSR=Z(I)-Z(I-1)
  ISN 0040              GO TO 100
                  C
                  C***  M=2 : FOR POINTS ON THE BOUNDARY J=1
                  C
  ISN 0041        2     IF(LX.EQ.1)GO TO 23
```

```
ISN 0043     21     PN=-1.
ISN 0044            BENQ(KQ)=AQ(I,J+1,KQ)
ISN 0045            BWSR(KQ)=AQ(I,J+2,KQ)
ISN 0046            BP(KQ)=AQ(I,J,KQ)
ISN 0047            XENQ=R(J+1)-R(J)
ISN 0048            XWSR=R(J+2)-R(J)
ISN 0049            GO TO 100
ISN 0050     23     IF(I.EQ.1) GO TO  31
ISN 0052            IF(I.EQ.IN) GO TO 51
ISN 0054            GO TO 12
             C
             C***   M=3 : FOR POINTS ON THE WALL OF I=IB AND THOSE ON THE INLET
             C
ISN 0055     3      IF(LX.NE.1) GO TO 32
ISN 0057     31     PN=-1.
ISN 0058            BENQ(KQ)=AQ(I+1,J,KQ)
ISN 0059            BWSR(KQ)=AQ(I+2,J,KQ)
ISN 0060            BP(KQ)=AQ(I,J,KQ)
ISN 0061            XENQ=Z(I+1)-Z(I)
ISN 0062            XWSR=Z(I+2)-Z(I)
ISN 0063            GO TO 100
ISN 0064     32     IF(J.EQ.JA) GO TO 41
ISN 0066            GO TO 13
             C
             C***   M=4 : FOR POINTS ON ALL WALLS PARALLEL TO THE J LINES
             C
ISN 0067     4      IF(LX.EQ.1 ) GO TO 43
ISN 0069     41     PN=-1.
ISN 0070            BENQ(KQ)=AQ(I,J-1,KQ)
ISN 0071            BWSR(KQ)=AQ(I,J-2,KQ)
ISN 0072            BP(KQ)=AQ(I,J,KQ)
ISN 0073            XENQ=R(J-1)-R(J)
ISN 0074            XWSR=R(J-2)-R(J)
ISN 0075            GO TO 100
ISN 0076     43     IF(I.EQ.IB) GO TO 31
ISN 0078            IF(I.EQ.IC) GO TO 51
ISN 0080            GO TO 12
             C
             C***   M=5 : FOR POINTS ON THE WALL OF I=IC AND THOSE ON THE EXIT
             C
ISN 0081     5      IF(LX.NE.1) GO TO 52
ISN 0083     51     PN=-1.
ISN 0084            BENQ(KQ)=AQ(I-1,J,KQ)
ISN 0085            BWSR(KQ)=AQ(I-2,J,KQ)
ISN 0086            BP(KQ)=AQ(I,J,KQ)
ISN 0087            XENQ=Z(I-1)-Z(I)
ISN 0088            XWSR=Z(I-2)-Z(I)
ISN 0089            GO TO 100
ISN 0090     52     IF(J.EQ.JP) GO TO 41
ISN 0092            GO TO 13
             C
ISN 0093     100    ADF=DF(PN,BENQ(KQ),BWSR(KQ),BP(KQ),XENQ,XWSR)
ISN 0094            RETURN
ISN 0095            END
```

```
LEVEL 21.6 ( MAY 72 )                                  OS/360   FORTRAN H

        COMPILER OPTIONS - NAME=  MAIN,OPT=02,LINECNT=56,SIZE=0000K,
                              SOURCE,EBCDIC,NOLIST,DECK,LOAD,NOMAP,NOEDIT,ID,NOXREF
  ISN 0002                SUBROUTINE PRINCT
  ISN 0003                COMMON/CVP/A(23,15,3),G1(23,15),G2(23,15),V1(23,15),V2(23,15)
  ISN 0004                COMMON/CNUMBR/NW,NF,NT,IE,IN,JN,INM,JNM,JA,JB,IB,IC,
                         1            JAM,JBM,IBP,ICM
  ISN 0005                COMMON/CGRID/Z(23),R(15),DELZ(23),DELR(15),IMIN(15),IMAX(15)
  ISN 0006                COMMON/CPARAM/VINL,RE,PR,BR
  ISN 0007                COMMON/CNAME/ANAME(9,7)
  ISN 0008                COMMON/CPRUP/RO(23,15),ZMU(23,15),ZK(23,15),CP(23,15)
  ISN 0009                DIMENSION W(23),AQ(23,15,7)
  ISN 0010                EQUIVALENCE (A(1,1,1),AQ(1,1,1))
                    C*******************************************************
                    C     THIS SUBROUTINE PRINTS OUT THE RESULTS
                    C*******************************************************
                    C
  ISN 0011                DO 100  K=1,7
  ISN 0012                WRITE(6,200) (ANAME(L,K),L=1,9)
  ISN 0013                DO 100  IP=1,2
  ISN 0014                IEMPTY=0
  ISN 0015                GO TO (11,12,13),IP
  ISN 0016          11    IEND=11
  ISN 0017                GO TO 20
  ISN 0018          12    IEND=22
  ISN 0019                IF(IN.LT.22)IEND=IN
  ISN 0021                GO TO 20
  ISN 0022          13    IEND=IN
  ISN 0023          20    DO 50  JJ=1,JN
  ISN 0024                J=JN+1-JJ
  ISN 0025                GO TO (21,22,23),IP
  ISN 0026          21    II1=IMIN(J)
  ISN 0027                IEMPTY=II1-1
  ISN 0028                II2=11
  ISN 0029                GO TO 30
  ISN 0030          22    II1=12
  ISN 0031                II2=IMAX(J)
  ISN 0032                IF(II2.GT.22) II2=22
  ISN 0034                GO TO 30
  ISN 0035          23    IF(IMAX(J).LT.23) GO TO 50
  ISN 0037                II1=23
  ISN 0038                II2=IMAX(J)
  ISN 0039          30    IF(K.NE.NW) GO TO 32
  ISN 0041                DO 31  I=II1,II2
  ISN 0042                W(I)=A(I,J,K)
  ISN 0043          31    A(I,J,NW)=W(I)*R(J)
  ISN 0044          32    IF(IEMPTY.GE.1) GO TO 33
  ISN 0046                WRITE(6,201) J,(AQ(I,J,K),I=II1,II2)
  ISN 0047                GO TO 44
  ISN 0048          33    GO TO (41,42,43),IEMPTY
  ISN 0049          41    WRITE(6,301) J,(AQ(I,J,K),I=II1,II2)
  ISN 0050                GO TO 44
  ISN 0051          42    WRITE(6,302) J,(AQ(I,J,K),I=II1,II2)
  ISN 0052                GO TO 44
  ISN 0053          43    WRITE(6,303) J,(AQ(I,J,K),I=II1,II2)
```

```
ISN 0054    44   IF(K.NE.NW) GO TO 50
ISN 0056         DO 45  I=II1,II2
ISN 0057    45   A(I,J,K)=W(I)
ISN 0058    50   CONTINUE
ISN 0059    5    GO TO (51,52,53),IP
ISN 0060    51   WRITE(6,202) (I,I=1,IEND)
ISN 0061         GO TO 54
ISN 0062    52   WRITE(6,202) (I,I=12,IEND)
ISN 0063         GO TO 54
ISN 0064    53   WRITE(6,202) (I,I=23,IEND)
ISN 0065    54   WRITE(6,203)
ISN 0066    100  CONTINUE
ISN 0067    200  FORMAT(1H1//35X,'THE DISTRIBUTION OF  ',9A4///)
ISN 0068    201  FORMAT(1H ,I2,2X,11(1PE11.3))
ISN 0069    202  FORMAT(1H0,11I11///)
ISN 0070    203  FORMAT(1H0///)
ISN 0071    301  FORMAT(1H ,I2,2X,11X,10(1PE11.3))
ISN 0072    302  FORMAT(1H ,I2,2X,22X, 9(1PE11.3))
ISN 0073    303  FORMAT(1H ,I2,2X,33X, 8(1PE11.3))
ISN 0074         RETURN
ISN 0075         END

*OPTIONS IN EFFECT*     NAME=  MAIN,OPT=02,LINECNT=56,SIZE=0000K,

*OPTIONS IN EFFECT*     SOURCE,EBCDIC,NOLIST,DECK,LOAD,NOMAP,NOEDIT,ID,NOXREF

*STATISTICS*     SOURCE STATEMENTS =      74 ,PROGRAM SIZE =    2032

*STATISTICS*  NO  DIAGNOSTICS GENERATED

****** END OF COMPILATION ******                                63K BYTES OF CORE
```

```
LEVEL 21.6 ( MAY 72 )                                  OS/360  FORTRAN H

          COMPILER OPTIONS - NAME=  MAIN,OPT=02,LINECNT=59,SIZE=0000K,
                                    SOURCE,EBCDIC,NOLIST,DECK,LOAD,NOMAP,NOEDIT,ID,NOXREF
  ISN 0002              SUBROUTINE HEAT
  ISN 0003              COMMON/CVP/A(23,15,3),G1(23,15),G2(23,15),V1(23,15),V2(23,15)
  ISN 0004              COMMON/CNUMBR/NN,NF,NT,IE,IN,JN,INM,JNM,JA,JB,IB,IC,
                       1           JAM,JBM, IBP,ICM
  ISN 0005              COMMON/CGRID/Z(23),R(15),DELZ(23),DELR(15),IMIN(15),IMAX(15)
  ISN 0006              COMMON/CPROP/RO(23,15),ZMU(23,15),ZK(23,15),CP(23,15)
  ISN 0007              COMMON/CREF/ROREF,ZMUREF,CPREF,ZKREF,TINL,TWALL
  ISN 0008              DIMENSION VIR(15),VITR(15)
                  C**********************************************************************
                  C     SUBROUTINE FOR CALCULATION OF LOCAL HEAT TRANSFER COEFFICIENT
                  C     AND LOCAL NUSSELT NUMBER
                  C**********************************************************************
                  C
  ISN 0009              WRITE(6,501)
                  C***  CALCULATE LOCAL HEAT TRANSFER RATE TO THE WALL
                  C
  ISN 0010              DO 500  I=IBP,ICM
  ISN 0011              Q=(ZK(I,JN)*ZKREF)*ADF(I,JN,2,NT)*(TINL-TWALL)
                  C
                  C***  CALCULATE LOCAL BULK TEMPERATURE OF THE GAS.
                  C     USING SIMPSON'S RULE FOR INTEGRATION
                  C
  ISN 0012              DO 510  J=2,JNM
  ISN 0013              VIR(J)=G1(I,J)*R(J)*CP(I,J)
  ISN 0014        510   VITR(J)=VIR(J)*(A(I,J,NT)*(TINL-TWALL)+TWALL)
  ISN 0015              ZINT1=VIR(2)*R(2)/2.0+(VIR(2)+VIR(3))*(R(3)-R(2))/2.0 +
                       1     (VIR(3)+3.0*VIR(4)+3.0*VIR(5)+2.0*VIR(6)+3.0*VIR(7)+
                       2      3.0*VIR(8)+VIR(9))*DELR(3)*3.0/8.0 + (7.0*VIR(9)+
                       3      32.0*VIR(10)+12.0*VIR(11)+32.0*VIR(12)+7.0*VIR(13))*
                       4     DELR(9)*2.0/45.0 + (VIR(13)+VIR(14))*(R(14)-R(13))/2. +
                       4     VIR(14)*(R(15)-R(14))/2.
  ISN 0016              ZINT2=VITR(2)*R(2)/2. + (VITR(2)+VITR(3))*(R(3)-R(2))/2. +
                       5     (VITR(3)+3.*VITR(4)+3.*VITR(5)+2.*VITR(6)+3.*VITR(7)+
                       6      3.*VITR(8)+VITR(9))*DELR(3)*3./8. + (7.*VITR(9)+
                       7      32.*VITR(10)+12.*VITR(11)+32.*VITR(12)+7.*VITR(13))*
                       8     DELR(9)*2./45. + (VITR(13)+VITR(14))*(R(14)-R(13))/2. +
                       8     VITR(14)*(R(15)-R(14))/2.
                  C
  ISN 0017              TBULK=ZINT2/ZINT1
  ISN 0018              TB=(TBULK-TWALL)/(TINL-TWALL)
                  C
                  C***  CALCULATE THE LOCAL HEAT TRANSFER COEFFICIENT AND
                  C     NUSSELT NUMBER
                  C
  ISN 0019              HCOEF=Q/(TBULK-TWALL)*(-1.)
  ISN 0020              CALL PROPTY(TB,ROB,ZMUB,ZKBULK,CPB)
  ISN 0021              ZNU=HCOEF*2.*R(JN)/(ZKBULK*ZKREF)
  ISN 0022              WRITE(6,502) Z(I),TBULK,Q,HCOEF,ZNU
  ISN 0023        500   CONTINUE
  ISN 0024        501   FORMAT('1'//T6,'DISTANCE FROM ENTRANCE',T30,'BULK TEMPERATURE',
                       1T48,'HEAT TRANSFER RATE',T70,'HEAT TRANSFER COEF.',
                       5T92,'NUSSELT NUMBER'/T14,'(IN)',T35,'(DEG K)',T50,'(CAL/CM**2/SEC)
```

-7905913

```
                  3' ,T63,'(CAL/CM**2/SEC/DEG K)'//)
ISN 0025     502  FORMAT(2F20.2,3(1PE21.4))
ISN 0026          RETURN
ISN 0027          END

*OPTIONS IN EFFECT*      NAME=  MAIN,OPT=02,LINECNT=56,SIZE=C000K,

*OPTIONS IN EFFECT*      SOURCE,EBCDIC,NOLIST,DECK,LOAD,NOMAP,NOEDIT,ID,NOXREF

*STATISTICS*   SOURCE STATEMENTS =     26 ,PROGRAM SIZE =    1712

*STATISTICS*  NO  DIAGNOSTICS GENERATED

****** END OF COMPILATION ******                                   67K BYTES OF CORE

*STATISTICS*  NO  DIAGNOSTICS THIS STEP
```

FINITE-DIFFERENCE ITERATIVE SOLUTION IS UNDERCONSIDERATION FOR THE CASE OF

LAMINAR INCOMPRESSIBLE FLOW IN A PIPE WITH A SUDDEN ENLARGEMENT AND A SUDDEN CONTRACTION

THE INITIAL INFORMATION SUPPLIED IS

```
RE,      REYNOLDS NUMBER BASED ON INLET DIAMETER  =   20.00
RORFF,   REFERENCE DENSITY FOR THE FLUID  . . . . =   1.62E-04
ZMUREF,  REFERENCE VISCOSITY FOR THE FLUID  . . . =   1.21E-03
RELAX'S, RELAXATION PARAMETERS FOR DEPENDENT VARIABLES ARE

         RELAX(1)= 0.70, RELAX(2)= 1.20,
CC,      THE CONVERGENCY CRITERION  . . . . . . . =   1.00E-03
IN,      THE NUMBER OF COLUMNS (Z-DIRECTION)  . . =    22
JN,      THE NUMBER OF ROWS (R-DIRECTION) . . . . =    16
```

DISTANCES IN DIRECTION-1

0.0	0.500	1.000	1.325	1.655	1.994	2.347	2.720
3.121	3.559	4.045	4.597	5.237	6.000	6.912	7.573
8.104	8.567	9.000	9.500	10.000	10.500		

DISTANCES IN DIRECTION-2

0.0	0.100	0.200	0.300	0.400	0.500	0.600	0.700
0.800	0.900	1.000	1.100	1.200	1.300	1.400	1.500

THE DISTRIBUTION OF VORTICITY - A(I,J,1)

	1	2	3	4	5	6	7	8	9	10	11
16			1.550E-02	-2.406E-01	-4.050E-01	-3.[illegible]E-01	-1.499E-01	3.191E-02	1.623E-01	2.380E-01	2.754E-01
15			5.145E-02	-1.655E-01	-2.520E-01	-1.964E-01	-6.641E-02	6.560E-02	1.641E-01	2.246E-01	2.566E-01
14			-6.578E-02	-9.807E-02	-1.030E-01	-5.626E-02	2.395E-02	1.069E-01	1.722E-01	2.153E-01	2.399E-01
13			-2.251E-01	-2.919E-02	5.202E-02	9.035E-02	1.215E-01	1.544E-01	1.855E-01	2.094E-01	2.250E-01
12			-4.25[illegible]E-01	5.574E-02	2.24[illegible]E-01	2.481E-01	2.263E-01	2.020E-01	2.030E-01	2.063E-01	2.117E-01
11			-6.67[illegible]E-01	1.955E-01	4.29[illegible]E-01	4.209E-01	3.381E-01	2.655E-01	2.234E-01	2.05[illegible]E-01	1.995E-01
10			-3.546E-01	3.896E-01	6.87[illegible]E-01	6.111E-01	4.557E-01	3.245E-01	2.446E-01	2.04[illegible]E-01	1.878E-01
9			-1.25[illegible]E 00	7.359E-01	9.971E-01	8.185E-01	5.735E-01	3.812E-01	2.638E-01	2.035E-01	1.759E-01
8			-1.652E 00	1.345E 00	1.388E 00	1.036E 00	6.851E-01	4.309E-01	2.774E-01	1.99[illegible]E-01	1.629E-01
7			-2.001E 00	2.437E 00	1.851E 00	1.245E 00	7.769E-01	4.635E-01	2.830E-01	1.912E-01	1.481E-01
6	4.00[illegible]E 00	8.377E 00	3.716E 00	4.352E 00	2.312E 00	1.404E 00	8.291E-01	4.727E-01	2.752E-01	1.767E-01	1.306E-01
5	6.4[illegible]E 00	6.653E 00	6.769E 00	4.21[illegible]E 00	2.454E 00	1.441E 00	7.174E-01	4.487E-01	2.511E-01	1.547E-01	1.100E-01
4	4.8[illegible]E 00	4.955E 00	4.98[illegible]E 00	3.575E 00	2.230E 00	1.304E 00	7.712E-01	3.347E-01	2.091E-01	1.24[illegible]E-01	6.612E-02
3	3.700E 00	3.287E 00	3.296E 00	2.550E 00	1.668E 00	9.816E-01	5.360E-01	2.809E-01	1.499E-01	8.786E-02	5.933E-02
2	1.600E 00	1.640E 00	1.641E 00	1.313E 00	8.795E-01	5.204E-01	2.829E-01	1.472E-01	7.809E-02	4.545E-02	3.034E-02
1	0.0	0.0	0.0	0.0	0.0	0.0	0.0	0.0	0.0	0.0	0.0

	12	13	14	15	16	17	18	19	20	21	22
16	2.914E-01	2.973E-01	2.988E-01	2.968E-01	2.780E-01	2.061E-01	6.403E-02	-2.840E-03			
15	2.714E-01	2.772E-01	2.787E-01	2.763E-01	2.581E-01	1.969E-01	9.223E-02	-3.538E-02			
14	2.522E-01	2.573E-01	2.587E-01	2.561E-01	2.397E-01	1.906E-01	1.025E-01	-2.594E-02			
13	2.337E-01	2.376E-01	2.387E-01	2.361E-01	2.225E-01	1.868E-01	1.270E-01	-6.343E-04			
12	2.154E-01	2.182E-01	2.189E-01	2.165E-01	2.061E-01	1.951E-01	1.582E-01	4.499E-02			
11	1.985E-01	1.999E-01	1.999E-01	1.970E-01	1.903E-01	1.851E-01	1.988E-01	1.178E-01			
10	1.815E-01	1.797E-01	1.791E-01	1.776E-01	1.748E-01	1.864E-01	2.526E-01	2.283E-01			
9	1.645E-01	1.605E-01	1.573E-01	1.582E-01	1.592E-01	1.887E-01	3.253E-01	3.954E-01			
8	1.47[illegible]E-01	1.413E-01	1.396E-01	1.388E-01	1.432E-01	1.909E-01	4.267E-01	6.460E-01			
7	1.241E-01	1.219E-01	1.198E-01	1.193E-01	1.764E-01	1.915E-01	5.750E-01	1.029E 00			
6	1.10[illegible]E-01	1.027E-01	9.991E-02	9.977E-02	[illegible]E-01	1.870E-01	8.077E-01	1.557E 01	8.835E 00	8.385E 00	8.219E 00
5	9.003E-02	8.229E-02	8.071E-02	8.004E-02	8.274E-02	1.691E-01	7.636E-01	5.182E 00	6.729E 00	6.579E 00	6.661E 00
4	6.890E-02	6.204E-02	6.076E-02	6.018E-02	6.345E-02	1.383E-01	6.228E-01	3.469E 00	4.760E 00	4.953E 00	5.018E 00
3	4.653E-02	4.152E-02	4.006E-02	4.[illegible]9E-02	4.638E-02	9.744E-02	4.327E-01	2.123E 00	3.025E 00	3.260E 00	3.338E 00
2	2.350E-02	2.081E-02	2.003E-02	2.011E-02	2.339E-02	5.906E-02	2.200E-01	1.014E 00	1.474E 00	1.617E 00	1.664E 00
1	0.0	0.0	0.0	0.0	0.0	0.0	0.0	0.0	0.0	0.0	0.0

THE DISTRIBUTION OF STREAM FUNCTION - A(I,J,2)

	1	2	3	4	5	6	7	8	9	10	11
16			1.250E-01	1.250E-01	1.250E-01	1.250E-01	1.250E-01	1.250E-01	1.250E-01	1.250E-01	1.250E-01
15			1.250E-01	1.265E-01	1.275E-01	1.271E-01	1.259E-01	1.247E-01	1.238E-01	1.233E-01	1.231E-01
14			1.250E-01	1.303E-01	1.334E-01	1.317E-01	1.276E-01	1.235E-01	1.205E-01	1.187E-01	1.178E-01
13			1.250E-01	1.351E-01	1.406E-01	1.369E-01	1.288E-01	1.210E-01	1.152E-01	1.117E-01	1.099E-01
12			1.250E-01	1.464E-01	1.474E-01	1.409E-01	1.286E-01	1.167E-01	1.081E-01	1.028E-01	1.001E-01
11			1.250E-01	1.493E-01	1.523E-01	1.424E-01	1.258E-01	1.103E-01	9.716E-02	9.237E-02	8.875E-02
10			1.250E-01	1.491E-01	1.542E-01	1.403E-01	1.220E-01	1.017E-01	8.968E-02	8.075E-02	[illegible]
9			1.250E-01	1.510E-01	1.517E-01	1.336E-01	1.107E-01	9.077E-02	7.685E-02	6.944E-02	6.392E-02
8			1.250E-01	1.493E-01	1.436E-01	1.213E-01	9.780E-02	7.760E-02	6.403E-02	5.578E-02	5.134E-02
7			1.250E-01	1.419E-01	1.288E-01	1.052E-01	8.190E-02	6.324E-02	5.071E-02	4.327E-02	3.528E-02
6	1.250E-01	1.250E-01	1.250E-01	1.250E-01	1.071E-01	8.410E-02	6.358E-02	4.793E-02	3.753E-02	3.143E-02	2.816E-02
5	[illegible]	1.081E-01	1.075E-01	9.767E-02	7.049E-02	6.055E-02	4.459E-02	[illegible]	2.524E-02	2.082E-02	1.842E-02
4	[illegible]	[illegible]	7.139E-02	[illegible]	4.777E-02	3.708E-02	2.677E-02	1.938E-02	1.465E-02	1.191E-02	1.045E-02
3	[illegible]	3.516E-02	3.462E-02	3.010E-02	2.356E-02	1.731E-02	1.232E-02	8.806E-03	6.581E-03	5.300E-03	4.614E-03
2	9.870E-03	1.014E-02	1.001E-02	8.669E-03	6.752E-03	4.926E-03	3.482E-03	2.471E-03	1.836E-03	1.470E-03	1.274E-03
1	0.0	0.0	0.0	0.0	0.0	0.0	0.0	0.0	0.0	0.0	0.0

	12	13	14	15	16	17	18	19	20	21	22
16	1.250E-01	1.250E-01	1.250E-01	1.250E-01	1.250E-01	1.250E-01	1.250E-01	1.250E-01			
15	[illegible]	[illegible]	1.229E-01	1.229E-01	1.231E-01	1.235E-01	1.245E-01	1.250E-01			
14	[illegible]	1.172E-01	1.172E-01	1.173E-01	1.178E-01	1.195E-01	1.229E-01	1.250E-01			
13	[illegible]	1.085E-01	1.087E-01	1.088E-01	1.098E-01	1.133E-01	1.203E-01	1.250E-01			
12	9.576E-02	9.825E-02	9.312E-02	9.432E-02	9.387E-02	1.053E-01	1.165E-01	1.250E-01			
11	8.704E-02	8.636E-02	8.617E-02	8.645E-02	8.851E-02	9.582E-02	1.114E-01	1.250E-01			
10	7.452E-02	7.370E-02	7.345E-02	7.382E-02	7.627E-02	8.509E-02	1.050E-01	1.250E-01			
9	6.174E-02	6.085E-02	6.061E-02	6.097E-02	6.363E-02	7.341E-02	9.707E-02	1.250E-01			
8	4.910E-02	4.830E-02	4.806E-02	4.843E-02	5.107E-02	6.108E-02	8.737E-02	1.250E-01			
7	3.732E-02	3.652E-02	3.640E-02	3.661E-02	3.904E-02	4.846E-02	7.559E-02	1.250E-01			
6	[illegible]	2.589E-02	2.570E-02	2.598E-02	2.797E-02	3.601E-02	6.138E-02	1.250E-01	1.250E-01	1.250E-01	1.250E-01
5	1.724E-02	1.675E-02	1.667E-02	1.682E-02	1.828E-02	2.432E-02	4.438E-02	9.819E-02	1.073E-01	1.080E-01	1.083E-01
4	9.723E-03	9.420E-03	9.337E-03	9.459E-03	1.036E-02	1.416E-02	2.710E-02	6.168E-02	7.082E-02	7.208E-02	7.250E-02
3	4.274E-03	4.131E-03	4.092E-03	4.149E-03	4.571E-03	6.370E-03	1.257E-02	2.886E-02	3.413E-02	3.505E-02	3.535E-02
2	1.176E-03	1.135E-03	1.123E-03	1.140E-03	1.260E-03	1.777E-03	3.564E-03	8.187E-03	9.824E-03	1.014E-02	1.025E-02
1	0.0	0.0	0.0	0.0	0.0	0.0	0.0	0.0	0.0	0.0	0.0

THE DISTRIBUTION OF Z-COMP MASS VELOCITY - G(I,J)

J	1	2	3	4	5	6	7	8	9	10	11
16			0.0	0.0	0.0	0.0	0.0	0.0	0.0	0.0	0.0
15			0.0	-1.881E-02	-3.010E-02	-2.392E-02	-9.221E-03	5.374E-03	1.603E-02	2.740E-02	2.567E-02
14			0.0	-3.302E-02	-5.018E-02	-3.769E-02	-1.142E-02	1.432E-02	3.315E-02	4.455E-02	5.054E-02
13			0.0	-4.203E-02	-5.806E-02	-3.937E-02	-4.021E-03	2.833E-02	5.189E-02	6.628E-02	7.379E-02
12			0.0	-4.696E-02	-5.342E-02	-2.528E-02	1.366E-02	4.829E-02	7.297E-02	8.864E-02	9.626E-02
11			0.0	-4.389E-02	-3.421E-02	3.076E-03	4.281E-02	7.491E-02	9.690E-02	1.102E-01	1.176E-01
10			0.0	-3.175E-02	3.637E-03	4.487E-02	8.429E-02	1.086E-01	1.24[illegible]E-01	1.330E-01	1.380E-01
9			0.0	-1.243E-03	6.653E-02	1.147E-01	1.388E-01	1.435E-01	1.541E-01	1.562E-01	1.575E-01
8			0.0	6.413E-02	1.672E-01	2.029E-01	2.067E-01	1.968E-01	1.867E-01	1.797E-01	1.760E-01
7			0.0	2.027E-01	3.037E-01	3.146E-01	2.852E-01	2.49[illegible]E-01	2.20[illegible]E-01	2.029E-01	1.932E-01
6	0.0	0.0	0.0	4.421E-01	4.934E-01	4.467E-01	3.721E-01	3.038E-01	2.547E-01	2.248E-01	2.086E-01
5	7.[illegible]E-01	6.601E-01	6.702E-01	7.777E-01	7.107E-01	[illegible]	4.601E-01	3.566E-01	2.851E-01	2.442E-01	2.214E-01
4	1.2[illegible] 00	1.215E 00	1.215E 00	1.126E 00	4.32[illegible]E-01	7.206E-01	5.378E-01	4.009E-01	3.110E-01	2.583E-01	2.300E-01
3	1.6[illegible] 00	1.550E 00	1.535E 00	1.353E 00	1.075E 00	9.038E-01	5.822E-01	4.226E-01	3.203E-01	2.610E-01	2.293E-01
2	1.920E 00	1.754E 00	1.731E 00	1.505E 00	1.178E 00	8.655E-01	6.162E-01	4.403E-01	3.231E-01	2.650E-01	2.307E-01
1	2.009E 00	1.927E 00	1.796E 00	1.556E 00	1.212E 00	8.361E-01	6.276E-01	4.462E-01	3.320E-01	2.663E-01	2.312E-01

J	12	13	14	15	16	17	18	19	20	21	22
16	0.0	0.0	0.0	0.0	0.0	0.0	0.0	0.0			
15	2.715E-02	2.771E-02	2.786E-02	2.764E-02	2.598E-02	1.959E-02	7.351E-03	0.0			
14	5.331E-02	5.440E-02	5.468E-02	5.425E-02	5.093E-02	3.931E-02	1.623E-02	0.0			
13	7.765E-02	7.912E-02	7.951E-02	7.890E-02	7.450E-02	5.912E-02	2.701E-02	0.0			
12	1.0[illegible]E-01	1.01[illegible]E-01	1.023E-01	1.017E-01	9.681E-02	7.956E-02	4.032E-02	0.0			
11	1.212E-01	1.229E-01	1.232E-01	1.225E-01	1.180E-01	1.012E-01	5.727E-02	0.0			
10	1.416E-01	1.417E-01	1.420E-01	1.415E-01	1.382E-01	1.245E-01	7.365E-02	0.0			
9	1.583E-01	1.587E-01	1.589E-01	1.567E-01	1.575E-01	1.501E-01	1.102E-01	0.0			
8	1.744E-01	1.719E-01	1.737E-01	1.739E-01	1.757E-01	1.782E-01	1.534E-01	0.0			
7	1.8[illegible]E-01	1.869E-01	1.863E-01	1.871E-01	1.925E-01	2.089E-01	2.166E-01	0.0			
6	2.0[illegible]E-01	1.976E-01	1.957E-01	1.981E-01	2.076E-01	2.415E-01	3.121E-01	0.0	0.0	0.0	0.0
5	2.1[illegible]4E-01	2.05[illegible]E-01	2.046E-01	2.065E-01	2.201E-01	2.732E-01	4.256E-01	7.915E-01	6.773E-01	6.615E-01	6.562E-01
4	2.162E-01	2.104E-01	2.08[illegible]E-01	2.112E-01	2.284E-01	2.991E-01	5.301E-01	1.155E 00	1.219E 00	1.217E 00	1.216E 00
3	2.137E-01	2.0[illegible]E-01	2.053E-01	2.080E-01	2.275E-01	3.095E-01	5.883E-01	1.337E 00	1.525E 00	1.548E 00	1.556E 00
2	2.137E-01	2.065E-01	2.046E-01	2.074E-01	2.295E-01	3.185E-01	6.286E-01	1.443E 00	1.704E 00	1.752E 00	1.768E 00
1	2.137E-01	2.063E-01	2.043E-01	2.078E-01	2.289E-01	3.215E-01	6.420E-01	1.479E 00	1.767E 00	1.820E 00	1.838E 00

THE DISTRIBUTION OF R-COMP MASS VELOCITY - G2(I,J)

16			0.0	0.0	0.0	0.0	0.0	0.0	0.0	0.0	0.0
15			0.0	-2.777E-03	-6.011E-04	1.488E-03	2.342E-03	1.912E-03	1.194E-03	6.124E-04	2.671E-04
14			0.0	-9.929E-03	-1.799E-03	6.395E-03	8.702E-03	7.122E-03	4.487E-03	2.337E-03	1.041E-03
13			0.0	-1.391E-02	-2.474E-03	1.394E-02	1.928E-02	1.487E-02	9.406E-03	4.951E-03	2.240E-03
12			0.0	-3.119E-02	-1.247E-03	2.440E-02	3.038E-02	2.441E-02	1.543E-02	8.177E-03	3.746E-03
11			0.0	-4.209E-02	3.554E-03	3.794E-02	4.433E-02	3.495E-02	2.199E-02	1.169E-02	5.407E-03
10			0.0	-4.997E-02	1.384E-02	5.455E-02	5.928E-02	4.567E-02	2.846E-02	1.514E-02	7.049E-03
9			0.0	-5.156E-02	3.14[illegible]E-02	7.380E-02	7.414E-02	5.544E-02	3.419E-02	1.815E-02	8.497E-03
8			0.0	-4.135E-02	[illegible]	9.435E-02	8.741E-02	6.331E-02	3.850E-02	2.035E-02	9.539E-03
7			0.0	-1.077E-02	9.071E-02	1.134E-01	9.711E-02	6.804E-02	4.074E-02	2.141E-02	1.004E-02
6	0.0	0.0	0.0	5.389E-02	1.217E-01	1.262E-01	1.008E-01	6.845E-02	4.034E-02	2.106E-02	9.883E-03
5	0.0	3.263E-03	4.697E-02	1.065E-01	1.398E-01	1.266E-01	9.625E-02	6.362E-02	3.694E-02	1.916E-02	8.591E-03
4	0.0	6.043E-03	5.551E-02	1.097E-01	1.283E-01	1.114E-01	8.212E-02	5.316E-02	3.049E-02	1.573E-02	7.384E-03
3	0.0	1.070E-02	4.418E-02	8.417E-02	9.577E-02	9.168E-02	5.919E-02	3.779E-02	2.149E-02	1.105E-02	5.174E-03
2	0.0	-2.094E-03	2.625E-02	4.955E-02	5.604E-02	4.753E-02	3.418E-02	2.167E-02	1.227E-02	6.310E-03	2.976E-03
1	0.0	0.0	0.0	0.0	0.0	0.0	0.0	0.0	0.0	0.0	0.0
	1	2	3	4	5	6	7	8	9	10	11

16	0.0	0.0	0.0	0.0	0.0	0.0	0.0	0.0			
15	9.959E-05	2.999E-05	3.651E-08	-8.337E-05	-4.294E-04	-1.093E-03	-1.139E-03	0.0			
14	3.973E-04	1.218E-04	-7.078E-07	-3.534E-04	-1.670E-03	-4.232E-03	-4.642E-03	0.0			
13	8.709E-04	2.714E-04	-2.812E-06	-7.767E-04	-3.616E-03	-9.256E-03	-1.074E-02	0.0			
12	1.479E-03	4.672E-04	-5.902E-06	-1.322E-03	-6.126E-03	-1.603E-02	-1.983E-02	0.0			
11	2.162E-03	6.911E-04	-9.457E-06	-1.937E-03	-9.920E-03	-2.440E-02	-3.249E-02	0.0			
10	2.849E-03	9.193E-04	-1.248E-05	-2.561E-03	-1.207E-02	-3.414E-02	-4.960E-02	0.0			
9	3.457E-03	1.125E-03	-1.463E-05	-3.123E-03	-1.500E-02	-4.436E-02	-7.252E-02	0.0			
8	3.912E-03	1.281E-03	-1.539E-05	-3.551E-03	-1.748E-02	-5.589E-02	-1.033E-01	0.0			
7	4.140E-03	1.364E-03	-1.457E-05	-3.777E-03	-1.912E-02	-6.596E-02	-1.454E-01	0.0			
6	4.090E-03	1.353E-03	-1.249E-05	-3.747E-03	-1.949E-02	-7.257E-02	-2.047E-01	0.0	0.0	0.0	0.0
5	3.734E-03	1.239E-03	-9.441E-06	-3.427E-03	-1.923E-02	-7.113E-02	-2.128E-01	-1.875E-01	-2.464E-02	-2.549E-03	0.0
4	3.077E-03	1.024E-03	-6.060E-06	-2.820E-03	-1.524E-02	-5.098E-02	-1.825E-01	-1.709E-01	-3.466E-02	-5.610E-03	0.0
3	2.172E-03	7.247E-04	-3.036E-06	-1.983E-03	-1.082E-02	-4.368E-02	-1.295E-01	-1.252E-01	-3.093E-02	-6.138E-03	0.0
2	1.250E-03	4.173E-04	-1.214E-06	-1.134E-03	-6.213E-03	-2.516E-02	-7.373E-02	-7.235E-02	-1.361E-02	-4.255E-03	0.0
1	0.0	0.0	0.0	0.0	0.0	0.0	0.0	0.0	0.0	0.0	0.0
	12	13	14	15	16	17	18	19	20	21	22

MAXIMUM RESIDUAL FOR EACH VARIABLE

NITER	VORTICITY	STREAM FCN
1	3.945E-02 (4, 5)	4.524E-03 (5, 6)
2	3.559E-02 (5, 4)	6.477E-03 (5, 6)
3	3.258E-02 (5, 3)	7.388E-03 (6, 7)
4	2.990E-02 (5, 2)	8.660E-03 (6, 7)
5	2.825E-02 (5, 2)	9.502E-03 (6, 7)
6	2.573E-02 (6, 2)	1.016E-02 (6, 8)
7	2.403E-02 (6, 2)	1.056E-02 (6, 8)
8	2.227E-02 (6, 2)	1.075E-02 (6, 8)
9	2.011E-02 (6, 2)	1.076E-02 (6, 8)
10	1.789E-02 (6, 2)	1.092E-02 (7, 9)
11	1.572E-02 (6, 2)	1.130E-02 (7, 9)
12	1.465E-02 (7, 2)	1.154E-02 (7, 9)
13	[illegible] (7, 2)	1.165E-02 (7, 9)
14	1.2[illegible]E-02 (7, 2)	1.164E-02 (7, 9)
15	1.197E-02 (7, 2)	1.153E-02 (7, 9)
16	1.103E-02 (7, 2)	1.132E-02 (7, 9)
17	1.010E-02 (7, 2)	1.103E-02 (7, 9)
18	9.204E-03 (7, 2)	1.067E-02 (7, 9)
19	9.532E-03 (8, 2)	1.024E-02 (7, 9)
20	8.221E-03 (8, 3)	9.926E-03 (8, 9)
21	7.881E-03 (8, 2)	9.812E-03 (8, 9)
22	7.514E-03 (8, 2)	9.644E-03 (8, 9)
23	7.138E-03 (8, 2)	9.425E-03 (8, 9)
24	6.745E-03 (9, 2)	9.161E-03 (8, 9)
25	6.346E-03 (8, 2)	8.558E-03 (8, 9)
26	5.944E-03 (8, 2)	9.521E-03 (8, 9)
27	5.543E-03 (8, 2)	8.153E-03 (8, 9)
28	5.146E-03 (8, 2)	7.762E-03 (8, 9)
29	4.768E-03 (9, 2)	7.354E-03 (8, 9)
30	4.625E-03 (9, 2)	6.932E-03 (8, 9)
31	4.468E-03 (9, 2)	6.615E-03 (9, 9)
32	4.238E-03 (9, 2)	6.427E-03 (9, 9)
33	4.117E-03 (9, 2)	6.222E-03 (9, 9)
34	3.927E-03 (9, 2)	5.998E-03 (9, 9)
35	3.732E-03 (9, 2)	5.758E-03 (9, 9)
36	3.531E-03 (9, 2)	5.505E-03 (9, 9)
37	3.328E-03 (9, 2)	5.242E-03 (9, 9)
38	3.123E-03 (9, 2)	4.972E-03 (9, 9)
39	2.920E-03 (9, 2)	4.695E-03 (9, 9)
40	2.719E-03 (9, 2)	4.416E-03 (9, 9)
41	2.519E-03 (9, 2)	4.135E-03 (9, 9)
42	2.338E-03 (10, 2)	3.855E-03 (9, 9)
43	2.252E-03 (10, 2)	3.599E-03 (10, 9)
44	2.162E-03 (10, 2)	3.462E-03 (10, 9)
45	2.068E-03 (10, 2)	3.319E-03 (10, 9)
46	1.971E-03 (10, 2)	3.170E-03 (10, 9)
47	1.873E-03 (10, 2)	3.019E-03 (10, 9)
48	1.772E-03 (10, 2)	2.864E-03 (10, 9)
49	1.671E-03 (10, 2)	2.708E-03 (10, 9)
50	1.570E-03 (10, 2)	2.552E-03 (10, 9)
51	1.470E-03 (10, 2)	2.395E-03 (10, 9)
52	1.371E-03 (10, 2)	2.24[illegible]E-03 (10, 9)
53	1.274E-03 (10, 2)	2.086E-03 (10, 9)
54	1.179E-03 (10, 2)	1.937E-03 (10, 8)
55	1.087E-03 (10, 2)	1.794E-03 (10, 8)

56	9.973E-04 (10, 2)	1.655E-03 (10, 8)
57	9.141E-04 (11, 2)	1.525E-03 (11, 9)
58	8.715E-04 (11, 2)	1.451E-03 (11, 9)
59	8.285E-04 (11, 2)	1.375E-03 (11, 9)
60	7.851E-04 (11, 2)	1.301E-03 (11, 9)
61	7.416E-04 (11, 2)	1.225E-03 (11, 9)
62	6.985E-04 (11, 2)	1.152E-03 (11, 9)
63	6.5[illegible]-04 (11, 2)	1.081E-03 (11, 8)
64	6.1[illegible]7E-04 (11, 2)	1.010E-03 (11, 8)
65	5.[illegible]24E-04 (11, 2)	9.422E-04 (11, 8)

THE DISTRIBUTION OF VORTICITY - A(I,J,1)

	1	2	3	4	5	6	7	8	9	10	11
16			1.447E-02	-2.195E-01	-4.536E-01	-5.364E-01	-4.968E-01	-3.714E-01	-1.976E-01	-1.607E-02	1.356E-01
15			5.308E-02	-1.646E-01	-3.071E-01	-3.539E-01	-3.166E-01	-2.215E-01	-9.313E-02	4.162E-02	1.546E-01
14			-5.327E-02	-1.116E-01	-1.593E-01	-1.672E-01	-1.295E-01	-6.289E-02	1.929E-02	1.042E-01	1.757E-01
13			-2.023E-01	-5.428E-02	-2.669E-03	2.882E-02	6.633E-02	1.035E-01	1.383E-01	1.708E-01	1.593E-01
12			-3.691E-01	1.718E-02	1.716E-01	2.405E-01	2.733E-01	2.775E-01	2.624E-01	2.408E-01	2.248E-01
11			-6.104E-01	1.193E-01	3.76[illegible]E-01	4.747E-01	4.930E-01	4.574E-01	3.893E-01	3.125E-01	2.514E-01
10			-6.650E-01	2.825E-01	6.295E-01	7.389E-01	7.249E-01	6.400E-01	5.156E-01	3.832E-01	2.776E-01
9			-1.151E 00	5.646E-01	9.597E-01	1.038E 00	9.663E-01	8.196E-01	6.353E-01	4.497E-01	3.007E-01
8			-1.457E 00	1.070E 00	1.405E 00	1.376E 00	1.259E 00	9.455E-01	7.392E-01	5.025E-01	3.173E-01
7			-1.757E 00	2.029E 00	2.000E 00	1.738E 00	1.433E 00	1.121E 00	8.144E-01	5.363E-01	3.231E-01
6	9.000E 00	8.414E 00	5.672E 00	3.958E 00	2.684E 00	2.069E 00	1.600E 00	1.199E 00	8.446E-01	5.409E-01	3.138E-01
5	6.400E 00	6.649E 00	6.741E 00	4.382E 00	3.046E 00	2.732E 00	1.647E 00	1.188E 00	8.124E-01	5.075E-01	2.854E-01
4	4.[illegible]30E 00	4.933E 00	4.975E 00	3.895E 00	2.875E 00	2.094E 00	1.505E 00	1.055E 00	7.040E-01	4.305E-01	2.361E-01
3	3.200E 00	3.266E 00	3.289E 00	2.812E 00	2.184E 00	1.608E 00	1.144E 00	7.885E-01	5.173E-01	3.113E-01	1.676E-01
2	1.600E 00	1.628E 00	1.638E 00	1.451E 00	1.157E 00	8.602E-01	6.105E-01	4.175E-01	2.715E-01	1.617E-01	8.587E-02
1	0.0	0.0	0.0	0.0	0.0	0.0	0.0	0.0	0.0	0.0	0.0

	12	13	14	15	16	17	18	19	20	21	22
16	2.323E-01	2.742E-01	2.941E-01	2.964E-01	2.824E-01	2.221E-01	8.833E-02	-3.737E-03			
15	2.277E-01	2.629E-01	2.752E-01	2.763E-01	2.625E-01	2.100E-01	9.983E-02	-4.238E-02			
14	2.237E-01	2.478E-01	2.583E-01	2.564E-01	2.437E-01	2.005E-01	1.140E-01	-2.490E-02			
13	2.2[illegible]E-01	2.330E-01	2.376E-01	2.363E-01	2.257E-01	1.927E-01	1.320E-01	1.150E-02			
12	2.187E-01	2.186E-01	2.199E-01	2.172E-01	2.083E-01	1.863E-01	1.551E-01	7.165E-02			
11	2.177E-01	2.044E-01	2.003E-01	1.974E-01	1.911E-01	1.807E-01	1.847E-01	1.628E-01			
10	2.172E-01	1.902E-01	1.818E-01	1.785E-01	1.741E-01	1.759E-01	2.235E-01	2.962E-01			
9	2.134E-01	1.755E-01	1.631E-01	1.591E-01	1.570E-01	1.714E-01	2.758E-01	4.892E-01			
8	2.07[illegible]E-01	1.599E-01	1.442E-01	1.397E-01	1.397E-01	1.671E-01	3.503E-01	7.694E-01			
7	1.974E-01	1.42?E-01	1.249E-01	1.202E-01	1.219E-01	1.620E-01	4.660E-01	1.182E 00			
6	1.912E-01	1.238E-01	1.052E-01	1.005E-01	1.034E-01	1.539E-01	6.653E-01	1.649E 01	9.280E 00	8.515E 00	8.260E 00
5	1.574E-01	1.025E-01	8.493E-02	8.070E-02	8.413E-02	1.361E-01	6.190E-01	5.119E 00	6.729E 00	6.706E 00	6.698E 00
4	1.257E-01	7.891E-02	6.413E-02	6.068E-02	6.396E-02	1.095E-01	4.927E-01	3.205E 00	4.521E 00	4.856E 00	4.968E 00
3	8.69?E-02	5.337E-02	4.290E-02	4.051E-02	4.304E-02	7.623E-02	3.354E-01	1.852E 00	2.748E 00	3.113E 00	3.235E 00
2	4.3?3E-02	2.672E-02	2.144E-02	2.126E-02	2.161E-02	3.889E-02	1.685E-01	8.548E-01	1.304E 00	1.519E 00	1.590E 00
1	0.0	0.0	0.0	0.0	0.0	0.0	0.0	0.0	0.0	0.0	0.0

THE DISTRIBUTION OF STREAM FUNCTION - A(I,J,2)

16			1.250E-01	1.250E-01	1.250E-01	1.250E-01	1.250E-01	1.250E-01	1.250E-01	1.250E-01	1.250E-01
15			1.250E-01	1.264E-01	1.279E-01	1.28[illegible]E-01	1.281E-01	1.273E-01	1.262E-01	1.250E-01	1.240E-01
14			1.250E-01	1.300E-01	1.348E-01	1.364E-01	1.354E-01	1.325E-01	1.285E-01	1.244E-01	1.209E-01
13			1.250E-01	1.347E-01	1.435E-01	1.461E-01	1.432E-01	1.381E-01	1.304E-01	1.225E-01	1.159E-01
12			1.250E-01	1.398E-01	1.521E-01	1.551E-01	1.510E-01	1.421E-01	1.306E-01	1.187E-01	1.088E-01
11			1.250E-01	1.444E-01	1.589E-01	1.614E-01	1.550E-01	1.430E-01	1.279E-01	1.126E-01	9.986E-02
10			1.250E-01	1.480E-01	1.625E-01	1.637E-01	1.543E-01	1.395E-01	1.218E-01	1.039E-01	8.923E-02
9			1.250E-01	1.495E-01	1.616E-01	1.593E-01	1.479E-01	1.311E-01	1.118E-01	9.272E-02	7.719E-02
8			1.250E-01	1.478E-01	1.549E-01	1.488E-01	1.352E-01	1.176E-01	9.613E-02	7.933E-02	6.415E-02
7			1.250E-01	1.407E-01	1.411E-01	1.313E-01	1.116E-01	9.948E-02	8.141E-02	6.431E-02	5.064E-02
6	1.250E-01	1.250E-01	1.250E-01	1.253E-01	1.193E-01	1.074E-01	9.326E-02	7.802E-02	6.271E-02	4.854E-02	3.734E-02
5	1.083E-01	1.080E-01	1.076E-01	9.950E-02	9.010E-02	7.878E-02	6.696E-02	5.511E-02	4.360E-02	3.316E-02	2.501E-02
4	7.380E-02	7.212E-02	7.153E-02	6.490E-02	5.726E-02	4.906E-02	4.100E-02	3.327E-02	2.597E-02	1.948E-02	1.445E-02
3	3.650E-02	3.511E-02	3.472E-02	3.140E-02	2.739E-02	2.318E-02	1.915E-02	1.537E-02	1.188E-02	8.815E-03	6.460E-03
2	9.800E-03	1.016E-02	1.094E-02	9.085E-03	7.891E-03	6.640E-03	5.451E-03	4.351E-03	3.343E-03	2.464E-03	1.792E-03
1	0.0	0.0	0.0	0.0	0.0	0.0	0.0	0.0	0.0	0.0	0.0
	1	2	3	4	5	6	7	8	9	10	11

16	1.250E-01	1.250E-01	1.250E-01	1.250E-01	1.250E-01	1.250E-01	1.250E-01	1.250E-01			
15	1.233E-01	1.230E-01	1.229E-01	1.229E-01	1.230E-01	1.234E-01	1.243E-01	1.250E-01			
14	1.187E-01	1.177E-01	1.173E-01	1.173E-01	1.176E-01	1.191E-01	1.224E-01	1.250E-01			
13	1.116E-01	1.096E-01	1.089E-01	1.088E-01	1.096E-01	1.126E-01	1.192E-01	1.250E-01			
12	1.025E-01	9.945E-02	9.841E-02	9.832E-02	9.947E-02	1.041E-01	1.147E-01	1.250E-01			
11	9.175E-02	8.788E-02	8.654E-02	8.643E-02	8.799E-02	9.422E-02	1.090E-01	1.250E-01			
10	7.989E-02	7.543E-02	7.390E-02	7.379E-02	7.564E-02	8.316E-02	1.020E-01	1.250E-01			
9	6.733E-02	6.265E-02	6.104E-02	6.093E-02	6.294E-02	7.127E-02	9.362E-02	1.250E-01			
8	5.456E-02	5.032E-02	4.848E-02	4.839E-02	5.038E-02	5.891E-02	8.364E-02	1.250E-01			
7	4.205E-02	3.803E-02	3.666E-02	3.658E-02	3.840E-02	4.644E-02	7.187E-02	1.250E-01			
6	3.033E-02	2.709E-02	2.599E-02	2.594E-02	2.744E-02	3.429E-02	5.903E-02	1.250E-01	1.250E-01	1.250E-01	1.250E-01
5	1.934E-02	1.761E-02	1.652E-02	1.679E-02	1.789E-02	2.303E-02	4.172E-02	9.733E-02	1.067E-01	1.078E-01	1.082E-01
4	1.136E-02	9.937E-03	9.459E-03	9.439E-03	1.012E-02	1.335E-02	2.534E-02	6.044E-02	6.980E-02	7.163E-02	7.223E-02
3	5.021E-03	4.364E-03	4.147E-03	4.139E-03	4.456E-03	5.985E-03	1.171E-02	2.800E-02	3.336E-02	3.466E-02	3.510E-02
2	1.384E-03	1.199E-03	1.139E-03	1.137E-03	1.227E-03	1.666E-03	3.311E-03	7.891E-03	9.554E-03	1.000E-02	1.015E-02
1	0.0	0.0	0.0	0.0	0.0	0.0	0.0	0.0	0.0	0.0	0.0
	12	13	14	15	16	17	18	19	20	21	22

THE DISTRIBUTION OF Z-COMP MASS VELOCITY - G1(I,J)

	1	2	3	4	5	6	7	8	9	10	11
16			0.0	0.0	0.0	0.0	0.0	0.0	0.0	0.0	0.0
15			0.0	-1.787E-02	-3.511E-02	-4.078E-02	-3.699E-02	-2.663E-02	-1.254E-02	7.204E-03	1.452E-02
14			0.0	-3.192E-02	-6.005E-02	-6.917E-02	-6.021E-02	-4.137E-02	-1.639E-02	9.596E-03	3.125E-02
13			0.0	-4.068E-02	[illegible]	-7.796E-02	-6.518E-02	-4.022E-02	-3.636E-03	2.775E-02	5.055E-02
12			0.0	-4.417E-02	-6.992E-02	-6.932E-02	-5.104E-02	-2.241E-02	1.138E-02	4.511E-02	7.270E-02
11			0.0	-4.109E-02	-5.230E-02	-4.743E-02	-1.654E-02	1.280E-02	4.410E-02	7.393E-02	9.786E-02
10			0.0	-2.931E-02	-1.524E-02	1.149E-02	3.976E-02	6.598E-02	8.966E-02	1.102E-01	1.260E-01
9			0.0	1.272E-03	4.776E-02	9.018E-02	1.193E-01	1.373E-01	1.477E-01	1.536E-01	1.568E-01
8			0.0	6.794E-02	1.469E-01	2.001E-01	2.230E-01	2.259E-01	2.170E-01	2.030E-01	1.896E-01
7			0.0	[illegible]	2.966E-01	3.451E-01	3.502E-01	3.237E-01	2.952E-01	2.565E-01	2.234E-01
6	0.0	0.0	0.0	4.122E-01	5.097E-01	5.252E-01	[illegible]	4.438E-01	3.781E-01	3.114E-01	2.564E-01
5	[illegible]	6.611E-01	6.684E-01	7.512E-01	7.755E-01	7.789E-01	6.925E-01	5.595E-01	4.592E-01	3.633E-01	2.862E-01
4	1.290E 00	1.215E 00	1.214E 00	1.135E 00	1.045E 00	9.266E-01	7.969E-01	6.623E-01	5.286E-01	4.058E-01	3.091E-01
3	1.659E 00	1.549E 00	1.537E 00	1.395E 00	1.234E 00	1.060E 00	[illegible]	7.229E-01	5.657E-01	4.253E-01	3.164E-01
2	1.920E 00	1.755E 00	1.736E 00	1.570E 00	1.370E 00	1.159E 00	9.575E-01	7.687E-01	5.942E-01	4.408E-01	3.230E-01
1	[illegible]	1.824E 00	1.802E 00	1.628E 00	1.415E 00	1.192E 00	9.804E-01	7.840E-01	6.037E-01	4.459E-01	3.252E-01

	12	13	14	15	16	17	18	19	20	21	22
16	0.0	0.0	0.0	0.0	0.0	0.0	0.0	0.0			
15	2.741E-02	2.618E-02	2.748E-02	2.763E-02	2.631E-02	2.097E-02	9.327E-03	0.0			
14	4.512E-02	5.174E-02	5.404E-02	5.426E-02	5.175E-02	4.185E-02	1.984E-02	0.0			
13	[illegible]	7.590E-02	7.873E-02	7.895E-02	7.562E-02	6.749E-02	3.189E-02	0.0			
12	9.029E-02	9.869E-02	1.016E-01	1.017E-01	9.307E-02	8.334E-02	4.611E-02	0.0			
11	1.130E-01	1.201E-01	1.225E-01	1.226E-01	1.192E-01	1.049E-01	6.352E-02	0.0			
10	1.357E-01	1.402E-01	1.417E-01	1.417E-01	1.392E-01	1.275E-01	8.566E-02	0.0			
9	1.583E-01	1.588E-01	1.589E-01	1.588E-01	1.579E-01	1.516E-01	1.150E-01	0.0			
8	1.805E-01	1.759E-01	1.742E-01	1.733E-01	1.753E-01	1.774E-01	1.553E-01	0.0			
7	2.017E-01	1.911E-01	1.874E-01	1.871E-01	1.912E-01	2.051E-01	2.134E-01	0.0			
6	2.211E-01	2.042E-01	1.993E-01	1.979E-01	2.051E-01	2.340E-01	3.015E-01	0.0	0.0	0.0	0.0
5	2.375E-01	2.145E-01	2.067E-01	2.062E-01	2.165E-01	2.618E-01	4.086E-01	8.070E-01	6.900E-01	6.672E-01	6.596E-01
4	2.490E-01	2.203E-01	2.113E-01	2.108E-01	2.239E-01	2.941E-01	5.002E-01	1.155E 00	1.222E 00	1.219E 00	1.219E 00
3	2.493E-01	2.183E-01	2.090E-01	2.076E-01	2.222E-01	2.920E-01	5.508E-01	1.314E 00	1.506E 00	1.541E 00	1.552E 00
2	2.511E-01	2.182E-01	2.072E-01	2.069E-01	2.228E-01	2.992E-01	5.854E-01	1.400E 00	1.668E 00	1.733E 00	1.755E 00
1	2.514E-01	2.191E-01	2.071E-01	2.067E-01	2.230E-01	3.016E-01	5.970E-01	1.429E 00	1.722E 00	1.797E 00	1.823E 00

THE DISTRIBUTION OF R-COMP MASS VELOCITY - G2(I,J)

J	1	2	3	4	5	6	7	8	9	10	11
16			0.0	0.0	0.0	0.0	0.0	0.0	0.0	0.0	0.0
15			0.0	-3.165E-03	-2.131E-03	-2.705E-04	1.058E-03	1.797E-03	1.987E-03	1.715E-03	1.163E-03
14			0.0	-1.155E-02	-7.485E-03	-7.077E-04	4.046E-03	6.747E-03	7.422E-03	6.404E-03	4.343E-03
13			0.0	-2.157E-02	-1.444E-02	-5.733E-04	9.061E-03	1.427E-02	1.552E-02	1.334E-02	9.035E-03
12			0.0	-3.762E-02	-2.124E-02	1.029E-03	1.599E-02	2.382E-02	2.547E-02	2.176E-02	1.473E-02
11			0.0	-5.185E-02	-2.584E-02	5.092E-03	2.493E-02	3.481E-02	3.641E-02	3.085E-02	2.076E-02
10			0.0	-6.486E-02	-2.595E-02	1.254E-02	3.577E-02	4.653E-02	4.743E-02	3.975E-02	2.663E-02
9			0.0	-7.024E-02	-1.903E-02	2.424E-02	4.910E-02	5.810E-02	5.751E-02	4.758E-02	3.163E-02
8			0.0	-6.566E-02	-2.915E-03	4.003E-02	6.102E-02	6.8[illegible]E-02	6.555E-02	5.344E-02	3.533E-02
7			0.0	-4.141E-02	2.279E-02	5.841E-02	7.291E-02	7.593E-02	7.038E-02	5.647E-02	3.723E-02
6	0.0	0.0	0.0	1.717E-02	5.227E-02	7.524E-02	8.079E-02	7.497E-02	7.0[illegible]E-02	5.591E-02	3.634E-02
5	0.0	3.055E-03	3.847E-02	6.662E-02	7.740E-02	8.362E-02	8.161E-02	7.574E-02	6.598E-02	5.124E-02	3.302E-02
4	0.0	7.582E-03	4.266E-02	7.252E-02	7.374E-02	7.843E-02	7.268E-02	6.503E-02	5.532E-02	4.237E-02	2.707E-02
3	0.0	1.037E-02	3.241E-02	5.597E-02	6.145E-02	5.967E-02	5.395E-02	4.717E-02	3.949E-02	2.993E-02	1.898E-02
2	0.0	-2.414E-03	1.874E-02	3.279E-02	3.655E-02	3.533E-02	3.165E-02	2.739E-02	2.273E-02	1.712E-02	1.080E-02
1	0.0	0.0	0.0	0.0	0.0	0.0	0.0	0.0	0.0	0.0	0.0

J	12	13	14	15	16	17	18	19	20	21	22
16	0.0	0.0	0.0	0.0	0.0	0.0	0.0	0.0			
15	5.996E-04	2.291E-04	5.850E-05	-5.781E-05	-3.565E-04	-1.004E-03	-1.236E-03	0.0			
14	2.241E-03	8.564E-04	2.164E-04	-2.349E-04	-1.392E-03	-3.903E-03	-5.015E-03	0.0			
13	4.644E-03	1.754E-03	4.466E-04	-5.214E-04	-3.022E-03	-8.557E-03	-1.155E-02	0.0			
12	7.56[illegible]E-03	2.901E-03	7.203E-04	-4.931E-04	-5.127E-03	-1.483E-02	-2.120E-02	0.0			
11	1.070E-02	4.087E-03	1.007E-03	-1.315E-03	-7.554E-03	-2.256E-02	-3.451E-02	0.0			
10	1.3[illegible]E-02	5.218E-03	1.276E-03	-1.746E-03	-1.011E-02	-3.153E-02	-5.233E-02	0.0			
9	1.623E-02	6.169E-03	1.497E-03	-2.136E-03	-1.257E-02	-4.137E-02	-7.594E-02	0.0			
8	1.86[illegible]E-02	6.814E-03	1.643E-03	-2.436E-03	-1.465E-02	-5.147E-02	-1.074E-01	0.0			
7	1.879E-02	7.073E-03	1.690E-03	-2.598E-03	-1.603E-02	-6.068E-02	-1.499E-01	0.0			
6	1.832E-02	6.859E-03	1.625E-03	-2.583E-03	-1.635E-02	-6.681E-02	-2.093E-01	0.0	0.0	0.0	0.0
5	1.654E-02	6.150E-03	1.445E-03	-2.367E-03	-1.528E-02	-6.522E-02	-2.146E-01	-1.937E-01	-2.626E-02	-3.775E-03	0.0
4	1.347E-02	4.974E-03	1.158E-03	-1.951E-03	-1.277E-02	-5.559E-02	-1.813E-01	-1.737E-01	-3.727E-02	-8.125E-03	0.0
3	9.379E-03	3.440E-03	7.336E-04	-1.373E-03	-9.052E-03	-3.774E-02	-1.270E-01	-1.256E-01	-3.332E-02	-8.721E-03	0.0
2	5.307E-03	1.934E-03	4.419E-04	-7.866E-04	-5.196E-03	-2.284E-02	-7.179E-02	-7.207E-02	-2.111E-02	-5.975E-03	0.0
1	0.0	0.0	0.0	0.0	0.0	0.0	0.0	0.0	0.0	0.0	0.0

FINITE-DIFFERENCE ITERATIVE SOLUTION IS UNDERCONSIDERATION FOR THE CASE OF

LAMINAR COMPRESSIBLE MCT GAS FLOW IN A PIPE WITH A SUDDEN ENLARGEMENT AND A SUDDEN CONTRACTION

THE INITIAL INFORMATION SUPPLIED IS

RE,	REYNOLDS NUMBER BASED ON INLET DIAMETER =	60.00	
PR,	PRANDTL NUMBER BASED ON INLET PROPERTIES =	0.66	
BR,	BRINKMANN NUMBER . . . . =	9.52E-06	
ROREF,	REFERENCE DENSITY FOR THE FLUID . . . . =	1.62E-04	GM/CC
ZMUREF,	REFERENCE VISCOSITY FOR THE FLUID . . . =	1.21E-03	GM/CM/SEC
CPREF,	REFERENCE HEAT CAPACITY FOR THE FLUID . =	1.24E-01	CAL/GM/DEG K
ZKREF,	REFERENCE HEAT CONDUCTIVITY FOR THE FLUID=	2.26E-04	CAL/CM/SEC/DEG K
TINL,	INLET TEMPERATURE OF THE FLUID . . . . . =	3000.00	DEG K
TWALL,	TEMPERATURE AT THE WALLS . . . . =	300.00	DEG K
VINL,	MEAN INLET FLOW RATE . . . . =	448.15	CM/SEC

RELAX'S, RELAXATION PARAMETERS FOR DEPENDENT VARIABLES ARE
RELAX(1)= 0.75, RELAX(2)= 0.55, RELAX(3)= 0.75,

CC,	THE CONVERGENCY CRITERION . . . . =	1.00E-03
IN,	THE NUMBER OF COLUMNS (Z-DIRECTION) . . =	23
JN,	THE NUMBER OF ROWS . .(R-DIRECTION) . . =	15

DISTANCES IN DIRECTION-1

0.0	0.500	1.000	1.401	1.813	2.248	2.720	3.248
3.861	4.600	5.440	6.091	6.620	7.067	7.457	7.806
8.126	8.427	8.717	9.000	9.500	10.000	10.500	

DISTANCES IN DIRECTION-2

0.0	0.050	0.125	0.250	0.375	0.500	0.625	0.750
0.875	1.000	1.125	1.250	1.375	1.440	1.500	

THE DISTRIBUTION OF VORTICITY - A(I,J,NW)

15			-3.537E-02	-2.046E-01	-3.415E-01	-4.395E-01	-5.209E-01	-5.928E-01	-6.574E-01	-7.180E-01	-7.779E-01
14			7.111E-02	-1.516E-01	-2.281E-01	-2.811E-01	-3.256E-01	-3.652E-01	-4.020E-01	-4.375E-01	-4.726E-01
13			1.896E-02	-7.327E-02	-9.017E-02	-1.031E-01	-1.154E-01	-1.270E-01	-1.385E-01	-1.495E-01	-1.595E-01
12			-1.178E-01	1.262E-01	2.104E-01	2.610E-01	2.991E-01	3.311E-01	3.586E-01	3.830E-01	4.059E-01
11			-2.809E-01	4.197E-01	5.866E-01	6.914E-01	7.708E-01	8.372E-C1	8.946E-01	9.450E-01	9.899E-01
1C			-6.001E-01	1.206E+00	1.382E+00	1.467E+00	1.536E+00	1.598E+00	1.655E+00	1.708E+00	1.758E+00
9			-9.222E-01	2.575E+C0	2.763E+00	2.760E+00	2.759E+00	2.771E+00	2.792E+00	2.819E+00	2.851E+00
8			-8.250E-01	3.845E+00	4.094E+00	4.131E+00	4.146E+00	4.163E+00	4.183E+00	4.201E+00	4.216E+00
7			-3.701E-04	4.773E+00	5.474E+00	5.648E+00	5.738E+00	5.781E+C0	5.789E+00	5.770E+00	5.731E+00
6	8.000E+00	6.395E+01	6.320E+01	7.265E+00	8.120E+00	8.010E+00	7.800E+00	7.560E+00	7.315E+00	7.075E+00	6.845E+00
5	6.C00E+00	1.293E+01	1.228E+01	1.083E+01	9.698E+00	8.861E+00	8.220E+00	7.706E+C0	7.279E+00	6.911E+00	6.589E+00
4	4.C00E+00	6.600E+00	6.768E+00	6.603E+00	6.478E+00	6.257E+00	6.002E+00	5.737E+C0	5.478E+00	5.228E+00	4.993E+00
3	2.C00E+00	3.289E+00	3.122E+00	2.839E+00	2.955E+00	2.999E+00	2.971E+00	2.900E+00	2.804E+00	2.695E+00	2.581E+00
2	8.000E-01	-1.505E+00	3.171E-01	1.870E+00	1.600E+00	1.367E+00	1.265E+00	1.207E+00	1.156E+00	1.106E+00	1.056E+00
1	0.0	0.0	0.0	0.0	0.0	0.0	0.0	0.0	0.0	0.0	0.0
	1	2	3	4	5	6	7	8	9	10	11

15	-8.404E-01	-9.082E-01	-9.861E-01	-1.070E+00	-1.170E+00	-1.208E+00	-1.809E+00	-3.964E+00	-5.223E-02		
14	-5.08CE-01	-5.433E-01	-5.780E-01	-6.094E-01	-6.394E-01	-6.713E-01	-7.465E-01	-5.348E-01	1.050E-01		
13	-1.679E-C1	-1.730E-01	-1.731E-01	-1.655E-01	-1.445E-01	-1.022E-01	2.827E-02	4.051E-01	-6.020E-01		
12	4.289E-01	4.535E-01	4.812E-01	5.098E-01	5.371E-01	5.290E-01	6.235E-01	1.125E+00	-1.361E+00		
11	1.031E+00	1.071E+00	1.112E+00	1.154E+00	1.214E+00	1.179E+00	1.004E+00	1.684E+00	-1.788E+00		
1C	1.805E+00	1.850E+00	1.894E+00	1.936E+C0	1.989E+00	1.992E+00	1.786E+00	1.978E+00	-1.710E+00		
9	2.883E+00	2.915E+00	2.946E+00	2.974E+00	3.004E+00	2.986E+00	2.770E+00	2.738E+C0	-1.379E+00		
8	4.228E+C0	4.234E+00	4.236E+00	4.231E+00	4.219E+00	4.151E+00	3.861E+00	3.517E+C0	-3.133E-01		
7	5.676E+00	5.609E+00	5.535E+00	5.453E+C0	5.366E+00	5.226E+00	4.839E+00	4.259E+00	1.973E+00		
6	6.625E+00	6.410E+00	6.210E+00	6.020E+00	5.845E+00	5.650E+00	5.240E+00	4.200E+00	5.720E+01	5.395E+01	5.310E+01
5	6.296E+C0	6.034E+C0	5.790E+00	5.561E+C0	5.362E+00	5.171E+00	4.856E+00	3.907E+00	1.058E+01	1.130E+01	1.154E+01
4	4.768E+00	4.557E+C0	4.362E+00	4.178E+C0	4.013E+00	3.872E+00	3.695E+00	3.235E+00	4.357E+00	4.670E+00	4.818E+00
3	2.469E+00	2.359E+00	2.254E+00	2.156E+00	2.070E+00	2.001E+00	1.936E+00	1.826E+00	2.129E+00	2.167E+00	2.156E+00
2	1.007E+00	9.590E-01	9.140E-01	8.715E-01	8.340E-01	7.990E-01	7.460E-01	5.840E-01	-1.166E-01	2.737E-01	5.315E-01
1	0.0	0.0	0.0	0.0	0.0	0.0	0.0	0.0	0.0	0.0	0.0
	12	13	14	15	16	17	18	19	20	21	22

THE DISTRIBUTION OF STREAM FUNCTION - A(I,J,NF)

15			0.0	0.0	0.0	0.0	0.0	0.0	0.0	0.0	0.0
14			0.0	4.824E-03	7.750E-03	9.789E-03	1.147E-02	1.293E-02	1.425E-02	1.548E-02	1.669E-02
13			0.0	1.786E-02	2.736E-02	3.380E-02	3.906E-02	4.361E-02	4.767E-02	5.143E-02	5.507E-02
12			0.0	5.055E-02	7.181E-02	8.603E-02	9.766E-02	1.076E-01	1.163E-01	1.241E-01	1.315E-01
11			0.0	6.014E-02	7.864E-02	9.307E-02	1.058E-01	1.168E-01	1.265E-01	1.351E-01	1.430E-01
10			0.0	1.957E-02	2.109E-02	2.908E-02	3.863E-02	4.767E-02	5.587E-02	6.331E-02	7.016E-02
9			0.0	-8.856E-02	-1.044E-01	-1.039E-01	-9.884E-02	-9.309E-02	-8.749E-02	-8.223E-02	-7.734E-02
8			0.0	-2.677E-01	-2.996E-01	-3.033E-01	-3.013E-01	-2.981E-01	-2.948E-01	-2.915E-01	-2.884E-01
7			0.0	-4.955E-01	-5.356E-01	-5.401E-01	-5.390E-01	-5.371E-01	-5.352E-01	-5.334E-01	-5.317E-01
6	0.0	0.0	0.0	-7.368E-01	-7.693E-01	-7.717E-01	-7.709E-01	-7.699E-01	-7.692E-01	-7.687E-01	-7.684E-01
5	-1.159E+00	-6.781E-01	-6.687E-01	-9.317E-01	-9.627E-01	-9.683E-01	-9.704E-01	-9.718E-01	-9.729E-01	-9.738E-01	-9.746E-01
4	-1.205E+00	-1.007E+00	-9.996E-01	-1.105E+00	-1.122E+00	-1.126E+00	-1.128E+00	-1.130E+00	-1.131E+00	-1.133E+00	-1.133E+00
3	-1.245E+00	-1.198E+00	-1.196E+00	-1.221E+00	-1.225E+00	-1.226E+00	-1.227E+00	-1.228E+00	-1.228E+00	-1.228E+00	-1.229E+00
2	-1.258E+00	-1.248E+00	-1.248E+00	-1.252E+00	-1.253E+00	-1.254E+00	-1.254E+00	-1.254E+00	-1.254E+00	-1.254E+00	-1.254E+00
1	-1.260E+00	-1.260E+00	-1.260E+00	-1.260E+00	-1.260E+00	-1.260E+00	-1.260E+00	-1.260E+00	-1.260E+00	-1.260E+00	-1.260E+00
	1	2	3	4	5	6	7	8	9	10	11

15	0.0	0.0	0.0	0.0	0.0	0.0	0.0	0.0	0.0		
14	1.794E-02	1.927E-02	2.076E-02	2.231E-02	2.408E-02	2.483E-02	3.481E-02	6.650E-02	0.0		
13	5.878E-02	6.262E-02	6.674E-02	7.089E-02	7.548E-02	7.803E-02	9.884E-02	1.493E-01	0.0		
12	1.386E-01	1.457E-01	1.528E-01	1.596E-01	1.664E-01	1.676E-01	1.900E-01	2.459E-01	0.0		
11	1.504E-01	1.575E-01	1.645E-01	1.710E-01	1.781E-01	1.785E-01	1.923E-01	2.502E-01	0.0		
10	7.656E-02	8.256E-02	8.841E-02	9.373E-02	9.982E-02	1.018E-01	1.153E-01	1.725E-01	0.0		
9	-7.279E-02	-6.862E-02	-6.463E-02	-6.106E-02	-5.693E-02	-5.371E-02	-3.544E-02	3.561E-02	0.0		
8	-2.856E-01	-2.830E-01	-2.806E-01	-2.787E-01	-2.765E-01	-2.734E-01	-2.526E-01	-1.624E-01	0.0		
7	-5.302E-01	-5.289E-01	-5.278E-01	-5.270E-01	-5.261E-01	-5.237E-01	-5.044E-01	-4.046E-01	0.0		
6	-7.682E-01	-7.681E-01	-7.680E-01	-7.681E-01	-7.682E-01	-7.670E-01	-7.534E-01	-6.697E-01	0.0	0.0	0.0
5	-9.753E-01	-9.759E-01	-9.765E-01	-9.770E-01	-9.775E-01	-9.774E-01	-9.710E-01	-9.304E-01	-7.252E-01	-6.925E-01	-6.845E-01
4	-1.134E+00	-1.135E+00	-1.136E+00	-1.136E+00	-1.136E+00	-1.137E+00	-1.135E+00	-1.122E+00	-1.062E+00	-1.046E+00	-1.041E+00
3	-1.229E+00	-1.229E+00	-1.229E+00	-1.230E+00	-1.230E+00	-1.230E+00	-1.229E+00	-1.227E+00	-1.215E+00	-1.211E+00	-1.210E+00
2	-1.254E+00	-1.254E+00	-1.254E+00	-1.254E+00	-1.254E+00	-1.254E+00	-1.254E+00	-1.254E+00	-1.251E+00	-1.250E+00	-1.250E+00
1	-1.260E+00	-1.260E+00	-1.260E+00	-1.260E+00	-1.260E+00	-1.260E+00	-1.260E+00	-1.260E+00	-1.260E+00	-1.260E+00	-1.260E+00
	12	13	14	15	16	17	18	19	20	21	22

THE DISTRIBUTION OF TEMPERATURE - A(I,J,NT)

	1	2	3	4	5	6	7	8	9	10	11
15			0.0	0.0	0.0	0.0	0.0	0.0	0.0	0.0	0.0
14			0.0	5.763E-03	8.252E-03	9.976E-03	1.138E-02	1.260E-02	1.371E-02	1.471E-02	1.565E-02
13			0.0	1.174E-02	1.677E-02	2.022E-02	2.300E-02	2.541E-02	2.758E-02	2.955E-02	3.136E-02
12			0.0	2.059E-02	3.050E-02	3.718E-02	4.250E-02	4.711E-02	5.120E-02	5.489E-02	5.827E-02
11			0.0	2.993E-02	4.441E-02	5.408E-02	6.182E-02	6.852E-02	7.450E-02	7.991E-02	8.488E-02
10			0.0	6.305E-02	7.813E-02	8.801E-02	9.616E-02	1.034E-01	1.101E-01	1.163E-01	1.221E-01
9			0.0	1.464E-01	1.601E-01	1.636E-01	1.672E-01	1.714E-01	1.760E-01	1.809E-01	1.859E-01
8			0.0	2.453E-01	2.609E-01	2.655E-01	2.687E-01	2.722E-01	2.761E-01	2.802E-01	2.846E-01
7			0.0	3.631E-01	3.839E-01	3.929E-01	3.999E-01	4.061E-01	4.115E-01	4.162E-01	4.201E-01
6	0.0	0.0	0.0	4.941E-01	5.540E-01	5.756E-01	5.858E-01	5.908E-C1	5.928E-01	5.928E-01	5.914E-01
5	1.COCE+CO	1.000E+CO	1.000E+00	9.662E-01	9.156E-01	8.755E-01	8.447E-01	8.202E-01	8.000E-01	7.829E-01	7.680E-01
4	1.000E+00	1.000E+00	1.000E+00	9.964E-01	9.841E-01	9.674E-01	9.495E-01	9.314E-01	9.138E-01	8.969E-01	8.807E-01
3	1.COOE+00	1.000E+00	1.000E+00	9.995E-01	9.966E-01	9.910E-01	9.830E-01	9.732E-C1	9.620E-01	9.498E-01	9.368E-01
2	1.COCE+CO	1.0CCE+CO	1.000E+00	9.998E-01	9.985E-01	9.952E-01	9.899E-01	9.825E-01	9.733E-01	9.628E-01	9.511E-01
1	1.000E+00	1.000E+00	1.000E+00	9.999E-01	9.988E-01	9.960E-01	9.912E-01	9.843E-01	9.755E-01	9.652E-01	9.538E-01

	12	13	14	15	16	17	18	19	20	21	22
15	0.0	0.0	0.0	0.0	0.0	0.0	0.0	0.0	0.0		
14	1.651E-02	1.731E-02	1.808E-02	1.884E-02	1.972E-02	2.082E-02	2.312E-02	2.743E-02	0.0		
13	3.303E-02	3.459E-02	3.606E-02	3.747E-02	3.898E-02	4.072E-02	4.536E-02	5.632E-02	0.0		
12	6.142E-02	6.436E-02	6.713E-02	6.956E-02	7.145E-02	7.086E-02	7.406E-02	9.705E-C2	0.0		
11	8.952E-02	9.389E-02	9.816E-02	1.022E-01	1.066E-01	1.060E-01	9.808E-02	1.287E-01	0.0		
10	1.277E-01	1.331E-01	1.384E-01	1.435E-01	1.487E-01	1.507E-01	1.419E-01	1.524E-01	0.0		
9	1.911E-01	1.963E-01	2.016E-01	2.067E-01	2.116E-01	2.134E-01	2.037E-01	2.025E-01	0.0		
8	2.891E-01	2.935E-01	2.980E-01	3.022E-01	3.058E-01	3.052E-01	2.896E-01	2.674E-01	0.0		
7	4.235E-01	4.264E-01	4.288E-01	4.307E-01	4.317E-01	4.275E-01	4.024E-01	3.434E-01	0.0		
6	5.892E-01	5.864E-01	5.832E-01	5.798E-01	5.758E-01	5.672E-01	5.342E-01	4.271E-01	0.0	0.0	0.0
5	7.546E-01	7.424E-01	7.311E-01	7.206E-01	7.108E-01	6.991E-01	6.669E-01	5.364E-01	3.356E-01	3.282E-01	3.253E-01
4	8.653E-01	8.505E-01	8.363E-01	8.227E-01	8.103E-01	7.981E-01	7.750E-01	6.831E-01	5.779E-01	5.560E-01	5.451E-01
3	9.235E-01	9.098E-01	8.960E-01	8.823E-01	8.694E-01	8.578E-01	8.422E-01	7.925E-01	7.338E-01	7.092E-01	6.929E-01
2	9.386E-01	9.255E-01	9.120E-01	8.984E-01	8.855E-01	8.742E-01	8.618E-01	8.323E-01	7.919E-01	7.634E-01	7.417E-01
1	9.414E-01	9.285E-01	9.151E-01	9.015E-01	8.886E-01	8.773E-01	8.655E-01	8.399E-01	8.030E-01	7.737E-01	7.510E-01

THE DISTRIBUTION OF Z-COMP. MASS VELOCITY - G1(I,J)

15			0.0	0.0	0.0	0.0	0.0	0.0	0.0	0.0	0.0
14			0.0	-6.686E-02	-1.006E-01	-1.232E-01	-1.415E-01	-1.574E-01	-1.714E-01	-1.844E-01	-1.969E-01
13			0.0	-6.521E-02	-8.869E-02	-1.042E-01	-1.169E-01	-1.277E-01	-1.370E-01	-1.451E-01	-1.525E-01
12			0.0	-3.109E-02	-2.243E-02	-2.319E-02	-2.672E-02	-3.030E-02	-3.341E-02	-3.591E-02	-3.769E-02
11			0.0	1.441E-C1	2.045E-01	2.274E-01	2.386E-01	2.457E-01	2.509E-01	2.550E-01	2.587E-01
10			0.0	4.331E-01	5.028E-01	5.328E-01	5.509E-01	5.641E-C1	5.745E-01	5.833E-01	5.911E-01
9			0.0	8.209E-01	8.947E-01	9.140E-01	9.280E-01	9.399E-01	9.502E-01	9.593E-01	9.676E-01
8			0.0	1.219E+CO	1.263E+00	1.267E+00	1.272E+00	1.279E+00	1.286E+00	1.294E+00	1.302E+00
7			0.0	1.550E+00	1.502E+00	1.489E+00	1.490E+00	1.496E+00	1.504E+00	1.512E+00	1.521E+00
6	0.0	C.0	0.0	1.567E+00	1.555E+00	1.580E+00	1.604E+00	1.623E+CO	1.637E+00	1.648E+00	1.657E+00
5	8.750E-01	3.532E+00	3.558E+00	1.854E+00	1.708E+00	1.693E+00	1.694E+00	1.697E+00	1.700E+00	1.702E+00	1.703E+00
4	1.500E+00	3.087E+00	3.166E+00	1.867E+00	1.662E+00	1.613E+00	1.588E+00	1.570E+00	1.555E+00	1.544E+00	1.533E+00
3	1.875E+00	3.361E+00	3.459E+00	2.118E+00	1.875E+00	1.814E+00	1.779E+00	1.750E+CO	1.726E+00	1.706E+00	1.689E+00
2	1.980E+00	2.777E+00	2.900E+00	1.818E+00	1.605E+00	1.549E+00	1.520E+00	1.498E+00	1.480E+00	1.466E+00	1.454E+00
1	2.000E+00	2.666E+00	2.793E+00	1.760E+00	1.553E+00	1.499E+00	1.470E+00	1.449E+00	1.433E+00	1.420E+00	1.410E+00
	1	2	3	4	5	6	7	8	9	10	11

15	0.0	0.0	0.0	0.0	0.0	0.0	0.0	0.0	0.0		
14	-2.095E-01	-2.223E-01	-2.359E-01	-2.492E-01	-2.637E-01	-2.729E-01	-3.285E-01	-4.248E-01	0.0		
13	-1.594E-01	-1.658E-01	-1.719E-01	-1.770E-01	-1.816E-01	-1.790E-01	-1.822E-01	-1.933E-01	0.0		
12	-3.868E-C2	-3.883E-02	-3.839E-02	-3.754E-02	-3.862E-02	-3.591E-02	-8.496E-03	-1.486E-02	0.0		
11	2.624E-01	2.662E-01	2.704E-01	2.744E-01	2.783E-01	2.724E-01	2.738E-01	2.760E-01	0.0		
10	5.986E-C1	6.059E-01	6.133E-01	6.204E-01	6.282E-01	6.234E-01	6.041E-01	5.490E-01	0.0		
9	9.753E-01	9.826E-01	9.902E-01	9.978E-01	1.007E+00	1.007E+00	9.953E-01	9.078E-01	0.0		
8	1.309E+00	1.316E+00	1.323E+00	1.329E+00	1.335E+00	1.339E+00	1.348E+00	1.296E+00	0.0		
7	1.529E+CO	1.537E+CO	1.544E+00	1.550E+00	1.556E+00	1.563E+00	1.599E+00	1.702E+00	0.8		
6	1.664E+00	1.670E+00	1.675E+00	1.679E+00	1.682E+00	1.691E+00	1.749E+00	2.094E+00	0.0	0.0	0.0
5	1.704E+00	1.705E+00	1.705E+00	1.705E+00	1.705E+00	1.708E+00	1.754E+00	2.052E+00	3.624E+00	3.797E+00	3.832E+00
4	1.525E+00	1.518E+00	1.511E+00	1.506E+00	1.501E+00	1.499E+00	1.525E+00	1.694E+CO	2.467E+00	2.665E+00	2.719E+00
3	1.674E+CO	1.662E+00	1.651E+00	1.642E+00	1.634E+00	1.630E+00	1.651E+00	1.785E+00	2.430E+00	2.644E+00	2.712E+00
2	1.445E+00	1.437E+00	1.430E+00	1.425E+00	1.422E+00	1.423E+00	1.445E+00	1.563E+00	2.090E+00	2.295E+00	2.371E+00
1	1.401E+00	1.394E+00	1.388E+00	1.384E+00	1.382E+00	1.384E+00	1.406E+00	1.521E+00	2.025E+00	2.229E+00	2.306E+00
	12	13	14	15	16	17	18	19	20	21	22

THE DISTRIBUTION OF R-COMP. MASS VELOCITY - G2(I,J)

	1	2	3	4	5	6	7	8	9	10	11
15			0.0	0.0	0.0	0.0	0.0	0.0	0.0	0.0	0.0
14			0.0	-3.934E-03	-2.428E-03	-1.734E-03	-1.439E-03	-1.260E-03	-1.138E-03	-1.071E-03	-1.061E-03
13			0.0	-1.502E-02	-8.226E-03	-5.731E-03	-4.714E-03	-4.091E-03	-3.665E-03	-3.420E-03	-3.339E-03
12			0.0	-4.571E-02	-2.022E-02	-1.391E-02	-1.145E-02	-9.801E-03	-8.603E-03	-7.798E-03	-7.330E-03
11			0.0	-5.901E-02	-1.998E-02	-1.588E-02	-1.393E-02	-1.209E-02	-1.059E-02	-9.471E-03	-8.693E-03
10			0.0	-2.054E-02	-3.453E-03	-1.049E-02	-1.196E-02	-1.121E-02	-1.015E-02	-9.220E-03	-8.480E-03
9			0.0	1.086E-01	1.850E-02	-1.958E-03	-7.466E-03	-8.258E-03	-7.972E-03	-7.459E-03	-6.918E-03
8			0.0	3.782E-01	4.501E-02	4.440E-03	-3.728E-03	-5.402E-03	-5.603E-03	-5.416E-03	-5.093E-03
7			0.0	8.329E-01	6.777E-02	6.972E-03	-2.415E-03	-3.896E-03	-3.823E-03	-3.546E-03	-3.256E-03
6	0.0	0.0	0.0	1.535E+00	6.825E-02	4.533E-03	-2.231E-03	-2.368E-03	-1.599E-03	-1.050E-03	-7.223E-04
5	0.0	-1.289E+00	1.507E-01	7.430E-01	8.872E-02	1.665E-02	6.658E-03	4.444E-03	3.557E-03	2.998E-03	2.608E-03
4	0.0	-8.022E-01	7.790E-02	4.501E-01	7.533E-02	1.936E-02	1.058E-02	8.054E-03	6.536E-03	5.403E-03	4.538E-03
3	0.0	-3.776E-01	3.354E-02	2.112E-01	3.938E-02	1.076E-02	6.317E-03	5.050E-03	4.218E-03	3.550E-03	2.968E-03
2	0.0	-1.840E-01	1.251E-02	9.708E-02	1.934E-02	5.373E-03	2.962E-03	2.221E-03	1.767E-03	1.450E-03	1.154E-03
1	0.0	0.0	0.0	0.0	0.0	0.0	0.0	0.0	0.0	0.0	0.0

	12	13	14	15	16	17	18	19	20	21	22
15	0.0	0.0	0.0	0.0	0.0	0.0	0.0	0.0	0.0		
14	-1.102E-03	-1.182E-03	-1.294E-03	-1.372E-03	-1.242E-03	-2.021E-03	-1.170E-02	-2.662E-02	0.0		
13	-3.394E-03	-3.537E-03	-3.733E-03	-3.821E-03	-3.491E-03	-5.098E-03	-2.389E-02	-4.084E-02	0.0		
12	-7.121E-03	-7.055E-03	-7.035E-03	-6.691E-03	-5.165E-03	-4.852E-03	-2.844E-02	-4.255E-02	0.0		
11	-8.183E-03	-7.836E-03	-7.621E-03	-7.275E-03	-5.792E-03	-3.001E-03	-2.251E-02	-4.938E-02	0.0		
10	-7.904E-03	-7.440E-03	-7.123E-03	-6.798E-03	-5.992E-03	-4.891E-03	-2.480E-02	-6.337E-02	0.0		
9	-6.391E-03	-5.895E-03	-5.533E-03	-5.226E-03	-5.227E-03	-8.107E-03	-3.742E-02	-1.128E-01	0.0		
8	-4.687E-03	-4.217E-03	-3.729E-03	-3.266E-03	-3.775E-03	-1.008E-02	-5.155E-02	-1.980E-01	0.0		
7	-2.938E-03	-2.572E-03	-2.106E-03	-1.625E-03	-2.382E-03	-1.037E-02	-6.102E-02	-3.035E-01	0.0		
6	-4.838E-04	-2.887E-04	-6.008E-05	2.147E-04	-6.064E-04	-8.231E-03	-5.779E-02	-3.924E-01	0.0	0.0	0.0
5	2.296E-03	2.013E-03	1.810E-03	1.772E-03	1.026E-03	-4.110E-03	-3.647E-02	-2.182E-01	-1.075E+00	-9.246E-02	-2.311E-02
4	3.832E-03	3.255E-03	2.817E-03	2.513E-03	1.748E-03	-1.172E-03	-1.749E-02	-1.016E-01	-4.710E-01	-6.999E-02	-2.052E-02
3	2.497E-03	2.115E-03	1.815E-03	1.538E-03	1.037E-03	-2.788E-04	-6.869E-03	-3.947E-02	-1.877E-01	-3.507E-02	-1.157E-02
2	9.442E-04	7.838E-04	6.569E-04	4.912E-04	1.945E-04	-4.891E-04	-3.651E-03	-1.913E-02	-8.722E-02	-1.865E-02	-6.843E-03
1	0.0	0.0	0.0	0.0	0.0	0.0	0.0	0.0	0.0	0.0	0.0

THE DISTRIBUTION OF Z-COMP. VELOCITY - V1(I,J)

J	1	2	3	4	5	6	7	8	9	10	11
15			0.0	0.0	0.0	0.0	0.0	0.0	0.0	0.0	0.0
14			0.0	-6.908E-03	-1.058E-02	-1.311E-02	-1.521E-02	-1.707E-02	-1.873E-02	-2.030E-02	-2.182E-02
13			0.0	-7.029E-03	-9.906E-03	-1.193E-02	-1.365E-02	-1.516E-02	-1.652E-02	-1.774E-02	-1.888E-02
12			0.0	-3.568E-03	-2.761E-03	-2.992E-03	-3.578E-03	-4.191E-03	-4.755E-03	-5.243E-03	-5.633E-03
11			0.0	1.766E-02	2.776E-02	3.302E-02	3.654E-02	3.939E-02	4.188E-02	4.412E-02	4.624E-02
10			0.0	6.689E-02	8.597E-02	9.718E-02	1.058E-01	1.133E-01	1.201E-01	1.265E-01	1.324E-01
9			0.0	2.084E-01	2.413E-01	2.500E-01	2.575E-01	2.649E-01	2.722E-01	2.793E-01	2.862E-01
8			0.0	3.996E-01	4.220E-01	4.283E-01	4.337E-01	4.404E-01	4.480E-01	4.565E-01	4.657E-01
7			0.0	6.767E-01	6.827E-01	6.877E-01	6.965E-01	7.065E-01	7.162E-01	7.251E-01	7.337E-01
6	0.0	0.0	0.0	8.568E-01	9.353E-01	9.805E-01	1.010E+00	1.029E+00	1.040E+00	1.047E+00	1.051E+00
5	8.750E-01	3.532E+00	3.558E+00	1.798E+00	1.579E+00	1.503E+00	1.457E+00	1.422E+00	1.394E+00	1.370E+00	1.348E+00
4	1.500E+00	3.087E+00	3.166E+00	1.861E+00	1.639E+00	1.566E+00	1.517E+00	1.474E+00	1.435E+00	1.401E+00	1.368E+00
3	1.875E+00	3.361E+00	3.459E+00	2.117E+00	1.869E+00	1.799E+00	1.752E+00	1.708E+00	1.668E+00	1.630E+00	1.594E+00
2	1.980E+00	2.777E+00	2.900E+00	1.818E+00	1.603E+00	1.542E+00	1.506E+00	1.475E+00	1.445E+00	1.418E+00	1.391E+00
1	2.000E+00	2.666E+00	2.793E+00	1.760E+00	1.551E+00	1.494E+00	1.459E+00	1.429E+00	1.402E+00	1.376E+00	1.352E+00

J	12	13	14	15	16	17	18	19	20	21	22
15	0.0	0.0	0.0	0.0	0.0	0.0	0.0	0.0	0.0		
14	-2.336E-02	-2.492E-02	-2.659E-02	-2.825E-02	-3.008E-02	-3.137E-02	-3.838E-02	-5.116E-02	0.0		
13	-1.997E-02	-2.100E-02	-2.200E-02	-2.288E-02	-2.373E-02	-2.367E-02	-2.489E-02	-2.850E-02	0.0		
12	-5.908E-03	-6.051E-03	-6.097E-03	-6.061E-03	-6.315E-03	-5.849E-03	-1.414E-03	-2.870E-03	0.0		
11	4.833E-02	5.041E-02	5.259E-02	5.472E-02	5.700E-02	5.559E-02	5.323E-02	6.411E-02	0.0		
10	1.383E-01	1.440E-01	1.498E-01	1.554E-01	1.612E-01	1.614E-01	1.501E-01	1.433E-01	0.0		
9	2.928E-01	2.992E-01	3.054E-01	3.113E-01	3.173E-01	3.184E-01	3.085E-01	2.806E-01	0.0		
8	4.791E-01	4.845E-01	4.939E-01	5.019E-01	5.091E-01	5.098E-01	4.900E-01	4.403E-01	0.0		
7	7.412E-01	7.482E-01	7.543E-01	7.593E-01	7.633E-01	7.621E-01	7.506E-01	7.122E-01	0.0		
6	1.052E+00	1.052E+00	1.051E+00	1.048E+00	1.044E+00	1.037E+00	1.021E+00	1.020E+00	0.0	0.0	0.0
5	1.329E+00	1.311E+00	1.294E+00	1.278E+00	1.263E+00	1.247E+00	1.229E+00	1.202E+00	1.489E+00	1.533E+00	1.536E+00
4	1.340E+00	1.314E+00	1.288E+00	1.265E+00	1.244E+00	1.226E+00	1.217E+00	1.212E+00	1.536E+00	1.608E+00	1.614E+00
3	1.559E+00	1.527E+00	1.497E+00	1.468E+00	1.442E+00	1.422E+00	1.416E+00	1.452E+00	1.850E+00	1.955E+00	1.965E+00
2	1.366E+00	1.341E+00	1.317E+00	1.295E+00	1.275E+00	1.262E+00	1.265E+00	1.327E+00	1.699E+00	1.808E+00	1.822E+00
1	1.328E+00	1.305E+00	1.282E+00	1.261E+00	1.243E+00	1.231E+00	1.236E+00	1.302E+00	1.666E+00	1.776E+00	1.791E+00

THE DISTRIBUTION OF R-COMP. VELOCITY - V2(I,J)

	1	2	3	4	5	6	7	8	9	10	11
15			0.0	0.0	0.0	0.0	0.0	0.0	0.0	0.0	0.0
14			0.0	-4.065E-04	-2.553E-04	-1.846E-04	-1.547E-04	-1.366E-04	-1.244E-04	-1.179E-04	-1.176E-04
13			0.0	-1.619E-03	-9.188E-04	-6.559E-04	-5.503E-04	-4.857E-C4	-4.419E-04	-4.181E-04	-4.135E-04
12			0.0	-5.245E-03	-2.489E-03	-1.795E-03	-1.533E-03	-1.356E-03	-1.224E-03	-1.139E-03	-1.096E-03
11			0.0	-7.234E-03	-2.712E-03	-2.306E-03	-2.133E-03	-1.938E-03	-1.767E-03	-1.639E-03	-1.554E-03
10			0.0	-3.172E-03	-5.904E-04	-1.913E-03	-2.297E-03	-2.252E-03	-2.123E-03	-1.999E-03	-1.900E-03
9			0.0	2.757E-02	4.990E-03	-5.357E-04	-2.071E-03	-2.327E-03	-2.284E-03	-2.172E-03	-2.046E-03
8			0.0	1.240E-01	1.504E-02	1.501E-03	-1.271E-03	-1.860E-03	-1.952E-03	-1.910E-03	-1.822E-03
7			0.0	3.636E-01	3.080E-02	3.220E-03	-1.129E-03	-1.840E-03	-1.821E-03	-1.701E-03	-1.571E-03
6	0.0	0.0	0.0	8.393E-01	4.105E-02	2.813E-03	-1.404E-03	-1.501E-03	-1.016E-03	-6.672E-04	-4.581E-04
5	0.0	-1.289E+00	1.507E-01	7.207E-01	8.200E-02	1.479E-02	5.727E-03	3.723E-03	2.916E-03	2.413E-03	2.065E-03
4	0.0	-8.022E-01	7.790E-02	4.487E-01	7.427E-02	1.880E-02	1.010E-02	7.560E-03	6.031E-03	4.902E-03	4.051E-03
3	0.0	-3.776E-01	3.354E-02	2.111E-01	3.926E-02	1.067E-02	6.222E-03	4.930E-03	4.076E-03	3.391E-03	2.801E-03
2	0.0	-1.840E-01	1.251E-02	9.706E-02	1.931E-02	5.350E-03	2.935E-03	2.187E-03	1.725E-03	1.402E-03	1.104E-03
1	0.0	0.0	0.0	0.0	0.0	0.0	0.0	0.0	0.0	0.0	0.0

	12	13	14	15	16	17	18	19	20	21	22
15	0.0	0.0	0.0	0.0	0.0	0.0	0.0	0.0	0.0		
14	-1.229E-04	-1.325E-04	-1.459E-04	-1.555E-04	-1.417E-04	-2.323E-04	-1.367E-03	-3.206E-03	0.0		
13	-4.252E-04	-4.481E-04	-4.778E-04	-4.939E-04	-4.561E-04	-6.743E-04	-3.264E-03	-6.022E-03	0.0		
12	-1.088E-03	-1.099E-03	-1.117E-03	-1.080E-03	-8.446E-04	-7.902E-04	-4.733E-03	-8.219E-03	0.0		
11	-1.507E-03	-1.484E-03	-1.482E-03	-1.451E-03	-1.186E-03	-6.124E-04	-4.376E-03	-1.147E-02	0.0		
10	-1.826E-03	-1.769E-03	-1.740E-03	-1.702E-03	-1.538E-03	-1.267E-03	-6.162E-03	-1.654E-02	0.0		
9	-1.919E-03	-1.795E-03	-1.707E-03	-1.630E-03	-1.647E-03	-2.563E-03	-1.160E-02	-3.487E-02	0.0		
8	-1.701E-03	-1.553E-03	-1.392E-03	-1.233E-03	-1.439E-03	-3.838E-03	-1.874E-02	-6.727E-02	0.0		
7	-1.424E-03	-1.252E-03	-1.029E-03	-7.960E-04	-1.169E-03	-5.056E-03	-2.864E-02	-1.270E-01	0.0		
6	-3.059E-04	-1.819E-04	-3.768E-05	1.340E-04	-3.764E-04	-5.047E-03	-3.369E-02	-1.912E-01	0.0	0.0	0.0
5	1.790E-03	1.548E-03	1.374E-03	1.328E-03	7.600E-04	-3.001E-03	-2.556E-02	-1.278E-01	-4.418E-01	-3.733E-02	-9.265E-03
4	3.368E-03	2.817E-03	2.402E-03	2.111E-03	1.449E-03	-9.589E-04	-1.396E-02	-7.271E-02	-2.932E-01	-4.222E-02	-1.218E-02
3	2.326E-03	1.944E-03	1.645E-03	1.375E-03	9.152E-04	-2.431E-04	-5.893E-03	-3.210E-02	-1.429E-01	-2.593E-02	-8.384E-03
2	8.925E-04	7.315E-04	6.050E-04	4.463E-04	1.745E-04	-4.338E-04	-3.197E-03	-1.624E-02	-7.089E-02	-1.469E-02	-5.257E-03
1	0.0	0.0	0.0	0.0	0.0	0.0	0.0	0.0	0.0	0.0	0.0

MAXIMUM RESIDUAL FOR EACH VARIABLE

NITER	VORTICITY	STREAM FCN	TEMPERATURE
1	3.896E+CO (2, 2)	2.549E-02 (19,12)	-1.454E-02 (11, 5)
2	5.856E+CO (2, 2)	3.461E-02 (19,11)	1.344E-02 (5, 6)
3	3.108E+CO (2, 2)	3.528E-02 (19,11)	1.686E-02 (6, 6)
4	1.981E+CO (2, 2)	3.364E-02 (19,11)	1.788E-02 (7, 6)
5	1.344E+CO (2, 2)	-3.616E-02 (6,11)	1.801E-02 (8, 7)
6	9.242E-01 (2, 2)	-3.944E-02 (7,11)	1.944E-02 (9, 7)
7	6.608E-C1 (2, 2)	-4.150E-02 (8,11)	2.004E-02 (10, 7)
8	5.240E-C1 (5, 3)	-4.330E-02 (9,12)	2.034E-02 (11, 8)
9	4.687E-01 (6, 3)	-4.484E-02 (9,11)	-2.217E-02 (6, 9)
10	5.032E-01 (20, 2)	-4.661E-02 (10,11)	-2.467E-02 (7, 9)
11	4.844E-01 (20, 2)	-4.722E-02 (11,11)	-2.632E-02 (8, 9)
12	4.328E-C1 (20, 2)	-4.768E-02 (12,12)	-2.669E-02 (9, 9)
13	3.730E-01 (20, 2)	-4.807E-02 (13,12)	-2.622E-02 (9, 9)
14	3.201E-C1 (2, 2)	-4.829E-02 (14,12)	-2.603E-02 (10, 9)
15	3.231E-01 (3, 2)	-4.863E-02 (16,12)	-2.556E-02 (11, 9)
16	3.456E-01 (3, 2)	-4.866E-02 (17,12)	-2.507E-02 (12, 9)
17	3.606E-C1 (3, 2)	-4.756E-02 (18,11)	-2.495E-02 (13, 9)
18	3.666E-01 (3, 2)	-4.366E-02 (18,11)	-2.442E-02 (14, 9)
19	3.646E-01 (3, 2)	-3.760E-02 (19,11)	-2.408E-02 (15, 9)
20	3.551E-C1 (3, 2)	3.340E-02 (8,12)	-2.374E-02 (17, 9)
21	3.397E-C1 (3, 2)	3.535E-02 (9,12)	-2.260E-02 (17, 9)
22	3.233E-01 (3, 2)	3.677E-02 (9,12)	-2.033E-02 (18, 9)
23	3.010E-01 (3, 2)	3.773E-02 (10,12)	-1.939E-02 (17, 8)
24	2.839E-C1 (3, 2)	3.864E-02 (10,12)	-1.840E-02 (18, 8)
25	2.650E-C1 (3, 2)	3.996E-02 (11,12)	-1.703E-02 (18, 8)
26	2.506E-01 (3, 2)	4.077E-02 (11,12)	-1.551E-02 (18, 8)
27	2.325E-C1 (3, 2)	4.224E-02 (12,12)	-1.446E-02 (18, 7)
28	2.134E-C1 (3, 2)	4.344E-02 (12,12)	-1.336E-02 (18, 7)
29	2.112E-01 (19, 2)	4.528E-02 (13,12)	-1.226E-02 (18, 7)
30	2.025E-C1 (19, 2)	4.698E-02 (13,12)	-1.122E-02 (18, 7)
31	1.895E-C1 (19, 2)	4.765E-02 (13,12)	-1.023E-02 (18, 7)
32	1.768E-01 (22, 2)	4.777E-02 (14,12)	-9.341E-03 (18, 7)
33	1.671E-01 (22, 2)	4.754E-02 (14,12)	-8.395E-03 (18, 7)
34	1.504E-C1 (22, 2)	4.635E-02 (14,12)	-7.439E-03 (18, 7)
35	1.402E-01 (18, 2)	4.435E-02 (14,12)	-6.486E-03 (18, 7)
36	1.440E-01 (17, 2)	4.206E-02 (15,12)	-5.745E-03 (18, 6)
37	1.455E-01 (17, 2)	4.008E-02 (15,12)	-5.225E-03 (16,12)
38	1.453E-01 (17, 2)	3.751E-02 (15,12)	-4.827E-03 (16,12)
39	1.429E-01 (17, 2)	3.454E-02 (16,12)	-4.494E-03 (17,11)
40	1.370E-C1 (17, 2)	3.229E-02 (16,12)	4.607E-03 (12,10)
41	1.334E-C1 (17, 2)	2.962E-02 (16,12)	4.142E-03 (12,10)
42	1.279E-C1 (17, 2)	2.660E-02 (16,12)	6.141E-03 (13,10)
43	1.205E-01 (17, 2)	2.381E-02 (17,12)	5.806E-03 (13,10)
44	1.167E-C1 (17, 2)	-2.237E-02 (12,12)	7.815E-03 (14,10)
45	1.082E-01 (16, 2)	-2.435E-02 (12,12)	8.186E-03 (14,10)
46	1.033E-01 (17, 2)	-2.485E-02 (13,12)	8.798E-03 (15,10)
47	9.340E-C2 (17, 2)	-2.673E-02 (13,12)	1.082E-02 (15,10)
48	8.692E-C2 (16, 2)	-2.673E-02 (13,12)	7.347E-03 (15,10)
49	7.798E-02 (16, 2)	-2.785E-02 (14,12)	1.381E-02 (16,10)
50	7.287E-C2 (17, 2)	-2.769E-02 (14,12)	9.931E-03 (16,11)
51	6.443E-02 (17, 2)	-2.761E-02 (15,12)	9.288E-03 (17,10)
52	[illegible] (17, 2)	-2.752E-02 (15,12)	1.253E-02 (17,10)
53	5.046E-02 (16, 2)	-2.605E-02 (15,12)	9.701E-03 (17,11)
54	4.366E-C2 (16, 2)	-2.601E-02 (17,11)	8.809E-03 (17,11)

59	[illegible]	(17, 2)	-1.904E-02	(17,12)	3.649E-03	(18,12)
60	[illegible]	(16, 2)	-1.643E-02	(18,12)	-3.474E-03	(17, 9)
61	1.454E-02	(15, 2)	-1.490E-02	(18,12)	[illegible]	(17, 9)
62	-1.300E-02	(20, 2)	-1.266E-02	(18,12)	[illegible]	(18, 9)
63	-1.488E-02	(20, 2)	1.192E-02	(12,12)	-2.980E-03	(18, 9)
64	-1.607E-02	(20, 2)	1.247E-02	(12,12)	-2.751E-03	(18, 9)
65	-1.223E-02	(20, 2)	1.274E-02	(12,12)	-2.583E-03	(18,10)
66	-1.042E-02	(21, 2)	1.319E-02	(13,12)	-2.454E-03	(18,11)
67	-1.424E-02	(20, 2)	1.392E-02	(13,12)	-2.469E-03	(18,11)
68	-7.719E-03	(20, 2)	1.438E-02	(13,12)	-2.386E-03	(18,11)
69	-7.733E-03	(20, 2)	1.488E-02	(14,12)	-2.277E-03	(18,11)
70	-8.930E-03	(20, 2)	1.557E-02	(14,12)	-2.206E-03	(16,12)
71	-1.077E-02	(20, 2)	1.594E-02	(14,12)	-2.248E-03	(16,12)
72	-1.088E-02	(20, 2)	1.596E-02	(14,12)	-2.254E-03	(16,12)
73	-1.090E-02	(20, 2)	1.585E-02	(15,12)	-2.231E-03	(16,12)
74	-1.312E-02	(20, 2)	1.586E-02	(15,12)	-2.180E-03	(16,12)
75	-1.034E-02	(20, 2)	1.556E-02	(15,12)	-2.105E-03	(16,12)
76	-1.193E-02	(20, 2)	1.498E-02	(15,12)	-2.011E-03	(16,12)
77	-6.022E-03	(19, 2)	1.413E-02	(15,12)	-1.900E-03	(16,12)
78	-1.020E-02	(20, 2)	1.332E-02	(16,12)	1.961E-03	(13,10)
79	-7.381E-03	(20, 2)	1.262E-02	(16,12)	1.984E-03	(13,10)
80	-1.155E-02	(20, 2)	1.173E-02	(16,12)	1.927E-03	(14,10)
81	6.560E-03	(14,10)	1.065E-02	(16,12)	2.077E-03	(14,10)
82	6.942E-03	(14,10)	9.429E-03	(16,12)	2.119E-03	(14,10)
83	-7.707E-03	(20, 2)	8.443E-03	(17,12)	1.976E-03	(14,10)
84	6.661E-03	(15,10)	7.513E-03	(17,12)	2.032E-03	(15,10)
85	6.977E-03	(15,10)	-6.665E-03	(13,12)	2.064E-03	(15,10)
86	6.559E-03	(15,10)	-7.112E-03	(13,12)	1.875E-03	(15,10)
87	5.906E-03	(15,10)	-7.418E-03	(13,12)	1.801E-03	(16,10)
88	5.938E-03	(16,10)	-7.406E-03	(13,12)	1.844E-03	(16,10)
89	5.709E-03	(16,10)	-7.410E-03	(14,12)	1.718E-03	(16,10)
90	5.311E-03	(16,10)	-7.633E-03	(14,12)	1.580E-03	(15,11)
91	-5.438E-03	(20, 2)	-7.725E-03	(14,12)	1.367E-03	(16,11)
92	3.897E-03	(16,10)	-7.589E-03	(14,12)	1.411E-03	(16,11)
93	3.767E-03	(17,10)	-7.495E-03	(15,12)	1.393E-03	(16,11)
94	3.512E-03	(17,10)	-7.361E-03	(15,12)	1.420E-03	(16,11)
95	3.039E-03	(17,10)	-7.133E-03	(15,12)	1.304E-03	(16,11)
96	2.519E-03	(17,10)	-6.871E-03	(16,12)	1.240E-03	(17,11)
97	-4.191E-03	(22, 2)	-6.753E-03	(16,12)	1.176E-03	(17,11)
98	-2.388E-03	(15,10)	-6.453E-03	(16,12)	1.067E-03	(17,11)
99	-2.468E-03	(15,10)	-6.076E-03	(16,12)	9.989E-04	(17,12)
100	-2.447E-03	(15,10)	-5.619E-03	(16,12)	9.325E-04	(17,12)
101	-2.394E-03	(15,10)	-5.176E-03	(17,12)	8.449E-04	(17,12)
102	3.219E-03	(22, 2)	-4.805E-03	(17,12)	-8.399E-04	(15,10)
103	-2.673E-03	(20, 2)	-4.349E-03	(17,12)	-8.202E-04	(15,10)
104	-2.222E-03	(16,10)	-3.827E-03	(17,12)	-7.985E-04	(16,10)
105	-2.143E-03	(16,10)	-3.264E-03	(17,12)	-7.770E-04	(16,10)
106	-2.031E-03	(16,10)	2.991E-03	(12,12)	-7.435E-04	(16,10)
107	-2.359E-03	(22, 2)	3.187E-03	(13,12)	-7.009E-04	(16,10)
108	-2.790E-03	(20, 2)	3.334E-03	(13,12)	-6.502E-04	(16,10)
109	-2.091E-03	(22, 2)	3.399E-03	(13,12)	-6.304E-04	(15,11)
110	-2.909E-03	(20, 2)	3.381E-03	(13,12)	-6.110E-04	(15,11)
111	-2.548E-03	(21, 2)	3.493E-03	(14,12)	-5.834E-04	(15,11)
112	2.732E-03	(22, 2)	3.595E-03	(14,12)	-5.756E-04	(16,11)
113	-3.327E-03	(20, 2)	3.610E-03	(14,12)	-5.726E-04	(16,11)
114	-3.600E-03	(20, 2)	3.540E-03	(14,12)	-5.612E-04	(16,11)
115	1.977E-03	(16, 2)	3.483E-03	(15,12)	-5.420E-04	(16,11)
116	-2.505E-03	(22, 2)	3.479E-03	(15,12)	-5.161E-04	(17,11)
117	-2.447E-03	(21, 2)	3.400E-03	(15,12)	-5.093E-04	(16,12)
118	-2.467E-03	(17, 2)	3.249E-03	(15,12)	-4.964E-04	(16,12)
119	1.958E-03	(15, 2)	3.036E-03	(15,12)	-4.746E-04	(16,12)
120	-1.683E-03	(21, 2)	2.904E-03	(16,12)	-4.451E-04	(16,12)
121	[illegible]	(18, 2)	2.752E-03	(16,12)	4.362E-04	(14,10)
122	[illegible]	(20, 2)	2.551E-03	(16,12)	4.241E-04	(14,10)
123	[illegible]	(17, 2)	2.308E-03	(16,12)	4.002E-04	(14,10)

[illegible]	[illegible]	[illegible]	[illegible]	[illegible]	[illegible]	[illegible]
127	-2.0[illegible]E-03	(22, 2)	-1.478E-03	(13,12)	3.4[illegible]E-04	(15,10)
128	-2.394E-03	(18, 2)	-1.548E-03	(13,12)	3.2[illegible]E-04	(16,10)
129	1.026E-03	(16,10)	-1.576E-03	(13,12)	3.183E-04	(16,10)
130	9.826E-04	(16,10)	-1.560E-03	(13,12)	3.024E-04	(16,10)
131	9.136E-04	(16,10)	-1.550E-03	(14,12)	2.833E-04	(15,11)
132	8.269E-04	(16,10)	-1.611E-03	(14,12)	2.768E-04	(15,11)
133	7.177E-04	(16,10)	-1.627E-03	(14,12)	2.633E-04	(15,11)
134	6.248E-04	(17,10)	-1.602E-03	(14,12)	2.593E-04	(16,11)
135	1.788E-03	(22, 2)	-1.547E-03	(14,12)	2.583E-04	(16,11)
136	2.289E-03	(22, 2)	-1.541E-03	(15,12)	2.503E-04	(16,11)
137	5.459E-04	(22, 2)	-1.532E-03	(15,12)	2.369E-04	(16,11)
138	-5.456E-04	(14,10)	-1.483E-03	(15,12)	2.233E-04	(17,11)
139	-5.568E-04	(14,10)	-1.407E-03	(15,12)	2.158E-04	(17,11)
140	-5.543E-04	(14,10)	-1.325E-03	(16,12)	-2.068E-04	(14,10)
141	-5.403E-04	(14,10)	-1.281E-03	(16,12)	-2.041E-04	(14,10)
142	-5.238E-04	(15,10)	-1.212E-03	(16,12)	-1.970E-04	(14,10)
143	-5.309E-04	(15,10)	-1.116E-03	(16,12)	-1.868E-04	(14,10)
144	-5.230E-04	(15,10)	-1.008E-03	(16,12)	-1.824E-04	(15,10)
145	-5.082E-04	(15,10)	-9.195E-04	(17,12)	-1.773E-04	(15,10)

THE CISTRIBUTION OF VORTICITY - A(I,J,NW)

15			-3.335E-02	-1.517E-01	-2.506E-01	-3.294E-01	-3.981E-01	-4.651E-C1	-5.349E-01	-6.258E-01	-7.361E-01
14			6.704E-02	-1.448E-C1	-2.269E-01	-2.811E-01	-3.278E-01	-3.747E-01	-4.266E-01	-4.919E-01	-5.700E-01
13			3.941E-02	-1.239E-01	-1.775E-01	-2.048E-01	-2.296E-01	-2.559E-01	-2.856E-01	-3.202E-01	-3.568E-01
12			-7.696E-02	-1.838E-02	7.352E-03	2.793E-02	4.271E-02	5.606E-02	6.966E-02	8.667E-02	1.101E-01
11			-2.300E-01	1.293E-01	2.467E-01	3.043E-01	3.548E-01	4.035E-01	4.525E-01	5.067E-01	5.612E-01
1C			-4.771E-01	5.053E-01	6.183E-01	7.151E-01	8.023E-01	8.888E-01	9.781E-01	1.080E+00	1.175E+00
9			-1.112E+C0	1.912E+00	1.924E+00	1.936E+00	1.966E+C0	2.021E+C0	2.105E+00	2.225E+00	2.349E+00
8			-1.596E+00	4.233E+00	4.276E+00	4.250E+00	4.254E+00	4.297E+C0	4.380E+00	4.505E+00	4.632E+00
7			-4.287E-01	4.803E+00	5.838E+00	6.408E+00	6.893E+00	7.313E+00	7.665E+00	7.934E+00	8.092E+00
6	8.C00E+00	6.310E+01	5.529E+01	1.001E+01	1.269E+01	1.320E+01	1.334E+01	1.331E+01	1.313E+01	1.284E+01	1.252E+01
5	6.COCE+C0	1.058E+01	2.202E+01	3.244E+01	2.775E+01	2.474E+01	2.229E+01	2.016E+01	1.825E+01	1.656E+01	1.528E+01
4	4.00CE+C0	1.832E+01	7.427E+00	5.952E+00	8.001E+00	9.337E+00	1.023E+01	1.076E+01	1.097E+01	1.088E+01	1.062E+01
3	2.000E+00	1.107E+01	8.493E+00	6.454E+00	5.663E+00	5.346E+00	5.233E+00	5.215E+00	5.216E+00	5.194E+00	5.158E+00
2	8.COCE-01	9.478E+C0	4.134E+00	1.942E+00	1.878E+00	1.992E+00	2.029E+00	2.027E+00	2.011E+00	2.000E+00	2.017E+00
1	0.0	0.0	0.0	0.0	0.0	0.0	0.0	0.0	0.0	0.0	0.0
	1	2	3	4	5	6	7	8	9	10	11

15	-8.485E-01	-9.727E-01	-1.089E+00	-1.169E+00	-1.243E+00	-1.602E+00	-2.983E+00	-5.296E+00	-3.453E-02		
14	-6.459E-01	-7.152E-01	-7.783E-01	-8.540E-01	-9.817E-01	-1.166E+00	-1.219E+00	-6.717E-01	6.941E-02		
13	-3.834E-01	-3.948E-01	-3.919E-01	-3.739E-01	-3.291E-01	-2.264E-01	-1.393E-02	3.933E-01	-8.461E-01		
12	1.405E-01	1.777E-01	2.203E-01	2.702E-01	3.408E-01	4.680E-01	7.091E-01	1.146E+C0	-1.919E+00		
11	6.096E-01	6.538E-01	6.791E-01	6.636E-01	6.150E-01	6.096E-01	8.168E-01	1.731E+00	-2.685E+00		
10	1.245E+00	1.312E+00	1.384E+00	1.451E+00	1.438E+00	1.192E+00	9.596E-01	1.750E+C0	-2.804E+00		
9	2.441E+00	2.514E+00	2.578E+00	2.646E+00	2.745E+00	2.750E+00	2.167E+00	2.062E+C0	-2.752E+00		
8	4.730E+00	4.805E+00	4.863E+00	4.894E+C0	4.905E+00	5.033E+00	5.251E+00	2.762E+00	-2.435E+00		
7	8.170E+00	8.208E+00	8.224E+00	8.221E+C0	8.165E+00	7.964E+00	8.518E+00	1.458E+01	-6.049E+00		
6	1.225E+C1	1.202E+01	1.182E+01	1.165E+01	1.150E+01	1.124E+01	9.123E+00	1.641E+01	6.876E+01	6.665E+01	6.424E+01
5	1.443E+01	1.381E+01	1.334E+01	1.295E+01	1.265E+01	1.256E+01	1.199E+01	4.291E+00	-1.447E+00	5.922E-01	3.365E+00
4	1.036E+01	1.013E+01	9.928E+00	9.751E+00	9.604E+00	9.567E+00	1.025E+01	1.178E+01	1.911E+01	1.628E+01	1.344E+01
3	5.128E+C0	5.109E+00	5.102E+00	5.104E+00	5.125E+00	5.223E+00	5,644E+00	6.450E+00	8.085E+00	8.290E+00	8.135E+00
2	2.047E+C0	2.088E+00	2.135E+00	2.183E+00	2.246E+00	2.414E+00	2.958E+00	3.931E+00	4.712E+00	3.973E+00	3.637E+00
1	0.0	0.0	0.0	0.0	0.0	0.0	0.0	0.0	0.0	0.0	0.0
	12	13	14	15	16	17	18	19	20	21	22

THE DISTRIBUTION OF STREAM FUNCTION - A(I,J,NF)

J \ I	1	2	3	4	5	6	7	8	9	10	11
15			0.0	0.0	0.0	0.0	0.0	0.0	0.0	0.0	0.0
14			0.0	3.878E-03	6.253E-03	8.029E-03	9.554E-03	1.104E-02	1.259E-02	1.456E-02	1.692E-02
13			0.0	1.576E-02	2.473E-02	3.093E-02	3.618E-02	4.128E-02	4.664E-02	5.332E-02	6.104E-02
12			0.0	5.440E-02	8.084E-02	9.709E-02	1.108E-01	1.241E-01	1.381E-01	1.547E-01	1.728E-01
11			0.0	9.349E-02	1.289E-01	1.494E-01	1.674E-01	1.852E-01	2.037E-01	2.255E-01	2.481E-01
10			0.0	1.138E-01	1.382E-01	1.551E-01	1.717E-01	1.888E-01	2.072E-01	2.290E-01	2.514E-01
9			0.0	7.593E-02	7.704E-02	8.523E-02	9.693E-02	1.105E-01	1.259E-01	1.448E-01	1.642E-01
8			0.0	-6.828E-02	-7.888E-02	-7.329E-02	-6.326E-02	-5.169E-02	-3.860E-02	-2.349E-02	-8.663E-03
7			0.0	-2.998E-01	-3.139E-01	-3.076E-01	-2.976E-01	-2.869E-01	-2.7[illegible]E-01	-2.652E-01	-2.555E-01
6	0.0	0.0	0.0	-5.469E-01	-5.597E-01	-5.568E-01	-5.525E-01	-5.483E-01	-5.448E-01	-5.416E-01	-5.388E-01
5	-1.159E+00	-6.628E-01	-6.167E-01	-7.562E-01	-7.846E-01	-7.937E-01	-7.996E-01	-8.045E-01	-8.091E-01	-8.132E-01	-8.163E-01
4	-1.205E+00	-9.748E-01	-9.730E-01	-1.032E+00	-1.044E+00	-1.047E+00	-1.049E+00	-1.051E+00	-1.053E+00	-1.056E+00	-1.058E+00
3	-1.245E+00	-1.186E+00	-1.187E+00	-1.201E+00	-1.205E+00	-1.206E+00	-1.207E+00	-1.207E+00	-1.208E+00	-1.209E+00	-1.210E+00
2	-1.258E+00	-1.246E+00	-1.246E+00	-1.249E+00	-1.250E+00	-1.250E+00	-1.250E+00	-1.250E+00	-1.250E+00	-1.250E+00	-1.250E+00
1	-1.260E+00	-1.260E+00	-1.260E+00	-1.260E+00	-1.260E+00	-1.260E+00	-1.260E+00	-1.260E+00	-1.260E+00	-1.260E+00	-1.260E+00

J \ I	12	13	14	15	16	17	18	19	20	21	22
15	0.0	0.0	0.0	0.0	0.0	0.0	0.0	0.0	0.0		
14	1.924E-02	2.166E-02	2.386E-02	2.554E-02	2.749E-02	3.429E-02	5.568E-02	8.586E-02	0.0		
13	6.833E-02	7.544E-02	8.180E-02	8.765E-02	9.595E-02	1.149E-01	1.540E-01	1.877E-01	0.0		
12	1.884E-01	2.020E-01	2.130E-01	2.220E-01	2.330E-01	2.559E-01	2.988E-01	3.195E-01	0.0		
11	2.660E-01	2.807E-01	2.915E-01	2.985E-01	3.044E-01	3.172E-01	3.484E-01	3.654E-01	0.0		
10	2.683E-01	2.821E-01	2.934E-01	3.025E-01	3.094E-01	3.143E-01	3.279E-01	3.378E-01	0.0		
9	1.787E-01	1.904E-01	2.001E-01	2.093E-01	2.203E-01	2.350E-01	2.523E-01	2.626E-01	0.0		
8	2.236E-03	1.078E-02	1.790E-02	2.481E-02	3.451E-02	5.543E-02	1.017E-01	1.467E-01	0.0		
7	-2.489E-01	-2.439E-01	-2.399E-01	-2.358E-01	-2.296E-01	-2.149E-01	-1.629E-01	-1.028E-03	0.0		
6	-5.371E-01	-5.359E-01	-5.348E-01	-5.335E-01	-5.307E-01	-5.241E-01	-5.051E-01	-3.695E-01	0.0	0.0	0.0
5	-8.183E-01	-8.198E-01	-8.209E-01	-8.215E-01	-8.211E-01	-8.184E-01	-8.131E-01	-7.945E-01	-7.689E-01	-7.553E-01	-7.403E-01
4	-1.059E+00	-1.061E+00	-1.061E+00	-1.062E+00	-1.062E+00	-1.061E+00	-1.058E+00	-1.049E+00	-1.029E+00	-1.029E+00	-1.031E+00
3	-1.210E+00	-1.210E+00	-1.210E+00	-1.211E+00	-1.211E+00	-1.210E+00	-1.209E+00	-1.207E+00	-1.202E+00	-1.202E+00	-1.202E+00
2	-1.250E+00	-1.250E+00	-1.250E+00	-1.250E+00	-1.250E+00	-1.250E+00	-1.250E+00	-1.249E+00	-1.248E+00	-1.248E+00	-1.248E+00
1	-1.260E+00	-1.260E+00	-1.260E+00	-1.260E+00	-1.260E+00	-1.260E+00	-1.260E+00	-1.260E+00	-1.260E+00	-1.260E+00	-1.260E+00

THE CISTRIBUTION OF TEMPERATURE - A(I,J,NT)

15			0.0	0.0	0.0	0.0	0.0	0.0	0.0	0.0	0.0
14			0.0	4.362E-03	5.960E-03	7.145E-03	8.235E-03	9.351E-03	1.058E-02	1.206E-02	1.389E-02
13			0.0	8.990E-03	1.220F-02	1.457E-02	1.674E-02	1.894E-02	2.135E-02	2.419E-02	2.766E-02
12			0.0	1.560E-02	2.158E-02	2.601E-02	2.997E-02	3.392E-02	3.810E-02	4.284E-02	4.830E-02
11			0.0	1.873E-02	2.656E-02	3.267E-02	3.829E-02	4.393E-02	4.981E-02	5.619E-02	6.289E-02
10			0.0	1.960E-02	2.946E-02	3.752E-02	4.536E-02	5.334E-02	6.164E-02	7.040E-02	7.857E-02
9			0.0	2.996E-02	4.561E-02	5.790F-02	6.871E-02	7.907E-02	8.960E-02	1.006E-01	1.103E-01
8			0.0	1.401E-01	1.471E-01	1.498E-01	1.534E-01	1.588E-01	1.662E-01	1.755E-01	1.846E-01
7			0.0	2.682E-01	2.789E-01	2.842E-01	2.899E-01	2.968E-01	3.049E-01	3.141E-01	3.220E-01
6	0.0	0.0	0.0	4.146E-01	4.713E-01	4.944E-01	5.080E-01	5.171E-01	5.229E-01	5.258E-01	5.265E-01
5	1.000E+00	1.000E+00	1.000E+00	9.670E-01	9.251E-01	8.888E-01	8.570E-01	8.284E-01	8.016E-01	7.764E-01	7.564E-01
4	1.000E+00	1.000E+00	1.000E+00	9.973E-01	9.904E-01	9.800E-01	9.668E-01	9.509E-01	9.320E-01	9.107E-01	8.913E-01
3	1.000E+00	1.000E+00	1.000E+00	9.997E-01	9.986E-01	9.962E-01	9.922E-01	9.860E-01	9.768E-01	9.642E-01	9.511E-01
2	1.000E+00	1.000E+00	1.000E+00	9.999E-01	9.995E-01	9.985E-01	9.964E-01	9.926E-01	9.862E-01	9.764E-01	9.654E-01
1	1.000E+00	1.000E+00	1.000E+00	1.000E+00	9.997E-01	9.990E-01	9.972E-01	9.938E-01	9.879E-01	9.787E-01	9.681E-01
	1	2	3	4	5	6	7	8	9	10	11

15	0.0	0.0	0.0	0.0	0.0	0.0	0.0	0.0	0.0		
14	1.588E-02	1.782E-02	1.976E-02	2.173E-02	2.376E-02	2.618E-02	2.988E-02	3.490E-02	0.0		
13	3.136E-02	3.489E-02	3.833E-02	4.176E-02	4.542E-02	5.012E-02	5.743E-02	6.754E-02	0.0		
12	5.382E-02	5.884E-02	6.340E-02	6.759E-02	7.204E-02	7.868E-02	9.099E-02	1.077E-01	0.0		
11	6.916E-02	7.480E-02	7.978E-02	8.377E-02	8.696E-02	9.152E-02	1.050E-01	1.409E-01	0.0		
10	8.524E-02	9.104E-02	9.679E-02	1.009E-01	1.045E-01	1.066E-01	1.134E-01	1.515E-01	0.0		
9	1.177E-01	1.237E-01	1.289E-01	1.332E-01	1.366E-01	1.384E-01	1.408E-01	1.679E-01	0.0		
8	1.917E-01	1.974E-01	2.021E-01	2.054E-01	2.066E-01	2.042E-01	1.998E-01	2.026E-01	0.0		
7	3.277E-01	3.320E-01	3.352E-01	3.369E-01	3.353E-01	3.251E-01	3.022E-01	2.957E-01	0.0		
6	5.261E-01	5.253E-01	5.241E-01	5.220E-01	5.174E-01	5.038E-01	4.595E-01	4.080E-01	0.0	0.0	0.0
5	7.429E-01	7.329E-01	7.234E-01	7.155E-01	7.070E-01	6.952E-01	6.581E-01	5.811E-01	4.675E-01	4.580E-01	4.503E-01
4	8.767E-01	8.650E-01	8.552E-01	8.467E-01	8.384E-01	8.292E-01	8.142E-01	7.860E-01	7.502E-01	7.254E-01	7.058E-01
3	9.402E-01	9.309E-01	9.228E-01	9.155E-01	9.086E-01	9.014E-01	8.920E-01	8.768E-01	8.603E-01	8.467E-01	8.328E-01
2	9.559E-01	9.475E-01	9.401E-01	9.334E-01	9.270E-01	9.206E-01	9.134E-01	9.037E-01	8.913E-01	8.783E-01	8.651E-01
1	9.589E-01	9.507E-01	9.434E-01	9.368E-01	9.305E-01	9.243E-01	9.175E-01	9.088E-01	8.972E-01	8.843E-01	8.712E-01
	12	13	14	15	16	17	18	19	20	21	22

THE DISTRIBUTION OF Z-COMP. MASS VELOCITY - G1(I,J)

	1	2	3	4	5	6	7	8	9	10	11
15			0.0	0.0	0.0	0.0	0.0	0.0	0.0	0.0	0.0
14			0.0	-8.427E-02	-1.324E-01	-1.658E-01	-1.941E-01	-2.216E-01	-2.504E-01	-2.864E-01	-3.281E-01
13			0.0	-1.644E-01	-2.477E-01	-3.003E-01	-3.445E-01	-3.875E-01	-4.327E-01	-4.871E-01	-5.473E-01
12			0.0	-2.487E-01	-3.332E-01	-3.791E-01	-4.200E-01	-4.604E-01	-5.025E-01	-5.509E-01	-5.985E-01
11			0.0	-2.114E-01	-2.039E-01	-2.063E-01	-2.166E-01	-2.301E-01	-2.457E-01	-2.641E-01	-2.791E-01
10			0.0	7.025E-02	2.073E-01	2.566E-01	2.820E-01	2.988E-01	3.109E-01	3.226E-01	3.356E-01
9			0.0	8.326E-01	9.923E-01	1.044E+00	1.074E+00	1.100E+00	1.123E+00	1.154E+00	1.189E+00
8			0.0	2.004E+00	2.085E+00	2.095E+00	2.104E+00	2.119E+00	2.144E+00	2.187E+00	2.238E+00
7			0.0	3.063E+00	3.077E+00	3.095E+00	3.131E+00	3.179E+00	3.240E+00	3.316E+00	3.393E+00
6	0.0	0.0	0.0	3.651E+00	3.766E+00	3.889E+00	4.016E+00	4.141E+00	4.264E+00	4.385E+00	4.486E+00
5	8.750E-01	1.040E+01	1.038E+01	5.171E+00	5.163E+00	5.228E+00	5.295E+00	5.362E+00	5.424E+00	5.485E+00	5.537E+00
4	1.500E+00	8.375E+00	9.120E+00	7.124E+00	6.727E+00	6.599E+00	6.516E+00	6.448E+00	6.386E+00	6.331E+00	6.293E+00
3	1.879E+00	9.029E+00	9.076E+00	7.231E+00	6.835E+00	6.726E+00	6.656E+00	6.587E+00	6.509E+00	6.426E+00	6.356E+00
2	1.980E+00	9.805E+00	9.700E+00	7.745E+00	7.268E+00	7.126E+00	7.037E+00	6.951E+00	6.857E+00	6.756E+00	6.673E+00
1	2.000E+00	9.953E+00	9.818E+00	7.843E+00	7.350E+00	7.202E+00	7.109E+00	7.021E+00	6.924E+00	6.819E+00	6.733E+00

	12	13	14	15	16	17	18	19	20	21	22
15	0.0	0.0	0.0	0.0	0.0	0.0	0.0	0.0	0.0		
14	-3.675E-01	-4.042E-01	-4.407E-01	-4.722E-01	-5.165E-01	-6.196E-01	-8.394E-01	-1.039E+00	0.0		
13	-6.003E-01	-6.477E-01	-6.876E-01	-7.245E-01	-7.767E-01	-8.737E-01	-1.012E+00	-1.012E+00	0.0		
12	-6.324E-01	-6.567E-01	-6.711E-01	-6.748E-01	-6.672E-01	-6.473E-01	-6.220E-01	-5.684E-01	0.0		
11	-2.843E-01	-2.850E-01	-2.859E-01	-2.863E-01	-2.717E-01	-2.079E-01	-1.035E-01	-6.478E-02	0.0		
10	3.490E-01	3.612E-01	3.657E-01	3.570E-01	3.365E-01	3.287E-01	3.842E-01	4.110E-01	0.0		
9	1.216E+00	1.240E+00	1.259E+00	1.269E+00	1.257E+00	1.184E+00	1.034E+00	8.736E-01	0.0		
8	2.280E+00	2.316E+00	2.347E+00	2.373E+00	2.399E+00	2.399E+00	2.215E+00	1.406E+00	0.0		
7	3.452E+00	3.498E+00	3.537E+00	3.573E+00	3.618E+00	3.709E+00	3.884E+00	3.303E+00	0.0		
6	4.556E+00	4.607E+00	4.648E+00	4.686E+00	4.732E+00	4.828E+00	5.202E+00	6.348E+00	0.0	0.0	0.0
5	5.572E+00	5.597E+00	5.616E+00	5.637E+00	5.668E+00	5.728E+00	5.899E+00	7.252E+00	1.097E+01	1.098E+01	1.100E+01
4	6.267E+00	6.248E+00	6.234E+00	6.226E+00	6.232E+00	6.270E+00	6.340E+00	6.600E+00	6.927E+00	7.142E+00	7.391E+00
3	6.307E+00	6.271E+00	6.243E+00	6.224E+00	6.219E+00	6.248E+00	6.342E+00	6.616E+00	7.252E+00	7.239E+00	7.182E+00
2	6.619E+00	6.583E+00	6.561E+00	6.549E+00	6.553E+00	6.595E+00	6.723E+00	7.061E+00	7.767E+00	7.785E+00	7.723E+00
1	6.678E+00	6.643E+00	6.621E+00	6.611E+00	6.616E+00	6.661E+00	6.795E+00	7.146E+00	7.865E+00	7.888E+00	7.826E+00

THE DISTRIBUTION OF R-COMP. MASS VELOCITY - G2(I,J)

J	1	2	3	4	5	6	7	8	9	10	11
15			0.0	0.0	0.0	0.0	0.0	0.0	0.0	0.0	0.0
14			0.0	-5.374E-03	-3.436E-03	-2.553E-03	-2.104E-03	-1.860E-03	-1.804E-03	-1.901E-03	-2.243E-03
13			0.0	-2.228E-02	-1.318E-02	-9.282E-03	-7.583E-03	-6.714E-03	-6.460E-03	-6.624E-03	-7.504E-03
12			0.0	-8.026E-02	-4.091E-02	-2.671E-02	-2.179E-02	-1.927E-02	-1.814E-02	-1.767E-02	-1.827E-02
11			0.0	-1.426E-01	-5.961E-02	-3.813E-02	-3.201E-02	-2.847E-02	-2.658E-02	-2.513E-02	-2.420E-02
10			0.0	-1.729E-01	-4.927E-02	-3.715E-02	-3.388E-02	-3.125E-02	-2.977E-02	-2.817E-02	-2.627E-02
9			0.0	-1.111E-01	-1.207E-02	-2.480E-02	-2.877E-02	-2.910E-02	-2.903E-02	-2.784E-02	-2.588E-02
8			0.0	1.318E-01	9.260E-03	-2.252E-02	-2.875E-02	-2.888E-02	-2.793E-02	-2.551E-02	-2.285E-02
7			0.0	6.325E-01	1.680E-02	-2.831E-02	-3.326E-02	-3.040E-02	-2.610E-02	-2.122E-02	-1.724E-02
6	0.0	0.0	0.0	1.411E+00	2.539E-02	-1.573E-02	-1.710E-02	-1.384E-02	-1.024E-02	-7.665E-03	-5.918E-03
5	0.0	-1.446E+00	4.047E-01	5.602E-01	1.216E-01	4.488E-02	2.920E-02	2.260E-02	1.775E-02	1.251E-02	8.918E-03
4	0.0	-9.295E-01	3.185E-01	3.547E-01	7.408E-02	2.343E-02	1.640E-02	1.542E-02	1.446E-02	1.194E-02	9.554E-03
3	0.0	-4.653E-01	1.663E-01	1.831E-01	4.562E-02	1.596E-02	1.081E-02	9.661E-03	8.850E-03	7.206E-03	5.530E-03
2	0.0	-2.325E-01	8.674E-02	8.962E-02	2.181E-02	7.190E-03	4.807E-03	4.389E-03	4.179E-03	3.455E-03	2.428E-03
1	0.0	0.0	0.0	0.0	0.0	0.0	0.0	0.0	0.0	0.0	0.0

J	12	13	14	15	16	17	18	19	20	21	22
15	0.0	0.0	0.0	0.0	0.0	0.0	0.0	0.0	0.0		
14	-2.863E-03	-3.306E-03	-3.194E-03	-3.467E-03	-9.536E-03	-3.255E-02	-6.112E-02	7.036E-02	0.0		
13	-9.040E-03	-1.008E-02	-1.066E-02	-1.428E-02	-3.065E-02	-6.953E-02	-8.955E-02	2.013E-01	0.0		
12	-1.988E-02	-2.010E-02	-1.904E-02	-2.211E-02	-4.187E-02	-8.634E-02	-8.811E-02	4.270E-01	0.0		
11	-2.457E-02	-2.302E-02	-1.860E-02	-1.548E-02	-2.559E-02	-6.459E-02	-7.177E-02	5.528E-01	0.0		
10	-2.607E-02	-2.560E-02	-2.422E-02	-2.157E-02	-1.752E-02	-3.056E-02	-3.945E-02	5.848E-01	0.0		
9	-2.532E-02	-2.502E-02	-2.597E-02	-3.178E-02	-4.456E-02	-5.930E-02	-5.302E-02	5.146E-01	0.0		
8	-2.187E-02	-2.137E-02	-2.255E-02	-3.073E-02	-6.309E-02	-1.477E-01	-2.061E-01	2.458E-01	0.0		
7	-1.555E-02	-1.470E-02	-1.582E-02	-2.298E-02	-5.167E-02	-1.779E-01	-5.922E-01	-4.461E-01	0.0		
6	-4.973E-03	-4.605E-03	-5.821E-03	-1.157E-02	-2.913E-02	-8.491E-02	-5.402E-01	-1.781E+00	0.0	0.0	0.0
5	7.826E-03	6.841E-03	5.144E-03	4.098E-04	-1.290E-02	-3.483E-02	-1.105E-01	-2.067E-01	-1.800E-01	-7.617E-02	-5.337E-02
4	8.691E-03	7.833E-03	6.601E-03	3.549E-03	-5.463E-03	-2.589E-02	-8.127E-02	-2.065E-01	-1.834E-01	8.598E-03	8.755E-03
3	4.720E-03	3.916E-03	2.975E-03	1.211E-03	-3.703E-03	-1.591E-02	-4.595E-02	-1.068E-01	-9.361E-02	3.365E-03	5.333E-03
2	1.681E-03	8.881E-04	2.918E-05	-1.108E-03	-3.660E-03	-1.056E-02	-2.873E-02	-6.185E-02	-5.315E-02	-1.144E-04	1.621E-03
1	0.0	0.0	0.0	0.0	0.0	0.0	0.0	0.0	0.0	0.0	0.0

THE CISTRIBUTION OF Z-COMP. VELOCITY - V1(I,J)

	1	2	3	4	5	6	7	8	9	10	11
15			0.0	0.0	0.0	0.0	0.0	0.0	0.0	0.0	0.0
14			0.0	-8.622E-03	-1.370E-02	-1.730E-02	-2.041E-02	-2.348E-02	-2.677E-02	-3.094E-02	-3.591E-02
13			0.0	-1.738E-C2	-2.679E-02	-3.302E-02	-3.847E-02	-4.395E-02	-4.992E-02	-5.734E-02	-6.602E-02
12			0.0	-2.755E-02	-3.851E-02	-4.520E-02	-5.149E-02	-5.805E-C2	-6.525E-02	-7.395E-02	-8.347E-02
11			0.0	-2.394E-02	-2.441E-02	-2.578E-02	-2.817E-02	-3.113E-02	-3.463E-02	-3.892E-02	-4.307E-02
10			0.0	8.005E-03	2.533E-02	3.319E-02	3.852E-02	4.316E-02	4.756E-02	5.238E-02	5.755E-02
9			0.0	1.021E-01	1.358E-01	1.557E-01	1.724E-01	1.892E-01	2.070E-01	2.279E-01	2.489E-01
8			0.0	4.936E-01	5.311E-01	5.404E-01	5.516E-01	5.685E-01	5.926E-01	6.255E-01	6.595E-01
7			0.0	1.043E+00	1.081E+00	1.106E+00	1.139E+00	1.183E+00	1.232E+00	1.292E+00	1.349E+00
6	0.0	0.0	0.0	1.747E+00	1.977E+00	2.127E+00	2.247E+00	2.352E+00	2.444E+00	2.525E+00	2.586E+00
5	8.750E-01	1.040E+01	1.038E+01	5.020E+00	4.817E+00	4.704E+00	4.614E+00	4.532E+00	4.455E+00	4.384E+00	4.327E+00
4	1.500E+00	8.379E+00	9.120E+00	7.107E+00	6.669E+00	6.482E+00	6.324E+00	6.166E+00	5.998E+00	5.824E+00	5.677E+00
3	1.875E+00	9.029E+00	9.076E+00	7.229E+00	6.827E+00	6.703E+00	6.610E+00	6.505E+00	6.375E+00	6.222E+00	6.080E+00
2	1.980E+00	9.805E+00	9.700E+00	7.745E+00	7.265E+00	7.116E+00	7.014E+00	6.905E+C0	6.773E+00	6.615E+00	6.468E+00
1	2.000E+00	9.953E+00	9.818E+00	7.843E+00	7.343E+00	7.176E+00	7.054E+00	6.923E+C0	6.773E+00	6.609E+00	6.457E+00

	12	13	14	15	16	17	18	19	20	21	22
15	0.C	0.0	0.0	0.0	0.0	0.0	0.0	0.0	0.0		
14	-4.080E-02	-4.571E-02	-5.028E-02	-5.462E-02	-6.060E-02	-7.394E-02	-1.028E-01	-1.319E-01	0.0		
13	-7.433E-02	-8.222E-02	-8.942E-02	-9.652E-02	-1.062E-01	-1.234E-01	-1.504E-01	-1.612E-01	0.0		
12	-9.166E-02	-9.854E-02	-1.039E-01	-1.075E-01	-1.095E-01	-1.111E-01	-1.156E-01	-1.172E-01	0.0		
11	-4.577E-02	-4.766E-02	-4.941E-02	-5.080E-02	-4.922E-02	-3.878E-02	-2.099E-02	-1.602E-02	0.0		
10	6.252E-02	6.717E-02	7.031E-02	7.063E-02	6.804E-02	6.733E-02	8.193E-02	1.068E-01	0.0		
9	2.658E-01	2.804E-01	2.928E-01	3.019E-01	3.042E-01	2.891E-01	2.559E-01	2.431E-01	0.0		
8	6.859E-01	7.072E-01	7.246E-01	7.385E-01	7.485E-01	7.445E-01	6.801E-01	4.347E-01	0.0		
7	1.392E+00	1.426E+00	1.452E+00	1.473E+00	1.486E+00	1.486E+00	1.467E+00	1.225E+00	0.0		
6	2.625E+00	2.651E+00	2.670E+00	2.682E+00	2.689E+00	2.683E+00	2.672E+00	3.007E+C0	0.0	0.0	0.0
5	4.285E+00	4.251E+C0	4.223E+00	4.199E+00	4.179E+00	4.162E+00	4.087E+00	4.535E+00	5.720E+00	5.625E+00	5.556E+00
4	5.571E+00	5.489E+00	5.422E+00	5.368E+00	5.325E+00	5.305E+00	5.277E+00	5.330E+00	5.374E+00	5.384E+00	5.442E+00
3	5.971E+00	5.884E+00	5.812E+00	5.752E+00	5.709E+00	5.694E+00	5.726E+00	5.883E+00	6.341E+00	6.241E+00	6.100E+00
2	6.360E+C0	6.276E+00	6.210E+00	6.159E+00	6.125E+00	6.126E+00	6.201E+00	6.450E+00	7.007E+00	6.932E+00	6.786E+00
1	6.329E+00	6.218E+00	6.117E+00	6.026E+00	5.953E+00	5.926E+00	5.973E+00	6.115E+00	6.469E+00	6.285E+00	6.077E+00

THE DISTRIBUTION OF R-COMP. VELOCITY - V2(I,J)

15			0.0	0.0	0.0	0.0	0.0	0.0	0.0	0.0	0.0
14			0.0	-5.498E-04	-3.555E-04	-2.664E-04	-2.213E-04	-1.971E-04	-1.928E-04	-2.053E-04	-2.455E-04
13			0.0	-2.355E-03	-1.425E-03	-1.021E-03	-8.468E-04	-7.615E-04	-7.453E-04	-7.797E-04	-9.053E-04
12			0.0	-8.891E-03	-4.728E-03	-3.184E-03	-2.672E-03	-2.430E-03	-2.356E-03	-2.371E-03	-2.548E-03
11			0.0	-1.615E-02	-7.135E-03	-4.765E-03	-4.162E-03	-3.852E-03	-3.746E-03	-3.702E-03	-3.734E-03
10			0.0	-1.970E-02	-6.020E-03	-4.804E-03	-4.629E-03	-4.514E-03	-4.554E-03	-4.574E-03	-4.505E-03
9			0.0	-1.362E-02	-1.652E-03	-3.696E-03	-4.619E-03	-5.006E-03	-5.349E-03	-5.497E-03	-5.418E-03
8			0.0	3.247E-02	2.359E-03	-5.809E-03	-7.536E-03	-7.747E-03	-7.719E-03	-7.296E-03	-6.732E-03
7			0.0	2.154E-01	5.903E-03	-1.012E-02	-1.211E-02	-1.131E-02	-9.950E-03	-8.268E-03	-6.856E-03
6	0.0	0.0	0.0	6.752E-01	1.333E-02	-8.607E-03	-9.568E-03	-7.860E-03	-5.871E-03	-4.415E-03	-3.412E-03
5	0.0	-1.446E+00	4.047E-01	5.438E-01	1.134E-01	4.039E-02	2.544E-02	1.910E-02	1.457E-02	9.997E-03	6.968E-03
4	0.0	-9.295E-01	3.185E-01	3.534E-01	7.344E-02	2.301E-02	1.592E-02	1.475E-02	1.358E-02	1.098E-02	8.620E-03
3	0.0	-4.653E-01	1.663E-01	1.830E-01	4.556E-02	1.590E-02	1.074E-02	9.541E-03	8.667E-03	6.977E-03	5.289E-03
2	0.0	-2.325E-01	8.674E-02	8.961E-02	2.181E-02	7.180E-03	4.792E-03	4.360E-03	4.128E-03	3.383E-03	2.353E-03
1	0.C	C.0	0.0	0.0	0.0	0.0	0.0	0.0	0.0	0.0	0.0
	1	2	3	4	5	6	7	8	9	10	11

15	0.0	C.0	0.0	0.0	0.0	0.0	0.0	0.0	0.0		
14	-3.177E-04	-3.721E-04	-3.644E-04	-4.011E-04	-1.119E-03	-3.886E-03	-7.490E-03	8.930E-03	0.0		
13	-1.119E-03	-1.280E-03	-1.386E-03	-1.903E-03	-4.189E-03	-9.821E-03	-1.331E-02	3.204E-02	0.0		
12	-2.882E-03	-3.016E-03	-2.948E-03	-3.523E-03	-6.874E-03	-1.482E-02	-1.582E-02	8.804E-C2	0.0		
11	-3.956E-03	-3.850E-03	-3.215E-03	-2.747E-03	-4.636E-03	-1.205E-02	-1.456E-02	1.367E-01	0.0		
10	-4.670E-03	-4.761E-03	-4.656E-03	-4.268E-03	-3.543E-03	-6.260E-03	-8.414E-03	1.520E-01	0.0		
9	-5.594E-03	-5.656E-03	-6.037E-03	-7.559E-03	-1.079E-02	-1.448E-02	-1.310E-02	1.432E-01	0.0		
8	-6.578E-03	-6.526E-03	-6.963E-03	-9.561E-03	-1.968E-02	-4.584E-02	-6.328E-02	7.600E-02	0.0		
7	-6.272E-03	-5.990E-03	-6.494E-03	-9.474E-C3	-2.122E-02	-7.129E-02	-2.237E-01	-1.655E-01	0.0		
6	-2.865E-03	-2.650E-03	-3.343E-01	-6.622E-03	-1.655E-02	-4.718E-02	-2.774E-01	-8.436E-01	0.0	0.0	0.0
5	6.018E-03	5.196E-03	3.883E-03	3.053E-04	-9.511E-03	-2.531E-02	-7.658E-02	-1.293E-01	-9.381E-02	-3.902E-02	-2.696E-02
4	7.727E-03	6.882E-03	5.741E-03	3.060E-03	-4.668E-03	-2.190E-02	-6.765E-02	-1.668E-01	-1.423E-01	6.481E-03	6.446E-03
3	4.469E-03	3.674E-03	2.770E-03	1.119E-03	-3.399E-03	-1.450E-02	-4.148E-02	-9.499E-02	-8.185E-02	2.901E-03	4.529E-03
2	1.615E-03	8.466E-04	2.762E-05	-1.042E-03	-3.421E-03	-9.805E-03	-2.650E-02	-5.650E-02	-4.795E-02	-1.019E-04	[illegible]
1	0.0	0.0	0.0	0.0	0.0	0.0	0.0	0.0	0.0	0.0	0.0
	12	13	14	15	16	17	18	19	20	21	22

DISTANCE FROM ENTRANCE (IN)	BULK TEMPERATURE (DEG K)	HEAT TRANSFER RATE (CAL/CM**2/SEC)	HEAT TRANSFER COEF. (CAL/CM**2/SEC/DEG K)	NUSSELT NUMBER
1.40	2023.22	-8.3079E-03	4.8211E-06	8.6879E-02
1.81	1992.93	-1.1420E-02	6.7458E-06	1.2299E-01
2.25	1984.91	-1.3733E-02	8.1504E-06	1.4908E-01
2.72	1981.72	-1.5875E-02	9.4395E-06	1.7288E-01
3.25	1980.10	-1.8083E-02	1.0763E-05	1.9725E-01
3.86	1978.79	-2.0539E-02	1.2234E-05	2.2432E-01
4.60	1978.85	-2.3514E-02	1.4006E-05	2.5680E-01
5.44	1980.53	-2.7255E-02	1.6218E-05	2.9717E-01
6.09	1980.83	-3.1378E-02	1.8668E-05	3.4202E-01
6.62	1980.48	-3.5459E-02	2.1100E-05	3.8662E-01
7.07	1979.51	-3.9631E-02	2.3597E-05	4.3254E-01
7.46	1977.79	-4.3906E-02	2.6169E-05	4.8002E-01
7.81	1974.23	-4.8216E-02	2.8799E-05	5.2902E-01
8.13	1961.87	-5.3075E-02	3.1937E-05	5.8960E-01
8.43	1918.06	-6.0372E-02	3.7311E-05	7.0133E-01
2.72	1923.43	-7.0140E-02	4.3205E-05	8.1031E-01